ZINC AND GENOMIC STABILITY

A thesis submitted to the University of Adelaide

for the degree of Doctor of Philosophy

Razinah Sharif

School of Medicine,

Faculty of Health Sciences, University of Adelaide

and

CSIRO Food and Nutritional Sciences, Adelaide

June 2012

TABLE OF CONTENTS

Abstract

Zinc (Zn) is an essential trace element required for both optimal human health and maintaining genomic stability. The main aim of this thesis was to address important knowledge gaps regarding the possible impact of Zn status on genomic stability events in both lymphocytes and epithelial cells using both *in vitro* and *in vivo* models. The project also aimed to study the differential impact of Zn Carnosine (ZnC) and Zn Sulphate ($ZnSO_4$) on genome stability as the former is a newly emerging commercially available supplement renown for its antioxidant capacity. The *in vitro* studies investigated the effects of $ZnSO_4$ and ZnC on cell proliferation via MTT assay and DNA damage rates and was measured using both the comet assay and the Cytokinesis-block micronucleus cytome (CBMN-Cyt) assay in the WIL2-NS human lymphoblastoid cell line and HOK cell line. This study also investigated the impact of Zn status on both telomere length and telomere base damage *in vitro*. An *in vivo* study was designed to further investigate the effect of Zn supplementation in minimising genome instability events in lymphocytes. An increased intake of Zn may reduce the risk of degenerative diseases but may be toxic if taken in excess. This study aimed to investigate whether taking daily supplements of 20 mg of Zn as Zn Carnosine can improve Zn status, genome stability events and Zn transporter genes in an elderly South Australian cohort characterised by having low plasma Zn levels. In conclusion, the *in vitro* studies suggest that 1) Zn deficiency (0 μM) and high Zn concentrations increase DNA damage; 2) Zn at 4-16 μM is optimal in maintaining genome stability events; 3) Zn at 16-32 μM is optimal in protecting the cell against DNA damage induced by irradiation and hydrogen peroxide challenges; and 4) Zn may play an important role in telomere maintenances. The *in vivo* study suggests that Zn supplementation may be beneficial in an elderly population with marginal lowered Zn status by raising plasma Zn levels, lowering DNA damage events and modifies Zn transporter gene expression.

Declarations

I, Razinah Sharif certify that this work contains no material which has been accepted for the award of any other degree or diploma in any university or other tertiary institution and, to the best of my knowledge and belief, contains no material previously published or written by another person, except where due reference has been made in the text.

I give consent for a copy of my thesis when deposited in the University Library, to be made available for loan and photocopying, subject to the provisions of the Copyright Act 1968.

The author acknowledges that copyright of published works contained within this thesis (as listed on page xv) resides with the copyright holders of those works. I also give permission for the digital version of my thesis to be made available on the web, via the University's digital research depository, the Library catalogue and also through web search engines, unless permission has been granted by the University to restrict access for a period of time.

CSIRO Food and Nutritional Sciences retain the copyright of any subsequent publications arising from this thesis.

Signature: …… Date: ……..

Acknowledgements

First and foremost, I would like to praise God for everything whilst travelling through this PhD journey. It has been a roller coaster ride and whenever I became stuck or felt unmotivated, God always listened to me and things worked out fine eventually.

Secondly, I would like to thank my amazing supervisors (Prof Michael Fenech, Dr Philip Thomas and Dr Peter Zalewski) for giving me the opportunity to undertake this PhD project and for their guidance through out the study. I would also like to thank Prof Robin Graham and Prof Ross Butler who were initially involved with the project design.

I'm also grateful to all the staff and students at CSIRO Nutrigenomics lab and also to Kylie Lange (CSIRO), Erin Symonds (IMVS), Steve Henderson (CSIRO Waite), Eugene Roscioli (QEH), Rhys Hamon (QEH), Teresa Fowles (Waite campus), Lyndon Palmer (Waite campus), and Nathan O'Callaghan (CSIRO) who have always listened and helped me with some of the experiments and making it a complete story line. I would also like to acknowledge the group of PhD students who shared the pain, sweat and tears (Arnida, Carly, Eva, Sau Lai, Ann, Penny, Kacie, Mansi), you guys are the best bunch! I would really appreciate all the advice, the conversations and all the help. Thanks a million!

In order to complete the biggest part of my PhD project which was the *in vivo* study, I needed to conduct a human trial and I would like to express my gratitude to the staff at the CSIRO clinical trial unit (Julia Weaver, Lyndi Lawson, Rosemary McArthur, Vanessa Courage and Peter Royle) who helped me in completing this study. Thank you so much! On this occasion, I would also like to acknowledge Metagenics Company who provided the pills for the Zinc study without any charges at all. I would also like to thank all the volunteers who completed the study without any provided renumeration. They were willing to participate for the sake of science only. I'm really thankful to them!

I would also like to acknowledge my parents, my housemates (Maisara, Fauziah, and Norhalisa) and my other Malaysian communities for their friendship, support and prayers during the course of my study.

A PhD is always a stressful journey and for this matter, I am really thankful to Fernwood Gym Adelaide City, a place where I can go and ease my stress and a place that I can go whenever I'm having breakdown moments. Special credit to Abby, Rachel, Lou, Tam, Eman, Sandy, Sophie and Katrina for being the best gym buddies and also to Tracey for being my personal trainer.

Last but not least, I would like to acknowledge CSIRO Food and Nutritional Sciences for the funding provided to support all the chemicals needed in my study and also to my employer (Universiti Kebangsaan Malaysia) and Ministry of Higher Education, Malaysia who provided the scholarship (tuition fees and living allowances).

Thank you everyone for all the help and support. This thesis wouldn't be a thesis without all of your support and prayers.

Thank you!

Presentations and Publications arising from the thesis

Abstract/Poster Presentations

1. **Sharif, R**., Thomas, P., Zalewski, P., Graham, R. & Fenech, M. The effect of Zinc Sulphate and Zinc Carnosine on cytotoxicity and genotoxicity in the WIL2-NS lymphoblastoid cell line. 19th International Conference on Nutrition. 4-9th October 2009, Bangkok, Thailand.

2. **Sharif, R**., Thomas, P., Zalewski, P., Graham, R. & Fenech, M. The effect of Zinc Sulphate and Zinc Carnosine on cytotoxicity and genotoxicity in the WIL2-NS lymphoblastoid cell line. Australian Science Medical Research 2010. 9-10th June 2010, Adelaide, Australia.

3. **Sharif, R**., Thomas, P., Zalewski, P., Graham, R. & Fenech, M. The effect of Zinc Sulphate and Zinc Carnosine on cytotoxicity and genotoxicity in the WIL2-NS lymphoblastoid cell line. Nutrigenomics Symposium, CSIRO. 30th July 2010, Adelaide, Australia.

4. **Sharif, R.** Thomas, P. Zalewski, P. and Fenech, M. Zinc deficiency increases genome instability in Human Oral Keratinocytes (HOK). Nutrition in Medicine Conference. 13–15th May 2011, Bondi, Australia.

5. **Sharif, R.** Thomas, P. Zalewski, P. and Fenech, M. Zinc deficiency increases genome instability in Human Oral Keratinocytes (HOK). Australian Science Medical Research 2011. 9-10th June 2011, Adelaide, Australia.

6. **Sharif, R.** Thomas, P. Zalewski, P. and Fenech, M. Zinc deficiency increases genome instability in Human Oral Keratinocytes (HOK). XI Asian Congress on Nutrition 2011. 13-16th July 2011, Singapore.

7. **Sharif, R.** Thomas, P. Zalewski, P. and Fenech, M. Zinc deficiency increases genome instability in Human Oral Keratinocytes (HOK). Postgraduate Research Conference, Faculty of Health Science, University of Adelaide. 25th August 2011, Adelaide, Australia.

8. **Sharif, R.** Thomas, P. Zalewski, P. and Fenech, M. The effect of Zinc Sulphate and Zinc Carnosine on cytotoxicity and genotoxicity in the WIL2-NS lymphoblastoid cell line. NSNZ & *NSA* Joint Annual Scientific Meeting. 30th November-2nd December 2011, Queenstown, New Zealand.

9. **Sharif, R.** Thomas, P. Zalewski, P. and Fenech, M. Zinc supplementation influences genomic instability biomarkers, antioxidant activity and Zn transporter genes in an elderly Australian population with low Zn status. International Society for Zinc Biology 2012 Conference. 15-19th January 2012, Melbourne, Australia.

Oral Presentations

1. Zinc and Genomic Stability. Wednesday Wrap. School of Medicine, University of Adelaide. 16th September 2009.

2. Zinc and Genomic Stability. Wednesday Wrap. School of Medicine, University of Adelaide. 14th December 2011.

3. Zinc and Genomic Stability. Special Seminar. Genome Stability Laboratory. Yong Loo Lin School of Medicine. National University of Singapore. 11th July 2011.

4. The effect of Zinc Sulphate and Zinc Carnosine on genome stability and cytotoxicity in the WIL2-NS lymphoblastoid cell line. International Society for Zinc Biology 2012 Conference. 15-19th January 2012. Melbourne, Australia.

Publications

1. **Sharif, R**., Thomas, P., Zalewski, P., Graham, R. & Fenech, M. (2011) The effect of Zinc Sulphate and Zinc Carnosine on cytotoxicity and genotoxicity in the WIL2-NS lymphoblastoid cell line. *Mutation Research*. **720(1-2)**: 22-33.

2. **Sharif, R**., Thomas, P., Zalewski, P. & Fenech, M. (2011) Zinc deficiency or excess within the physiological range increases genome instability and cytotoxicity, respectively, in human oral keratinocyte cells. Genes and Nutrition. In press.

3. **Sharif, R**., Thomas, P., Zalewski, P. & Fenech, M. (2011) The role of zinc in genomic stability. Mutation Research. In press.

4. O'Callaghan, N., Baack, N., **Sharif, R**., and Fenech, M. (2011) A qPCR-based assay to quantify oxidized guanine and other FPG-sensitive base lesions within telomeric DNA. Biotechniques. Vol. 51 (6): 403–412.

List of Abbreviations

ACCV	Anti Cancer Council of Victoria
AOA	Antioxidant Activity
ANOVA	Analysis of Variance
AP1	Activator Protein 1
APE	Apyrimidinic Endonuclease
ATCC	American Type Culture Collection
aTL	Absolute Telomere Length
ATM	Ataxia Telangiectasia Mutated
ATR	Ataxia Telangiectasia and Rad3 Related
ATRIP	Ataxia Telangiectasia and Rad3 Related Interacting Protein
AU	Arbitrary Unit
BCA	Bicinchoninic Acid
BER	Base Excision Repair
BN	Binucleate
BNed	Binucleated
BHMT	Betaine-homocysteine-S-methyltranferase
BSA	Bovine Serum Albumin
Ca	Calcium
CBMN Cyt assay	Cytokinesis Block Micronucleus Cytome assay
cDNA	Complementary Deoxyribonucleic Acid
CRP	C-Reactive Protein
CSIRO	Commonwealth Scientific and Industrial Research Organisation
C_T	Cycle Threshold
Cu	Copper
$CuSO_4$	Copper Sulphate
Cu/ZnSOD	Copper Zinc Superoxide Dismutase
CV	Coefficient of Variation
Cyto-B	Cytochalasin B
DCF	2′7′-dichlorofluorescein
DCFH	2′7′-dichlorofluorescein hydrochloride
dH_2O	Distilled Water
DMSO	Dimethyl Sulfoxide
DNA	Deoxyribonucleic Acid
DNMT	Deoxyribonucleic Acid Methyltransferase
DTT	Dithiothreitol

EDTA	Ethylenediaminetetraacetic Acid
ELISA	Enzyme-linked Immunosorbent Assay
eSOD	Erythrocyte Superoxide Dismutase
FapyGua	2,6-diamino-4-hydroxy-5-formamidopyrimidine
FapyAde	4,6-diamino-5-formamidopyrimidine
FBS	Foetal Bovine Serum
Fe	Iron
$FeCl_3.6H_2O$	Iron Chloride
FFQ	Food Frequency Questionnaire
Fpg	Formanidopyrimidine-DNA Glycosylase
FRAP	Ferric reducing Ability of Plasma
GAPDH	Glyceraldehyde 3-Phosphate Dehydrogenase
gDNA	Genomic Deoxyribonucleic Acid
H_2O_2	Hydrogen Peroxide
HBSS	Hanks Balanced Salt Solution
HCy	Homocysteine
HCl	Hydrochloric Acid
HOK	Human Oral Keratinocyte
HUMN	HUman MicroNucleus/ The International Collaborative Project on Micronucleus Frequency in Human Populations
H_2O	Water
ICPOES	Inductively Coupled Plasma Optical Emission Spectrometry
IL-6	Interleukin-6
IMVS	Institute of Medical and Veterinary Science
IR	Irradiated
K	Potassium
Kb	Kilobases
MDA	Malondialdehyde
Mg	Magnesium
$MgCl_2$	Magnesium Chloride
MNi	Micronuclei
MNed	Micronucleated
MnSOD	Manganese Superoxide Dismutase
mRNA	Messenger Ribonucleic Acid
MT	Metallothionein
MT1A	Metallothionein-1A
MTR	Methionine Synthase
MTT	3-(4,5-Dimethylthiazol-2-yl)-2,5-diphenyltetrazolium Bromide
MZnD	Marginal Zinc Deficiency

Na	Sodium
NaCl	Sodium Chloride
NaF	Sodium Fluoride
NaOH	Sodium Hydroxide
NBud	Nuclear Bud
NDI	Nuclear Division Index
NFκB	Nuclear Factor kappa-light-chain-enhancer of activated B cells
NI	Non Irradiated
NK	Natural Killer
NPB	Nucleoplasmic Bridge
NO	Nitric Oxide
$Na_4P_2O_7.10H_2O$	Sodium Pyrophosphate
Na_3VO_4	Sodium Orthovanadate
8-OHdG	8-Hydroxy-2-deoxyguanosine
8-oxoG	8-Oxoguanine
8-oxodG	8-Oxo-2'-deoxyguanosine
OGG1	8-Oxoguanine DNA glycosylase
OKM	Oral Keratinocyte Medium
OKGS	Oral Keratinocyte Growth Supplement
P	Phosphorus
p53	p53 Tumor Suppressor genes
PARP	Poly (ADP-ribose) Polymerase
PBL	Peripheral Blood Lymphocyte
PBS	Phosphate Buffered Saline
PCR	Polymerase Chain Reaction
PHA	Phytohemagglutinin
PMSF	Phenylmethanesulfonylfluoride
Q-FISH	Quantitative Fluorescent In Situ Hybridization
RDA	Recommended Daily Allowance
RDI	Recommended Daily Intake
Ref1	Redox Factor-1
RPMI	Roswell Park Memorial Institute
ROS	Reactive Oxygen Species
RT	Real Time
RT	Room Temperature
RTPCR	Real Time Polymerase Chain Reaction
S	Sulphur
SAM	S-adenosyl Methionine
SE	Standard Error
SD	Standard Deviation
SDS	Sodium Dodecyl Sulfate

SDS-PAGE	Sodium Dodecyl Sulfate Polyacrylamide Gel Electrophoresis
SNP	Single Nucleotide Polymorphism
SOD	Superoxide Dismutase
TANK1	Human Tankyrase 1
TBAR	Thiobarbituric Acid Reaction
TBD	Telomere Base Damage
TI	Tail Intensity
TL	Telomere Length
TM	Tail Moment
TPEN	N,N,N'N'-tetrakis(-)[2-pyridylmethyl]-ethylenediamine
TPTZ	Tripyridyl Triazine
WAS	Waite Analytical Service
WHO	World Health Organization
WIL2-NS	WIL2-NS Lymphoblastoid Cell Line
WST-1	2-(4-Iodophenyl)-3-(4-nitrophenyl)-5-(2,4-disulfophenyl)-2H-tetrazolium monosodium salt
Zn	Zinc
ZnC	Zinc Carnosine
ZnD	Zinc Deficiency
ZnAD	Zinc Adequate
$ZnSO_4$	Zinc Sulphate
ZIP1	ZIP1 human Zinc transporter gene
γ-H2AX	genes coding for Histone 2A (phosphorylated)

Chapter 1

The Role of Zinc in Genomic Stability

Sharif, R.[1,2,3], Thomas, P.[1], Zalewski, P.[2] & Fenech, M.[1]

[1]CSIRO Food and Nutritional Sciences, Adelaide, Australia

[2]School of Medicine, Faculty of Health Sciences, University of Adelaide, Adelaide, Australia

[3]Nutrition Program, Faculty of Health Sciences, Universiti Kebangsaan Malaysia, Malaysia

Mutation Research. 2011.

Statement of Authorship

The Role of Zinc in Genomic Stability

Razinah Sharif

Wrote manuscript and contributed to planning of article

Signed ……. Date ……

Philip Thomas

Contributed to planning of article and provided critical evaluation of the manuscript

Signed ……. Date ……

Peter Zalewski

Contributed to planning of article and provided critical evaluation of the manuscript

Signed ……. Date ……

Michael Fenech

Contributed to planning of article and provided critical evaluation of the manuscript and acted as corresponding author

Signed ……. Date ……

Chapter 1

The Role of Zinc in Genomic Stability

1.1 Abstract

Zinc (Zn) is an essential trace element required for maintaining both optimal human health and genomic stability. Zn plays a critical role in the regulation of DNA repair mechanisms, cell proliferation, differentiation and apoptosis involving the action of various transcriptional factors and/or DNA or RNA polymerases. Zn is an essential cofactor or structural component for important antioxidant defence proteins and DNA repair enzymes such as Cu/Zn SOD, OGG1, APE and PARP and may also affect activities of enzymes such as BHMT and MTR involved in methylation reactions in the folate-methionine cycle. This review focuses on the role of Zn in the maintenance of genome integrity and the effects of deficiency or excess on genomic stability events and cell death.

1.2 Introduction

In 2004, cancer caused 7.4 million deaths worldwide (accounting for 13% of all deaths) and in 2030, it is estimated that the mortality rate of cancer will continue to rise to at least 12 million cases per annum [1] . The links between diet and cancer have been under investigation for several decades and the evidence suggests a significant causal or preventative role for various dietary factors [2]. Although unravelling the links between diet and cancer is complex, the need for research in this area is important as individual dietary components may significantly modify a multitude of cellular processes affecting the initiation and progression of cancer pathways [3, 4]. In order to unravel the association between diet and cancer

development, the biological processes underlying cancer etiology and the modulating role of micronutrients need to be more clearly understood [2].

The involvement of genomic stability in the development of cancer has been well established [2]. Cancer is now recognised as a disease of altered gene expression caused by genome and epigenome alterations. Apart from the effect of environmental genotoxins, one of the key components in cancer initiation is loss of genome stability due to nutritional imbalances and their interaction with genotype [2-5]. Recent research has focussed on the involvement of micronutrients and their role in fundamental processes such as DNA synthesis, DNA methylation, DNA repair and apoptosis [5, 6]. Figure 1 illustrates the potential of gene-diet and gene-toxin interactions to affect genome integrity and health outcomes. It has been shown that micronutrient deficiency can produce DNA damage resulting in increased cancer risk, higher incidence of infertility and accelerated ageing [6-8].

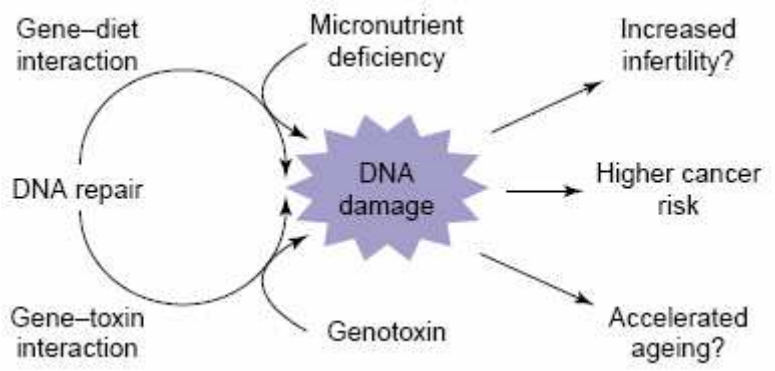

Figure 1.1: The concept of gene-diet and gene-toxin interaction and their effects on DNA damage and possible health consequences (adapted from Fenech 2002 [8])

Dietary deficiency in key micronutrients required for DNA maintenance may lead to DNA damage [5]. A number of laboratory and epidemiological studies suggest that low intake of vitamins and minerals could also be a major risk factor for several types of cancers and other degenerative diseases [9, 10]. It has been shown that dietary deficiencies in certain micronutrients such as folate or antioxidant vitamins, such as

vitamin C or E can result in DNA-strand breaks and DNA base lesions to a similar extent to that induced by carcinogenic doses of ionising radiation [11, 12].

The need to understand the role of micronutrients and the relevant effects on genomic stability is important in order to provide a better strategy for cancer prevention by exploiting potential nutrient-nutrient and nutrient-gene interactions. One of the aims of this review is to provide a better understanding for the role of one of the more important micronutrients, namely Zinc (Zn), and to investigate its role in maintaining genomic stability.

Zn is an essential component for more than 1000 proteins including Copper/Zn super oxide dismutase (SOD) as well as a number of other Zn finger proteins [13, 14]. Table 1.1 lists several important Zn requiring proteins that are crucial for maintenance of genome integrity.

The function of Zn involves a wide range of biological processes including cell proliferation, immune function and defence against free radicals [13-18]. In addition, Zn appears to regulate key physiological processes such as cellular response is to oxidative stress, DNA repair, cell cycle regulation and apoptosis [14]. Several studies have shown a correlation between increased apoptosis and Zn deficiency in various cells types such as human Chang liver cells, vascular endothelial cells as well as in rat testes [19-26]. The fact that Zn plays an important role in the determination and regulation of apoptosis in mammalian cells is well established [27-31]. The mechanisms and capabilities of cellular uptake and accumulation of Zn may vary in different cell types which depend on various factors such as Zn transporters (see Table 1.2).

Zn deficiency has been shown to affect the DNA repair response via regulation of one of the most important tumor suppressor proteins, p53. p53 is a zinc-binding protein containing several reactive cysteines, and its key biochemical property, sequence-specific DNA binding, is dependent upon metal and redox regulation *in vitro [32]*. p53 protein functions as a coordinator for events leading to

DNA repair and also for modulating cell cycle progression, cell proliferation, differentiation and apoptosis [33]. p53 is well known for its ability to induce G_1 arrest in the cell cycle, allowing the cells to induce adequate repair of DNA before DNA replication and nuclear division [34]. In low Zn medium, p53 expression is up-regulated indicating that it may be one of the cellular responses to DNA damage induced by Zn deficiency [10, 35]. Studies showed that p53 expression is notably higher in low Zn culture medium (<4μM) compared to replete medium (>4 μM) with a marked decrease in the ability of p53 to bind to DNA [36].

Under conditions of low zinc status, p53 becomes oxidized and dysregulated but is still capable of repressing and inducing genes including p53-mediated apoptosis [37,38], but the set of genes affected is different from the wild type p53. This is an apparent paradox as Zn is needed for the normal function of p53 to bind to DNA and induce pro-apoptotic genes while low Zn can lead to increased expression and activation of p53. p53 can promote apoptosis by two mechanisms a) transcriptionally, via the up and down regulation of pro and anti-apoptotic genes, respectively and b) by direct interaction with Bcl-2/Bax and induction of mitochondrial membrane permeabilization leading to caspase activation [37]. Therefore, low Zn may be differentially affecting two p53-dependent pathways, one dependent on gene expression and the other only indirectly affected by gene expression. These two pathways may be functionally dissimilar in different cellular types.

Another possible mechanism by which Zn may affect a response to DNA damage is its involvement in Poly (ADP-ribose) polymerase (PARP) which is a DNA binding protein catalysing the poly (ADP-ribosyl)ation of protein. PARP has two Zn fingers called F1 and F2 which play a role in the recognition of DNA breaks. PARP binds to DNA single-strand breaks created during base excision repair (BER), via its Zn-finger motifs and recruits other DNA repair factors (e.g., XRCC and DNA ligase) to the damaged site allowing the completion of BER [38]. A recent study using peripheral blood mononuclear cells (PBMC) from Zn supplemented elderly people has revealed a positive correlation between cellular poly (ADP-ribosyl)ation capacity and Zn

status. This suggests that Zn supplementation in elderly individuals can increase cellular PARP capacity resulting in the maintenance of efficient genome stability and integrity [39]. PARP is also activated by the accumulation of DNA strand breaks and by 8-hydroxydeoxyguanosine (8-OHdG), an oxidatively damaged form of guanine in nuclear DNA. PARP also plays pivotal roles in DNA-repair and cell check-point pathways [40]. The involvement of Zn in p53 and PARP regulation emphasizes the essential role played by Zn in crucial cellular processes. Besides PARP and p53, Zn is also involved in DNA repair via 8-oxoguanine glycosylase (OGG1), apyrimidinic endonuclease (APE) and activator protein 1 (AP1), as reviewed in [14].

OGG1 functions in the first step of the BER pathway to recognize and remove 8-hydroxy-2'-deoxyguanosine [41]. A previous study showed that marginal and severe Zn depletion caused an increase in OGG1 expression indicating increased oxidative DNA damage [42]. Interestingly, although both OGG1 and PARP are involved in DNA repair, PARP capacity and expression is decreased or only slightly altered with Zn deficiency [39]. This lack of response or negative response of PARP to Zn depletion could markedly interrupt the overall BER pathway and contribute to the accumulation of DNA damage. Marginal and severe Zn deficiency was found to disable the cells' capacity to repair oxidative DNA damage [42, 43].

Zn status is also important in affecting APE because Zn deficiency increases APE expression in cultured cells [36]. APE acts as an important endonuclease in BER [44]. Human APE/Ref-1 acts both as a DNA repair protein (exhibiting 3′-phosphodiesterase and 5′AP-endonuclease activity) and as a positive or negative regulator of transcription (via redox-based activation of transcription factors such as AP1, p53, and NFκB) [44]. It is plausible that Zn-regulated APE expression is attributed to cellular redox status, as there are data indicating that APE expression is increased under conditions of oxidative stress [45]. Consistent with the view that Zn deficiency is associated with cancer predisposition, APE expression has been found to be elevated in lung carcinoma [46]. Increases in APE expression may be expected to be associated with increases in the binding activity of several redox-sensitive

transcription factors such as NFκB (nuclear factor kappa-light chain-enhancer of activated B cells) and AP1 that regulate gene expression [14].

However, Ho *et al* reported a marked reduction in both NFκB and AP1 binding with Zn deficiency [36]. NFκB is a transcription factor involved in determining the balance between proliferation and apoptotic stress response [47]. AP1 is another transcriptional factor produced by a variety of dimeric combinations of proteins from the Jun and Fos families [48]. AP1 is regulated via phosphorylation by mitogen-activated protein kinases (MAPKs) and interacts with other factors such as NFκB, CBP/p300 and Rb, thus regulating target genes common to NFκB. Like NFκB, AP1 is also considered to be a proliferation and tumor growth promoter [48]. These transcription factors play important roles in controlling response to oxidative stress and cell proliferation [49], and their inactivation of binding impairs the ability of the cell to respond to oxidative stress and damage [50]. Mackenzie *et al.* (2002) reported that low Zn medium leads to an impairment of NFκB nuclear translocation and thus inhibits the transactivation of NFκB driven genes that can potentially affect cell survival [51].

Various *in vitro* and *in vivo* approaches have also shown that Zn deficiency leads to oxidative stress [19-22, 35, 52]. These findings suggest that Zn depletion may increase DNA damage which leads to genomic instability. The role of Zn in protecting biological structures from damage by free radicals includes (i) maintaining an adequate level of metallothionein (which is a free radical scavenger), (ii) as an essential component of Cu/ZnSOD and (iii) as a protective agent for thiols, as reviewed in [13, 14]. Previous studies have shown that Zn and metallothionein are genome-protective against oxidative stress insults [30, 53, 54].

Metallothionein (MT) is a small sized protein which serves as a Zn specific chaperone and functions by a similar redox mechanism distributing Zn to enzymes in the metabolic network [55, 56]. There are several forms of metallothionein which are isoforms of MT. These isoforms include MT-1, MT-2, MT-3 and MT-4 [57]. MT-1 and MT-2 are found in all organs, whereas MT-3 is expressed mainly in the central

nervous system, and MT-4 is most abundant in stratified tissues [56]. Table 1B summarizes several important Zn proteins involved in Zn transport and storage. MT has been found to affect release of Zn for the activity of PARP-1 which is involved in base excision DNA-repair [58]. A previous study showed that the abnormal sequester of Zn by MT in ageing is deleterious because it leads to low Zn bioavailability with impairment of PARP-1 and NK cell activity [58].

Table 1.1: Zn associated proteins involved in antioxidant response, DNA damage response and folate/methionine metabolism

Functions	Protein	Role	References
Antioxidant	1) Cu/Zn SOD	- remove superoxide anion	Dreosti 2001 [13]
	2) Metallothionein	- potent scavenger of hydroxyl radical	Bell 2009 [56]
DNA Repair/DNA damage response	1)PARP	- binds to DNA single strand breaks created during base excision repair	Petrucco & Percudani 2008 [38]
	2)OGG1	- base excision repair; recognize and remove 8-hydroxy-2'-deoxyguanosine	Boiteux & Radicella 2000 [41]
	3)APE	- important endonuclease in base excision repair, cleavage of damaged sites in DNA	Fritz 2000 [44]
	4)AP1	- control oxidative stress responses and help control cell proliferation and apoptosis	Karin & Shaulian 2001 [49]
	5)NFκB	- control oxidative stress responses and help control cell proliferation and apoptosis	Karin & Shaulian 2001 [49]
Apoptosis/DNA Repair	1) p53	- coordinating events leading to appropriate DNA repair. Induce G_1 arrest in the cell cycle, allowing the cell to induce adequate repair of DNA before cellular division	Lane 1992 [34]
Methionine Synthesis	1)BHMT	- catalyses the transfer of methyl groups from betaine to homocysteine to produce dimethylglycine (DMG) and methionine	Breksa & Garrow 1999 [112]
	2) MTR	- catalyses the transfer of methyl groups from 5-methyl tetrahydrofolate to homocysteine to produce methionine	Mathew and Goulding 1997 [116] Koutmos *et al* [115]

Table 1.2: Important Zn associated proteins involved in Zn transport and storage

Functions	Protein	Zn proteins	Cellular distributions	Role	References
Zn transport	1) ZnT (ZnT1 – ZnT8)	ZnT1	Plasma membrane	- Zn efflux from the cytoplasm towards either intracellular vesicles and/or the extracellular space	Liuzzi & Cousins 2004 [130], Sekler *et al* 2007 [131]
		ZnT2	Vesicles, lysosomes; small intestine, kidney, placenta, pancreas, seminal testis and mammary gland		
		ZnT3	Synaptic vesicles (Glutamatergic and GABAergic); brain		
		ZnT4	Intracellular compartments; (mammary gland, brain, small intestine and mast cells)		
		ZnT5	Insulin secretory vesicles, Golgi; pancreatic β-cells, intestine, heart, brain, liver, kidney		
		ZnT6	Complexed with ZnT5; liver, brain and small intestine		
		ZnT7	Golgi body; small intestine, liver, retina, spleen, kidney and lung		
		ZnT8	Insulin secretory vesicles; pancreatic β-cells		
	2) ZIP (ZIP1-ZIP4)	ZIP1	Organs and glands	- controls Zn uptake from the extracellular matrix and/or intracellular organelle into the cytoplasm	Lichten & Cousins 2009 [132], Liuzzi and Cousins 2004 [130]
		ZIP2	Liver, spleen, small intestine and bone marrow		
		ZIP3	Bone marrow, spleen, small intestine and liver		

		ZIP4	Small intestine		
Zn transport and storage	1)MT (MT1 – MT4)	MT1	All organs	- distribution of intracellular zinc as zinc undergoes rapid inter- and intracluster exchange	Krezel & Maret 2007 [55]
		MT2	All organs		
		MT3	Central nervous systems		
		MT4	Stratified tissues		

1.3 Zinc deficiency, DNA damage and chromosomal instability

Various lines of evidence have shown that genomic instability events are one of the main indicators for increased cancer risk [8, 9, 13, 59-62]. As Zn is required as a cofactor in DNA metabolism, this suggests that deficiency in this micronutrient may induce important chromosomal mutations that increase individual cancer risk. The link between Zn deficiency and cancer has been established in both *in vivo* and *in vitro* studies. Zn status is compromised in cancer patients compared with healthy controls [63-66]. In rats, dietary Zn deficiency causes an increased susceptibility to tumor incidence when exposed to carcinogenic compounds (N-nitrosomethylbenziamine) [67]. Insufficient intake of Zn may also increase the risk of oesophageal cancer in both humans [68, 69] and rats [70]. Zn deficiency has also been shown to lead to testicular cell DNA damage [19-22] via an increase in reactive oxygen species secondary to tissue iron accumulation and/or reductions in Zn dependent antioxidant processes.

It has been shown that an increase in cytosolic Zn in both breast and pancreatic cancers was associated with increased expression of the Zn transporters Zip7 and Zip4 and also leads to enhanced tyrosine phosphorylation and downstream cell growth signals [71, 72]. However in prostate cancer, a decrease in cellular Zn and Zip1 expression was found to be associated with enhanced tumour growth [73]. Why Zn depletion or repletion influences certain cancer types and not others has not been thoroughly investigated and needs to be the subject of future studies. It may be that the net effect of Zn depletion on cancer initiating events and cancer growth differs between tissues depending on their dependency for this element for normal function.

8-OHdG was also found to be significantly higher in Zn deficient rats ($p<0.05$) [19]. In the same study, they also found disruptions in NFκB binding activity in the Zn deficient group which resembles an early response to Zn deficiency induced oxidative stress; levels of Cu/Zn SOD and MnSOD were also significantly higher in the Zn deficient group indicative of high oxidative stress in rats fed on a low Zn diet. In

addition, Zn deficiency may impair cognitive function in both experimental animals and humans, especially in children [74-79]. In the following section, the effect of Zn deficiency and DNA damage response in both *in vitro* and *in vivo* models will be examined in more detail.

i) In vitro studies

Previous studies have shown that Zn depleted cells have impaired DNA repair mechanisms and an elevated rate of DNA damage [13, 36, 80]. Ho *et al* has previously shown that low intracellular Zn induces oxidative DNA damage, disrupts p53, NFκB, and AP1 DNA binding and affects DNA repair in a rat glioma cell line [36]. Significant increased single strand breaks ($p<0.05$) were observed in Zn depleted cells together with an increase in oxidant production measured via nitrite formation which is an indirect measure of nitric oxide (NO) production. It was also observed that there was a significant increase ($p<0.05$) in 2′7′-dichlorofluorescein hydrochloride (DCFH) fluorescence in these Zn depleted cells. DCFH becomes oxidized to 2′7′-dichlorofluorescein (DCF), a fluorescent product, and indicates increased oxidant production and oxidative stress. An increase in p53 and APE expression indicating elevated DNA damage rates was also observed [36].

In 2003, another study showed that Zn deficiency can induce oxidative DNA damage and increased p53 expression in human lung fibroblasts [35]. This confirmed the hypothesis that Zn deficiency caused an increase in DNA damage and alteration in DNA repair mechanisms. In this study, differential gene expression in cells was observed with chemically-induced Zn deficiency using the intracellular Zn chelator, N,N,N',N'-tetrakis-(2-pyridylmethyl)ethylenediamine (TPEN, a membrane permeable metal chelator with a high specificity for Zn) and medium chelated with chelex-100 (to produce Zn-deficient medium). In the same study, several genes involved in DNA damage/repair and oxidative stress were affected by both Zn deficiency induction methods. Glutathione peroxidase expression was induced in both TPEN treatment and Zn deficiency but proteasome 26S and chromosomal segregation 1 genes were down regulated. An induction of superoxide dismutase 1 (also known as CuZnSOD)

was also seen in TPEN treatment. A reduction in metallothionein-1 mRNA expression and an increase in ferritin (light chain) expression were observed in cells grown in Zn deficient medium. Several DNA damage response factors (eg. GADD-inducible, ADP-ribosyltransferase, chromosome segregation 1, kinesin-like 5) were also down regulated, indicating that certain DNA repair mechanisms may be impaired under conditions of Zn deficiency. Although similar classes of genes were affected, few were common to both treatments. This suggests that the cellular effects and responses to these different intracellular Zn depletion methods are different. Some decrease in several proteins involved in both stress response (Chaperonin, Hsp70, Hsp105, MAPKK 5, heme Oxygenase 2 – TPEN; Hsp90, Hsp60, stress induced phosphoprotein – Zn deficient medium) and protein degradation (proteasome 26S, casein kinase 2, cathepsin L- TPEN; proteasome 26S, proteasome subunit beta – Zn deficient medium) were also observed. The down regulation of these factors could alter cellular stress response and indirectly affect transcription of DNA damage/repair genes [35]. In addition, an increase in DNA strand breaks and p53 expression in Zn depleted cells with both treatments was also observed. Although there is an upregulation of p53 expression, the depletion of Zn to 50% of normal levels (4 µM) rendered this protein nonfunctional [36] leading to the possibility that Zn deficiency provides an environment that results in both increased DNA damage together with a decreased DNA damage response capacity.

Recently, Zn deficiency was found to alter DNA damage response genes in normal human prostate epithelial cells [80]. In this study, low cellular Zn levels caused DNA damage and altered expression of cell cycle genes, apoptosis, DNA damage, repair and transcription. A significant increase in single strand DNA breaks ($p<0.05$) was observed in cells grown in Zn deficient (ZnD) media compared with cells grown in Zn adequate (ZnAD) media for 7 days. Zn status in ZnAD cells was 0.1969 ± 0.0211 and in ZnD cells, 0.0479 ± 0.0083 nmol/million cells which indicated a 75% reduction compared to ZnAD cells ($p<0.001$). Differential expression of genes involved in DNA damage response and repair (TP73, MRE11A, XRCC4, and BRCA2) early onset genes were down-regulated, and TP53 was up-regulated and it was shown by western blot that increased p53 expression was evident in ZnD cells. This

study confirms an important role for Zn in maintaining DNA integrity and that Zn depletion may impair cellular mechanisms that could result in accumulation of DNA mutations leading to increased cancer risk.

In our recently published study, it was found that both lower and excess Zn concentrations caused an increase in DNA damage as measured via the alkaline comet assay in a WIL2-NS lymphoblastoid cell line and HOK cells [81, 82]. Zn depleted cells showed an increase in both tail moment and tail intensity ($p<0.05$) and a similar trend was observed in Zn supplemented cells at 32 µM ($p<0.05$) suggesting that a U-shaped dose response is involved. The mechanism of how Zn can exert the cytotoxicity and genotoxicity effects are still unclear. Based on cytotoxicity and necrosis data, it is probable that the increased DNA damage measured by comet assay at 32 µM Zn concentration was partly due to necrosis [81].

There are various methods to measure genome stability but to date the cytokinesis blocked micronucleus cytome (CBMN-Cyt) assay appears to be the best validated tool for measuring DNA damage as a result of micronutrient deficiency (as reviewed in [83]). This comprehensive method can provide data on cytostatic and cytotoxic effects as well as chromosomal damage and instability events. In the CBMN-Cyt assay, a cytokinesis blocking agent (cytochalasin B) is used to produce once-divided binucleated cells that can express micronuclei (MNi) which are biomarkers of whole chromosome loss and/or breakage. MNi originate from acentric chromosomal fragments or whole chromosomes that lag behind at anaphase during nuclear division. In addition, it is also possible to measure nucleoplasmic bridges (NPBs), which arise from dicentric chromosomes (caused by DNA misrepair or telomere end fusions) and nuclear buds (NBuds), a biomarker of gene amplification, replication stress or unresolved DNA repair-DNA protein complexes [84-86]. The presence of these DNA damage endpoints are a strong indicator of chromosomal damage and instability within a cell [84]. These DNA damage events have been shown to be sensitive to small changes in micronutrient concentration (eg. folic acid, riboflavin, selenomethionine) within the physiological range [87-89].

To date, there are only 7 studies that have used the CBMN assay to observe the genomic stability effect of Zn. The first study in 2001, showed that Zn dimethyldithiocarbamate and Zn diisonyldithiocarbamate at 0.1, 1.0, 10.0 μg/ml did not induce any MNi in human peripheral blood lymphocyte cultures [90]. In contrast, Santra *et al* (2002) showed that induction of MNi in Zn chloride treated human leukocytes at 15 mM and 30 mM was significant when compared to negative controls, but that this was not in a linear dose-dependent manner [91].

Recently, we have published data on how Zn can affect genomic stability events *in vitro* [81]. In this study, the effects of Zn sulphate ($ZnSO_4$) and Zn carnosine (ZnC) were investigated in the WIL2-NS human lymphoblastoid cell line and measured chromosomal damage and instability as well as cytoxicity using the CBMN-Cyt assay. Zn deficient medium (0 μM) was produced using Chelex treatment, and the two Zn compounds (i.e. ZnSO4 and ZnC) were tested at concentrations of 0.0, 0.4, 4.0, 16.0, 32.0 and 100.0 μM. Results from an MTT assay showed that cell growth and viability were decreased in Zn depleted cells (0 μM) as well as at 32 μM and 100 μM for both Zn compounds (p<0.0001). The CBMN-Cyt assay showed a significant increase in the frequency of both apoptotic and necrotic cells under Zn deficient conditions (p<0.0001). Elevated frequencies of MNi, NPBs and NBuds were induced in Zn depleted cells (p<0.0001), whereas genome damage was reduced in supplemented cultures for both Zn compounds at 4 μM and 16 μM, indicating that these concentrations are optimal for genome stability. The potential protective effect of $ZnSO_4$ and ZnC were also investigated following exposure to 1.0 Gy γ-radiation. Cultures in medium containing these compounds at 4-32 μM prior to irradiation displayed significantly reduced frequencies of MNi, NPBs and NBuds compared with cells maintained in 0 μM medium (p<0.0001). Expression of γ-H2AX and 8-oxoguanine glycosylase (OGG1) measured by western blotting was increased in Zn-depleted cells. These results suggest that Zn plays an important role in genomic stability and that the optimal Zn concentration range for prevention of DNA damage and cytotoxicity *in vitro* lies between 4 and 16 μM.

The same experimental design was applied to an epithelial tissue type known as the Human Oral Keratinocyte cell line [82]. A significant increase in the frequency of both apoptotic and necrotic cells measured via CBMN Cyt assay under Zn deficient conditions ($p<0.05$) was observed. Furthermore, elevated frequencies of MNi, NPBs and NBuds were observed at 0 and 0.4 μM Zn whereas these biomarkers were minimised for both Zn compounds at 4 μM and 16 μM Zn ($p<0.05$), suggesting these concentrations are optimal to maintain genome stability. Expression of PARP, p53 and OGG1 measured by western blotting was increased in Zn depleted cells indicating that DNA repair mechanisms are activated. To conclude, maintaining Zn concentrations within the range of 4-16 μM is essential for DNA damage prevention in cultured human oral keratinocytes.

ii) In vivo studies

Dietary Zn restriction in rats (< 1 ppm of Zn in diet) for 3 weeks showed an alteration in antioxidant status measured via ferritin-reducing ability of plasma assay (20% decrease - $p<0.05$) and a 50% reduction in plasma uric acid ($p<0.05$). An increase in plasma F2-isoprostanes resulting in increased oxidative stress was also observed indicating increased lipid peroxidation which has been shown to lead to an increase in DNA damage [92].

A further study in 2009 [43] revealed that severe Zn depletion in rats caused an increase in DNA damage in peripheral blood cells compared to Zn replete controls and this was associated with impairment in DNA repair, compromised p53 DNA binding, and upregulation of the BER proteins, OGG1 and PARP [43]. Song *et al* [42] showed that marginal Zn deficiency (MZnD) in rats caused an increase in oxidative DNA damage in the prostate after chronic exercise. MZnD treated groups also showed increased p53 and PARP expression but no change in plasma 8-OHdG levels compared to Zn Adequate (ZnAD) group. Results utilizing the comet assay showed that the tail moment of peripheral blood cells in MZnD group was 20% higher than in the ZnAD group and prostate 8-OHdG in MZnD group was 32% higher than ZnAD

group. 8-OHdG concentration in the prostate was significantly correlated with the tail moments of peripheral blood cells (*r=0.66, p=0.03*) [42].

In relation to *in vivo* studies, pretreatment with $ZnSO_4$ at 100 µmol/kg suppressed bone marrow injury caused by low doses of X-irradiation in wild type mice but not in metallothionein (MTI/MTII) null mice. A significant increase in the MNi frequency in both reticulocytes and polychromatic erthrocytes in MTI/MTII null mice was evident [93]. This study suggests that metallothionein which is normally induced in the presence of Zn plays a protective role against low dose X-ray insults. Metallothionein may exert its radioprotective effects via its capacity to neutralise hydroxyl radicals which is greater than that of glutathione, the most abundant antioxidant in the cytosol [56].

In particular, dietary Zn restriction and repletion of Zn to its normal status was found to affect DNA integrity in healthy men aged 19-50 years old [94]. In this study, the number of DNA strand breaks increased significantly during the Zn depletion period (6 weeks). The increases were shown to be reversible following Zn repletion suggesting that the extent of DNA damage is related to dietary Zn status. In this study, plasma Zn levels measured at the beginning (day 13) and at the end of the Zn depletion period (day 55) did not differ significantly. Mean plasma Zn concentrations were 0.79 ± 0.9 and 0.79 ± 1.0 μg/mL on days 13 and 55, respectively. However, plasma Zn concentrations were found to be 13% higher at the end of the Zn repletion period (0.86 ± 1.0 μg/mL on day 83) than at the end of the Zn depletion period. Plasma Zn concentrations showed a negative correlation with DNA damage measures (*r=-0.47, p=0.014*) [94]. This study illustrates the importance of Zn in maintaining DNA integrity *in vivo* in humans.

The outcomes of these studies suggest that Zn deficiency may influence DNA damage via 2 different mechanisms: 1) Zn deficiency may increase oxidative stress resulting in increased DNA damage; 2) Zn deficiency may impair DNA damage responses. Table 2 summarizes current knowledge on Zn and DNA damage in both *in vitro* (Table 1.3) and *in vivo* studies (Table 1.4).

1.4 Zinc excess, DNA damage and toxicity

Although it is well proven that Zn deficiency may lead to increased DNA damage, limited studies have been undertaken in order to understand the effect of Zn supplementation or excess in relation to cellular functions. What is the Zn concentration range or intake level that does not harm the genome? Is there any toxicity caused by Zn concentration in excess of the normal upper limits of the physiological range? Does the toxicity of Zn supplement depend on the composition of the non-Zn fraction of the molecule? An *in vitro* study showed that excess Zn chromate can induce chromosomal instability and DNA double strand breaks in human lung cells [95]. MRE11 expression was increased, ATM and ATR were phosphorylated indicating that the DNA double strand break repair system was initiated. ATR is an upstream initiator of the checkpoint response from various types of DNA lesions and is recruited by ATR-interacting protein (ATRIP) to stalled DNA replication forks [96, 97]. ATR phosphorylates a number of substrates which in turn target other proteins to induce cell-cycle arrest and facilitate DNA repair. ATM kinase signals the presence of DNA double strand breaks by phosphorylating downstream proteins that initiate cell-cycle arrest, apoptosis, and DNA repair [97].

In another study, Zn chromate was found to be clastogenic as measured via chromosome aberrations in WTHBF-6 cells, a clonal cell line derived from primary human bronchial fibroblasts [98]. On the other hand, Zn citrate (CIZAR) at 1 mM was shown to be cytotoxic as measured via Cell Counting Kit (CCK)-8 assay and induced apoptotic response within choriocarcinoma cell lines [99]. A recent study published by our group showed that Zn at 32 µM (present as either $ZnSO_4$ or ZnC) started to show an increase in DNA damage events in WIL2-NS lymphoblastoid cell line, and at 100 µM, severe cytotoxicity was observed [81]. Studies with other cell types report different cytotoxicity concentrations [100] suggesting that the effect of Zn may differ according to different cell type [27]. However, the mechanism of why and how Zn can cause such cytotoxic effects is still unknown.

A previous study in Algerian mice treated with Zn acetate showed that micronuclei in bone marrow polychromatic erythrocytes (a biomarker of chromosome damage) were significantly elevated compared to the control group (rats fed with distilled water) suggesting potential dose related Zn genotoxicity [101]. High concentrations of Zn in drinks, up to 2500 mg/L have been associated with individual poisoning, causing nausea, abdominal cramping, vomiting, tenesmus and diarrhoea with or without bleeding [102]. Data by WHO (2001) suggested Zn excess during embryogenesis can be teratogenic or lethal. However, Zn appears not to be classified as either a mutagen or carcinogen when excess levels are reached [102, 103]. Biochemical analysis has shown that Zn excess can inhibit the activity of some DNA repair proteins, including N-methylpurine-DNA glycosylase and DNA ligase 1 [104].

Table 1.3: Current literature on the effect of Zn on DNA damage *in vitro*

In vitro Study	Target cells	Zn Concentration	Assay	Comments	Author
Zn deficiency alters DNA damage response genes in normal human prostate epithelial cells	PrEC (normal prostate epithelial cells)	ZnAD - 3 µM ZnD – Zn deficient media (Intracellular Zn concentration – ZnD : 0.0479 ± 0.0083 nmol/million cells; ZnAD : 0.1969 ± 0.0211 nmol/million cells)	Alkaline comet assay	Increased single strand breaks were observed in Zn depleted cells ($p<0.05$)	Yan *et al* 2008 [80]
			Gene expression	Differential expression of genes involved in DNA damage response were identified with low cellular Zn – (downregulated) p73; MRE11A; XRCC4; BRCA2, (upregulated) p53; ATP-binding cassette, sub Family F (GCN20) member 2	
	- Zn deficiency may compromise DNA integrity in the prostate				
Zn deficiency induces oxidative DNA damage and increases p53 expression in human lung fibroblast	IMR90 (Human lung fibroblast)	ZnAD- 4 µM ZnD	Alkaline comet assay	Increased single strand breaks were observed in Zn depleted cells (*$p<0.05$*)	Ho *et al* 2003 [35]
			Western blot	Increase in p53 expression in Zn depleted cells (*$p<0.05$*)	
	-Zn deficiency induces oxidative DNA damage and increases p53 expression				

Low intracellular Zn induces oxidative DNA damage, disrupts p53, NFκB, and AP1 DNA binding and affects DNA repair in a rat glioma cell line	C6 (rat glioma cell line)	ZnAD – 4 μM ZnD	Alkaline Comet assay	Increased single strand breaks were observed in Zn depleted cells (*p<0.05*)	Ho *et al* 2002 [36]
			Oxidant Production	Increase in oxidant production measured via nitrite formation which is an indirect measure of nitric oxide (NO) production and 2′7′-dichlorofluorescein (DCF) production in Zn depleted cells (*p<0.05*)	
			Western blot	Increase in p53 and APE production indicating an increase in DNA damage in Zn depleted cells	
	- Zn deficiency induces oxidative DNA damage in rat glioma cell line				
The effect of Zn sulphate and Zn carnosine on genome stability and cytotoxicity in WIL2-NS human lymphoblastoid cell line	WIL2-NS (human lymphoblastoid cell line)	$ZnSO_4$/ZnC – 0.4, 4, 16, 32, 100 μM ZnD	Alkaline Comet assay	Increased single strand breaks were observed in both Zn depleted cells and higher concentration of Zn (32 μM) (*p<0.05*)	Sharif *et al* 2011 [81]
			CBMN-Cyt assay	Increased micronuclei, nucleoplasmic bridges, nuclear buds in both Zn depleted cells and higher concentration of Zn (32 μM) (*p<0.05*)	
			Western Blot	Increased in OGG1, PARP and γ-H2AX in Zn depleted cells (*p<0.05*)	
	Zn deficiency induced DNA damage and chromosomal instability and Zn excess > 32 μM induces cytotoxicity				
Zn deficiency or excess increases genome instability	HOK (Human Oral Keratinocytes)	$ZnSO_4$/ZnC – 0.4, 4, 16, 32, 100 μM ZnD	Alkaline Comet assay	Increased single strand breaks were observed in both Zn depleted cells and higher concentration of Zn (32 μM)	Sharif *et al* 2011 [82]

and cytotoxicity, respectively in Human Oral Keratinocytes cell				(*p<0.05*)	
			CBMN-Cyt assay	Increased micronuclei, nucleoplasmic bridges, nuclear buds in both Zn depleted cells and higher concentration of Zn (32 µM) (*p<0.05*)	
			Western blot	Increased in OGG1, PARP and γ-H2AX in Zn depleted cells (*p<0.05*)	

Abbreviations: 8-OHdG (8-hydroxydeoxyguanosine), ZnD (Zn Deficient), ZnAD (Zn Adequate), APE (Apurinic Endonuclease), OGG1 (8-oxoguanine glycosylase), PARP (poly (ADP-ribose) polymerase), γ-H2AX (genes coding for Histone 2A).

Table 1.4: Current literature on the effect of Zn on DNA damage *in vivo*

In vivo Study (Human)	Target cells	Zn Concentration	Assay	Comments	Author
Dietary Zn restriction and repletion affects DNA integrity in healthy men	Peripheral blood cells	Zn depletion period : 12.08 ± 15.29 µM Zn repletion period : 13.15 ± 15.29 µM	Alkaline Comet assay	The number of DNA strand breaks increased during the Zn depletion period (*p<0.05*)	Song *et al* 2009 [94]
	- increase in DNA damage was reversible after Zn repletion - Consuming a Zn-adequate diet (11 mg Zn/d) for 13 d may have helped to reduce DNA damage; adequate Zn is important in maintaining DNA integrity				

Abbreviations: 8-OHdG (8-hydroxydeoxyguanosine), ZnD (Zn Deficient), ZnAD (Zn Adequate), MZnD (Marginal Zn Deficient). MZnAD (Marginal Zn Adequate), APE (Apurinic Endonuclease), OGG1 (8-oxoguanine glycosylase), PARP (poly (ADP-ribose) polymerase), γ-H2AX (genes coding for Histone 2A).

1.5 Zinc and telomeres

Telomeres consist of a universally conserved hexanucleotide repeat sequence (TTAGGG) that caps the ends of chromosomes. They have an important role in protecting the chromosome ends from recombining with each other and thus preventing chromosomal end-to-end fusions [105]. Degradation of telomeres has been shown to lead to chromosomal instability, via telomere end fusions. This results in generation of breakage-fusion-bridge cycles within chromosomes, which lead to gene amplification and gene dosage imbalance which is an important risk factor for cancer [106]. Accelerated telomere length shortening can result in a DNA damage response leading to chromosomal end-to-end fusions, cell arrest and apoptosis [107]. Although telomere shortening has been proposed as one of the fundamental mechanisms that determine chromosomal instability, the rate of cellular ageing [107] and increased cancer risk [106], the relationship between dietary factors and telomere biology remains unclear [108].

There are very few studies that have investigated the impact of Zn on maintaining telomere integrity. Liu and colleagues (2004) found that Zn sulphate at 80 μM accelerated telomere loss in hepatoma cells (SMMC-7721) after 4 weeks of treatment [109]. A further study revealed that cells with short telomeres are associated with impaired Zn homeostasis in hypertensive patients [110]. However, it is known that Zn is part of Human Tankyrase 1 (TANK1) which plays a role in maintaining telomere integrity [111]. TANK1 is a member of the growing family of poly ADP-ribose polymerases (PARPs) that interacts with the telomere-binding protein TRF1 [112]. The role of TANK1 involves displacing TRF1 from telomeric DNA, which suggests that TANK1 may be a positive regulator of telomere length in telomerase-expressing cells [113-115].

1.6 Knowledge gaps and future directions

As reviewed elsewhere [59, 83, 116, 117], it is important to determine dietary reference values for a micronutrient based on DNA damage prevention, using the

best validated biomarkers of genome integrity. Most of the *in vitro* experiments indicate that DNA breaks and chromosomal instability in cells are minimized when Zn concentration in culture medium is between 4-16 μM [35, 36, 81]. However, whether this optimal concentration range is applicable *in vivo* and/or to all tissues or differs depending on alterations in phenotype due to development, ageing or disease remains unknown. There is limited information on the relationship between Zn status and DNA damage/chromosomal instability, and therefore there is an urgent need to conduct robust and reproducible intervention *in vivo* studies with well-validated biomarkers of DNA integrity.

In addition, prevention of diseases caused by genome damage need to take into consideration differences in individual Zn metabolism genotypes due to single nucleotide polymorphisms (SNPs) which may influence bioavailability and homeostasis of Zn within cells. Bioavailability of Zn is controlled by Zn homeostatic mechanisms that influence Zn uptake, efflux and Zn distribution within cells. There are two protein families of Zn transporters, which include ZnT and ZIP families. The ZnT family includes the solute linker carrier 30A (SLC30A, ZnT) family and SLC39A (ZIP) family of metal ion transporters. The ZnT family of transporters function in Zn efflux from the cytoplasm towards either intracellular vesicles and/or the extracellular space [118, 119] while the ZIP family consist of 14 members, which controls Zn uptake from the extracellular matrix and/or intracellular organelles into the cytoplasm [120]. Besides ZnT, Zn is also mobilized by binding with specific ligands such as metallothionein [56, 121].

In the ZincAge project, it was shown that polymorphisms of the metallothionein gene MT1A influences the efficacy of Zn supplementation [122, 123]. MT induction and expression is also mediated by IL-6, a multifunctional cytokine, regulating differentiation and activity of different cell types, stress reactions and inflammatory response [122-126]. Recent studies suggest that the common IL-6-174 G/C and MT1A +647 polymorphisms interactively affect zinc bioavailability and bioefficacy and are likely to be a useful indicator for the selection of elderly people who need Zn supplementation [122, 123, 126-129]. Future studies should explore whether

polymorphisms in ZnT, ZIP, MT1A and IL6 genes modify the relationship between Zn status and genome stability.

Finally, in this brief review, a new schematic diagram is proposed (Figure 1.2) highlighting the potential effects of Zn deficiency or excess on multiple aspects of genomic stability based on the currently available published evidence.

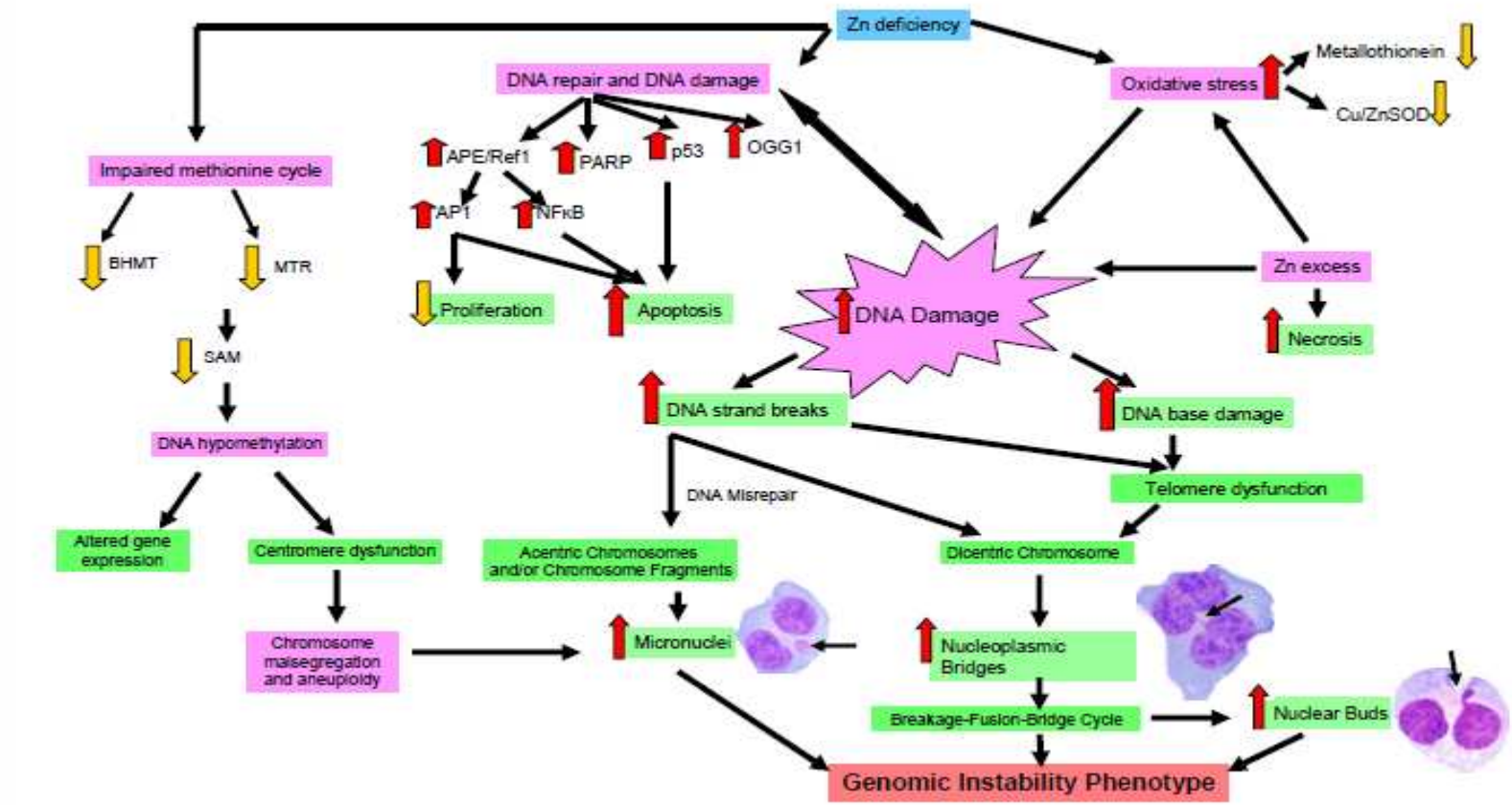

Figure 1.2: Schematic diagram proposing potential effects of Zn deficiency or excess on genomic stability and DNA integrity. Abbr : ZnDF – Zn Deficiency, AP1 - activator protein 1, NFκB - nuclear factor kappa-light-chain-enhancer of activated B cells, APE/Ref-1 - apyrimidinic endonuclease/redox factor-1, p53 – p53 tumor suppressor genes, BHMT - Betaine-homocysteine-S-methyltranferase, MTR – methionine synthase, SAM - S-adenosyl methionine

Chapter 2

Aims, Hypotheses and Models

Chapter 2

Aims, Hypotheses and Models

2.1 Aims and hypotheses

The main aim of this thesis was to address important knowledge gaps regarding the possible impact of Zn on genomic stability events in both lymphocytes and epithelial cells using both *in vitro* and *in vivo* models. The project aimed to study the differential impact of two different Zn salts on genome stability, including Zn Sulphate which is the commonly used in the laboratory and Zn Carnosine which is a newly emerging commercially available supplement known for its antioxidant capacity.

The experiments and investigations tested the following hypotheses:

1. Zn deficiency or excess increases DNA damage in an *in vitro* cell model.
2. ZnC will give better genome stability because it is readily absorbed than Zn Sulphate and a stronger antioxidant.
3. *In vivo* Zn supplementation improves cellular and plasma Zn status and lowers the rates of DNA damage in an elderly South Australian population.

2.2 Experimental models

2.2.1 *In vitro* model

These hypotheses were tested *in vitro* in both WIL2-NS lymphoblastoid and human oral keratinocyte cell lines. These models were also used to investigate the effect of Zn deficiency at various concentrations in relation to genomic instability events.

WIL2-NS is a human B lymphoblastoid cell line containing a mutation in the p53 gene and is therefore characterized by a deficiency in cellular apoptotic response that allows cells with chromosomal damage to survive. This feature, together with clearly defined cellular and nuclear morphology, make WIL2-NS cells ideal for measuring DNA damage as cells with chromosomal damage are not eliminated via apoptosis. Previous studies conducted at CSIRO's Nutrigenomics and Genome Health laboratory have shown that the WIL2-NS cell line is a sensitive and accurate model for determining chromosomal damage [130, 131].

Also in this study, a human oral keratinocyte (HOK) cell line was used as a model for cells derived from an epithelial origin to determine the cytotoxicity and genotoxicity effect of Zn. Oral keratinocytes play a major role in somatic cellular protection by providing a major barrier to physical, microbial, and chemical agents that may potentially cause local cell injury [132]. These cells share major structural, functional, and gene expression patterns with the well-characterized dermal keratinocytes and provide a suitable model for cells derived from the buccal mucosa [132].

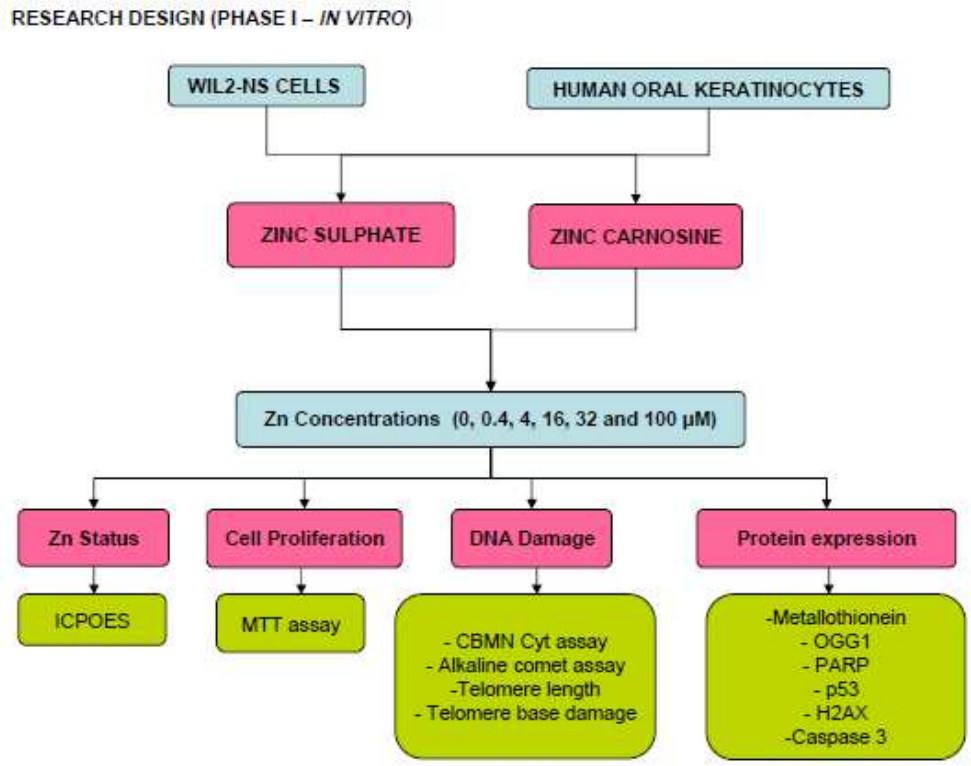

Figure 2.1: Simplified diagram outlying the assays performed using the human lymphoblastoid and oral keratinocyte *in vitro* models.

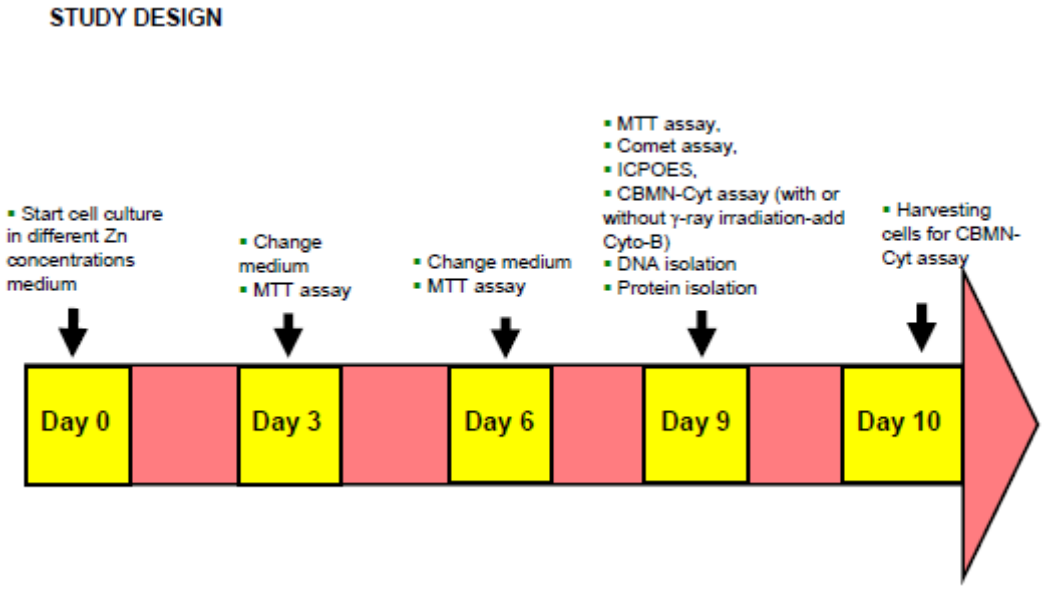

Figure 2.2: Schematic diagram for 9 day culture protocol for WIL2-NS cells tested for cytotoxic and genotoxic effects of Zn. The same protocol was used for HOK cells except that harvesting cells for the CBMN-Cyt assay was conducted on day 11 after 48 hours incubation with Cytochalasin B.

2.2.2 *In vivo* model

To test the impact of Zn on genomic stability in an *in vivo* model, a 12 week placebo-controlled human trial was conducted. The study was designed as a randomised, controlled intervention in a free-living healthy elderly population. This study aimed to investigate whether taking daily supplements (Zn Carnosine) can improve Zn status, genome stability events and Zn transporter genes in an elderly South Australian cohort characterised by having low plasma Zn levels.

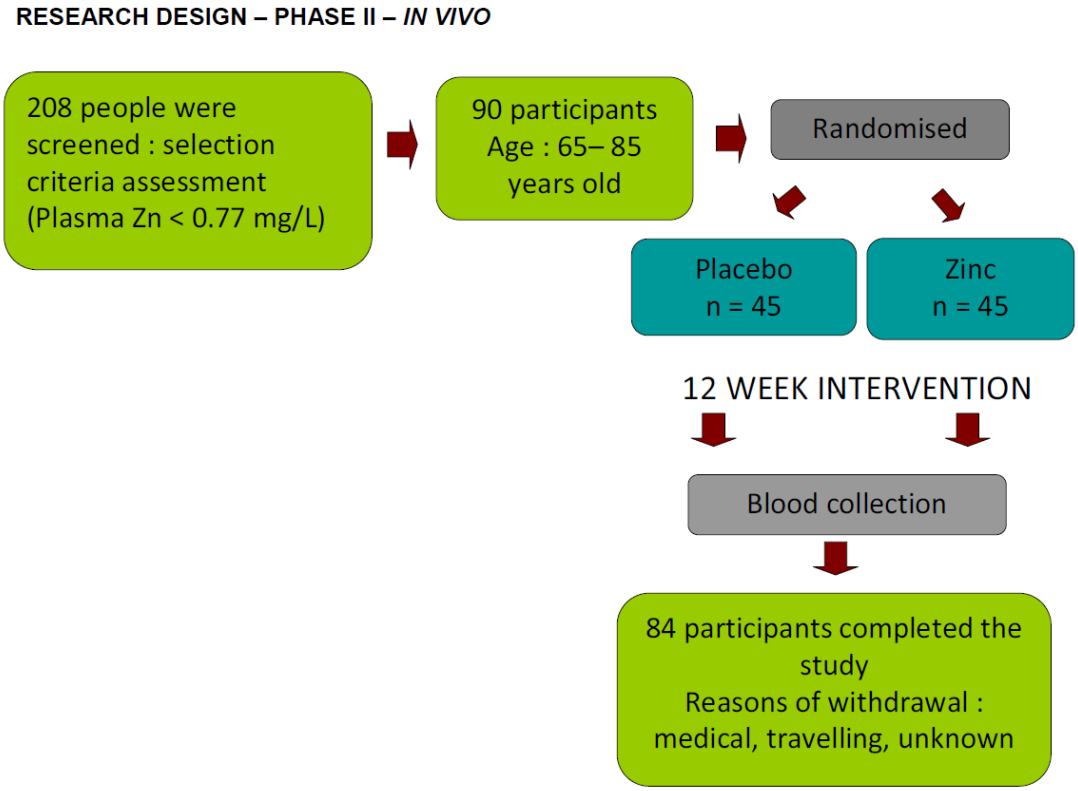

Figure 2.3: Simplified chart illustrating the research design for *in vivo* investigations.

More detailed study design and method assays are explained in greater detail in the subsequent chapters contained within this thesis.

Chapter 3

The Effect of Zinc Sulphate and Zinc Carnosine on Genome Stability and Cytotoxicity in the Human WIL2-NS Lymphoblastoid Cell Line

Sharif, R.[1,2,3], Thomas, P.[1], Zalewski, P.[2], Graham RD[4] & Fenech, M.[1]

[1]CSIRO Food and Nutritional Sciences, Adelaide, Australia

[2]School of Medicine, Faculty of Health Sciences, University of Adelaide, Adelaide, Australia

[3]Nutrition Program, Faculty of Health Sciences, Universiti Kebangsaan Malaysia, Malaysia

[4]School of Plant and Food Science, University of Adelaide, Adelaide, Australia

Mutation Research 720 (2011) 22–33

Statement of Authorship

The Effect of Zinc Sulphate and Zinc Carnosine on Genome Stability and Cytotoxicity in the Human WIL2-NS Lymphoblastoid Cell Line

Razinah Sharif

Performed analysis on all samples, interpreted data, wrote manuscript and contributed to planning of article

Signed ……. Date ……

Philip Thomas

Supervised development of work, helped in data interpretation, contributed to planning of article and provided critical evaluation of the manuscript

Signed ……. Date ……

Peter Zalewski

Supervised development of work, helped in data interpretation, contributed to planning of article and provided critical evaluation of the manuscript

Signed ……. Date ……

Robin Graham

Contributed to planning of article and provided critical evaluation of the manuscript

Signed ……. Date ……

Michael Fenech

Supervised development of work, helped in data interpretation, contributed to planning of article and provided critical evaluation of the manuscript and acted as corresponding author

Signed ……. Date ……

Chapter 3

The Effect of Zinc Sulphate and Zinc Carnosine on Genome Stability and Cytotoxicity in the Human WIL2-NS Lymphoblastoid Cell Line

---

3.1 Abstract

Zinc (Zn) is an essential cofactor required by numerous enzymes essential for cell metabolism and the maintenance of DNA integrity. The effect of Zn deficiency or excess on genomic instability events was investigated and the optimal concentration of two Zn compounds that minimize DNA damage events was determined. The effects of Zn Sulphate ($ZnSO_4$) and Zn Carnosine (ZnC) on cell proliferation were investigated in the WIL2-NS human lymphoblastoid cell line. DNA damage was determined using both the comet assay and the Cytokinesis-block micronucleus cytome (CBMN-Cyt) assay. Zn deficient medium (0 μM) was produced using Chelex treatment, and the two Zn compounds (ie. $ZnSO_4$ and ZnC) were tested at concentrations of 0.0, 0.4, 4.0, 16.0, 32.0 and 100.0 μM. Results from the MTT assay showed that cell growth and viability were decreased in Zn depleted cells (0 μM) as well as at 32 μM and 100 μM for both Zn compounds (p<0.0001). DNA strand breaks, as measured by the comet assay, were found to be increased in Zn depleted cells compared to the other treatment groups (p<0.05). The CBMN-Cyt assay showed a significant increase in the frequency of both apoptotic and necrotic cells under Zn deficient conditions (p<0.0001). Elevated frequencies of micronuclei (MNi), nucleoplasmic bridges (NPBs) and nuclear buds (NBuds) were induced in Zn depleted cells (p<0.0001) whereas genome damage was reduced in supplemented cultures for both Zn compounds at 4 μM and 16 μM, possibly suggesting these concentrations

may be optimal for genome stability. The potential protective effect of $ZnSO_4$ and ZnC was also investigated following exposure to 1.0 Gy γ-radiation and a hydrogen peroxide (H_2O_2) challenge. Culture in medium containing these compounds at 4-32 µM prior to irradiation displayed a significantly reduced frequency of MNi, NPBs and NBuds compared to cells maintained in 0 µM medium (p<0.0001). Similarly, cells in 16-32 µM for both Zn compounds were found to be protective against H_2O_2 induced cytotoxicity and DNA damage events compared to Zn depleted cells (*p<0.0001*) as measured via the CBMN-Cyt assay. Expression of γ-H2AX and 8-oxoguanine glycosylase measured by western blot was increased in Zn depleted cells. These results suggest that Zn plays an important role in genomic stability and the optimal Zn concentration range for prevention of DNA damage and cytotoxicity *in vitro* lies between 4-16 µM.

3.2 Introduction

Recent research has focussed on the role played by micronutrients in determining genomic stability events, as it has been shown previously that alterations in the concentration of certain micronutrients can affect DNA repair, DNA synthesis and apoptosis [5, 6]. Previous reports showed that micronutrient deficiency can induce DNA damage which may increase risk for infertility, cancer and accelerated ageing [6, 7]. A number of experimental and epidemiological studies suggest that low intake of certain minerals could be a risk factor for several types of cancers [9, 10]. Furthermore evidence shows that dietary deficiencies in minerals such as selenium, magnesium and Zn can result in DNA-strand breaks and oxidative lesions that may be similar to radiation-induced DNA damage [11, 12].

Zn plays a critical role in a wide range of cellular processes including cell proliferation, apoptosis and defence against free radicals [13, 14, 16-18]. It is an essential micronutrient for human health, reproduction and immune system function [15] and there is now a growing body of evidence to suggest an important role for this metal in maintaining DNA integrity [13, 14]. It is known that more than 100 specific enzymes require Zn for their catalytic function, including those which are

critical for antioxidant defence and genomic stability. This group includes copper/Zn superoxide dismutase (Cu/ZnSOD) which plays an important role in the cellular defence system [18] and hOGG1, a glycosylase involved in the repair of oxidised guanine in DNA [41]. The optimal concentration of Zn for genome stability in human cells *in vitro* and/or *in vivo*, however is currently undefined. Furthermore, the impact of excess Zn on genome stability has not been adequately explored.

In this study, we investigated Zn carnosine [*N*-(3-aminopropionyl)-L-histidinato Zn], which is a chelate of Zn and L-carnosine and is one of the new commercially available supplements. Zn carnosine (ZnC) as a supplement originated in Japan and was designed to combine the beneficial effects of both Zn and the antioxidant carnosine. There is now accumulating evidence highlighting the protective potential of ZnC against gastric lesions induced by ethanol and hydrogen peroxide [13, 133, 134]. A study in 2006 by Mahmood *et al* showed that ZnC can stabilise the integrity of the small bowel and stimulate gut repair processes in both *in vitro* and *in vivo* models [135]. Recent research suggests that ZnC may induce anti-oxidative stress enzymes in an *in vivo* model [136] and decrease p53, p21(WAF1/CIP1) and Bax expression after irradiation of rat jejunal crypt cells [137]. The effect of ZnC on genomic instability relative to other commonly used Zn supplements (eg. Zn Sulphate - $ZnSO_4$) has remained unexplored.

The CBMN-Cyt assay was chosen as the main outcome measure in this study because it is a comprehensive, robust and validated system for measuring DNA damage, cytostasis and cytotoxicity [84, 138, 139]. DNA damage events are scored specifically in once-divided binucleated (BN) cells and include i) micronuclei (MNi), a biomarker of whole chromosome loss and/or breakage, ii) nucleoplasmic bridges (NPBs), a biomarker of dicentric chromosomes resulting from DNA misrepair and/or telomere end-fusions, and iii) nuclear buds (NBuds) a biomarker of gene amplification events that may be generated as a result of breakage fusion bridge cycles initiated by NPBs [84]. To our knowledge, there have been no studies investigating the effects of Zn depletion and/or excess in relation to chromosomal damage and cytotoxicity utilising the CBMN-Cyt assay. A growing body of evidence

has shown that the genome damage biomarkers measured in this CBMN-Cyt assay are predictive of cancer risk. A multinational study conducted by the HUMN international collaborative project showed that MNi frequency in peripheral blood lymphocytes (PBL) is predictive of cancer risk within a population of healthy subjects [140], while El-Zein *et al* showed that frequency of MNi, NPBs and NBuds in PBL is significantly associated with lung cancer risk in smokers [141]. A recent review of the literature identified the CBMN-Cyt assay as the best validated biomarker of DNA damage that is sensitive to nutritional status as well as being associated with and predictive of degenerative diseases [83]. Hence, this assay was used as the primary outcome measure to investigate the potential genomic and cancer-related effects of Zn, depending on its concentration and its source compound.

In this study, the human B-lymphoblastoid model (WIL2-NS) was used, because it has been previously shown to be sensitive to the genotoxic and cytotoxic effects of essential minerals within the physiological range [142, 143]. In addition, WIL2-NS cells are p53 deficient [144], which prevents DNA-damage induced apoptosis and allows cells with DNA damage to survive, be visualized and quantified. The CBMN-Cyt assay in the WIL2-NS assay system has also been proven to be sensitive in detecting Reactive Oxygen Species (ROS)-induced DNA damage [131].

The primary aim of the study was to test the hypothesis that both Zn deficiency and excess can cause DNA damage and cytotoxicity, and to define the optimal concentrations of Zn for genome stability for cultured human cells. To test the hypothesis, two Zn compounds were compared; $ZnSO_4$ as the most commonly used form of Zn in research applications and ZnC as a novel form of Zn that is increasingly being used as a dietary supplement. A secondary aim was to determine the potential protective effects of these compounds against genomic damage induced by ionising radiation and H_2O_2 challenges.

3.3 Materials and methods

3.3.1 WIL2-NS cell culture

WIL2-NS cells are a human B lymphoblastoid cell line derived from the spleen of a Caucasian male with hereditary spherocyte anaemia and was obtained from the American Type Culture Collection (ATCC No. CRL-8155, Manassas, VA, USA). Cells were cultured in RPMI 1640 tissue culture media (Sigma, St. Louis, MO, USA) supplemented with 5% (v/v) foetal bovine serum (FBS) (Thermo Trace, Australia), 1% (v/v) penicillin [5000 IU/ml]/streptomycin [5 mg/ml] (Sigma, USA), 1 mM L-glutamine (Sigma, USA) at 37°C in a 5% CO_2, humidified atmosphere. WIL2-NS cells were cultured in 500 µl volumes in 24 well plates (Thermo Fisher Scientific, NY, USA) at an initial density of 2 X 10^3 cells/ml (based on growth curve data) for 9 days and the medium was replaced every 3 days (Figure 3.1).

3.3.2 Cell counting using the Coulter Counter

Cell count was measured using a Coulter Counter (Z1 Coulter® Particle Counter, Beckman Coulter, USA). The count of each sample was taken in duplicate and the mean value of samples containing cells measured. The mean of blank counts was substracted from the mean cell count before calculating the cell concentration. Cell concentration (cells/ml) was determined by multiplying the value by 2000 (dilution factor 1000 and counting volume of 0.5 ml).

3.3.3 Culture medium

For all experiments, cells were cultured in Zn-depleted medium (0 µM) to which $ZnSO_4$ (Sigma Aldrich St. Louis, MO, USA) or ZnC (Hamari Chemicals Osaka, Japan) was added to obtain Zn concentrations of 0.4, 4.0, 16.0, 32.0 and 100.0 µM. Zn depleted medium was prepared using RPMI medium (Zn deficient) and FBS that was depleted of Zn as follows: FBS was mixed with 10% Chelex-100 (Sigma, St. Louis, MO, USA) for two hours and the cycle of depletion was repeated again for another 4

hours. Mineral levels and Zn levels were measured by inductively coupled plasma optical emission spectrometry (ICPOES).

Because chelex-100 is chelating not just Zn, we determined the mineral level and added Fe, Ca, and Mg according to the table 3.1 below:

Table 3.1: Preparation of additional mineral mix to the chelated culture medium (per 500 ml)

Mineral	Amount (mg)
Iron (Fe)	0.125
Calcium (Ca)	11
Magnesium (Mg)	6.085

Calculations for preparing a total final volume of 100 ml culture medium with chelated FBS are specified in Table 3.2.

Table 3.2: Preparations of Zn chelated medium (100 ml)

Solutions	Volume (ml)
RPMI-1640 medium (Zn deficient)	93
FBS chelated (5% final)	5
Penicillin [5000 IU/ml]/Streptomycin [5 mg/ml]	1
L-Glutamine (1mM)	1

Calculations for preparing a total final volume of 100 ml culture medium with different Zn concentrations are specified in Table 3.3.

Table 3.3: Preparations of culture medium with varying Zn concentrations (20 ml)

Treatment	0	0.4	4	16	32	100
Zn Chelated medium (µl)	20 000	19 992	19 996	19 984	19 968	19 900
$ZnSO_4$ or ZnC (1 mM) (µl)	-	8	-	-	-	-
$ZnSO_4$ or ZnC (20 mM) (µl)	-	-	4	16	32	100

pH of the medium was checked and no changes in pH were observed in each culture medium with different Zn concentrations.

3.3.4 9-day WIL2-NS culture in 24 well plates

WIL2-NS cells were cultured in 24 well plates (NUNC flat bottom, sterile with lid, 500 µl per well) (Figure 3.2) with appropriate Zn-supplemented culture medium at an initial density of 2 X 10^3 cells/ml (based on growth curve) in 500 µl volume. The seeding concentration of WIL2-NS cells was determined in preliminary experiments aimed at optimising cell growth after 9 days. Cells were cultured in a humidified incubator at 37°C with 5% CO_2 (Sanyo MCO-17 AIC, Japan) for 9 days. On day 3 and 6, half of the culture medium was removed carefully without disturbing the cells and replaced with fresh culture medium with the same Zn concentration used on day 0. For the alkaline comet and CBMN-Cyt assay, WIL2-NS cells were cultured for 9 days as described above. On day 9, 100 µl of the cell suspension was transferred into eppendorf tubes for the alkaline comet assay and the rest of the cells were used for the CBMN-Cyt assay as described in 3.3.8.

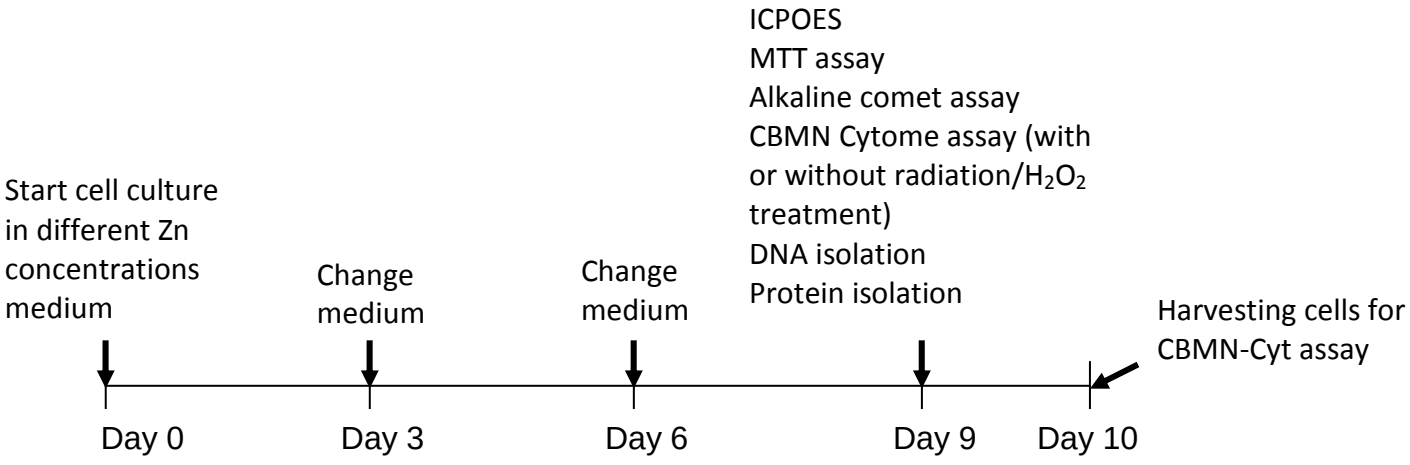

Figure 3.1: Schematic diagram for a 9 day WIL2-NS cell culture protocol testing for cytotoxic and genotoxic effects of Zn deficiency and excess.

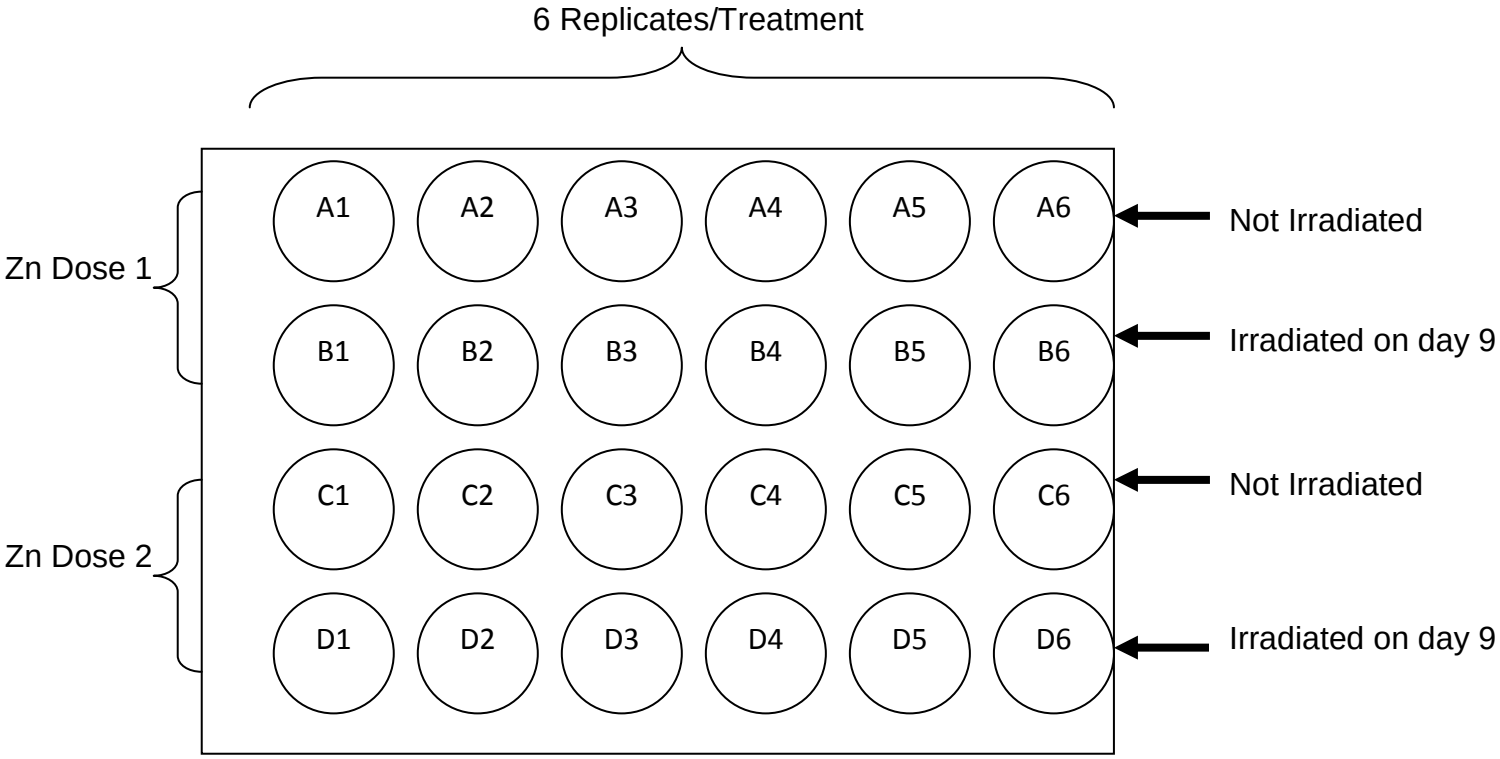

Figure 3.2: Schematic diagram of 24 well (500 µl) plate used for 9 day culture of WIL2-NS for both alkaline comet and CBMN-Cyt assays. Two doses of Zn were studied on each plate and multiple plates were used to study all doses and the two types of Zn compound.

All experimental data were based on six replicate measurements within each experiment and each experiment was repeated six times on separate days to ensure that the impact of intra- and inter-experimental variation was properly addressed.

3.3.5 Inductively coupled plasma optical emission spectrometry (ICPOES)

ICPOES was used to determine Zn levels in both media and within cells after culturing for 9 days. Analysis was performed at the Waite Analytical Services (W.A.S. - School of Agriculture and Wine, University of Adelaide). Briefly, either 2 ml of medium or cell pellets (4 X 10^6 cells/ml) were incubated with 4% nitric acid and hydrogen peroxide in 50 ml polypropylene centrifuge tubes which were sealed using a secure lid (Greiner Bio-One, Germany). These specific tubes were used because we had previously verified that they do not contaminate samples with Zn that might otherwise be present in certain tubes. Samples were then diluted and analysed by

ICPOES as described previously with slight modification [145]. The intra- and inter-assay coefficient of variation (CV) for the Zn measurements was 8.4% and 8.5% respectively.

3.3.6 MTT assay

MTT assay was used to measure cell growth and viability at the biochemical level. It provides a measure of mitochondrial activity in viable cells, and is therefore indicative of the number of viable cells with intact mitochondria [146]. 100 µl of WIL2-NS cells (2 X 10^3 cells/ml) were cultured at different Zn concentrations for 9 days in 96-well plates (Thermo Fisher Scientific, NY, USA) (six replicates per treatment, repeated on six different ocassions). Medium was changed on day 3 and day 6. 10 µl of MTT salt solution (5 mg/ml – Sigma, St. Louis, MO, USA) was added on day 9 to each well and incubated for 4 hours. Solubilizing solution was added [10% SDS (Sodium Dodecyl Sulphate (Sigma, St. Louis, MO, USA) in 0.01M HCl (BDH, Analar, England)] to the plate and further incubated overnight at 37°C. Absorbance was read with an ELISA microplate reader (SpectraMax 250, Molecular Devices, CA, USA) and the difference of optical density at 650nm and 570nm measured. Mitochondria will convert MTT salt to the blue formazan crystal which is solubilised by SDS and quantified by absorbance at 650 nm and 570 nm. This absorbance level is indicative of cellular number and viability. The intra- and inter-assay CV for the MTT assay was 6.1% and 7.2% respectively.

3.3.7 Alkaline comet assay

Single cell gel electrophoresis (comet assay) was used to measure DNA strand breaks and alkaline labile sites in cells cultured for 9 days. The assay was conducted under alkaline conditions as previously described [147, 148] with slight modification for use with a high throughput CometSlide HT (Trevigen Inc. Cat 4252-02K-01). 100 µl cell suspension in 1% low melting point agarose was spread onto precoated high throughput Comet slides before being immersed in lysis buffer [100 mM EDTA disodium salt dehydrate (Sigma, St. Louis, MO, USA), 2.5 M NaCl (Sigma, St. Louis,

MO, USA), 10 mM Trizma base (Sigma, St. Louis, MO, USA), 1% Triton X-100 (Sigma, St. Louis, MO, USA), pH adjusted to 10.0], for 1 h at 4°C. Slides were incubated in ice-cold alkaline electrophoresis buffer [1 mM EDTA (Sigma, St. Louis, MO, USA), 300 mM NaOH (Sigma, St. Louis, MO, USA), pH adjusted to 13.0] for 20 minutes. Electrophoresis was then conducted at 25V, 350 mA for 20 minutes in the same alkaline buffer in a horizontal Comet assay electrophoresis tank (Thistle Scientific). Slides were washed (3 times with neutralization buffer – 0.4 M Tris-HCl, pH adjusted to 7.5), drained and immersed in 70% ethanol for 5 minutes and air dried at room temperature overnight. Staining was performed using Propidium Iodide solution (Sigma, St. Louis, MO, USA - 50 ug/ml in Phosphate Buffer Saline) for 10 minutes. The above procedures were performed under subdued light conditions using UVA and UVB fliters on fluorescent lamps to avoid light-induced DNA breaks. Nuclei with/without DNA damage were observed at 20X magnification using an Eclipse fluorescence microscope (Nikon, Tokyo, Japan) with a triple band filter (excitation wavelength of 530 nm and emission wavelength of 615 nm) and captured with an attached Spot video camera (Diagnostic Instrument Inc.; Model – 254015, USA). 100 cells were randomly selected from each spot and scored with online software (Tritek - http://autocomet.com/main_home.php) for tail moment and tail intensity. Tail moment (tail length X DNA density) and tail intensity (% DNA in tail) were used as indicators of DNA damage. The intra- and inter-assay CV for the tail moment measured was 20.94% and 25.99%, and for tail intensity was 28.64% and 14.40%, respectively.

3.3.8 CBMN-Cyt assay

After 9 days in culture (Figure 3.1), cells were resuspended in fresh culture medium in the presence of Cytochalasin-B (Cyto-B, Sigma, St. Louis, MO, USA - 4.5 µg/ml) in 24 well plates (37°C, 5% CO_2) for a further 24 hours. Cells were then harvested onto microscope slides on day 10 using a cytocentrifuge as per the manufacturer's instructions (Shandon Products, UK). Slides were air-dried for 10 minutes, fixed in Diff-Quik fixative for 10 minutes and stained using Diff-Quik stains (Lab Aids,

Australia). For each treatment, a total of 500 cells were scored and classified to determine the ratios of mononucleate, binucleate (BN), multinucleate, apoptotic and necrotic cells. These ratios were used to determine the nuclear division index (NDI) a biomarker of cytostatic effect and cytotoxicity events were assessed by the frequency of necrotic and apoptotic cells. A total of 1000 BN cells were scored for genome damage indices (MNi, NPBs and NBuds). Scoring criteria for the CBMN-Cyt assay were followed as previously described [84]. To estimate the induced frequency following radiation, baseline values of cultures without radiation exposure were subtracted from those of corresponding irradiated cultures. The intra-assay and inter-assay CV for CBMN-Cyt assay biomarkers in non-irradiated (NI) and irradiated (IR) cultures was as follows: Apoptotic cells (NI 16.7%, 14.5%; IR 78.4%, 189.3%); Necrotic cells (NI 16.3%; 31.8%; IR 89.9%, 198.5%); NDI (NI 2.3%, 2.4%; IR 31.3, 256.2%); MNi (NI 23.5%; 24.3%; IR 30.9%, 27.0%); NPB (NI 20.4%; 24.7%; IR 34.9%, 32.1%); and NBuds (NI 65.1%; 61.6%; IR 39.2%, 63.3%) respectively. For H_2O_2 treatment, the intra and inter-assay CV were as follows: Apoptotic cells (53.57%; 148.04%); Necrotic cells (54.52%; 111.15%); NDI (74.37%, 53.22%); MNi (47.01%; 55.83%), NPB (49.92%; 43.20%) and NBuds (84.75%; 77.25%).

3.3.8.1 Scoring criteria

a) Criteria for scoring viable mono-, bi- and multinucleated cells

Frequency of viable mono-, bi-, and multinucleated cells were measured to determine cytostatic effects and the rate of mitotic divisions, as calculated using the nuclear division index. These cell types have the following characteristics [84]:

- Mono-, bi- and multinucleated cells are viable cells with an intact cytoplasm and normal nucleus morphology containing one, two and three or more nuclei, respectively.
- They may or may not contain one or more MNi or NBuds and in the case of bi- and multinucleated cells they may or may not contain one or more NPBs.

Necrotic and apoptotic cells should not be included among the viable cells scored.

b) Criteria for scoring apoptotic cells

Apoptotic lymphocytes are cells undergoing programmed cell death. They have the following characteristics:

- Early apoptotic cells can be identified by the presence of chromatin condensation within the nucleus and intact cytoplasmic and nuclear membranes.
- Late apoptotic cells exhibit nuclear fragmentation into smaller nuclear bodies within an intact cytoplasm/cytoplasmic membrane.
- Staining intensity of the nucleus, nuclear fragments and cytoplasm in both kinds of apoptotic cells is usually greater than that of viable cells.

c) Criteria for scoring necrotic cells

Necrosis is an alternative form of cell death that is thought to be caused by damage to cellular membranes, organelles and/or critical metabolic pathways required for cell survival such as energy metabolism. Necrotic cells have the following characteristics:

- Early necrotic cells can be identified by their pale cytoplasm, the presence of numerous vacuoled (mainly in the cytoplasm but sometimes in the nucleus), damaged cytoplasmic membrane and a fairly intact nucleus.
- Late necrotic cells exhibit loss of cytoplasm and damaged/irregular nuclear membranes with only a partially intact nuclear structure and often with nuclear material leaking from the nuclear boundary.
- Staining intensity of the nucleus and cytoplasm in both types of necrotic cells is usually less than that observed in viable cells.

d) Criteria for selecting BN cells suitable for scoring MNi, NPBs and NBuds

The cytokinesis-blocked BN cells that may be scored for MNi, NPBs and NBuds frequency should have the following characteristics:

- The cell should be binucleated.
- The two nuclei in a binucleated cell should have intact nuclear membranes and be situated within the same cytoplasmic boundary.
- The two nuclei in a binucleated cell should be approximately equal in size, staining pattern and staining intensity.
- The two nuclei within a BN cell may touch but ideally should not overlap each other. A cell with two overlapping nuclei can be scored only if the nuclear boundaries of each nucleus are distinguishable.
- The cytoplasmic boundary or membrane of a binucleated cell should be intact and clearly distinguishable from the cytoplasmic boundary of adjacent cells.

e) Criteria for scoring micronuclei (MNi)

MNi are morphologically identical to but smaller than the main nuclei. They also have the following characteristics:
- the diameter of MNi in human lymphocytes usually varies between $1/16^{th}$ and $1/3^{rd}$ the mean diameter of the main nucleus, which corresponds to $1/256^{th}$ and $1/9^{th}$ of the area of one of the main nuclei in a BN cell, respectively.
- MNi are non-refractile and they can therefore be readily distinguished from artefacts such as staining particles.
- MNi are not linked or connected to the main nuclei.
- MNi may touch but not overlap the main nuclei and the micronuclear boundary should be distinguishable from the nuclear boundary.
- MNi usually have the same staining intensity as the main nuclei but occasionally staining may be more intense.

f) Criteria for scoring nucleoplasmic bridges (NPBs)

NPB is a continuous DNA-containing structure linking the nuclei in a binucleated cell. NPBs originate from dicentric chromosomes (resulting from misrepaired DNA breaks or telomere end fusions) in which the centromeres are pulled to opposite poles of the cells during anaphase. They have the following characteristics:

- The width of a NPB may vary considerably but usually does not exceed 1/4th of the diameter of the nuclei within the cell.
- NPBs should also have the same staining characteristics as the main nuclei.
- On rare ocassions, more than one NPB may be observed within one binucleated cell.
- A binucleated cell with a NPB may contain one or more MNi.
- BN cells with one or more NPBs and no MNi may also be observed.

g) Criteria for scoring nuclear buds (NBuds)

NBuds represent the mechanism by which a nucleus eliminates amplified DNA and/or DNA repair complexes. NBuds have the following characteristics:
- NBuds are similar to MNi in appearance with the exception that they are connected to the nucleus via a bridge that can be slightly narrower than the diameter of the bud or by a much thinner bridge depending on the stage of the extrusion process.
- NBuds usually have the same staining intensity as MNi.
- Ocassionally, NBuds may appear to be located within a vacuole adjacent to the nucleus.

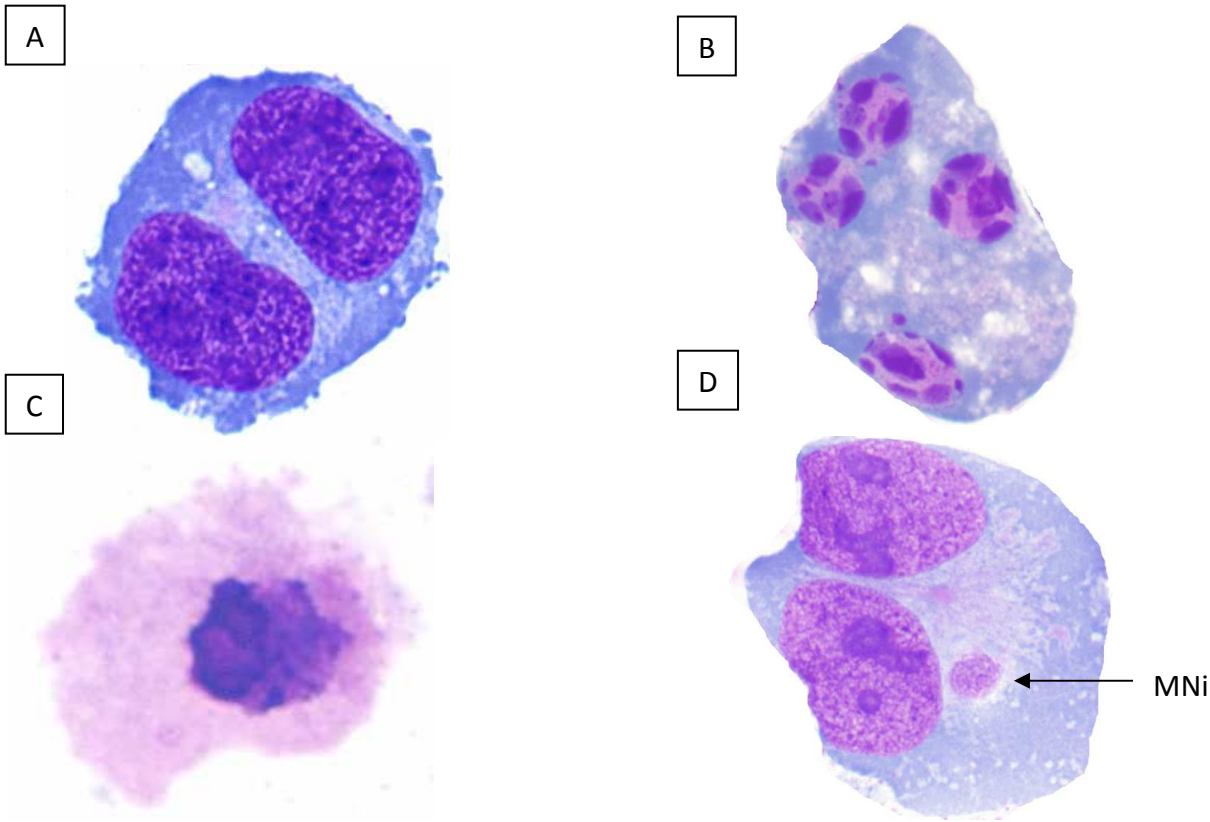

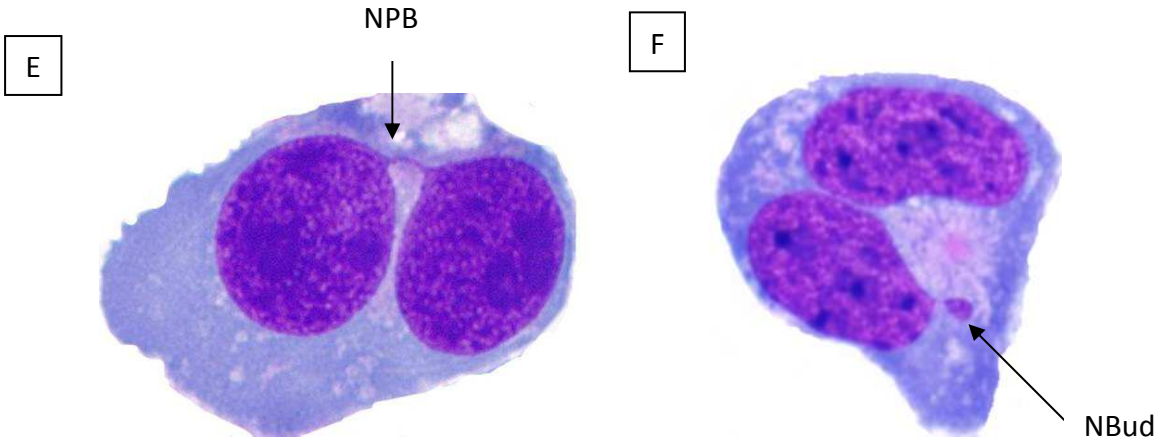

Figure 3.3: Example of morphological characteristics used to score cells in the cytokinesis blocked micronucleus cytome (CBMN-Cyt) assay. (A) binucleated cell; (B) apoptotic cells; (C) necrotic cell; (D) micronuclei; (E) nucleoplasmic bridges; and (F) nuclear buds (1000X magnification).

3.3.9 Gamma-ray-irradiation of cells

After nine days in culture, 500µl of cell suspension per treatment was transferred into eppendorf tubes (Axygen Scientific Inc., USA). Samples were challenged with 1.0-Gy gamma radiation at room temperature (22°C) with a CIS BIO International IBL 437 blood-cell irradiator comprising three stationary ^{137}Cs double-encapsulated radiation sources emitting gamma-radiation at 5.3 Gy/min. After irradiation, the 500µl suspensions were transferred into 24-well plates and incubated for 30 minutes at 37°C prior to addition of Cyto-B (Sigma, St. Louis, MO, USA—4.5µg/ml). Cells were harvested and microscope slides prepared to determine the frequency of CBMN-Cyt assay biomarkers following a further 24 hour incubation period at 37°C in a 5%-CO_2, humidified atmosphere.

3.3.10 H_2O_2 treatment of cells

After nine days in culture, cells were challenged with or without 30 µM H_2O_2 solution (Sigma, USA) prior to the CBMN Cyt assay. Briefly, 30 µM of H_2O_2 solution was added to the cell culture and incubated at 37°C for 30 minutes prior to the CBMN Cyt assay.

3.3.11 Western blotting

Cells were collected and transferred into a fresh eppendorf tube to be lysed. Preparation of cell lysis buffer is listed in Table 3.4:

Table 3.4: Preparation of working solution for cell lysis buffer. This buffer contains 50 mM HEPES, 100 mM Sodium Chloride (NaCl), 1% Triton X-100, 4 mM ($Na_4P_2O_7.10H_2O$), 2 mM Sodium orthovanadate *(*Na_3VO_4), 10 mM Sodium Fluoride (NaF).

Chemical	Initial Concentration (M)	Gram	Volume (ml)	ml to make lysis buffer (100 ml)
HEPES	0.5	2.383	20	10
NaCl	5	5.844	20	2
EDTA - pH 8	0.125	2.921	80	8
$Na_4P_2O_7.10H_2O$	0.1	0.892	20	4
Na_3VO_4	0.2	0.736	20	1
NaF	0.5	0.419	20	2
Triton X – 100	1 %		1	1

Cell lysis buffer was prepared in 80 ml of miliQ water (resistivity 18.2Ω) and the pH was set to 7.5 with Sodium Hydroxide (NaOH). As the pH was set, extra miliQ water was added to make up to 100 ml of solution which was stored at 4°C. Just before use, phenylmethanesulphonylfluoride or phenylmethylsulphonyl fluoride (PMSF) was added to a final concentration of 1 mM and 1 tablet of protease inhibitor (1 tablet per 10 ml) was also added to the solution.

To prepare cell lysates, cells were spun for 1200 rpm for 5 minutes at 4°C and then washed with cold Phosphate Buffered saline (PBS). Cells were spun and washed twice more prior to the pellet being resuspended in 1 ml of lysis buffer and incubated for 30 minutes at 4°C. Cells were then spun at 14,000 rpm at 4°C for 15 minutes. Supernatant was transferred to fresh tubes and aliquoted to several tubes (50 µl/tube). Cell aliquots can be stored at -80°C until further use.

To determine the protein concentration for each of the cell lysates, a BCA assay was performed (Sigma, Australia). Cell aliquots were thawed from -80°C and

lysis buffer was used as a diluent. To prepare standard curve dilutions, 100 µl of each standard was prepared and BCA at 1 mg/ml standard (Sigma, Australia) was used. Preparation of the standard curve dilutions is listed in Table 3.5.

Table 3.5: Preparations of standard curve dilutions for BCA assay

Conc. of standard (µg/ml)	Vol. of standard solution (µl)	Vol of diluent (µl)
1000	100	0
800	80	20
600	60	40
400	40	60
200	20	80
0	0	100

25 µl of a standard or sample (in triplicate) was added to 96 well plates. Subsequently, 200 µl of working reagent was added to each well (Reagent A and Reagent B from the BCA kit [Sigma, Australia]). The plate was then incubated at 37°C for 30 minutes and read at 562 nm using an ELISA microplate reader (SpectraMax 250, Molecular Devices, CA, USA). An example of a standard protein curve is shown in Figure 3.4.

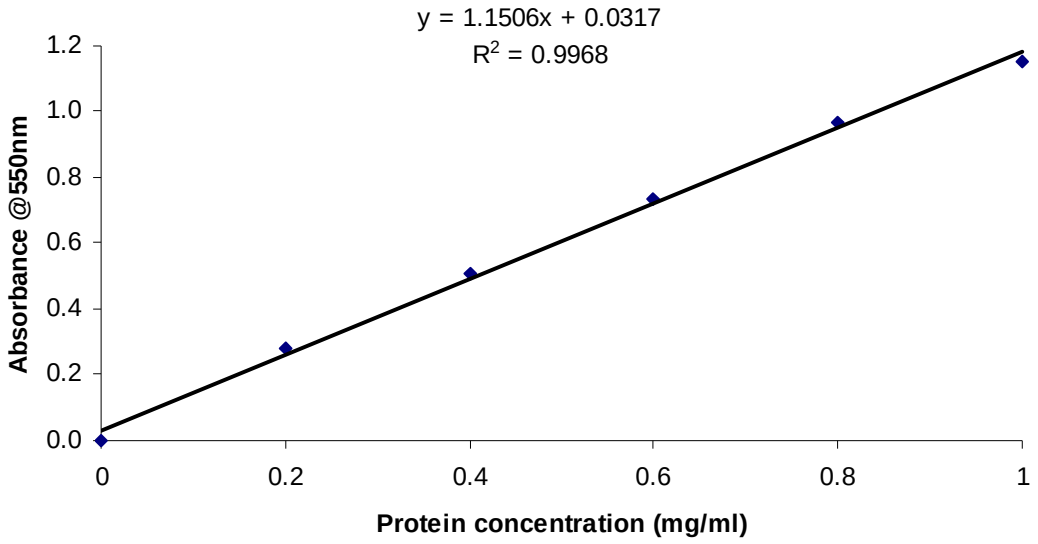

Figure 3.4: Standard curve for protein determination

Equal amounts of lysate protein (20 mg/lane) was separated using SDS-PAGE on a 4-12% bis-Tris gel (Invitrogen, CA, USA) and transferred to a nitrocellulose membrane

(Amersham Hybond™ ECL™, GE Healthcare, UK). The membranes were probed with antibodies to specific proteins as follows: mouse anti-poly-ADP ribose polymerase (PARP; BD Pharmingen, CA, USA), rabbit anti-8-oxoguanine glycosylase (OGG1; Novus Biologicals, USA), mouse anti-metallothionein (MT; Dako, Denmark), mouse anti γ-H2AX (Millipore, USA) and mouse anti β-actin (Sigma, St. Louis, MO, USA). Bound antibodies were detected using either goat anti-mouse IgG horseradish peroxidase or goat anti-rabbit IgG horseradish peroxidase (Dako, Denmark) and developed with Amersham™ ECL™ western blotting detection reagent (GE Healthcare, UK). Bands of interest were acquired using a luminescent image analyser LAS-4000 (FujiFilm, Tokyo, Japan) and quantification of Western blot analysis was done using the Multi Gauge version 3.0 program (FujiFilm, Tokyo, Japan). The data was presented as a ratio of samples to β-actin. The intra-assay and inter-assay CV for protein expression were as follows: Caspase 3 (10.86%, 17.76%); Metallothionein (13.34%, 18.60%); PARP (14.14%, 16.69%); OGG1 (27.39%, 35.74%); γ-H2AX (17.68%, 26.11%) respectively.

3.3.12 Statistical analysis

For each treatment, six replicate measurements were performed within each of six separate experiments performed on separate days (n=6). The intra- and inter-assay CV was calculated for each biomarker based on these repeated measurements after combining data for each culture at each different Zn concentration, excluding those at 100µM Zn in which extreme cytotoxicity occurred. All end points measured were tested for Gaussian distribution by using the Kolmogorov–Smirnov test. One-way analysis of variance (ANOVA) followed by Tukey's *post hoc* tests for data with Gaussian distribution was performed to compare the effects of different Zn concentrations. The non-parametric Friedman test followed by Dunn's multiple comparison test was used for data that did not exhibit Gaussian distribution. Two-way ANOVA was used in this study to measure the difference in effects between $ZnSO_4$ and ZnC and the % variance for biomarker results that could be explained by Zn concentration and Zn compound used. Data are expressed as mean ± standard

error with *p<0.05* considered statistically significant. Statistical analyses were performed using Prism 5.0 (GraphPad Inc., San Diego, CA).

3.3.13 Optimization of cell growth for long term culture

The aim of this study was to determine the optimal starting cell concentration for a 9-day WIl2-NS cell culture. Cells were seeded in 96 well culture plates at different concentrations (0.15 X 10^5 cells/ml, 0.075 X 10^5 cells/ml, 0.0375 X 10^5 cells/ml and 0.01875 X 10^5 cells/ml). Cells were continuously cultured in 96 well-microwell plate for 9 days and half of the culture medium was changed on day 3 and day 6. Cell proliferation was measured using the MTT assay as described in section 3.3.6. Figure 3.5 showed the WIL2-NS cell growth curve obtained.

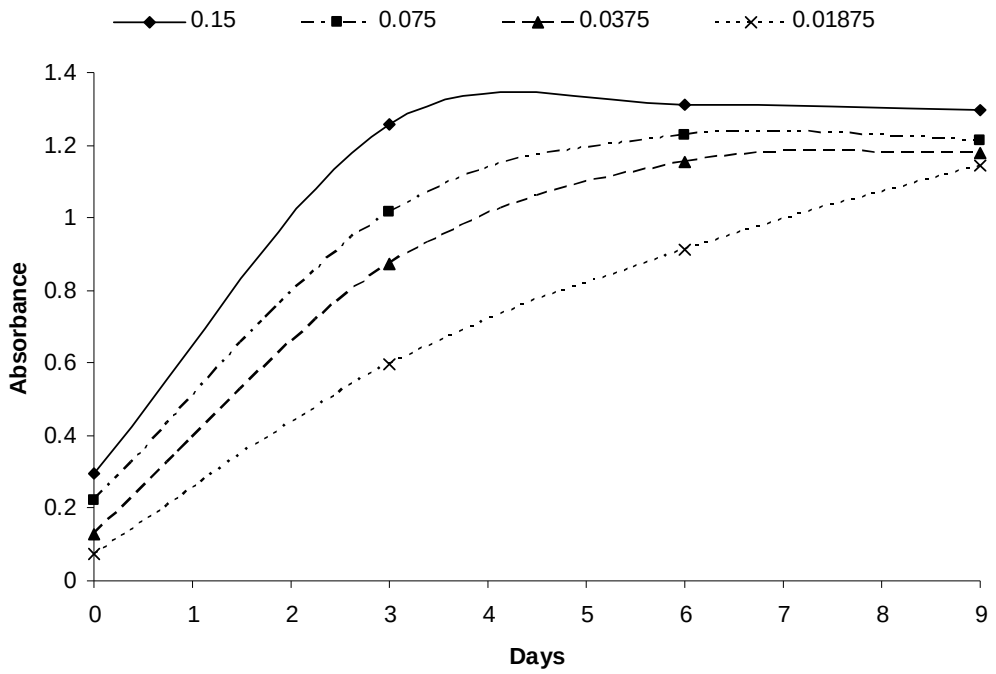

Figure 3.5: WIL2-NS cell growth curve following 9 day culture.

From the growth curve, 0.01875 X 10^5 cells/ml appeared to be the most optimal cell seeding density for WIL2-NS cells following 9 days culture. Considering cell number

and volume required for all the assays and practicality of the protocol, the seeding concentration of 2 X 10^3 cells/ml was chosen as the optimal choice for the study.

3.4 Results

3.4.1 Cellular Zinc concentrations

Figure 3.6A and 3.6B show concentrations of cellular Zn in WIL2-NS cells following 9 day cultures in different concentrations of $ZnSO_4$ and ZnC, respectively. Zn depleted cells showed a significant reduction in cellular Zn levels (p<0.0001) and there was no effect on other divalent metals (Copper and Iron) (Table 3.5). Cells supplemented with either $ZnSO_4$ or ZnC showed a significant dose related increase in cellular Zn (p<0.0001) with increased concentration of Zn in medium. The increment however, appeared to be significantly greater for $ZnSO_4$ relative to ZnC based on the observed trends and the associated % variance estimates (Effect of type of Zn compound: 22.16%, p<0.0001, Concentration: 67.29%, p<0.0001).

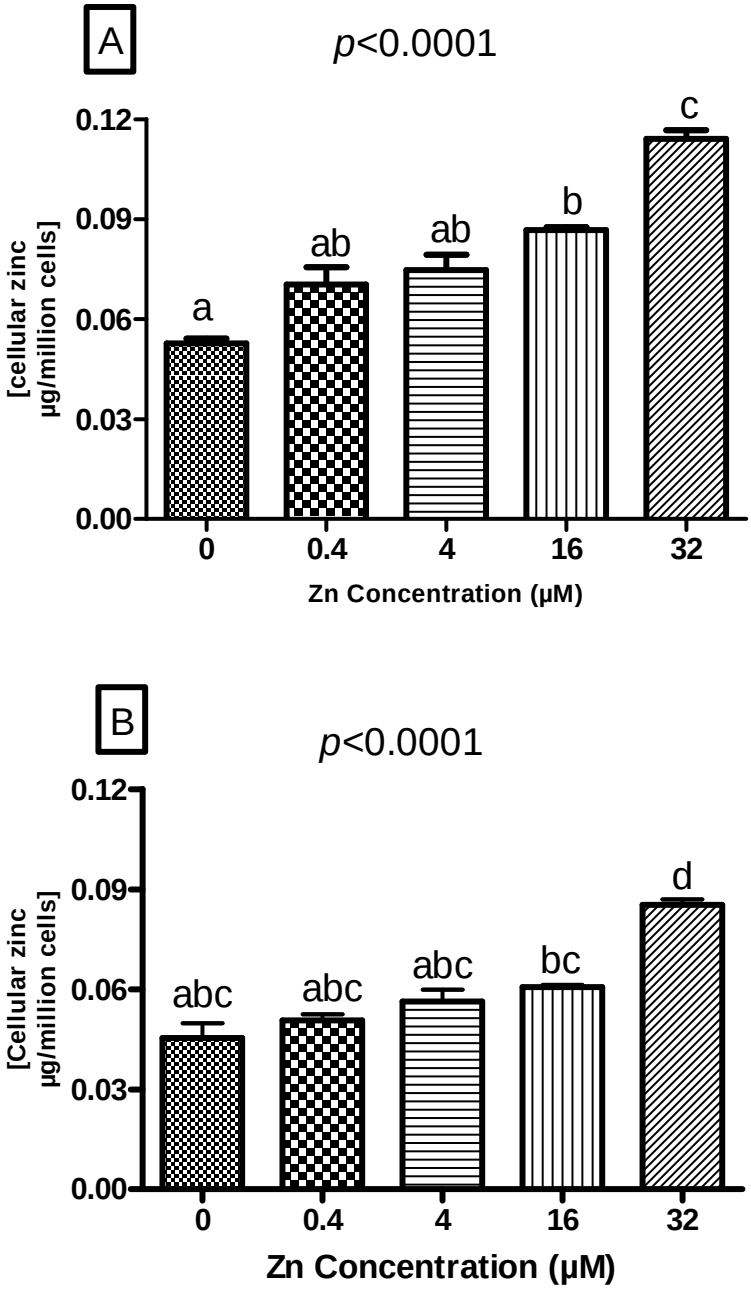

Figure 3.6: Levels of intracellular zinc in WIL2-NS cells treated with (A) $ZnSO_4$ and (B) ZnC, at increasing concentrations of Zn. 0 µM represents cells grown in Zn depleted medium. Groups not sharing the same letter are significantly different to each other (One way ANOVA: $p<0.0001$). Results shown are mean ± standard error (n=6).

Table 3.5: Levels of Fe (Iron), Cu (Copper), Ca (Calcium) and Mg (Magnesium) in Zn culture medium at various concentrations.

Treatment	Fe (Iron)	Cu (Copper)	Ca (calcium)	Mg (Magnesium)
Zinc Depleted cells	0.076 ± 0.005	0.110 ± 0.010	0.456 ± 0.005	1.100 ± 0.100
$ZnSO_4$ 0.4 µM	0.077 ± 0.005	0.113 ± 0.015	0.443 ± 0.028	1.033 ± 0.152
$ZnSO_4$ 4 µM	0.076 ± 0.005	0.113 ± 0.015	0.456 ± 0.005	1.100 ± 0.100
$ZnSO_4$ 16 µM	0.080 ± 0.010	0.111 ± 0.010	0.451 ± 0.025	1.083 ± 0.076
$ZnSO_4$ 32 µM	0.076 ± 0.005	0.105 ± 0.012	0.452 ± 0.007	1.133 ± 0.152
ZnC 0.4 µM	0.076 ± 0.005	0.110 ± 0.009	0.456 ± 0.005	1.071 ± 0.062
ZnC 4 µM	0.077 ± 0.004	0.107 ± 0.006	0.460 ± 0.001	0.996 ± 0.052
ZnC 16 µM	0.078 ± 0.004	0.103 ± 0.015	0.455 ± 0.005	1.071 ± 0.062
ZnC 32 µM	0.076 ± 0.005	0.110 ± 0.011	0.450 ± 0.010	1.033 ± 0.057

3.4.2 MTT assay

Figure 3.7A and 3.7B shows the effect of $ZnSO_4$ and ZnC on WIL2-NS cell culture on different days (Day 0, Day 3, day 6 and Day 9). Similarly, for both Zn treatments, no detrimental effect was observed on day 3 and day 6 (except for 0 µM) while on day 9, the effect was more apparent except for cells grown in 100 µM $ZnSO_4$ and ZnC. At 100 µM treatment, no cell proliferation was observed. On day 9, MTT results showed a significant decrease in viable cells in Zn depleted cultures and with excess Zn (p< 0.0001) (Figure 3.8A and B). Cell viability appeared to be optimal between the range 0.4 µM to 16 µM for both ZnC and $ZnSO_4$. At 32 µM both Zn compounds showed a non-significant decrease in viable cell number, and at 100 µM both Zn compounds exhibited severe cytotoxic effects (p<0.0001). Two way ANOVA analysis showed no significant differences in viability of cells treated with $ZnSO_4$ or ZnC, with the greatest % variance attributable to Zn concentration (Effect of type of Zn compound: 0.12%, p=0.1996; Concentration: 68.56%, p<0.0001).

A

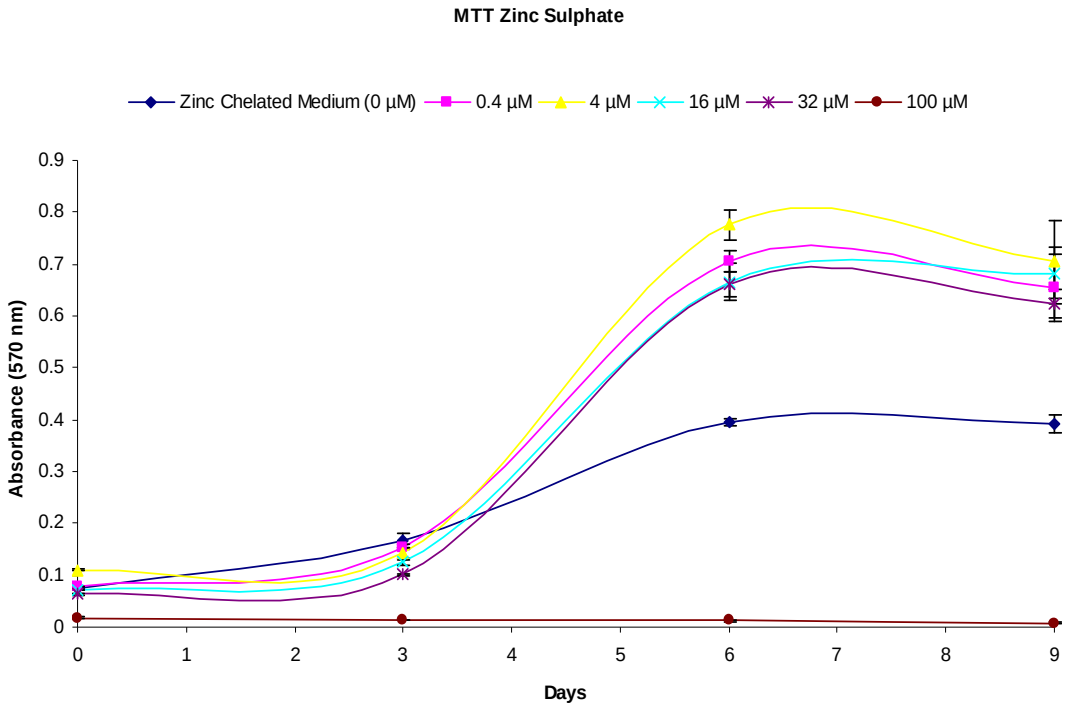

B

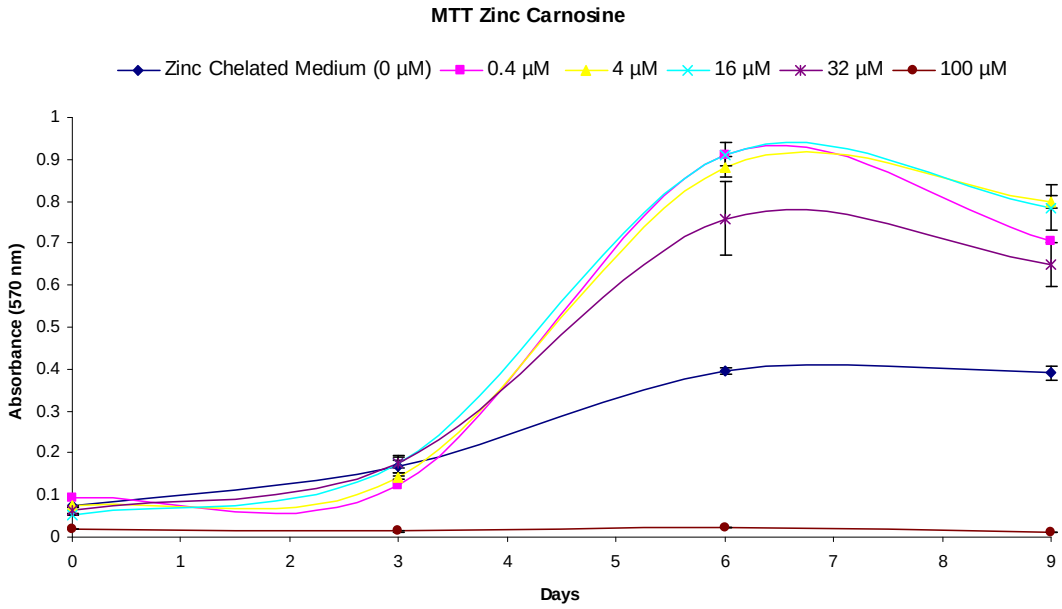

Figure 3.7: MTT assay absorbance of cells treated with (A) $ZnSO_4$ and (B) ZnC at increasing Zn concentration on different days (Day 0, Day 3, Day 6 and day 9). Results shown are mean ± standard error (n=6). MTT assay absorbance is directly correlated with cell growth and viability.

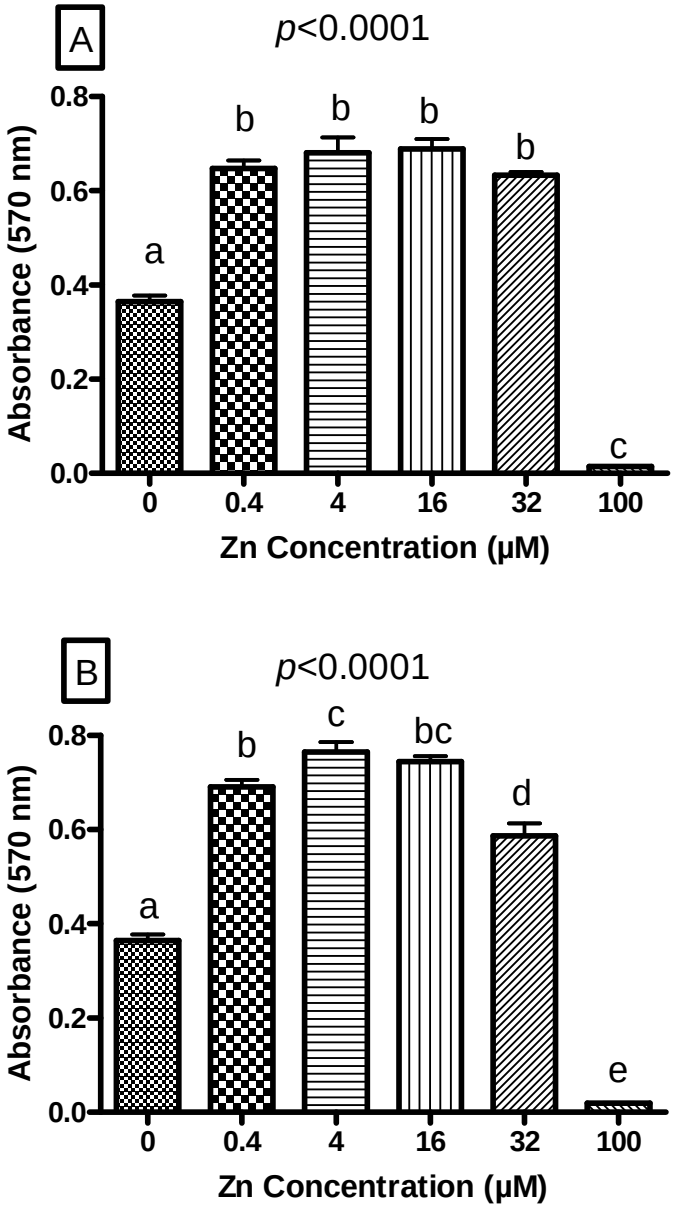

Figure 3.8: MTT assay absorbance of cells treated with (A) $ZnSO_4$ and (B) ZnC at increasing Zn concentration on day 9. Groups not sharing the same letter are significantly different to each other (One way ANOVA: $p<0.0001$). Results shown are mean ± standard error (n=6). MTT assay absorbance is directly correlated with cell growth and viability.

3.4.3 Alkaline comet assay

DNA strand breaks and alkali-labile sites were determined using the comet assay. DNA damage is often associated with cell death; therefore, it is critical that the highest dose tested will not induce excessive cytotoxicity. Hence, treatment with $ZnSO_4$ and ZnC at 100 µM was excluded as cell viability was less than 5%. Two endpoints were measured: tail moment (TM) and tail intensity (TI). TI represents percentage of DNA in the tail and TM represents a measure of tail length X measure of DNA in tail as a metric for DNA migration [149]. Figures 3.9A-D show a significant increase in both TM and TI for Zn depleted cells (p<0.05). With increasing Zn supplementation, a reduction in both TM and TI was observed using both types of Zn compounds. However, at 32 µM, values for TM and TI started to increase, suggesting a U-shaped dose response curve. There were relatively small differences in values for both TM and TI for cells treated with $ZnSO_4$ or ZnC (Tail moment - Effect of type of Zn compound: 0.00%, p=0.9121, Concentration: 13.46%, p<0.0001; Tail Intensity - Effect of type of Zn compound: 0.17%, p=0.3938, Concentration: 18.54%, p<0.0001).

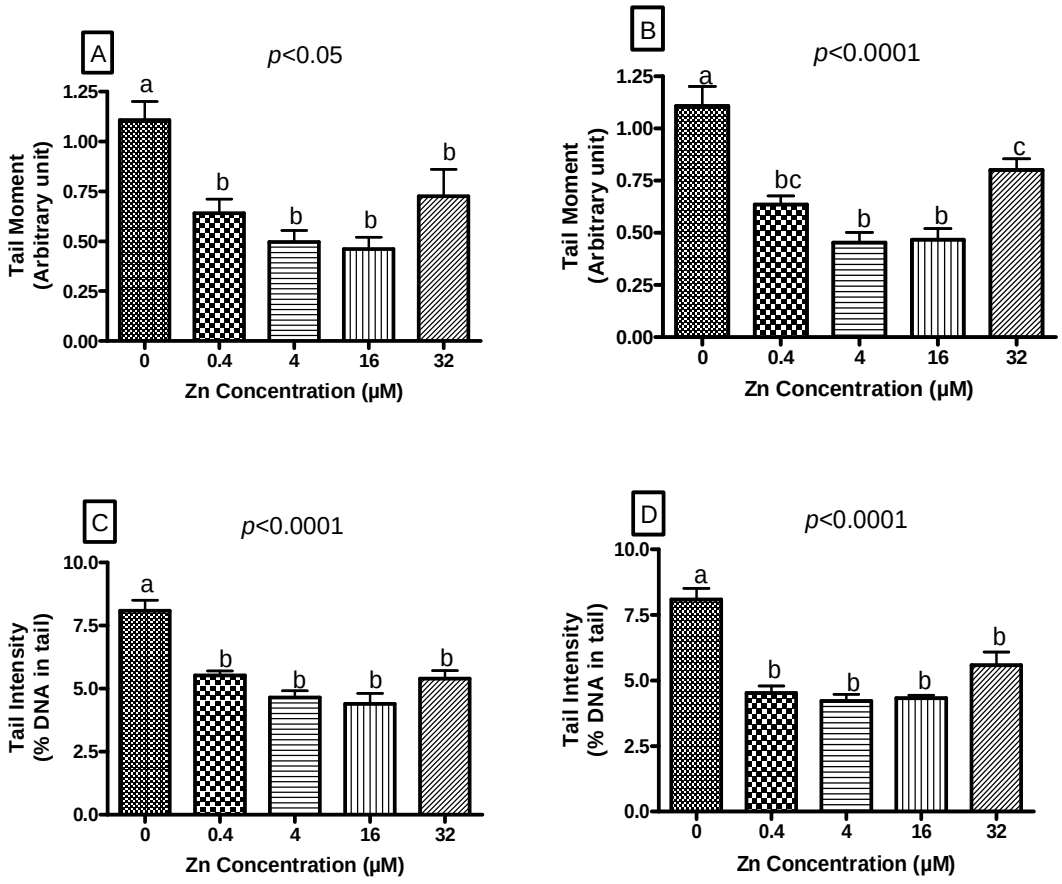

Figure 3.9: Tail moment values for cells treated with (A) $ZnSO_4$ and (B) ZnC; Tail intensity values for cells treated with (C) $ZnSO_4$ and (D) ZnC at increasing concentrations of Zn. Groups not sharing the same letter are significantly different to each other (One way ANOVA: $p<0.05$). Results are shown as mean ± standard error (n=6).

3.4.4 Effect of Zinc concentration on baseline levels of cytotoxicity and chromosome damage as measured by the CBMN-Cyt assay

The highest percentages of necrotic and apoptotic cells were observed in Zn depleted cells ($p<0.0001$). Figures 3.10A-D show a reduction in the percentage of both necrotic and apoptotic cells with increasing concentrations of Zn treatment ($p<0.0001$). Figures 3.10E and 3.10F show a reduction in NDI for Zn depleted cells ($p<0.0001$), while NDI increased with increasing Zn concentration indicating a significant cystostatic effect of Zn deficiency. These effects were virtually identical for ZnC and $ZnSO_4$.

MNi, NPBs and NBuds in binucleated cells were scored to measure chromosome damage and these results are shown in Figures 3.11A-F. Zn depleted cells showed the highest frequency for each of the three DNA damage endpoints measured (MNi, NPBs and NBuds) (p<0.0001). Overall, Zn supplemented cells showed a dose-related reduction in DNA damage events compared to Zn depleted cells (p<0.05). Both Zn compounds showed lowest total DNA damage at 4 µM and 16 µM (Figure 3.11A-F). There was no difference in combined total DNA damage events (i.e MNi, NPBs and NBuds added together) between $ZnSO_4$ and ZnC at any of the Zn concentrations tested (Effect of type of Zn compound: 0.04%, p=0.4691; Concentration: 69.03%, p<0.0001).

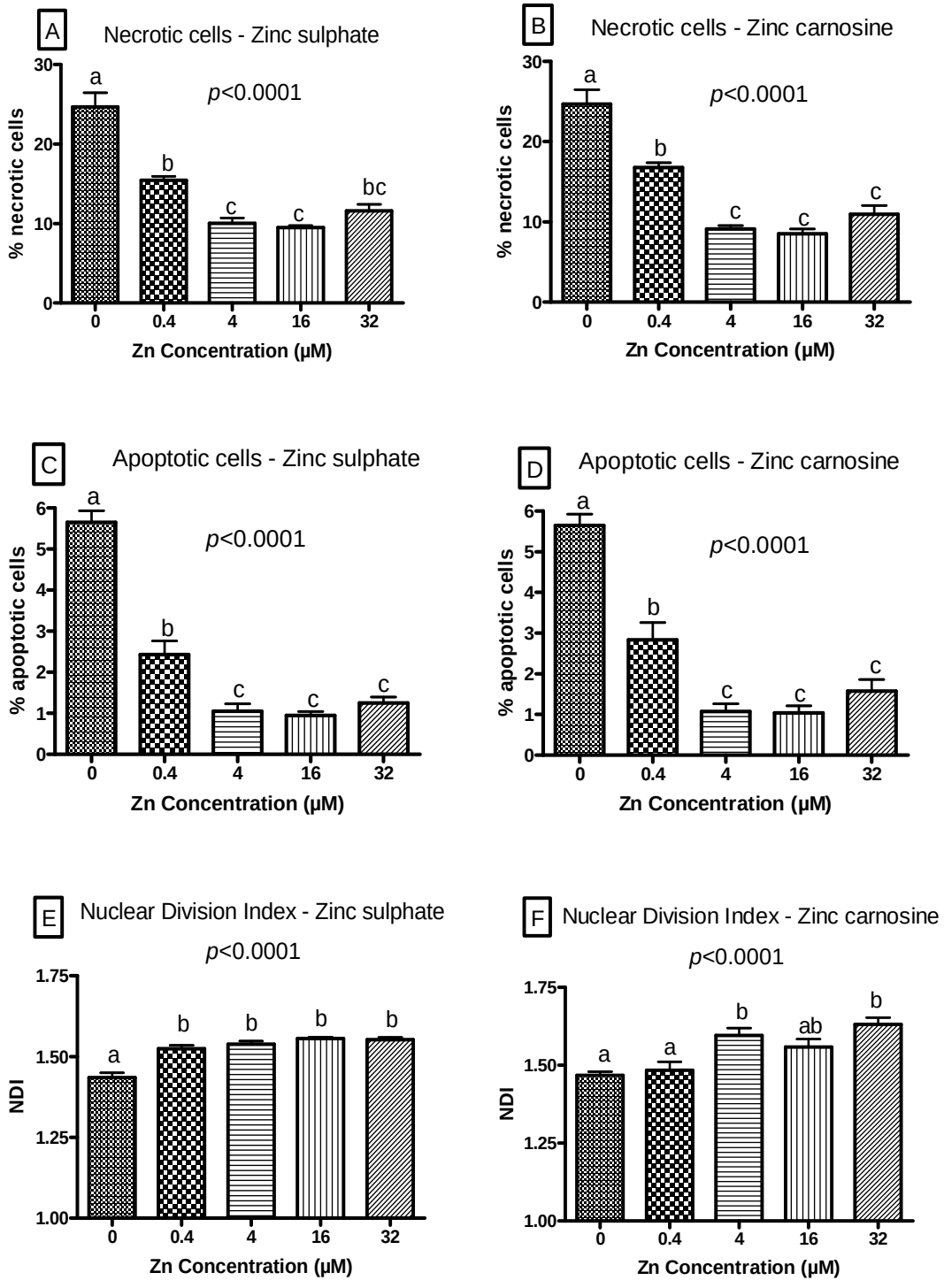

Figure 3.10: Cytotoxicity and cytostatic end points at increasing Zn concentration scored using CBMN-Cyt assay in WIL2-NS cells on day 10: (A) percentage of necrotic cells from cultures treated with $ZnSO_4$, (B) percentage of necrotic cells from cultures treated with ZnC, (C) percentage of apoptotic cells from cultures treated with $ZnSO_4$, (D) percentage of apoptotic cells from cultures treated with ZnC, (E) NDI of cultures treated with $ZnSO_4$, and (F) NDI of cultures treated with ZnC. Groups not sharing the same letter are significantly different to each other (p<0.0001). Results are shown as mean ± standard error (n=6).

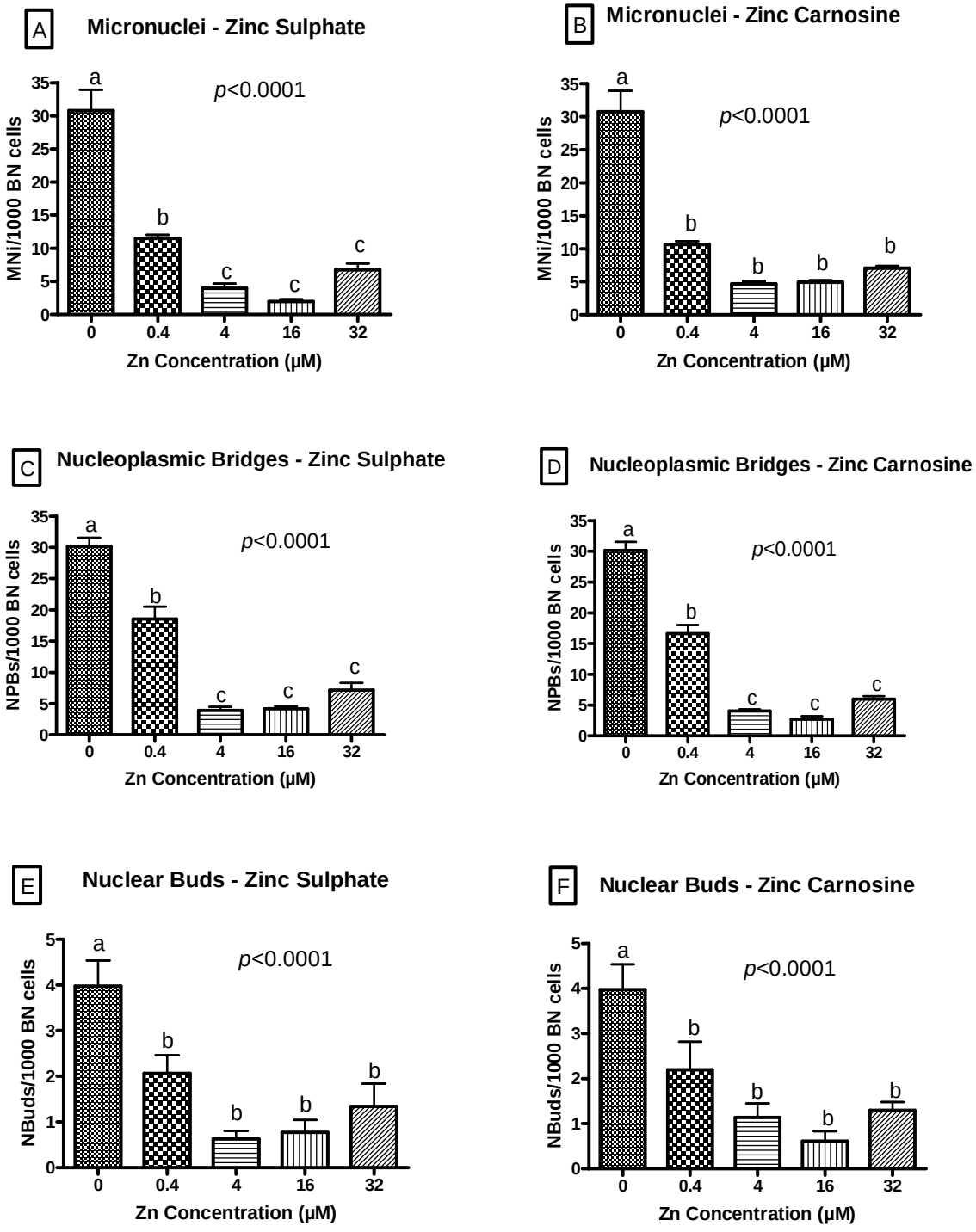

Figure 3.11: DNA damage biomarker end points scored using CBMN-Cyt assay in WIL2-NS cells on day 10 in relation to Zn concentration: (A) frequency of MNi in 1000 BN cells from cultures treated with $ZnSO_4$, (B) frequency of MNi in 1000 BN cells from cultures treated with ZnC, (C) frequency of NPBs in 1000 BN cells from cultures treated with $ZnSO_4$, (D) frequency of NPBs in 1000 BN cells from cultures treated with ZnC, (E) frequency of NBuds in 1000 BN cells from cultures treated with $ZnSO_4$, and (F) frequency of NBuds in 1000 BN cells from cultures treated with ZnC. Groups not sharing the same letter are significantly different to each other (*p<0.05*). Results shown are mean ± standard error (n=6).

3.4.5 Effect of Zinc concentration on γ-radiation induced cytotoxicity and chromosome damage as measured by the CBMN-Cyt assay

There was a significant reduction in the percentage of γ-ray-induced necrotic and apoptotic cells with increasing Zn concentration (*p<0.0001*). The lowest levels occurred at 4 and 16 µM Zn for both compounds. Zn concentration also showed a significant impact on γ-ray-induced changes in NDI with an apparent reduction in NDI at the higher doses (Figure 3.12A-F).

Zn depleted cells showed the highest frequency of γ-ray induced MNi, NPBs and NBuds (*p<0.05*). As Zn concentration increases, a significant reduction in the frequency of MNi, NPBs and NBuds was evident for both compounds (Figure 3.13A-F). There was no significant difference between $ZnSO_4$ and ZnC for effects on total induced DNA damage biomarkers (Effect of type of Zn compound: 0.02%, *p*=0.7112, Concentration: 44.80%, *p*<0.0001).

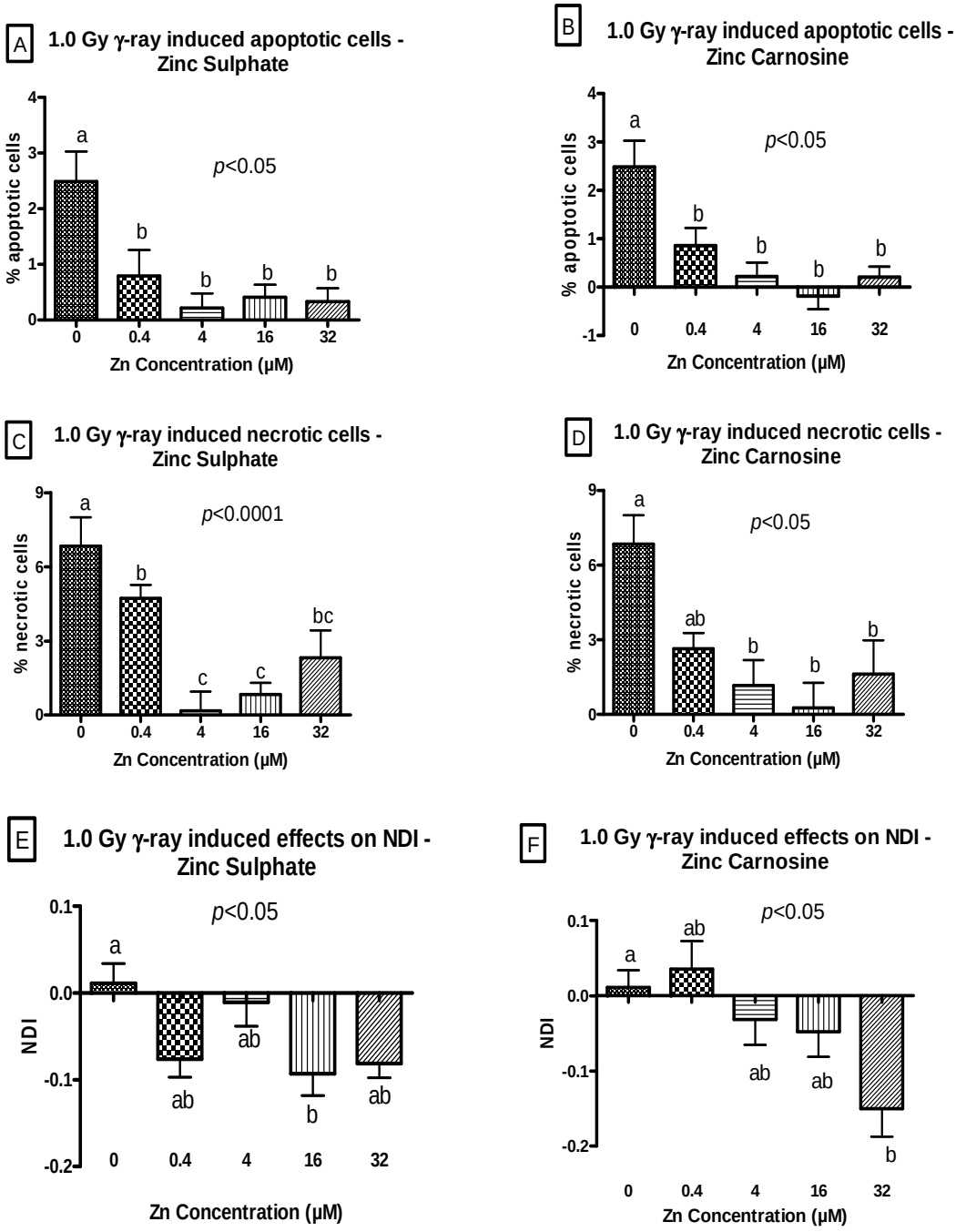

Figure 3.12: γ-ray induced cytotoxicity and cytostatic end points at increasing Zn concentration scored in WIL2-NS cells using CBMN-Cyt assay on day 10: (A) percentage of apoptotic cells from cultures treated with $ZnSO_4$, (B) percentage of apoptotic cells from cultures treated with ZnC, (C) percentage of necrotic cells from cultures treated with $ZnSO_4$, (D) percentage of necrotic cells from cultures treated with ZnC, (E) NDI of cultures treated with $ZnSO_4$, and (F) NDI of cultures treated with ZnC. Groups not sharing the same letter are significantly different to each other (p<0.05). Results are shown as mean ± standard error (n=6).

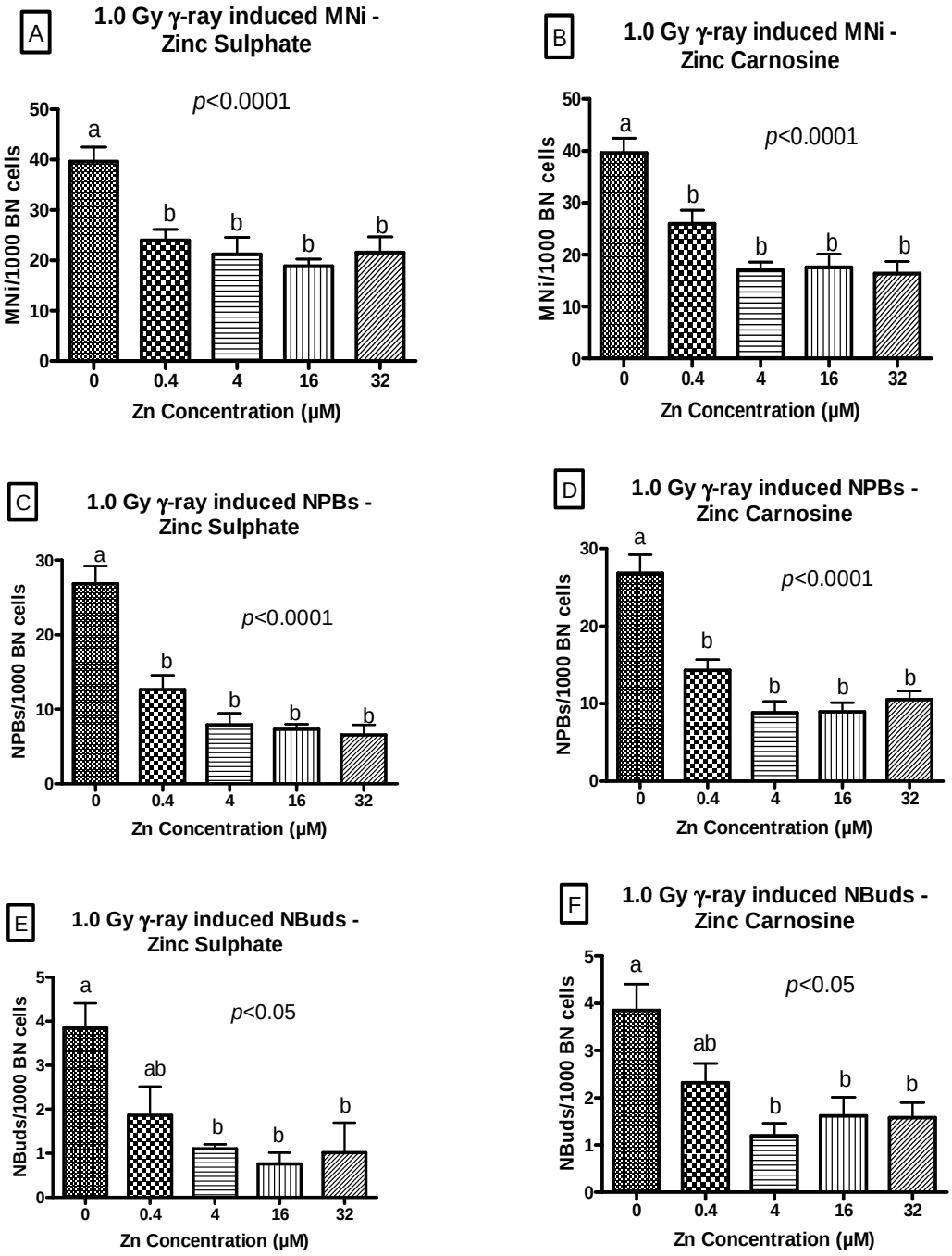

Figure 3.13: γ-ray induced DNA damage biomarker end points with increasing Zn concentration scored in WIL2-NS cells using CBMN-Cyt assay on day 10: (A) frequency of MNi in 1000 BN cells from cultures treated with $ZnSO_4$, (B) frequency of MNi in 1000 BN cells from cultures treated with ZnC, (C) frequency of NPBs in 1000 BN cells from cultures treated with $ZnSO_4$, (D) frequency of NPBs in 1000 BN cells from cultures treated with ZnC, (E) frequency of NBuds in 1000 BN cells from cultures treated with $ZnSO_4$, and (F) frequency of NBuds in 1000 BN cells from cultures treated with ZnC. γ-ray-induced values measured by subtracting values for non-irradiated controls from those of irradiated cultures. Groups not sharing the same letter are significantly different to each other (p<0.05). Results are shown as mean ± standard error (n=6).

3.4.6 Effect of Zinc concentration on H_2O_2 induced cytotoxicity and chromosome damage as measured by the CBMN-Cyt assay

Figure 3.14A-F showed the cytotoxic and cytostasis effect of H_2O_2 treatment against cells cultured in Zn treatment at various concentrations. Following H_2O_2 treatment, cells tended to have higher percentages of necrotic cells especially in the Zn depleted culture (23.56 ± 2.17%) compared to the other treatment groups (*p<0.0001*). Zn at 16 µM showed the lowest percentages of necrotic cells for both Zn types with 2.56 ± 1.08 for $ZnSO_4$ and 1.397 ± 1.61 for ZnC, respectively. There was no effect on type of Zn on % of necrotic cells (Effect of type of Zn compound: 0.03%, *p*=0.5424, Concentration: 67.94%, *p*<0.0001). Zn depleted cells also showed the highest percentage of apoptotic cells with 2.48 ± 1.33%. Zn concentration at 16 µM appeared to be the most optimal concentration for both Zn types to reduce apoptosis with only 0.122 ± 1.784% for $ZnSO_4$ treated culture and 0.2417 ± 0.4792% for ZnC. Similarly with necrotic cells, the concentration of each treatment appeared to explain the most variation observed in this experiment and there was no significant difference observed with type of Zn (Effect of type of Zn compound: 0.01%, *p*=0.8594, Concentration: 13.39%, *p*<0.0001). There were no significant changes for H_2O_2 induced effects on NDI for both Zn types.

Highest MNi frequency per 1000 BN cells was observed in Zn depleted cells although the frequency was not as high as γ-ray-induced with only 28.50 ± 1.01 compared to 39.61 ± 6.98 (Figure 3.15A and B). Both Zn cultures at 32 µM showed the lowest MNi frequency after H_2O_2 treatment with 8.50 ± 2.57 for $ZnSO_4$ and 9.42 ± 4.42 for ZnC. There was no difference with the type of Zn as analysed with 2-way ANOVA (Effect of type of Zn compound: 0.08%, *p*=0.3954, Concentration: 59.61%, *p*<0.0001). Frequency of NPBs was also higher in Zn depleted cells compared to the other treatment group with 16.87 ± 2.52 (*p<0.001*) (Figure 3.15C and D). $ZnSO_4$ at concentrations of 32 µM showed the lowest frequency of NPB-induced with only 6.59 ± 3.29. Similarly with MNi frequency, there was no significant difference comparing both Zn compounds (Effect of type of Zn compound: 0.01%, *p*=0.8594, Concentration: 13.39%, *p*<0.0001). For NBuds, $ZnSO_4$ at the concentrations of 32 µM

showed the lowest frequency with 0.2278 ± 1.03 and ZnC at the concentrations of 16 µM showed only 0.958 ± 0.792 compared to Zn depleted cultures which showed 5.03 ± 0.68 (*p<0.001*) (Figure 3.15E and F). Concentrations appeared to explain the most variation in this experiment compared to the effect of Zn compounds (Effect of type of Zn compound: 0.22%, *p*=0.2727, Concentration: 34.96%, *p*<0.0001).

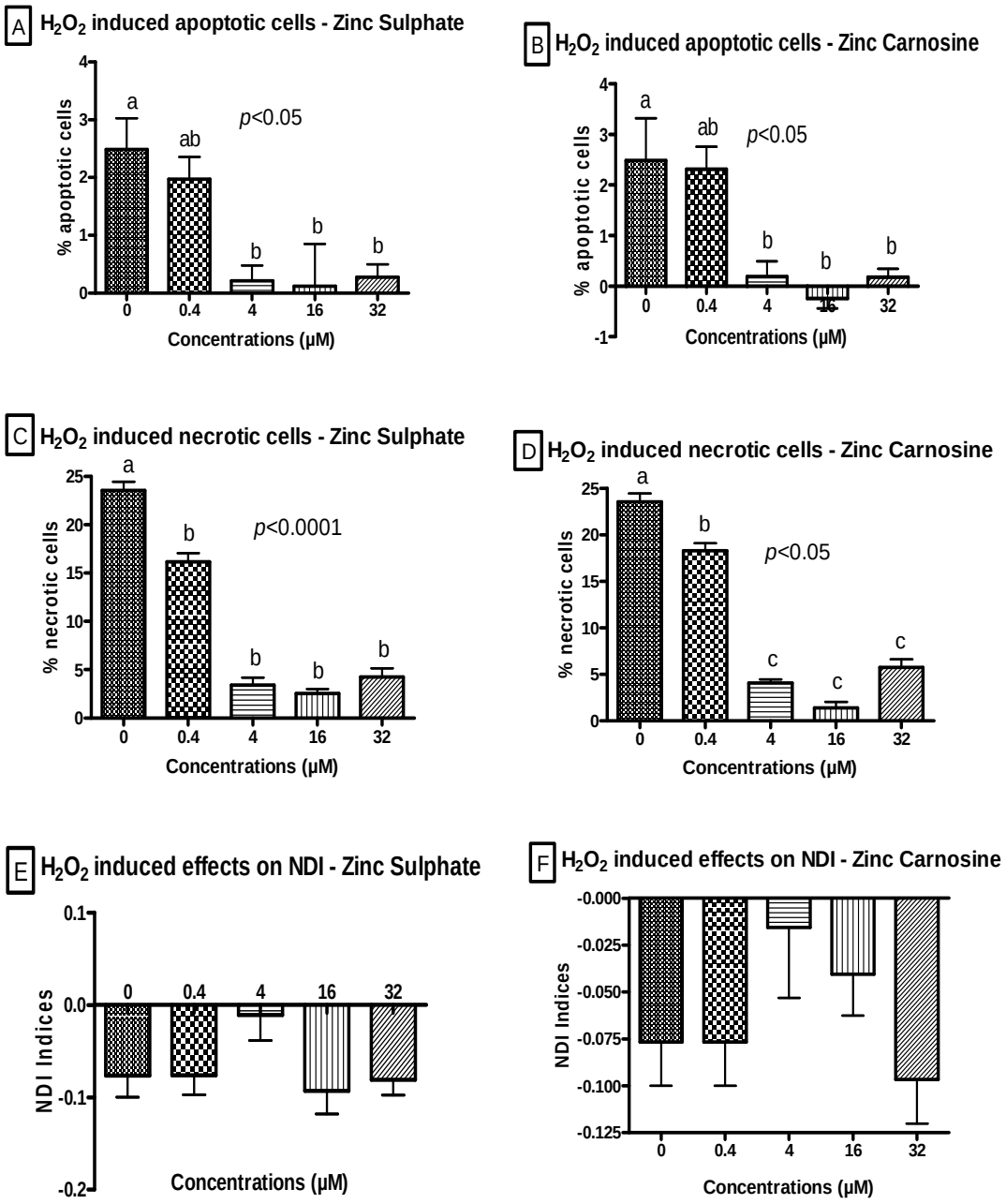

Figure 3.14: H_2O_2 induced cytotoxicity and cytostatic end points at increasing Zn concentration scored in WIL2-NS cells using CBMN-Cyt assay on day 10: (A) percentage of apoptotic cells from cultures treated with $ZnSO_4$, (B) percentage of apoptotic cells from cultures treated with ZnC, (C) percentage of necrotic cells from cultures treated with $ZnSO_4$, (D) percentage of necrotic cells from cultures treated with ZnC, (E) NDI of cultures treated with $ZnSO_4$, and (F) NDI of cultures treated with ZnC. H_2O_2 induced values measured by subtracting values for non-treated cultures from those of treated cultures. Groups not sharing the same letter are significantly different to each other (p<0.05). Results are shown as mean ± standard error (n=6).

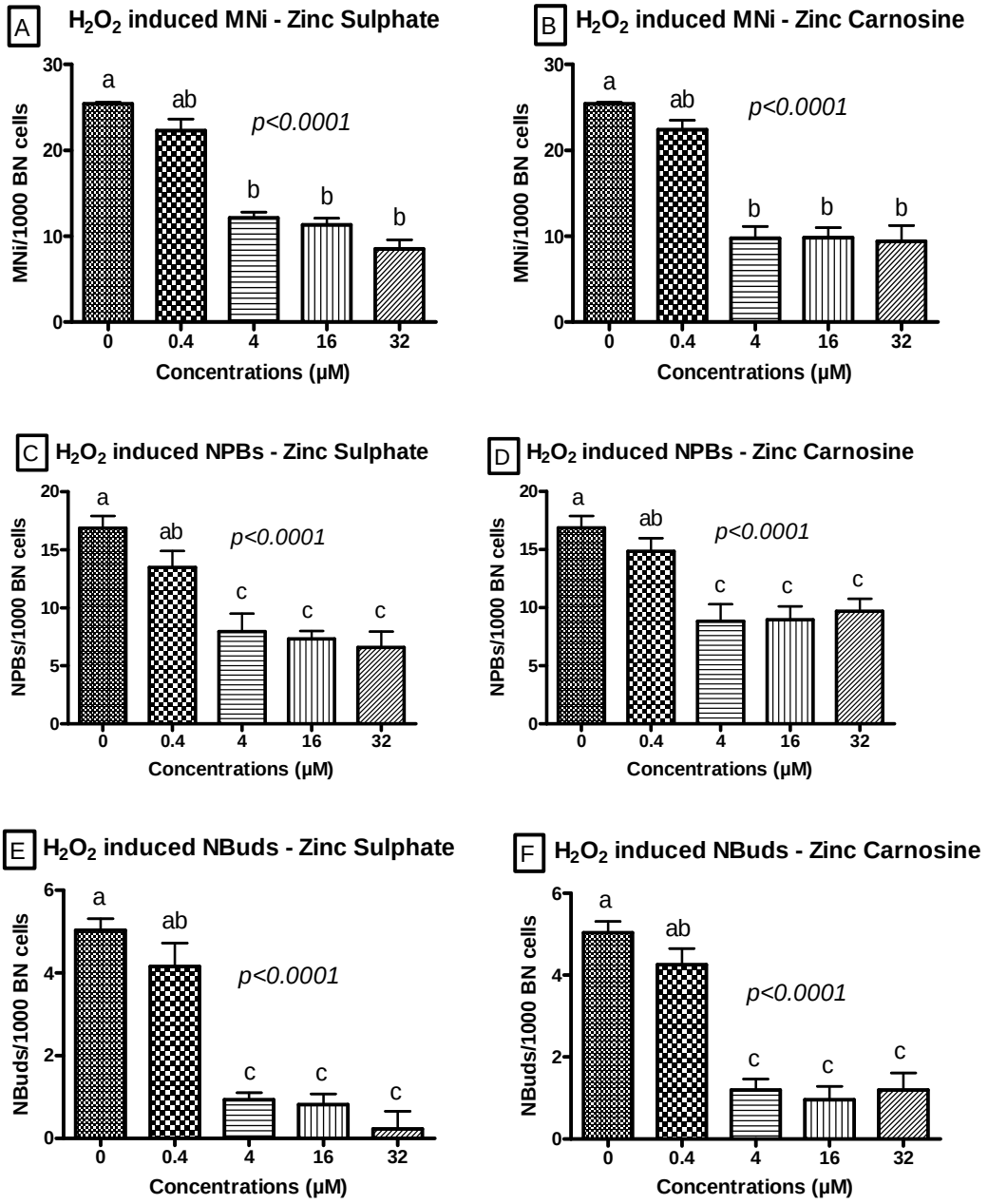

Figure 3.15: H_2O_2 induced DNA damage biomarker end points with increasing Zn concentration scored in WIL2-NS cells using the CBMN-Cyt assay on day 10: (A) frequency of MNi in 1000 BN cells from cultures treated with $ZnSO_4$, (B) frequency of MNi in 1000 BN cells from cultures treated with ZnC, (C) frequency of NPBs in 1000 BN cells from cultures treated with $ZnSO_4$, (D) frequency of NPBs in 1000 BN cells from cultures treated with ZnC, (E) frequency of NBuds in 1000 BN cells from cultures treated with $ZnSO_4$, and (F) frequency of NBuds in 1000 BN cells from cultures treated with ZnC. H_2O_2 induced values measured by subtracting values for non-treated cultures from those of treated cultures. Groups not sharing the same letter are significantly different to each other (p<0.05). Results are shown as mean ± standard error (n=6).

3.4.7 Western blot analysis

To obtain some insights into the molecular mechanisms by which Zn depletion or excess may alter DNA damage and cytotoxicity, expression of key proteins involved in these events were measured. Higher levels of PARP and OGG1 (DNA repair proteins) were observed in Zn depleted cells ($p<0.05$) (Figure 3.16A-B), however, Zn supplemented cells did not show any significantly different levels of these proteins. Increased levels of γ-H2AX levels were observed in Zn depleted cells suggesting increased DNA breaks ($p<0.05$) (Figure 3.16C). To determine apoptotic activity, Caspase 3 levels were measured and no cleaved fragments were observed in any treatment (data not shown) indicating limited apoptotic activity induced via Caspase 3. However, Zn depleted cells showed higher expression of pro-caspase 3 (39 kDa) as compared to the other groups ($p<0.05$) (Figure 3.16D). Levels of metallothionein (MT) (Zn-bound antioxidant) were lowest in Zn depleted cells compared with all other groups confirming the relevance of this biomarker as an indicator of Zn status (Figure 3.16E).

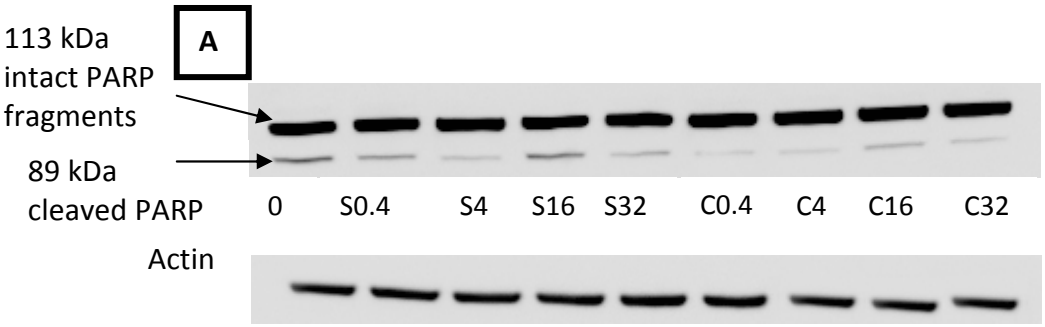
A
113 kDa
intact PARP
fragments
89 kDa
cleaved PARP
0
S0.4
S4
S16
S32
C0.4
C4
C16
C32
Actin

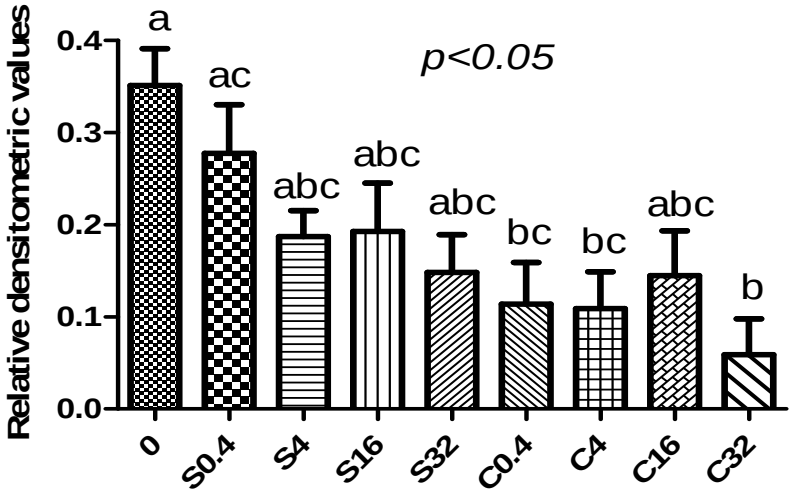
Relative densitometric values
0.4
0.3
0.2
0.1
0.0
a
ac
abc
abc
abc
bc
bc
abc
b
p<0.05
0
S0.4
S4
S16
S32
C0.4
C4
C16
C32


B
OGG1
0
S0.4
S4
S16
S32
C0.4
C4
C16
C32
Actin

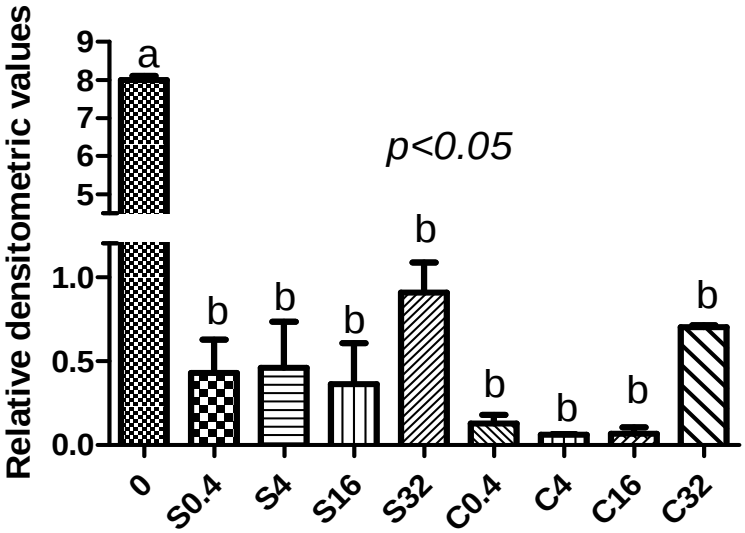
Relative densitometric values
9
8
7
6
5
1.0
0.5
0.0
a
b
b
b
b
b
b
b
b
p<0.05
0
S0.4
S4
S16
S32
C0.4
C4
C16
C32

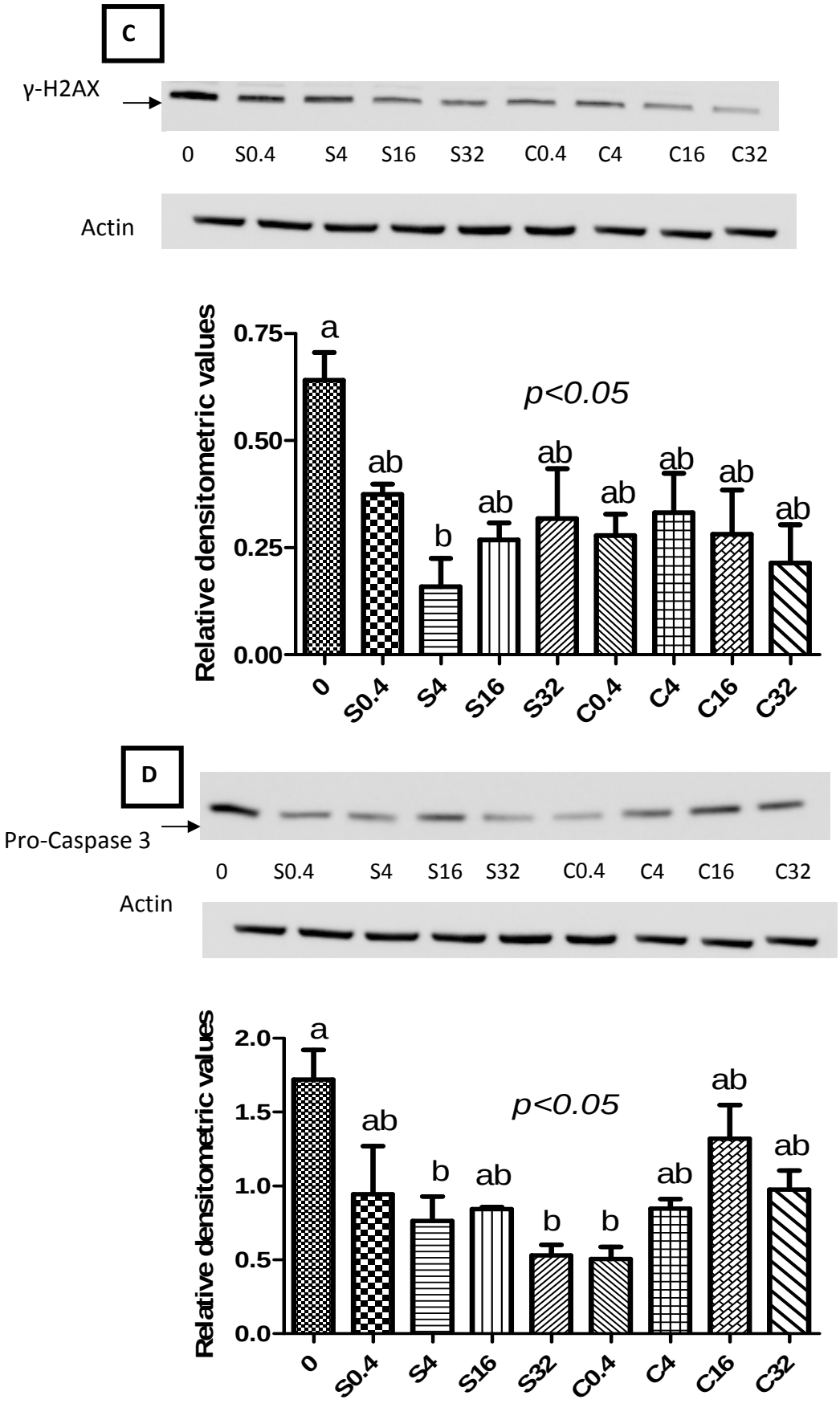
C
γ-H2AX
0
S0.4
S4
S16
S32
C0.4
C4
C16
C32
Actin
Relative densitometric values
0.75
0.50
0.25
0.00
a
ab
b
ab
ab
ab
ab
ab
ab
p<0.05
D
Pro-Caspase 3
0
S0.4
S4
S16
S32
C0.4
C4
C16
C32
Actin
Relative densitometric values
2.0
1.5
1.0
0.5
0.0
a
ab
b
ab
b
b
ab
ab
ab
p<0.05

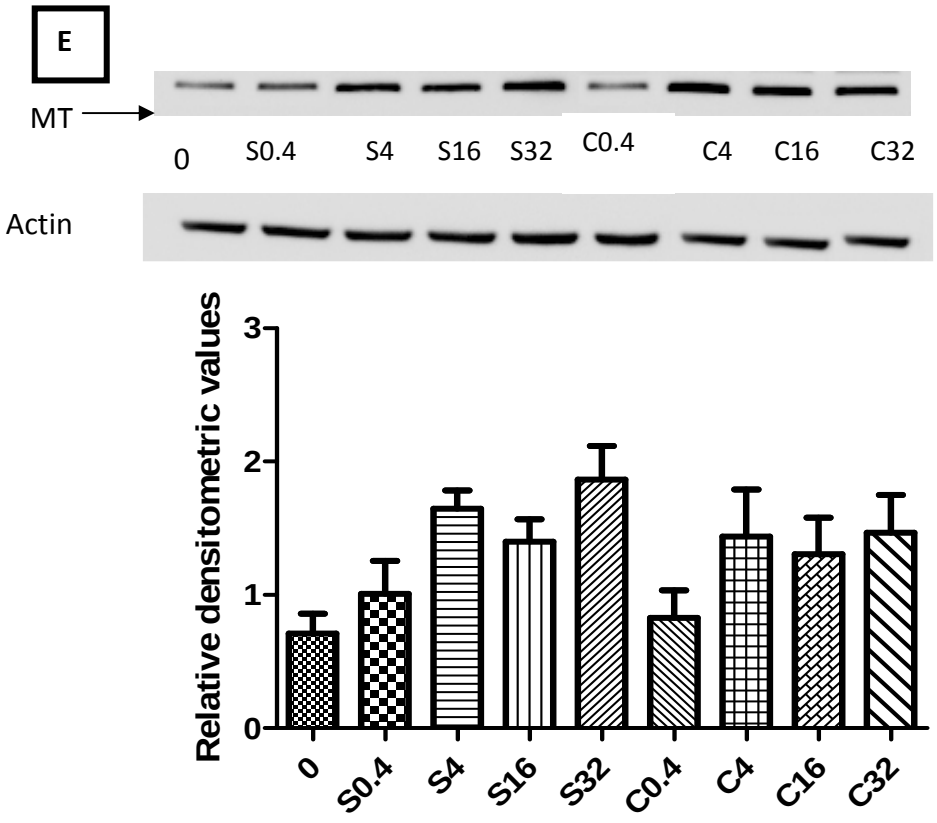

Figure 3.16: The effects of Zn concentration in WIL2-NS cells on levels of (A) 8-oxoguanine glycosylase (OGG1); (B) Poly (ADP-ribose) polymerase (PARP); (C) γ-H2AX; (D) Caspase 3; (F) Metallothionein (MT) expressed in WIL2-NS cells following 9 days of culture, as determined by western blot analysis. Abbr: S – Zinc Sulphate; C-Zinc Carnosine; 0 – Zn depleted cells. Representative western blot are shown in the inserts. Relative densitometric values are values for each sample divided by β-actin. Groups not sharing the same letter are significantly different to each other (One way ANOVA - $p<0.05$). Results shown are mean ± standard error (n=6).

3.4.8 Cytotoxicity and genotoxicity effect of WIL2-NS cells in optimal medium

Data on WIL2-NS cells grown in optimal medium were presented in Table 3.6. Optimal medium consist of RPMI 1640 tissue culture media (Sigma, St. Louis, MO, USA) supplemented with 5% (v/v) foetal bovine serum (FBS) (Thermo Trace, Australia), 1% (v/v) penicillin [5000 IU/ml]/streptomycin [5 mg/ml] (Sigma, USA), 1 mM L-glutamine (Sigma, USA)] and cells were cultured at 37°C in a 5% CO_2, humidified atmosphere. The optimal culture medium contains 3.8 µM of Zn (from FBS). Cells grown in optimal medium did not show any cytotoxicity and genotoxicity effects as compared to Zn depleted cells. The relationship between DNA damage and

cells grown in optimal medium was very similar to cells grown in additional 4 μM of Zn.

Table 3.6: Levels of Zn, cytoxicity and genome stability measurements for WIL2-NS cells cultured in standard normal medium.

Levels of Zn (µg/million cells)	Absorbance (570 nm)	Tail moment (arbitrary unit)	Tail intensity (% DNA in tail)	Apoptotic cells (% apoptotic cells)	Necrotic cells (% necrotic cells)	NDI (NDI Indices)	Micronuclei (MNi/1000 BN)	Nucleoplasmic Bridges (NPB/1000 BN)	Nuclear Buds (NBuds/1000 BN)
0.075 ± 0.004	0.6807 ± 0.032	0.496 ± 0.060	4.644 ± 0.260	1.047 ± 0.180	10.051 ± 0.676	1.538 ± 0.010	3.980 ± 0.710	3.903 ± 0.560	0.633 ± 0.170

3.5 Discussion

Results from this study showed that total Zn within cells treated with $ZnSO_4$ was higher compared to cells treated with ZnC. This finding suggests that Zn from ZnC may be less bioavailable than that from $ZnSO_4$ possibly due to the chelating property of carnosine in ZnC. However, bioefficacy effects in terms of genome stability were not dissimilar between the two forms of Zn. It is possible that carnosine from ZnC may have contributed to the protective effects of this compound and could explain why ZnC was as efficacious as $ZnSO_4$ despite a lower cellular Zn concentration; this is discussed in further detail below. Further work to measure labile Zn in the culture medium and within the cells will be conducted to determine the difference of Zn uptake in both Zn compounds using molecular probes of free Zn such as Zinquin [34].

Findings from this study suggest that supplementation with Zn at 4 µM and 16 µM proved to be most beneficial in reducing genomic instability, as well as potentially providing a protective effect in cells exposed to ionising radiation. Both deficient (Zn depleted medium, 0 µM) and the higher concentrations of Zn (32 and 100 µM) were found to induce elevated levels of cell death and DNA strand breaks suggesting a U-shaped dose response. It is known that the physiological range for Zn is between 2-15 µM and the pharmacological range is between 15-100 µM [31]. In this study, we found that physiological concentrations of Zn had beneficial effects on the genomic stability of WIL2-NS cells, whereas, lower concentration of Zn and maximal pharmacologic concentration of 100 µM, Zn appeared to adversely affect several parameters of cellular health. For example, treatment of WIL2-NS cells with Zn compounds at a concentration of 100 µM was shown to produce increased cytotoxic effects resulting in reduced viability as shown by the MTT assay. This finding is in contrast to that reported by Sliwinski and colleagues (2009) [100] who showed that $ZnSO_4$ at 100 µM did not affect the viability of normal human lymphocytes suggesting that sensitivity to Zn toxicity may be dependent on cell type. Zn depleted cells in our study were shown to have a reduced cell viability compared to cells that were supplemented with either $ZnSO_4$ or ZnC. Both apoptosis and

necrosis were found to be significantly elevated in Zn deficient medium in our study. It has previously been shown that low cellular Zn concentrations induce programmed cell death in various cell types including fibroblasts, hepatocytes, T-cell precursors, glioma and testicular cells [35, 36, 80, 150, 151].

The mechanisms underlying the induction of apoptosis under conditions of Zn deficiency may involve the activation of Caspase 3, a cysteine protease responsible for cleaving various substrates in the apoptotic pathway including the key protein (poly (ADP ribose) polymerase (PARP)) [152], a DNA-binding enzyme which catalyses the post-translational poly(ADP-ribosyl)ation of proteins. However, no cleavage of Caspase 3 fragments was observed in western blot analysis. This could be due to the fact that WIL2-NS cells are known to have a mutation in codon 237 of the p53 gene leading to dysfunctional protein and causing a reduced apoptotic response to DNA damage events [144]. WIL2-NS cells with genome damage that would normally be eliminated through apoptosis may proceed through the cell cycle and survive to express micronuclei in binucleated cells. This may explain the findings that show a lower percentage of apoptosis cells (1-6%) relative to necrotic cells (9-30%) observed in the CBMN-Cyt assay.

Interestingly, we also observed higher levels of cleaved PARP in Zn depleted cells, however, the increase was not strong. Our result is consistent with another study by Song *et al* (2009) where they found PARP expression is slightly increased with Zn deficiency. The response of PARP to Zn depletion could alter the overall base excision repair pathway which leads to accumulation of DNA damage [43] as observed in this present study (higher frequency of MNi, NPB and NBuds, higher DNA strand breaks). The higher DNA damage levels observed in Zn deficient cells can be explained by the role of this element in PARP activity. Zn is an essential component for PARP-1, which binds via its Zn domain to DNA strand breaks and thereby assists in the recruitment of DNA repair complexes [153]. A previous study reported a positive correlation between cellular poly(ADP-ribosyl)ation and Zn status in human peripheral blood mononuclear cells [39], further suggesting that Zn plays a pivotal role in maintaining genome integrity and stability [13].

To investigate the effects of Zn deficiency or excess on DNA damage induction, we used the CBMN-Cyt assay and the alkaline comet assay to obtain a comprehensive and complimentary assessment of the induced DNA damage profile. The alkaline comet assay provides a measure of single and double strand breaks in DNA that are induced but remain unrepaired. In contrast, micronuclei and nucleoplasmic bridges occur due to mis-repair of DNA strand breaks which leads to formation of acentric chromosome fragments and dicentric chromosomes from which they originate respectively. The results from this study suggest that low intracellular Zn generates an increase in DNA strand break frequency compared to Zn supplemented cells. It is well documented that Zn depleted cells have a higher rate of DNA damage as measured by the comet assay [36, 43, 80, 94, 154]. In the current study, it was found that additional Zn even at 0.4 μM can reduce both tail moment and tail intensity values. Higher concentrations of Zn further reduced DNA strand breaks (4 and 16 μM) but at the highest concentration tested (32 μM), increases in DNA strand breaks were observed suggesting a potential genotoxic effect for both Zn compounds when present in excess. In addition, we also found that Zn depleted cells showed higher levels of γ-H2AX which is a sensitive molecular marker for DNA strand breaks [155]. These results provide further evidence of the important role of Zn in maintaining DNA integrity.

Findings on baseline DNA damage measured in the CBMN-Cyt assay showed that Zn depleted cells expressed a higher frequency of MNi, NPBs and NBuds while Zn supplemented cells showed significant reductions in DNA damage. To our knowledge, this is the first cytogenetic study to investigate the effects of various concentrations of Zn on MNi, NPBs and NBuds expression simultaneously in WIL2-NS cells. An earlier study in 2002, showed the efficiency of cytokinesis-block micronucleus assay as a means to evaluate the genotoxic effects of Zn excess [91]. This study found a significant increase in micronucleated cytokinesis-blocked cells (MNCBs) in Zn-chloride-treated cells compared to the negative control. Recent research also showed that excess of Zn acetate can induce significant increases of both MNi and sister chromatid exchange in bone marrow cells in an Algerian mouse

model [101]. The results from our study suggest a narrow physiological concentration range of Zn between 4 μM and 16 μM for optimising chromosomal stability.

The increase of NPBs observed with Zn deficiency may be due to DNA break mis-repair or telomere end fusion, possibly caused by accelerated telomere shortening. Telomere stability has been shown to correlate with the risk of cancer [106, 156-160] and zinc status [99, 109, 161]. Recent research in humans has shown that accumulation of cells with short telomeres is associated with reduced Zn status [110]. It is plausible that optimal Zn concentrations may reduce genomic instability events and the risk of cancer by enhancing telomere stability and limiting the rate of telomere shortening [106, 108]. This may lead to reduced formation of dicentric chromosomes which are expressed as NPBs [162]. Future investigations examining the relationship between Zn and telomere length will be required to either confirm or refute these potential mechanisms. The use of centromeric and telomeric probes in combination with the CBMN-Cyt assay in future studies may enhance mechanistic information by allowing discrimination between MNi originating from acentric fragments or lagging whole chromosomes and between NPB originating from telomere end fusions or from those due to dicentric chromosomes caused by mis-repair of double strand breaks in DNA [84].

The elevated frequency in DNA damage biomarkers in Zn depleted cells observed in this study may be a result of increased DNA oxidation and/or DNA breaks and elevated chromosome damage rates [14]. In recent studies, low intracellular Zn was shown to affect DNA damage, oxidative stress, antioxidant defence and DNA repair in rats [43]. Zn is involved in both base excision repair and nucleotide excision repair where Zn finger and Zn associated proteins play an important role [13]. Zn is part of OGG1 which is another DNA repair enzyme that plays an important role in base excision repair by removing 8-hydroxyl-2'-deoxyguanosine, one of the more prevalent oxidative DNA damage events [41]. This present study showed that OGG1 expression is significantly increased in Zn depleted

cells suggesting that oxidative stress is one of the mechanisms by which Zn deficiency may cause DNA damage.

Our results also suggest that the optimal radioprotective effect of Zn occurs in the 4-16 µM range as measured via the CBMN-Cyt assay. These observations are in agreement with other studies showing that Zn can be protective against the harmful cellular and physiological effects of radiation [54, 163-167]. Zn concentration at 16-32 µM was optimal in reducing cytotoxicity and DNA damage biomarkers after treatment with H_2O_2. However, more necrotic cells were observed in our experiments with H_2O_2 treatment. This is in agreement with a previous study by Fenech *et al* (1999) that showed that the main event induced by H_2O_2 in G_0 lymphocytes is necrosis and not MN formation [168]. Previous studies showed similar results to our study where they found that pre treatment with Zn was shown to have a protective effect against H_2O_2 induced cytoxicity [29, 169, 170]. Interestingly, simultaneous exposure to Zn and H_2O_2 was shown to exacerbate oxidative damage [29, 170].

One of the possible mechanisms underlying this genome-protective effect is the involvement of Zn in the regulation of metallothionein [14]. It is known that Zn can modulate the expression of metallothionein (MT), which is one of the important metalloenzymes involved in cellular defence against free radicals and oxidative stress [13]. Our baseline data showed that MT expression is decreased in Zn-depleted cells indicating low antioxidant defence systems against oxidative insult. Previous studies have shown that cells with low levels of MT are more susceptible to DNA damage and apoptotic cell death following exposure to stress stimuli, including oxidative stress, whereas prior induction of MT appears to offer cellular protection [30, 53, 171, 172].

Besides MT, Zn can also protect against oxidative damage via Fenton type reactions where less redox active Zn displaces bound iron from macromolecules and thus reduce the OH radical production. An *in vitro* study showed that as intracellular Zn concentration increased, more iron was displaced and less OH radical-driven DNA

damage was evident [173]. In addition, Zn is also part of Cu/Zn SOD which is one of the main defence enzymes against ROS. Further investigation possibly via knock-down of key genes coding for Zn-induced or Zn-requiring proteins is necessary to determine the critical role of Zn in anti-oxidant cellular mechanisms.

In this current study, only a small difference in the response to DNA damage between $ZnSO_4$ and ZnC was observed. Interestingly, this was despite lower intracellular Zn in cells grown in ZnC medium relative to $ZnSO_4$. Involvement of carnosine may contribute to these observed effects due to its action as a natural antioxidant. Derived from the amino acids β-histidine and L-alanine, carnosine has been shown to protect against radiation and promote wound healing [174-178]. Several mechanisms are suggested in relation to the antioxidant properties of carnosine ie. a) its chelating action against metal ions; b) superoxide-dismutase (SOD)-like activity, and; c) ROS and free radical scavenging [179-181]. We therefore cannot exclude the possibility that some of the genome protective effects of ZnC observed in our experiments may have been due to carnosine rather than Zn and future studies will require the inclusion of carnosine as a control to test this possibility.

In conclusion, both $ZnSO_4$ and ZnC were shown to provide optimal cell viability and minimal DNA damage as well as improved resistance to γ-radiation-induced and H_2O_2 – induced genome damage at 4 - 32 μM Zn concentration. Higher concentrations of Zn (32 and 100 μM) or Zn deficiency (=< 0.4 μM) may cause severe cytotoxic and genotoxic effects. It is evident that more attention should be given to Zn levels in culture medium which should be carefully maintained at an optimal concentration to maintain genome stability. Whether the optimal concentration of Zn should be determined for each specific cell line needs to be tested as it is quite possible that requirements may vary depending on genotype.

Chapter 4

Zinc Deficiency or Excess within the Physiological Range Increases Genome Instability and Cytotoxicity, respectively, in Human Oral Keratinocyte Cells

Sharif, R.[1,2,3], Thomas, P.[1], Zalewski, P.[2] & Fenech, M.[1]

[1]CSIRO Food and Nutritional Sciences, Adelaide, Australia

[2]School of Medicine, Faculty of Health Sciences, University of Adelaide, Adelaide, Australia

[3]Nutrition Program, Faculty of Health Sciences, Universiti Kebangsaan Malaysia, Malaysia

Genes Nutrition. 2011

Statement of Authorship

Zinc Deficiency or Excess within the Physiological Range Increases Genome Instability and Cytotoxicity, respectively, in Human Oral Keratinocyte Cells

Razinah Sharif

Performed analysis on all samples, interpreted data, wrote manuscript and contributed to planning of article

Signed ……. Date ……

Philip Thomas

Supervised development of work, helped in data interpretation, contributed to planning of article and provided critical evaluation of the manuscript

Signed ……. Date ……

Peter Zalewski

Supervised development of work, helped in data interpretation, contributed to planning of article and provided critical evaluation of the manuscript

Signed ……. Date ……

Michael Fenech

Supervised development of work, helped in data interpretation, contributed to planning of article and provided critical evaluation of the manuscript and acted as corresponding author

Signed ……. Date ……

Chapter 4

Zinc Deficiency or Excess within the Physiological Range Increases Genome Instability and Cytotoxicity, respectively, in Human Oral Keratinocyte Cells

---

4.1 Abstract

Zinc (Zn) is an essential component of Zn finger proteins and plays a role as a cofactor for enzymes required for cellular metabolism and the maintenance of DNA integrity. This study investigated the genotoxic and cytotoxic effects of Zn deficiency or excess in a primary human oral keratinocyte cell line and determined the optimal concentration of two Zn compounds, Zn Sulphate ($ZnSO_4$) and Zn Carnosine (ZnC) to minimize DNA damage. Zn deficient medium (0 µM) was produced using Chelex treatment, and the two Zn compounds, $ZnSO_4$ and ZnC were tested at concentrations of 0.0, 0.4, 4.0, 16.0, 32.0 and 100.0 µM. Cell viability was decreased in Zn depleted cells (0 µM) as well as at 32 µM and 100 µM for both Zn compounds (*p<0.0001*) as measured via the MTT assay. DNA strand breaks, as measured by the comet assay, were found to be increased in Zn depleted cells compared to the other treatment groups (*p<0.05*). The Cytokinesis Block Micronucleus Cytome assay showed a significant increase in the frequency of both apoptotic and necrotic cells under Zn deficient conditions (*p<0.05*). Furthermore, elevated frequencies of micronuclei (MNi), nucleoplasmic bridges (NPBs) and nuclear buds (NBuds) were observed at 0 and 0.4 µM Zn whereas these biomarkers were minimised for both Zn compounds at 4 µM and 16 µM Zn (*p<0.05*), suggesting these concentrations are optimal to maintain genome stability. The potential protective effect of $ZnSO_4$ and ZnC was also investigated following exposure to 1.0 Gy γ-radiation and a 30 µM hydrogen

peroxide (H_2O_2) challenge. The frequency of MNi, NPBs and NBuds were not measurable due to the irregular shape of cells and a higher frequency of necrotic and mononucleated cells. Expression of PARP, p53 and OGG1 measured by western blotting were increased in Zn depleted cells indicating that DNA repair mechanisms were activated. These results suggest that maintaining Zn concentrations within the range of 4-16 µM is essential for DNA damage prevention in cultured human oral keratinocytes.

4.2 Introduction

Extensive research has been undertaken to investigate the effect of zinc deficiency on DNA damage events in both *in vitro* and *in vivo* systems [35, 36, 43, 80, 94, 154]. However, little is known on the effect of zinc concentration on epithelial cells within the buccal mucosa. Buccal cells can be easily obtained in a minimally invasive manner and have been used extensively in human *in vivo* studies investigating the genotoxic effects of environmental and life style factors [182-191]. Determining the nutritional requirements for optimal genome integrity in human tissue is a high priority for disease prevention as risk for developmental and degenerative diseases increases with elevated rates of genetic damage [83]. However, the mineral micronutrient requirement for DNA damage prevention in ectodermal tissues such as the buccal mucosa is virtually unexplored.

In order to better understand the effect of Zn on genome integrity in buccal cells, Human Oral Keratinocyte (HOK) primary cells were used as a model [132]. Oral keratinocytes play a major role in cell protection by providing a major barrier to physical, microbial, and chemical agents that may potentially cause local cell injury. Their involvement in proinflammatory processes results in the production of cytokines either constitutively or after a variety of stimuli [192], implying that they may potentially participate in controlling oral infections through an inflammatory process involving different interleukins, such as IL-1ß and IL-18 [193]. Oral keratinocytes express a variety of differentiation markers, which are influenced by calcium-induced changes in the transcription of target genes [194]. These cells share

major structural and functional features as well as same gene expression patterns with the well-characterized dermal keratinocytes and provide a suitable model for cells of the buccal mucosa [132].

To date, there are no studies on the effect of Zn on genomic stability in primary HOK cells even though Zn is recognised as one of the key minerals that is essential in maintaining DNA integrity [13, 14]. The Cytokinesis Block Micronucleus Cytome (CBMN-Cyt) assay has been identified as currently the best validated biomarker of DNA damage and cytotoxocity that is sensitive to nutritional status as well as being associated with and predictive of degenerative diseases [83]. Thus, this assay was chosen as the primary outcome measure to investigate the potential genomic stability effects of Zn, depending on its concentration and its source compound. To provide some insight into potential molecular mechanisms the expression of important DNA damage response proteins was measured such as γ-H2AX, Caspase 3, p53, PARP and OGG1 [14] and metallothionein was investigated as a biomarker for Zn status [195].

In this present study, it was hypothesized that both deficiency and excess of Zn could cause DNA damage and cytotoxicity, and the effect of Zn on these DNA damage events may be different depending on the different chemical forms. In addition, we aimed to define the optimal concentrations of Zn for genome stability of cultured human oral keratinocytes and to identify those biomarkers in the CBMN-Cyt assay that are most sensitive to alterations in Zn concentration. A secondary aim was to determine the potential protective effects of these compounds against genomic damage induced by ionising radiation and H_2O_2 treatment.

In order to test these hypotheses, two Zn compounds were compared; Zinc Sulphate ($ZnSO_4$) as the most commonly used form of Zn in research studies and Zinc Carnosine (ZnC) as a novel form of Zn that is increasingly being used as a dietary supplement possessing health promoting effects for gastrointestinal function [135].

4.3 Materials and Methods

4.3.1 HOK cell culture and study design

HOK cells are human oral keratinocytes isolated from the normal human oral mucosa, and were obtained from the ScienCell Research Laboratories (Cat No 2610; ScienCell, Ca, USA) (Figure 4.1). Cells were cultured in Oral Keratinocyte Medium (OKM) which is a complete medium for optimal growth of normal human oral keratinocytes *in vitro*. OKM consists of 500 ml of basal medium, 5 ml of oral keratinocyte growth supplement (OKGS, Cat. No. 2652 ScienCell Research Laboratories, Ca, USA) and 5 ml of penicillin/streptomycin solution (P/S, Cat. No. 0503, ScienCell Research Laboratories, Ca, USA). The medium is serum-free, HEPES and bicarbonate buffered with a pH of 7.4. Cells were cultured in T75cm^2 flasks coated with poly-L-lysine (Sigma, USA) solution in an incubator at 37°C in a 5% CO_2 humidified atmosphere. HOK cells were cultured in 500 µl volumes in 24 well plates (Thermo Fisher Scientific, NY, USA) at an initial density of 2 X 10^3 cells/ml (based on growth curve) for 9 days and the medium was replaced every 3 days (Figure 4.2). Viable cell counts were performed via a trypan blue exclusion assay as described previously [196]. For all experiments, cells were cultured in Zn-depleted medium (0 µM) to which $ZnSO_4$ (Sigma Aldrich St. Louis, MO, USA) or ZnC (Hamari Chemicals Osaka, Japan) was added to obtain Zn concentrations of 0.4, 4.0, 16.0, 32.0 and 100.0 µM. Zn depleted medium was prepared as follows : HOK medium was mixed with 10% Chelex-100 (Sigma, St. Louis, MO, USA) for two hours and the cycle of depletion was repeated again for another 4 hours. The chelex-treated medium was filter-sterilised prior to use in cultures.

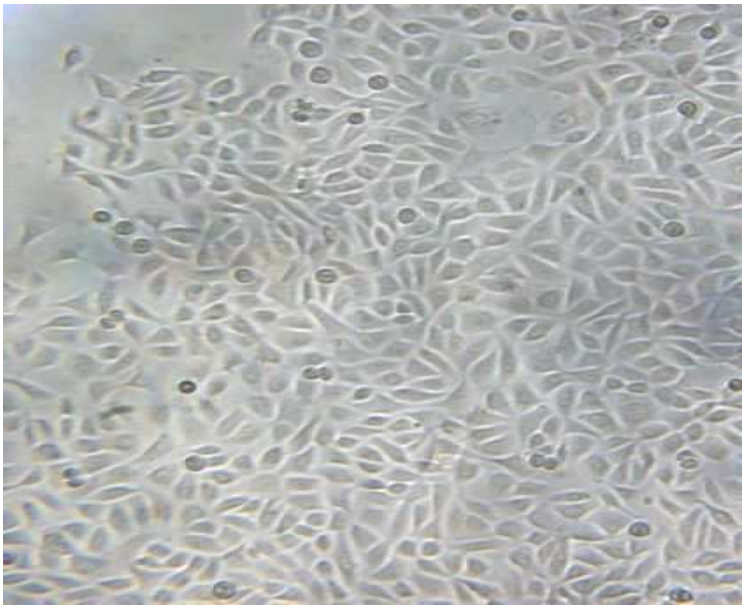

Figure 4.1: Photomicrograph of human oral keratinocyte cell line (X40)

4.3.2 Cell counting using the Coulter Counter

Cell count was measured using a Coulter Counter (Z1 Coulter® Particle Counter, Beckman Coulter, USA). The count of each sample was taken in duplicate and the mean value of samples containing cells measured. The mean of blank counts was substracted from the mean cell count before calculating the cell concentration. Cell concentration (cells/ml) was determined by multiplying the value by 2000 (dilution factor 1000 and counting volume of 0.5 ml).

4.3.3 Culture medium

For all experiments, cells were cultured in Zn-depleted medium (0 µM) to which $ZnSO_4$ (Sigma Aldrich St. Louis, MO, USA) or ZnC (Hamari Chemicals Osaka, Japan) was added to obtain Zn concentrations of 0.4, 4.0, 16.0, 32.0 and 100.0 µM. Zn depleted medium was prepared as follows : HOK medium was mixed with 10% Chelex-100 (Sigma, St. Louis, MO, USA) for two hours and the cycle of depletion was repeated again for another 4 hours. Mineral levels and Zn levels were measured by inductively coupled plasma optical emission spectrometry (ICPOES).

Because chelex-100 is chelating not just Zn, we determined the mineral level and added Fe, Ca, and Mg as according to the Table 4.1:

Table 4.1: Preparation of additional mineral mix to the chelated culture medium (per 500 ml)

Mineral	Amount (mg)
Iron (Fe)	0.85
Calcium (Ca)	14.67
Magnesium (Mg)	131.85

Calculations for preparing a total final volume of 500 ml culture medium are specified in Table 4.2.

Table 4.2: Preparations of Zn chelated medium (500 ml)

Solutions	Volume (ml)
HOK chelated medium	490
Oral keratinocyte growth supplement	5
Penicillin/Streptomycin solution	5

Calculations for preparing a total final volume of 20 ml culture medium with different Zn concentrations are specified in Table 4.3.

Table 4.3: Preparations of culture medium with varying Zn concentrations (20 ml)

Treatment	0	0.4	4	16	32	100
HOK Chelated medium (µl)	20 000	19 992	19 996	19 984	19 968	19 900
$ZnSO_4$ or ZnC (1 mM) (µl)	-	8				
$ZnSO_4$ or ZnC (20 mM) (µl)			4	16	32	100

pH of the medium was checked and no changes in pH was observed in each culture medium with different Zn concentrations.

4.3.4 10-day HOK culture in 24 well plates

HOK cells were cultured for 9 days (Figure 4.2) in 24 well plates (NUNC flat bottom, sterile with lid, 500 µl per well) (Figure 4.3) with appropriate Zn-supplemented culture medium at an initial density of 2 X 10^3 cells/ml (based on growth curve) in 500 µl volume. The seeding concentration of HOK cells was determined in preliminary experiments aimed at optimising cell growth after 9 days. Cells were cultured in a humidified incubator at 37°C with 5% CO_2 (Sanyo MCO-17 AIC, Japan) for 9 days. On day 3 and 6, half of the culture medium was removed carefully without disturbing the cells and replaced with fresh culture medium with the same Zn concentration used on day 0. For the alkaline comet assay and CBMN-Cyt assay, HOK cells were cultured for 9 days as described above. On day 9, 100 µl of the cell suspension was trypsinized and transferred into eppendorf tubes for the alkaline comet assay and the rest of the cells used for the CBMN-Cyt assay as described in 4.3.8.

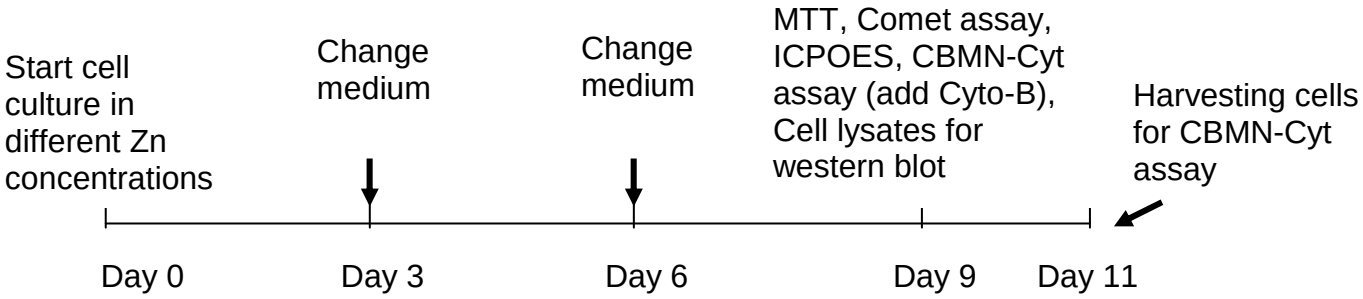

Figure 4.2: Schematic diagram for 10 day culture protocol of HOK cells testing for cytotoxic and genotoxic effects of Zn. HOK – Human Oral Keratinocytes; MTT - [3-(4,5-Dimethylthiazol-2-yl)-2,5-diphenyltetrazolium bromide]; ICPOES – Inductively Coupled Plasma Optical Emission Spectrometry; CBMN Cyt – Cytokinesis Block Micronucleus Cytome; Cyto-B – Cytochalasin B. The initial concentration of cells was 2 X 10^3 cells/ml on day 0 and cells were cultured in 500µl volumes.

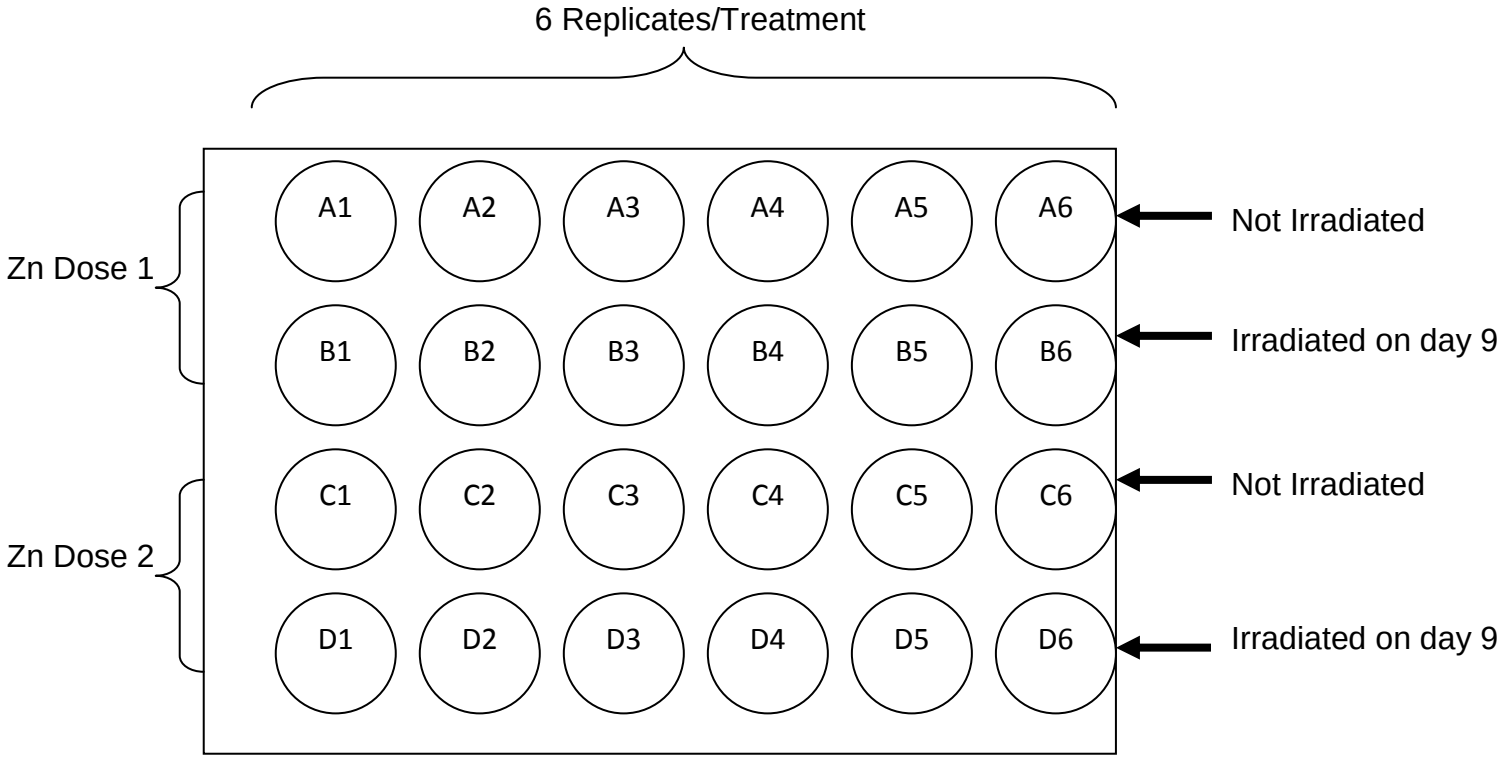

Figure 4.3: Schematic diagram of 24 well (500 µl) plate used for 9 day culture of HOK cells for alkaline comet assay and CBMN-Cyt assay. Two doses of Zn were studied on each plate and multiple plates used to study all doses and the two types of Zn compound.

All experimental data were based on six replicate measurements within each experiment and each experiment was repeated six times on separate days to ensure that the impact of intra- and inter-experimental variation was properly addressed.

4.3.5 Inductively coupled plasma optical emission spectrometry (ICPOES)

ICPOES was used to determine Zn levels both in media and within cells after culturing for 9 days. Analysis was conducted at the Waite Analytical Services (W.A.S. - School of Agriculture and Wine, University of Adelaide). Briefly, either 2 ml of medium or cell pellets (4 X 10^6 cells/ml) were incubated with 4% nitric acid and H_2O_2 in 50 ml polypropylene centrifuge tubes which were sealed using a secure lid (Greiner Bio-One, Germany). These specific tubes were used because we had previously verified that they do not contaminate samples with Zn that might otherwise be present in certain tubes. Samples were then diluted and analysed by

ICPOES as described previously with slight modification [145]. The intra- and inter-assay coefficient of variation (CV) for the Zn measurements was 9.18% and 10.59% respectively.

4.3.6 MTT cell growth and viability assay

The level of viable cells was measured using the MTT assay as described previously in section 3.3.6 (Chapter 3) [146]. Briefly, 100 µl of HOK cells (1 X 10^3 cells/ml) were cultured at different Zn concentrations for 9 days in 96-well plates (Thermo Fisher Scientific, NY, USA) coated with poly-L-Lysine (Sigma, St. Louis, MO, USA). Medium was changed on day 3 and day 6. 10 µl of MTT salt solution (5 mg/ml – Sigma, St. Louis, MO, USA) was added on day 9 to each well and incubated for 4 hours. Solubilizing solution [10% Sodium Dodecyl Sulphate (SDS) (Sigma, St. Louis, MO, USA)] in 0.01M HCl (BDH, Analar, England) was added to the plate and further incubated overnight at 37°C. Absorbance was read with an ELISA microplate reader (SpectraMax 250, Molecular Devices, CA, USA) and the difference in optical density at 650 nm and 570 nm measured. The intra- and inter-assay coefficient of variation (CV) for the MTT assay was 18.16% and 25.29% respectively.

4.3.7 Alkaline comet assay

Single cell gel electrophoresis (comet assay) was used to measure DNA strand breaks and alkaline labile sites in cells cultured for 9 days. The assay was conducted under alkaline conditions as previously described [147, 148] with slight modification for use with a high throughput CometSlide HT (Trevigen Inc. Cat 4252-02K-01). 100 µl cell suspension in 1% low melting point agarose was spread onto precoated high throughput Comet slides before being immersed in lysis buffer [100 mM EDTA disodium salt dehydrate (Sigma, St. Louis, MO, USA), 2.5 M NaCl (Sigma, St. Louis, MO, USA), 10 mM Trizma base (Sigma, St. Louis, MO, USA), 1% Triton X-100 (Sigma, St. Louis, MO, USA), pH adjusted to 10.0], for 1 h at 4°C. Slides were incubated in ice-cold alkaline electrophoresis buffer [1 mM EDTA (Sigma, St. Louis, MO, USA), 300 mM NaOH (Sigma, St. Louis, MO, USA), pH adjusted to 13.0] for 20 minutes.

Electrophoresis was then conducted at 25V, 350 mA for 20 minutes in the same alkaline buffer in a horizontal Comet assay electrophoresis tank (Thistle Scientific). Slides were washed (3 times with neutralization buffer – 0.4 M Tris-HCl, pH adjusted to 7.5), drained and immersed in 70% ethanol for 5 minutes and air dried at room temperature overnight. Staining was performed using Propidium Iodide solution (Sigma, St. Louis, MO, USA - 50 ug/ml in Phosphate Buffer Saline) for 10 minutes. The above procedures were performed under subdued light conditions using UVA and UVB fliters on fluorescent lamps to avoid light-induced DNA strand breaks. Nuclei with/without DNA damage were observed at 20X magnification under an Eclipse fluorescence microscope (Nikon, Tokyo, Japan) with a triple band filter (excitation wavelength of 530 nm and emission wavelength of 615 nm) and captured with an attached Spot video camera (Diagnostic Instrument Inc.; Model – 254015, USA). 100 cells were randomly selected from each spot and scored with online software (Tritek - http://autocomet.com/main_home.php) for tail moment and tail intensity. Tail moment (tail length X DNA density) and tail intensity (% DNA in tail) were used as indicators of DNA damage. The intra- and inter-assay CV for the tail moment measured was 21.49% and 32.22%, and for tail intensity was 12.63% and 17.94%, respectively.

4.3.8 CBMN-Cyt assay

In the CBMN-Cyt assay, DNA damage biomarkers are scored in cytokinesis-blocked binucleated cells. The DNA damage biomarkers scored are micronuclei (MNi, a biomarker for whole chromosome loss and/or chromosome breakage), nucleoplasmic bridges (NPBs, a biomarker or DNA misrepair and/or telomere to telomere end fusions) and nuclear buds (NBuds, a biomarker of gene amplification) [84]. Cytochalasin B (Sigma, St. Louis, MO, USA - 4.5 µg/ml) was added and cells further incubated for another 48 hrs (37°C, 5% CO_2). Cells were then harvested onto microscope slides on day 11 using a cytocentrifuge as per the manufacturer's instructions (Shandon Products, UK). Slides were air-dried for 10 mins, fixed in Diff-Quik fixative for 10 minutes and stained using Diff-Quik stains (Lab Aids, Australia).

A total of 3600 cells were scored per dose (treatment) (100 X 6 slides X 6 experiments) and classified to determine the ratios of mononucleate, binucleate (BN), multinucleate, apoptotic and necrotic cells. These ratios were used to determine the nuclear division index (NDI) which is a biomarker of cytostasis where cytostatic effects are readily estimated from the ratio of mono-, bi- and multinucleated cells. The NDI provides a measure of the proliferative status of the viable cell fraction. It is therefore an indicator of cytostatic effects and, in the case of lymphocytes, it is also a measure of mitogenic response, which is useful as a biomarker of immune function [84]. NDI is calculated according to the method of Eastmond and Tucker [197]. 500 viable cells are scored to determine the frequency of cells with 1, 2, 3 or 4 nuclei, and calculate the NDI using the formula NDI = (M1 + 2M2 + 3M3 + 4M4)/N, where M1–M4 represent the number of cells with 1–4 nuclei and N is the total number of viable cells scored (excluding necrotic and apoptotic cells). The NDI is a useful parameter for comparing the mitogenic response of lymphocytes and cytostatic effects of agents examined in the assay.

Cytotoxicity events were assessed by the frequency of necrotic and apoptotic cells. A total of 18 000 BN cells per dose (treatment) (500 X 6 slides X 6 experiments) were scored for genome damage indices (MNi, NPBs and NBuds).The scoring criteria for these cells are based on those originally described by Fenech (2007) [84]. Photomicrographs of the different cell types and nuclear anomalies scored in the CBMN-Cyt assay are shown in Figure 4.4. The intra-assay and inter-assay CV for CBMN-Cyt assay biomarkers in non-irradiated (NI) and irradiated (IR) cultures was as follows: Apoptotic cells (NI 23.82%, 48.73%; IR 40.10%, 191.54%); Necrotic cells (NI 31.63%; 45.56%; IR 182.75%, 374.37%); NDI (NI 2.19%, 5.23%; IR 29.48, 49.45%); MNi (NI 73.21%; 102.58%); NPB (NI 62.61%; 86.37%); and NBuds (NI 57.13%; 91.58%) respectively. For H_2O_2 treatment, the intra and inter-assay CV were as follows: Apoptotic cells (44.69%; 249.66%); Necrotic cells (109.73%; 237.76%); and NDI (8.03%, 10.15%). Frequency of MNi, NPB and NBuds for cells treated with γ-radiation and H_2O_2 treatment were not measurable due to irregular cell shape and sizes and a higher frequency of mononucleated cells and necrotic cells.

4.3.8.1 Scoring criteria

a) Criteria for scoring viable mono-, bi- and multinucleated cells

Frequency of viable mono-, bi-, and multinucleated cells is measured to determine cytostatic effects and the rate of mitotic divisions, which can be calculated using the nuclear division index. These cell types have the following characteristics:

- Mono-, bi- and multinucleated cells are viable cells with an intact cytoplasm and normal nucleus morphology containing one, two, three or more nuclei, respectively.
- They may or may not contain one or more MNi or NBuds and in the case of bi- and multinucleated cells they may or may not contain one or more NPBs.

Necrotic and apoptotic cells should not be included among the viable cells scored.

b) Criteria for scoring apoptotic cells

Apoptotic human oral keratinocytes cells are cells undergoing programmed cell death. They have the following characteristics:

- Early apoptotic can be identified by the presence of chromatin condensation within the nucleus and intact cytoplasmic and nuclear membranes.
- Late apoptotic cells exhibit nuclear fragmentation into smaller nuclear bodies within an intact cytoplasm/cytoplasmic membrane.
- Staining intensity of the nucleus, nuclear fragments and cytoplasm in both kinds of apoptotic cells is usually greater than that of viable cells.

c) Criteria for scoring necrotic cells

Necrosis is an alternative form of cell death that is thought to be caused by damage to cellular membranes, organelles and/or critical metabolic pathway required for cell survival such as energy metabolism. Necrotic cells have the following characteristics:

- Early necrotic cells can be identified by their pale cytoplasm, the presence of numerous vacuoled (mainly in the cytoplasm and sometimes in the nucleus), damaged cytoplasmic membrane and a fairly intact nucleus.
- Late necrotic cells exhibit loss of cytoplasm and damaged/irregular nuclear membrane with only a partially intact nuclear structure and often with nuclear material leaking from the nuclear boundary.
- Staining intensity of the nucleus and cytoplasm in both types of necrotic cell is usually less than that observed in viable cells.

d) Criteria for selecting BN cells suitable for scoring MNi, NPBs and NBuds

The cytokinesis-blocked BN cells that may be scored for MNi, NPBs and NBuds frequency should have the following characteristics:
- The cell should be binucleated.
- The two nuclei in a binucleated cell should have intact nuclear membranes and be situated within the same cytoplasmic boundary.
- The two nuclei in a binucleated cell should be approximately equal in size, staining pattern and staining intensity.
- The two nuclei within a BN cell may touch but ideally should not overlap each other. A cell with two overlapping nuclei can be scored only if the nuclear boundaries of each nucleus are distinguishable.
- The cytoplasmic boundary or membrane of a binucleated cell should be intact and clearly distinguishable from the cytoplasmic boundary of adjacent cells.

e) Criteria for scoring micronuclei

MNi are morphologically identical to but smaller than nuclei. They also have the following characteristics:
- The diameter of MNi in human oral keratinocytes usually varies between $1/16^{th}$ and $1/3^{rd}$ the mean diameter of the main nuclei, which corresponds to $1/256^{th}$ and $1/9^{th}$ of the area of one of the main nuclei in a BN cell, respectively.

- MNi are non-refractile and can therefore be readily distinguished from artefact such as staining particles.
- MNi are not linked or connected to the main nuclei.
- MNi may touch but not overlap the main nuclei and the micronuclear boundary should be distinguishable from the nuclear boundary.
- MNi usually has the same staining intensity as the main nuclei but occasionally staining may be more intense.

f) Criteria for scoring nucleoplasmic bridges

A NPB is a continuous DNA-containing structure linking the nuclei in a binucleated cell. NPBs originate from dicentric chromosomes (resulting from misrepaired DNA breaks or telomere end fusions) in which the centromeres are pulled to opposite poles during anaphase. They have the following characteristics:
- The width of a NPB may vary considerably but usually does not exceed $1/4^{th}$ of the diameter of the nuclei within the cell.
- NPBs should also have the same staining characteristics as the main nuclei.
- On rare occasions, more than one NPB may be observed within one binucleated cell.
- A binucleated cell with a NPB may contain one or more MNi.
- BN cells with one or more NPBs and no MNi may also be observed.

g) Criteria for scoring nuclear buds

NBuds represent the mechanism by which a nucleus eliminates amplified DNA and/or DNA repair complexes. NBuds have the following characteristics:
- NBuds are similar to MNi in appearance with the exception that they are connected with the nucleus via a bridge that can be slightly narrower than the diameter of the bud or by a much thinner bridge depending on the stage of the extrusion process.
- NBuds usually have the same staining intensity as MNi.
- Ocassionally, NBuds may appear to be located within a vacuole adjacent to the nucleus.

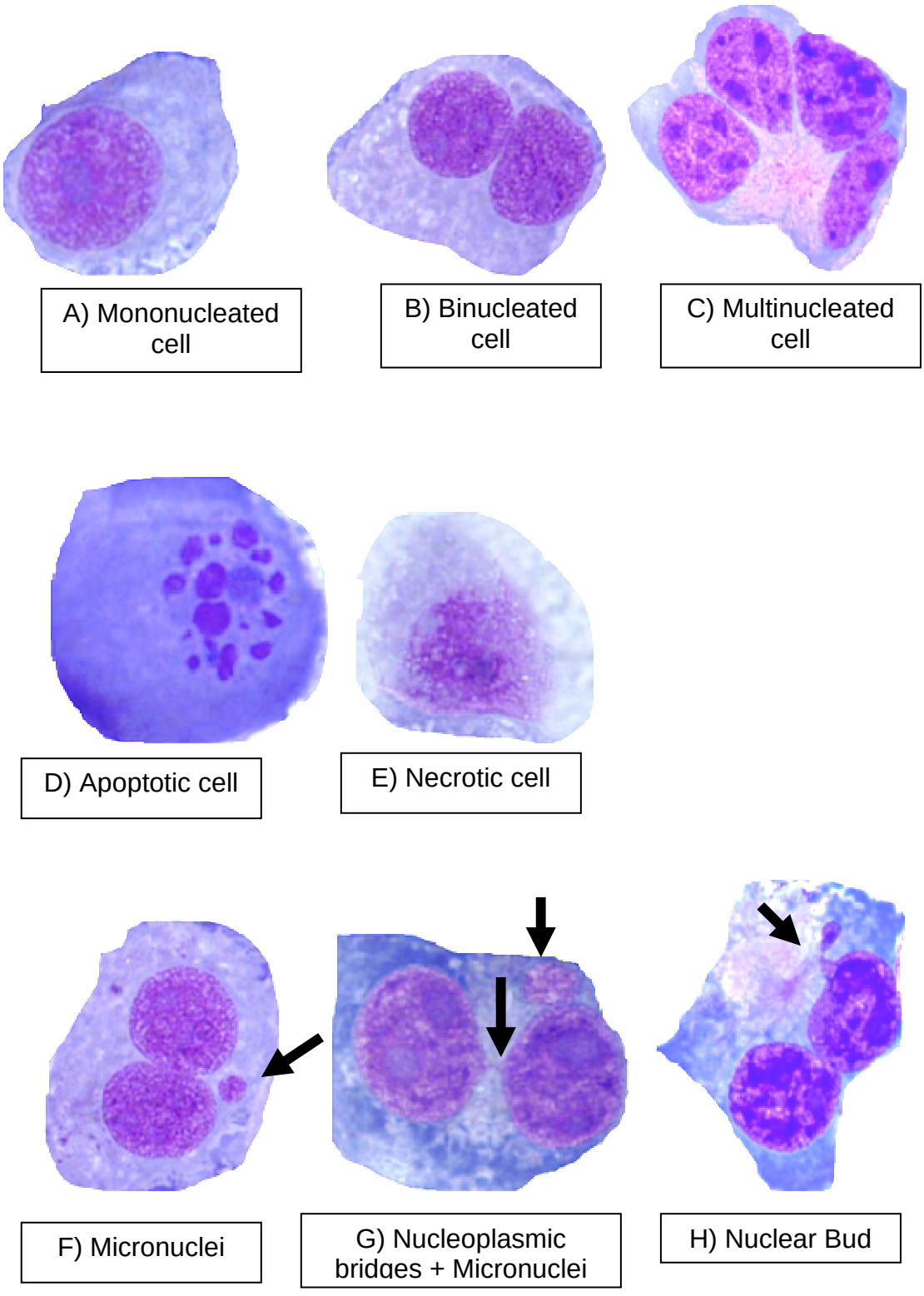

Figure 4.4: Photomicrographs of the human oral keratinocyte cells scored in the CBMN-Cyt assay (X1000); (**A**) mononucleated cell; (**B**) binucleated cell; (**C**) multinucleated cell; (**D**) apoptotic cell; (**E**) necrotic cell; (**F**) binucleated cell containing a micronucleus (indicated by arrow); (**G**) binucleated cell containing a nucleoplasmic bridge and a micronucleus (indicated by arrows); and (**H**) binucleated cell containing a nuclear bud (indicated by arrow).

4.3.9 Gamma-ray-irradiation of cells

After nine days in culture, 500µl of cell suspension per treatment was trypsinized and transferred into eppendorf tubes (Axygen Scientific Inc., USA). Samples were challenged with 1.0-Gy gamma radiation at room temperature (22°C) with a CIS BIO International IBL 437 blood-cell irradiator comprising three stationary ^{137}Cs double-encapsulated radiation sources emitting gamma-radiation at 5.3 Gy/min. Following irradiation, the 500µl suspensions were transferred into 24-well plates and incubated for 30 minutes at 37°C prior to addition of Cyto-B (Sigma, St. Louis, MO, USA—4.5µg/ml). Cells were harvested for scoring CBMN-Cyt assay biomarkers following a further 48 hour incubation period at 37°C in a 5%-CO_2, humidified atmosphere.

4.3.10 H_2O_2 treatment of cells

After nine days in culture, cells were challenged with or without 30 µM H_2O_2 solution (Sigma, USA) prior to the CBMN Cyt assay. Briefly, 30 µM of H_2O_2 solution was added to the cell culture and incubated at 37°C for 30 minutes prior to the CBMN Cyt assay.

4.3.11 Western Blotting

Cells were collected and transferred into a fresh eppendorf tube to be lysed. Preparation of cell lysis buffer is listed in Table 4.4.

Table 4.4: Preparation of working solution for cell lysis buffer. This buffer contains 50 mM HEPES, 100 mM Sodium Chloride (NaCl), 1% Triton X-100, 4 mM Sodium Pyrophosphate ($Na_4P_2O_7.10H_2O$), 2 mM Sodium orthovanadate *(*Na_3VO_4), 10 mM Sodium Fluoride (NaF).

Chemical	Initial Concentration (M)	Gram	Volume (ml)	ml to make lysis buffer (100 ml)
HEPES	0.5	2.383	20	10
NaCl	5	5.844	20	2
EDTA - pH 8	0.125	2.921	80	8
$Na_4P_2O_7.10H_2O$	0.1	0.892	20	4
Na_3VO_4	0.2	0.736	20	1
NaF	0.5	0.419	20	2
Triton X – 100	1 %		1	1

Cell lysis buffer was prepared in 80 ml of miliQ water (resistivity 18.2 Ω) and the pH was set to 7.5 with Sodium Hydroxide (NaOH). As the pH was set, extra miliQ water was added to make up to 100 ml of solution which was stored at 4°C. Just before use, phenylmethanesulphonylfluoride or phenylmethylsulphonyl fluoride (PMSF) was added to a final concentration of 1 mM and 1 tablet of protease inhibitor (1 tablet per 10 ml) was also added to the solution.

To prepare cell lysates, cells were spun for 1200 rpm for 5 minutes at 4°C and then washed with cold Phosphate Buffered saline (PBS). Cells were spun and washed twice more prior to the pellet being resuspended in 1 ml of lysis buffer and incubated for 30 minutes at 4°C. Cells were then spun at 14,000 rpm at 4°C for 15 minutes. Supernatant was transferred to fresh tubes and aliquoted to several tubes (50 µl/tube). Cell aliquots can be stored at -80°C until further use.

To determine the protein concentration for each of the cell lysates, a BCA assay was performed (Sigma, Australia). Cell aliquots were thawed from -80°C and lysis buffer was used as a diluent. To prepare standard curve dilutions, 100 µl of each standard was prepared and BSA at 1 mg/ml standard (Sigma, Australia) was used. Preparation of the standard curve dilutions is listed in Table 4.5.

Table 4.5: Preparations of standard curve dilutions for BCA assay

Conc. of standard (µg/ml)	Vol. of standard solution (µl)	Vol of diluent (µl)
1000	100	0
800	80	20
600	60	40
400	40	60
200	20	80
0	0	100

25 µl of a standard or sample (in triplicates) was added to 96 well plates. Subsequently, 200 µl of working reagent was added to each well (Reagent A and Reagent B from the BCA kit [Sigma, Australia]). The plate was then incubated at 37°C for 30 minutes and read at 562 nm using an ELISA microplate reader (SpectraMax 250, Molecular Devices, CA, USA). An example of a standard protein curve is shown in Figure 4.5.

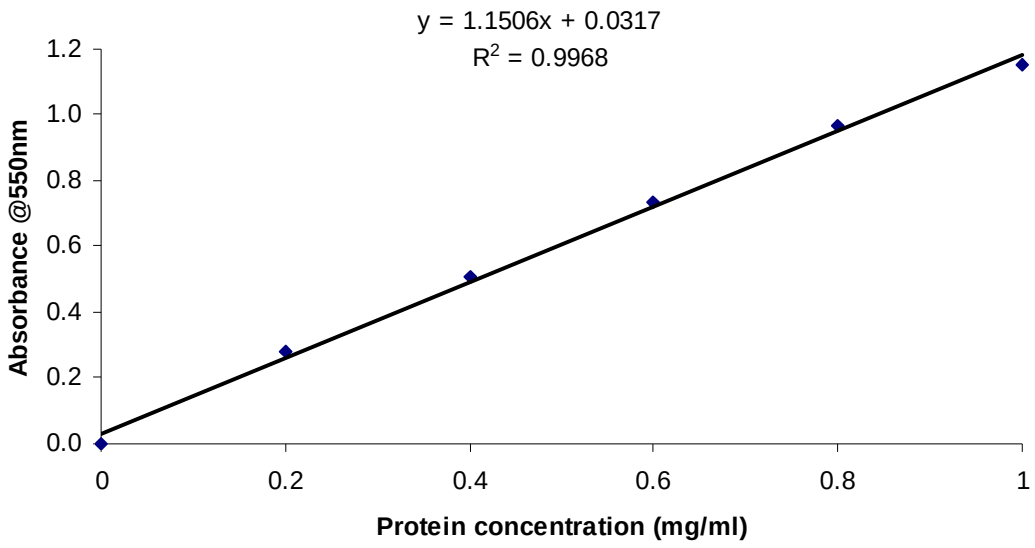

Figure 4.5: Standard curve for protein determination

Equal amounts of lysate protein (20 mg/lane) were separated using SDS-PAGE on a 4-12% bis-Tris gel (Invitrogen, CA, USA) and transferred to a nitrocellulose membrane (Amersham Hybond™ ECL™, GE Healthcare, UK). The membranes were probed with antibodies to specific proteins as follows: mouse anti-poly-ADP ribose polymerase (PARP; BD Pharmingen, CA, USA), rabbit anti-8-oxoguanine glycosylase

(OGG1; Novus Biologicals, USA), mouse anti-metallothionein (MT; Dako, Denmark), mouse anti γ-H2AX (Millipore, USA) and mouse anti β-actin (Sigma, St. Louis, MO, USA). Bound antibodies were detected using either goat anti-mouse IgG horseradish peroxidase or goat anti-rabbit IgG horseradish peroxidase (Dako, Denmark) and developed with Amersham™ ECL™ western blotting detection reagent (GE Healthcare, UK). Bands of interest were acquired using a luminescent image analyser LAS-4000 (FujiFilm, Tokyo, Japan) and quantification of Western blot analysis was done using Multi Gauge version 3.0 program (FujiFilm, Tokyo, Japan). The data is presented as a ratio of protein expression relative to β-actin. The intra-assay and inter-assay CV for protein expression were as follows: Caspase 3 (10.86%, 17.76%); Metallothionein (13.34%, 18.60%); PARP (14.14%, 16.69%); OGG1 (27.39%, 35.74%); p53 (7.36%, 10.19%); γ-H2AX (17.68%, 26.11%) respectively.

4.3.12 Statistical analysis

For each treatment, six replicate measurements were performed within each of six separate experiments performed on separate days (n=6) except for the H_2O_2 treatment where the experiments were performed in triplicate for only 3 separate experiments (n=3). The intra- and inter-assay CV was calculated for each biomarker based on these repeated measurements after combining data for each culture at each different Zn concentration, excluding those at 100µM Zn in which extreme cytotoxicity occurred. All end points measured were tested for Gaussian distribution by using the Kolmogorov–Smirnov test. One-way analysis of variance (ANOVA) followed by Tukey's *post hoc* tests for data with Gaussian distribution was performed to compare the effects of different Zn concentrations. The non-parametric Friedman test followed by Dunn's multiple comparison test was used for data that did not exhibit Gaussian distribution. Two-way ANOVA was used in this study to measure the difference in effects between $ZnSO_4$ and ZnC and the % variance for biomarker results that could be explained by Zn concentration and Zn compound used. Data are expressed as mean ± standard error with $P<0.05$ considered statistically significant. Statistical analyses were performed using Prism 5.0 (GraphPad Inc., San Diego, CA).

4.3.13 Optimization of cell growth for long term culture

The aim of this study was to determine the optimal starting cell concentration for a 9-day HOK cell culture. Cells were seeded in 96 well culture plates at different concentrations (0.15 X 10^5 cells/ml, 0.075 X 10^5 cells/ml, 0.0375 X 10^5 cells/ml and 0.01875 X 10^5 cells/ml). Cells were continuously cultured in a 96 well-microwell plate for 9 days and half of the culture medium was changed on day 3 and day 6. Cell proliferation was measured using the MTT assay as described in section 4.3.6. Figure 4.6 showed the HOK cell growth curve obtained.

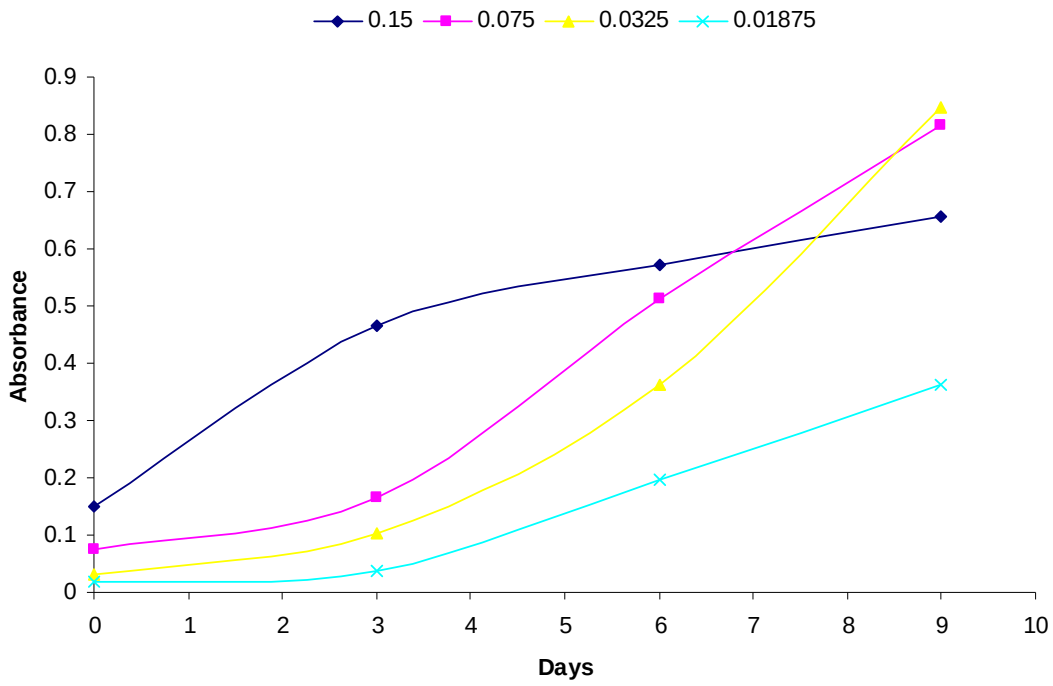

Figure 4.6: HOK cell growth curve following 9 day culture (n=3).

From the growth curve, 0.01875 X 10^5 cells/ml appeared to be one of the most optimal cell seeding density for HOK cells following 9 days culture. Considering cell number and volume required for all the assays and practicality of the protocol, the seeding concentration of 2 X 10^3 cells/ml was chosen as the optimal choice for the study.

4.3.14 Optimization of Cytochalasin B (Cyto B) concentration

The aim of this pilot study is to determine the optimal concentration of Cyto B for optimal number of binucleates with minimal number of necrotic cells. HOK cells were seeded in a 24 well plate (500 µl/ 2x10^3 cells/ml) for 9 days and medium was changed on day 3 and day 6. On day 9, different concentrations of Cyto B were added (4.5 µg/ml, 9.0 µg/ml and 18 µg/ml) and cells were harvested on different incubation time (after 24 hours, after 48 hours and after 72 hours). Binucleated cells, necrotic cells and NDI of the cells were reported as in Figure 4.7A-C. Based on Figure 4.7, 4.5 µg/ml of Cyto B and incubation time of 48 hours were chosen as the optimal concentration and incubation time for performing CBMN-Cyt assay.

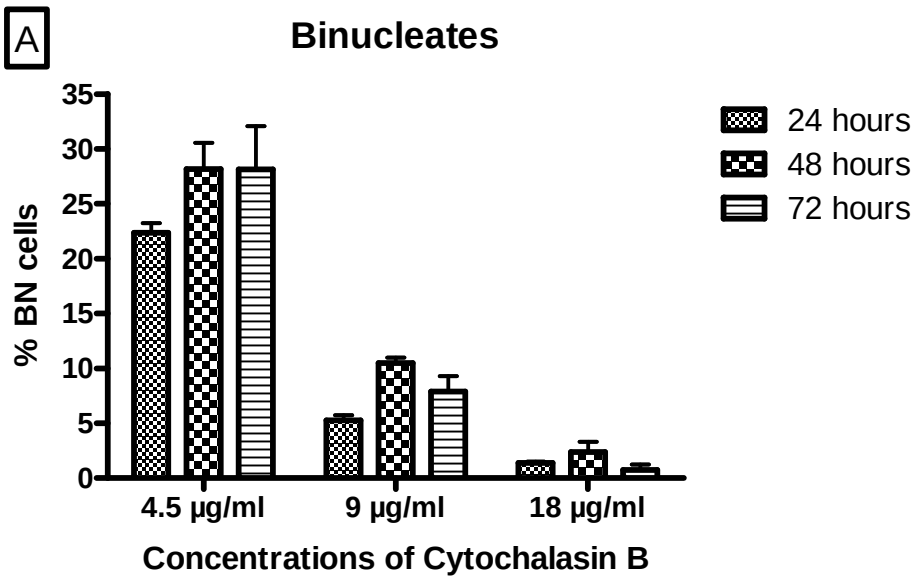

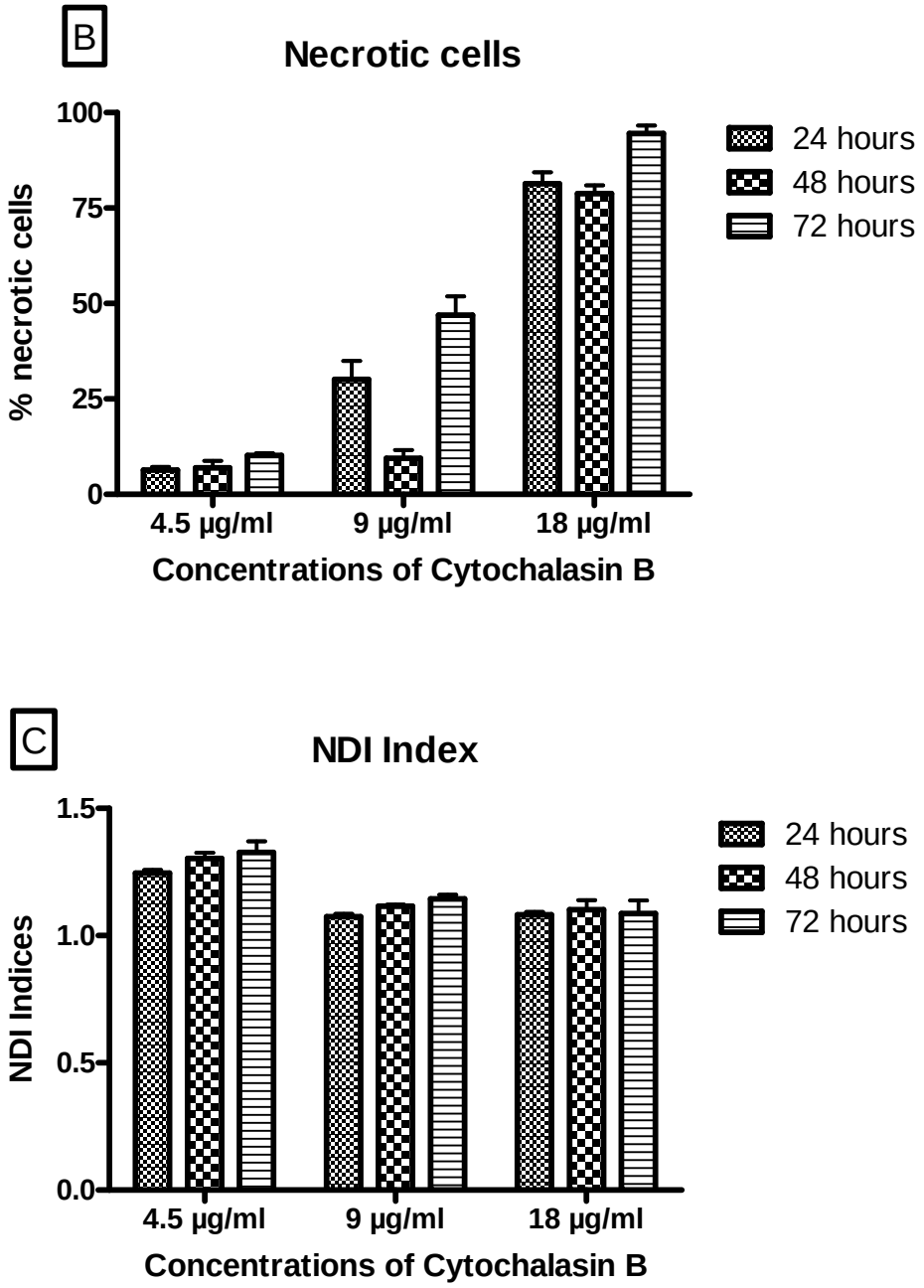

Figure 4.7: Optimization of Cytochalasin B. A) Binucleated cells; B) Necrotic cells; and C) Nuclear Division Index. Results shown are mean ± standard error (n=3).

4.4 Results

4.4.1 Cellular Zinc concentrations

Zn depleted cells showed a significant reduction in cellular Zn levels (*p<0.0001*) and there was no effect on other divalent metals (Copper and Iron) (Table 4.6). Cells supplemented with either $ZnSO_4$ or ZnC showed a significant dose related increase in cellular Zn (*p*<0.0001) with increased concentration of Zn in medium (Figure 4.8). The increment however, appeared to be slightly greater for $ZnSO_4$ relative to ZnC based on the observed trends and the associated % variance estimates (Effect of type of Zn compound: 1.47%, *p=0.0004*, Effect of concentration: 92.92%, *p*<0.0001).

Table 4.6: Levels of Iron, Copper, Magnesium and Calcium for various Zn concentrations. Abbreviations: ZS – Zinc Sulphate, ZC – Zinc Carnosine

Zinc Concentrations	**0 µM**	**ZS 0.4 µM**	**ZS 4 µM**	**ZS 16 µM**	**ZS 32 µM**	**ZC 0.4 µM**	**ZC 4 µM**	**ZC 16 µM**	**ZC 32 µM**
Iron (µg/million cells)	0.08 ± 0.00022	0.078 ± 0.00015	0.08 ± 0.00020	0.081 ± 0.00022	0.08 ± 0.00017	0.08 ± 0.00019	0.082 ± 0.00021	0.08 ± 0.00023	0.081 ± 0.00018
Copper (µg/million cells)	0.19 ± 0.00021	0.20 ± 0.00022	0.21 ± 0.00018	0.22 ± 0.00021	0.20 ± 0.00017	0.20 ± 0.00021	0.21 ± 0.00022	0.21 ± 0.00023	0.20 ± 0.00024
Magnesium (µg/million cells)	13.05 ± 0.00022	13.07 ± 0.00015	13.06 ± 0.00020	13.00 ± 0.00022	13.02 ± 0.00017	13.10 ± 0.00019	13.01 ± 0.00021	13.00 ± 0.00023	13.01 ± 0.00018
Calcium (µg/million cells)	4.05 ± 0.00022	4.00 ± 0.00015	4.02 ± 0.00020	4.00 ± 0.00022	4.03 ± 0.00017	4.00 ± 0.00019	4.05 ± 0.00021	4.05 ± 0.00023	4.01 ± 0.00018

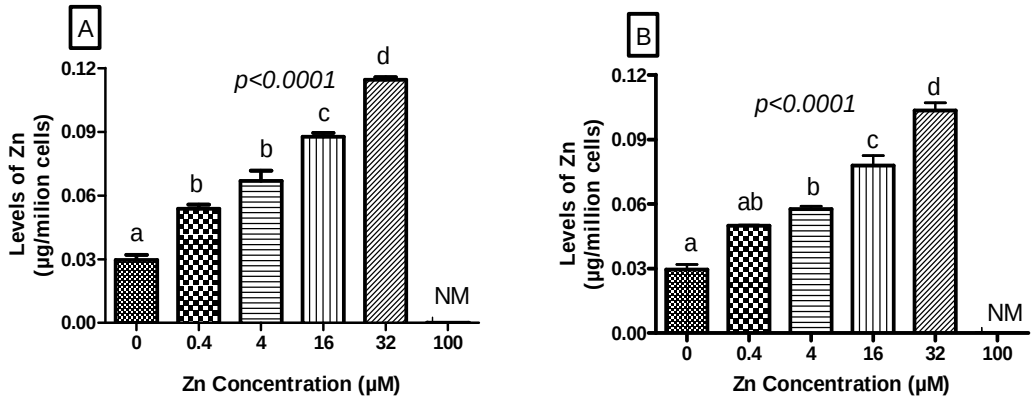

Figure 4.8: Concentration of intracellular Zn in HOK cells treated with (A) $ZnSO_4$ and (B) ZnC, at increasing concentrations of Zn. 0 µM represents cells grown in Zn depleted medium. Groups not sharing the same letter are significantly different to each other (*p* values refer to One way ANOVA analysis: *p<0.05*). Results shown are mean ± standard error (n=6). NM – Not measureable.

4.3.2 Effect of Zinc concentrations on cell viability as measured via the MTT assay

Figure 4.9A and 4.9B showed the effect of both ZnC and $ZnSO_4$ on HOK cells on different days (Day 0, Day 3, Day 6 and Day 9). No obvious effect was observed on day 3 and day 6 (except for 0 µM and 100 µM) while on day 9, the effect was more apparent. On day 9, a significant decrease in viable cells in Zn depleted cultures and with excess Zn ($p< 0.0001$) is shown in Figure 4.10A and 4.10B. Cell viability appeared to be optimal between the range 4 µM to 16 µM for both ZnC and $ZnSO_4$. At 32 µM both Zn compounds showed a significant decrease in viable cell number, and at 100 µM both Zn compounds exhibited severe cytotoxic effects (p<0.0001). Two way ANOVA analysis showed better viability for cells treated with $ZnSO_4$ compared to ZnC, at 4, 16 and 32 µM ($p<0.05$), but the greatest % variance was attributable to Zn concentration (Effect of type of Zn compound: 9.59%, $p<0.0001$, Effect of concentration: 68.63%, $p<0.0001$).

A

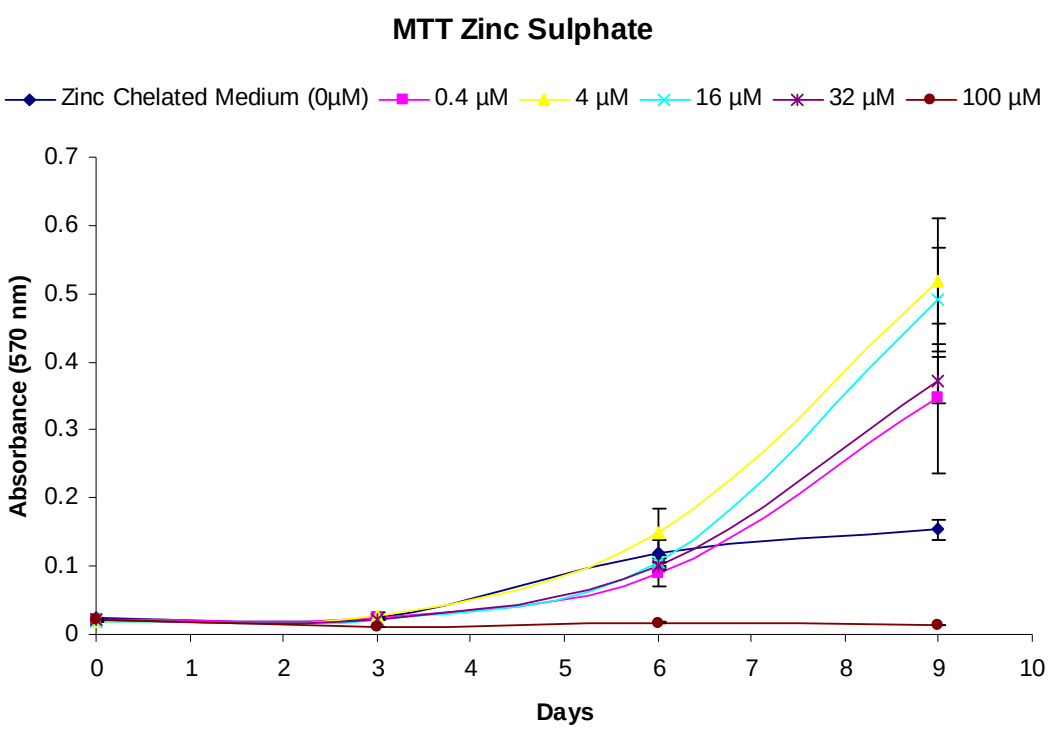

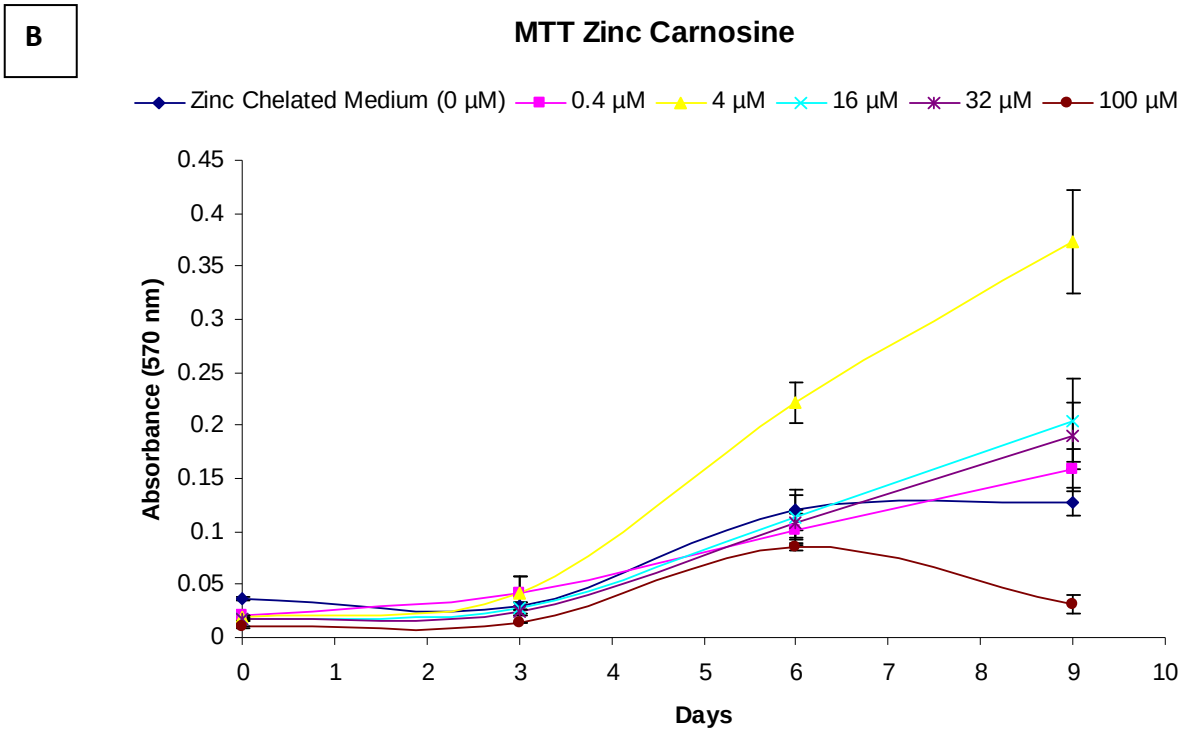

Figure 4.9: MTT assay absorbance of cells treated with (A) $ZnSO_4$ and (B) ZnC at increasing Zn concentration on different days (Day 0, Day 3, Day 6 and day 9). Results shown are mean ± standard error (n=6). MTT assay absorbance is directly correlated with cell growth and viability.

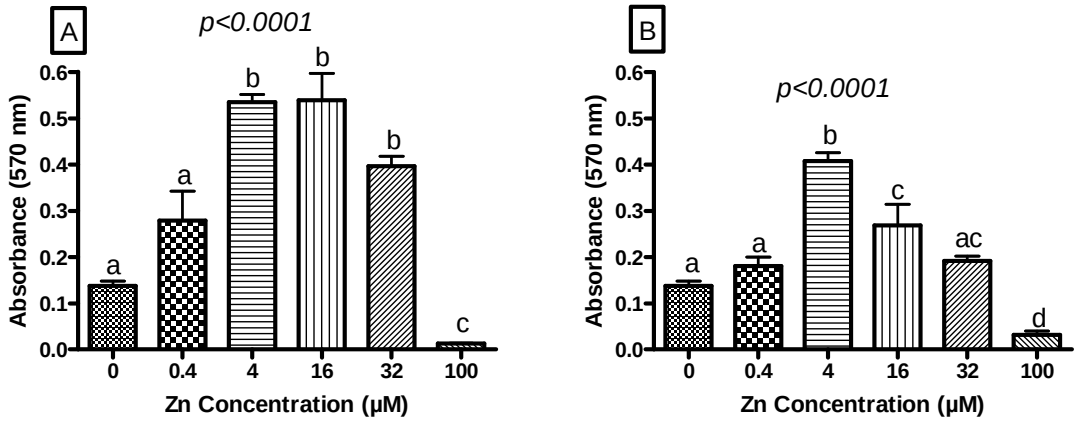

Figure 4.10: Level of viable cells in cultures treated with (A) $ZnSO_4$ and (B) ZnC at increasing Zn concentration measured via MTT assay. Groups not sharing the same letter are significantly different to each other (*p* values refer to One way ANOVA analysis: *p<0.05*). Results shown are mean ± standard error (n=6).

4.4.3 Effect of Zinc concentrations on DNA strand breaks as measured via the comet assay

Comet assay was used to determine DNA strand breaks and alkali-labile sites. DNA damage is often associated with cell death; therefore, it is critical that the highest dose tested should not induce excessive cytotoxicity. Hence, treatment with $ZnSO_4$ and ZnC at 100 µM was excluded as cell viability was less than 5%. Two endpoints were measured in this assay: tail moment (TM) and tail intensity (TI). TI represents percentage of DNA in the tail and TM represents a measure of tail length multiplied by the measure of DNA in the tail as a metric for DNA migration [149]. Figures 4.11A-D showed a significant increase in both TM and TI for Zn depleted cells (p<0.05). A reduction in both TM and TI was observed with increasing zinc concentrations. However, at 32 µM, values for TM and TI started to increase, suggesting a U-shaped dose response curve. There were no significant differences in values for both TM and TI for cells treated with $ZnSO_4$ or ZnC (Tail moment - Effect of type of Zn compound: 0.45%, *p=0.3950*, Effect of concentration: 66.70%, p<0.0001; Tail Intensity - Effect of type of Zn compound: 0.01%, *p=0.9121*, Effect of concentration: 55.87%, *p<0.0001*).

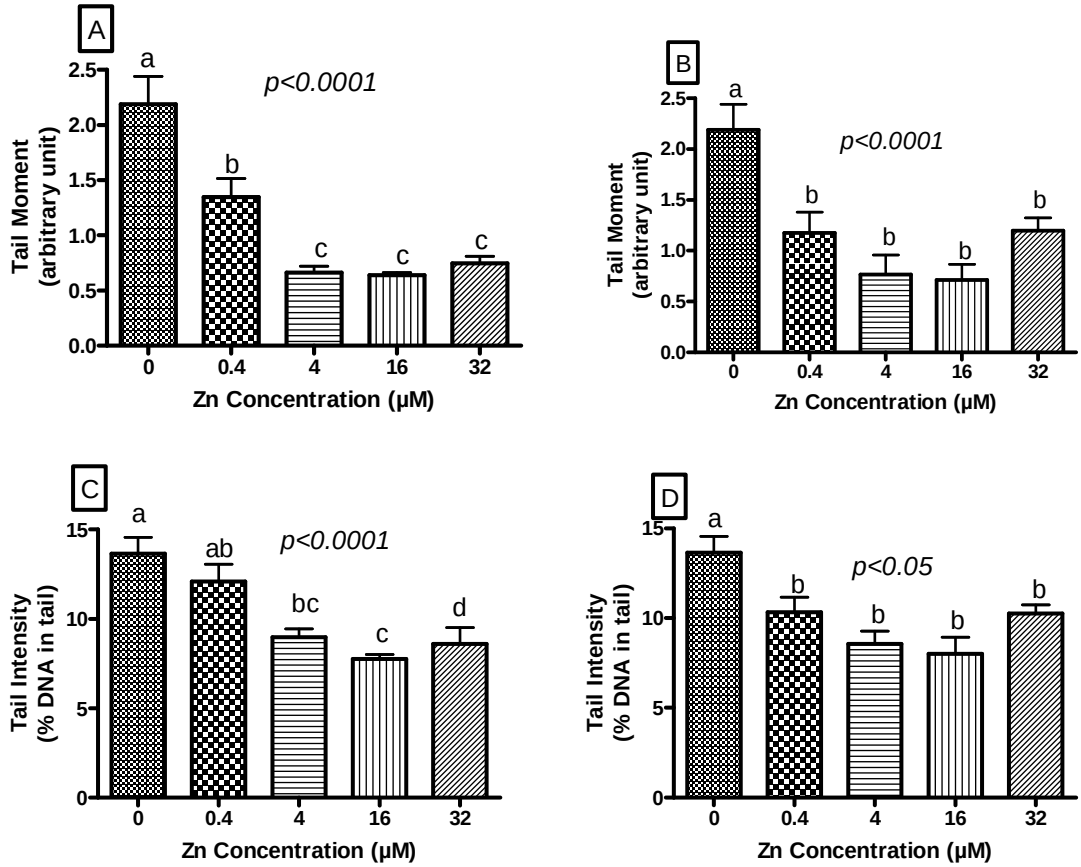

Figure 4.11: Tail moment values for cells treated with (A) $ZnSO_4$ and (B) ZnC; Tail intensity values for cells treated with (C) $ZnSO_4$ and (D) ZnC at increasing concentrations of Zn. Groups not sharing the same letter are significantly different to each other (*p* values refer to One way ANOVA analysis: *p<0.05*). Results are shown as mean ± standard error (n=6).

4.4.4 Effect of Zinc concentration on baseline levels of cytotoxicity and chromosome damage as measured by the CBMN-Cyt assay

Zn depleted cells showed the highest percentages of necrotic and apoptotic cells (*p<0.05*) (Figure 4.12A-D). Increasing concentrations of Zn showed a reduction in the percentage of both necrotic and apoptotic cells (*p<0.05*). Figures 4.12E and 4.12F show a reduction in NDI for Zn depleted cells (*p<0.05*), while NDI increased with increasing Zn concentration indicating a cystostatic effect of Zn deficiency. There was no difference in apoptosis, necrosis and cytostasis (NDI) between $ZnSO_4$ and ZnC at any of the concentrations tested (Apoptosis – Effect of type of Zn compound: 0.00%, *p=0.9798*, Effect of concentration: 55.73%, *p<0.0001*; Necrosis – Effect of type of Zn compound: 0.06%, *p=0.8107*, Effect of concentration: 49.13%, *p<0.0001*; NDI – Effect of type of Zn compound: 5.27%, *p=0.0432*, Effect of concentration: 31.83%, *p<0.05*).

In order to measure chromosome damage, MNi, NPBs and NBuds were scored in binucleated cells as shown in Figure 4.4. Figures 4.13A-F show a significant increase in frequency of MNi, and NPBs for Zn depleted cells (*p<0.05*). A non-significant increase in NBuds frequency was observed in Zn depleted cells. Zn supplemented cells showed a dose-related reduction in DNA damage events compared to Zn depleted cells (*p<0.05*). Lowest DNA damage was observed at 4 µM and 16 µM and this trend is similar for both $ZnSO_4$ and ZnC. There were no significant differences in frequencies of MNi, NPBs, NBuds for cells treated with $ZnSO_4$ and ZnC (MNi – Effect of type of Zn compound: 0.66%, *p=0.4884*; Effect of concentration: 30.41%, *p<0.05*; NPBs - Effect of type of Zn compound: 0.08%, *p=0.8155*, Effect of concentration: 26.90%, *p<0.05*; NBuds - Effect of type of Zn compound: 0.14%, *p=0.7556*, Effect of concentration: 26.03%, *p<0.05*).

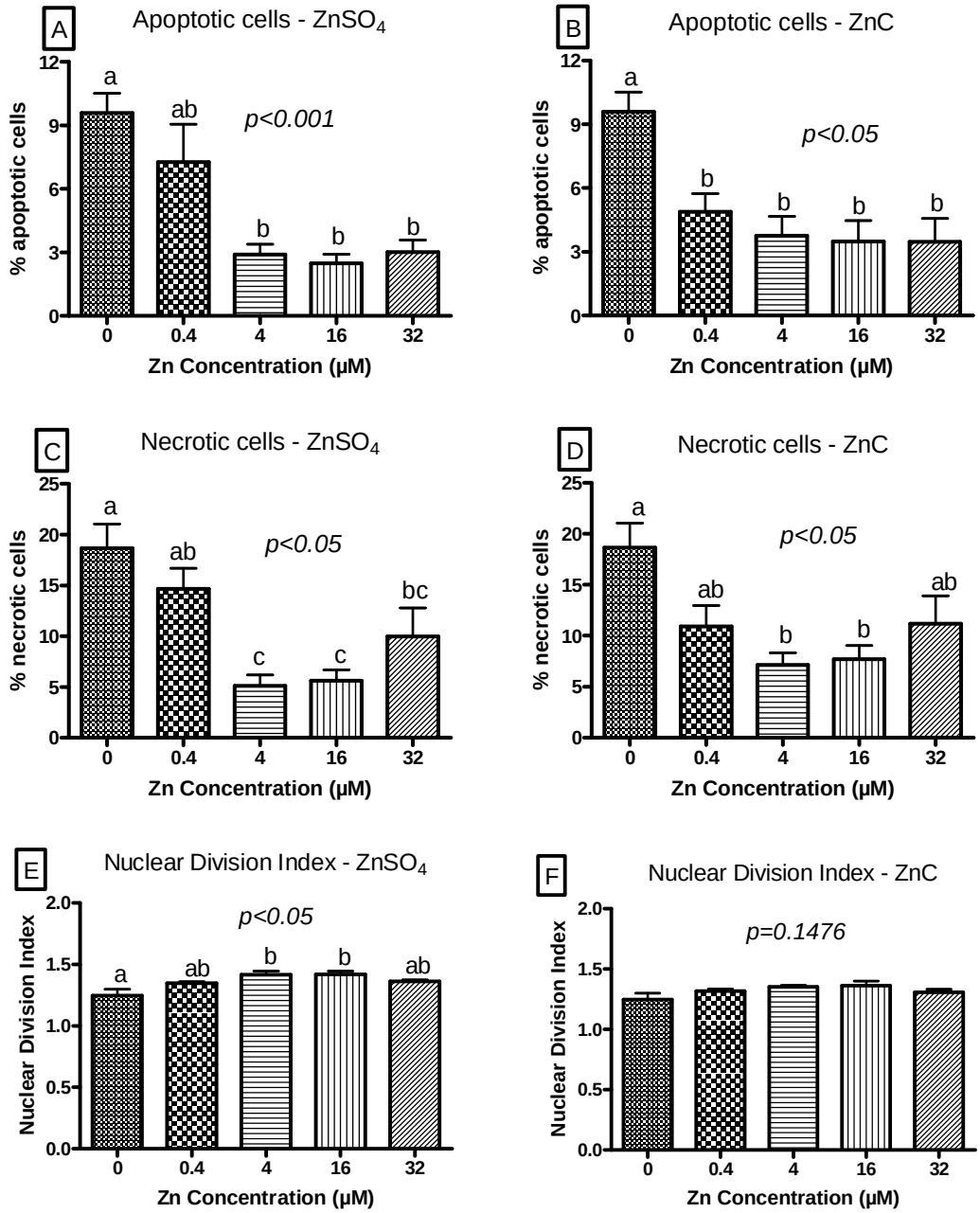

Figure 4.12: Cytotoxicity and cytostatic end points with increasing Zn concentration scored using CBMN-Cyt assay in HOK cells on day 11: **(A)** percentage of apoptotic cells from cultures treated with $ZnSO_4$, **(B)** percentage of apoptotic cells from cultures treated with ZnC, **(C)** percentage of necrotic cells from cultures treated with $ZnSO_4$, **(D)** percentage of necrotic cells from cultures treated with ZnC, **(E)** NDI of cultures treated with $ZnSO_4$, and **(F)** NDI of cultures treated with ZnC. Groups not sharing the same letter are significantly different to each other. Results shown are mean ± standard error (n=6). (*p* values refer to One way ANOVA analysis: *p<0.05*).

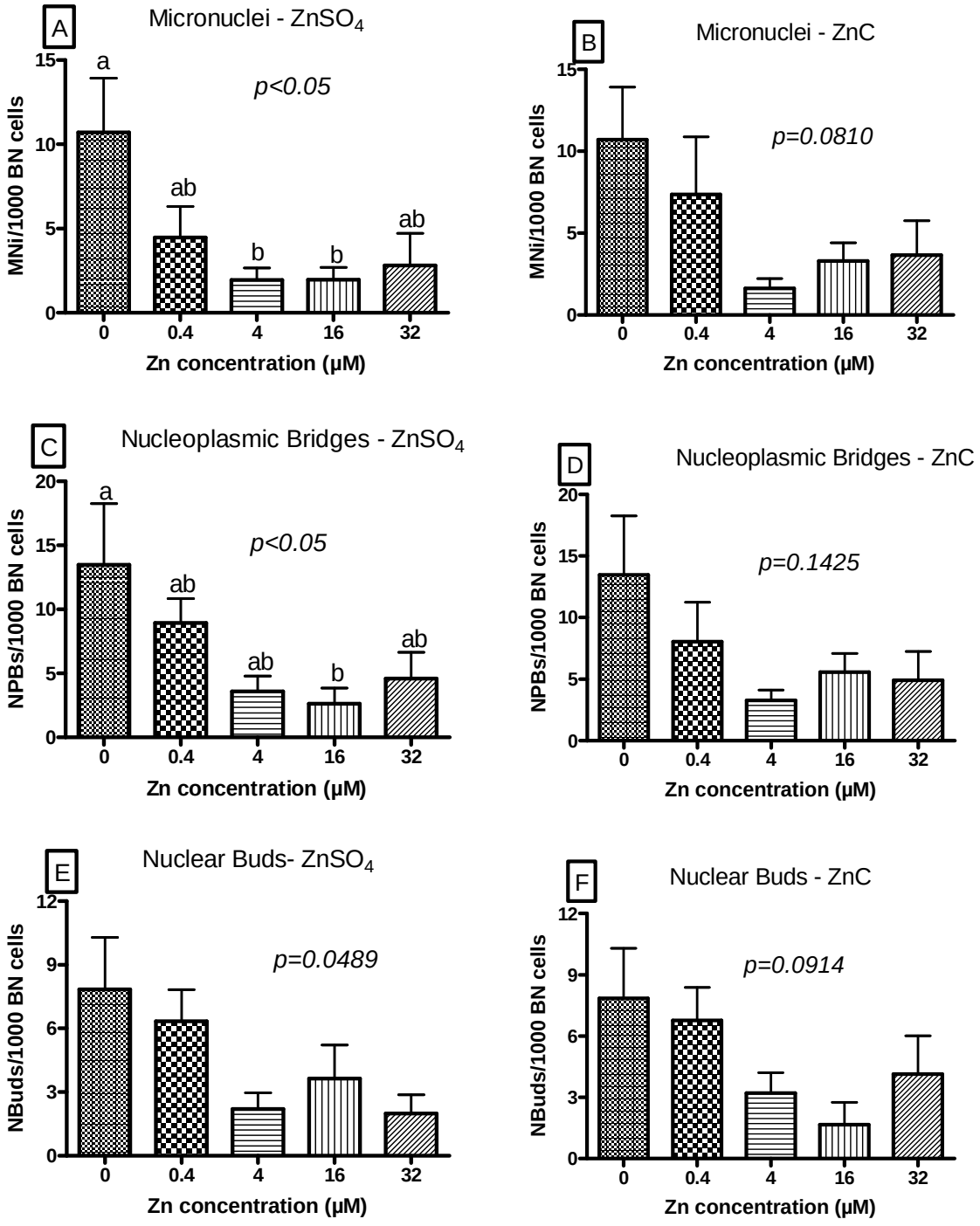

Figure 4.13: DNA damage biomarker end points scored using CBMN-Cyt assay in HOK cells on day 11 in relation to increasing Zn concentration: **(A)** frequency of MNi in 1000 BN cells from cultures treated with $ZnSO_4$, **(B)** frequency of MNi in 1000 BN cells from cultures treated with ZnC, **(C)** frequency of NPBs in 1000 BN cells from cultures treated with $ZnSO_4$, **(D)** frequency of NPBs in 1000 BN cells from cultures treated with ZnC, **(E)** frequency of NBuds in 1000 BN cells from cultures treated with $ZnSO_4$, and **(F)** frequency of NBuds in 1000 BN cells from cultures treated with ZnC. Groups not sharing the same

letter are significantly different to each other. (*p* values refer to One way ANOVA analysis: *p<0.05*). Results shown are mean ± standard error (n=6).

4.4.5 Effect of Zinc concentration on γ-radiation induced cytotoxicity and chromosome damage as measured by the CBMN-Cyt assay

Figure 4.14A-D showed that there was a significant reduction in the percentage of γ-ray-induced necrotic and apoptotic cells with increasing Zn concentration (*p<0.05*). The lowest levels occurred at 16 and 32 µM Zn for both compounds. There was no difference with the type of Zn as analysed with 2-way ANOVA for both apoptotic and necrotic cells (Apoptotic - Effect of type of Zn compound: 0.49%, *p*=0.2143, Concentration: 71.11%, *p*<0.0001; Necrotic - Effect of type of Zn compound: 0.01%, *p*=0.8907, Concentration: 52.98%, *p*<0.0001). There was no significant effect with both Zn treatments in the NDI. There was no significant difference with the type of Zn (Effect of type of Zn compound: 2.62%, *p*=0.0754, Concentration: 22.98%, *p*<0.0001).

Frequency of micronucleated cell, nucleoplasmic bridges and nuclear buds were not measured due to higher number of mononucleated cells, necrotic cells and irregular shape of the cells (Figure 4.15).

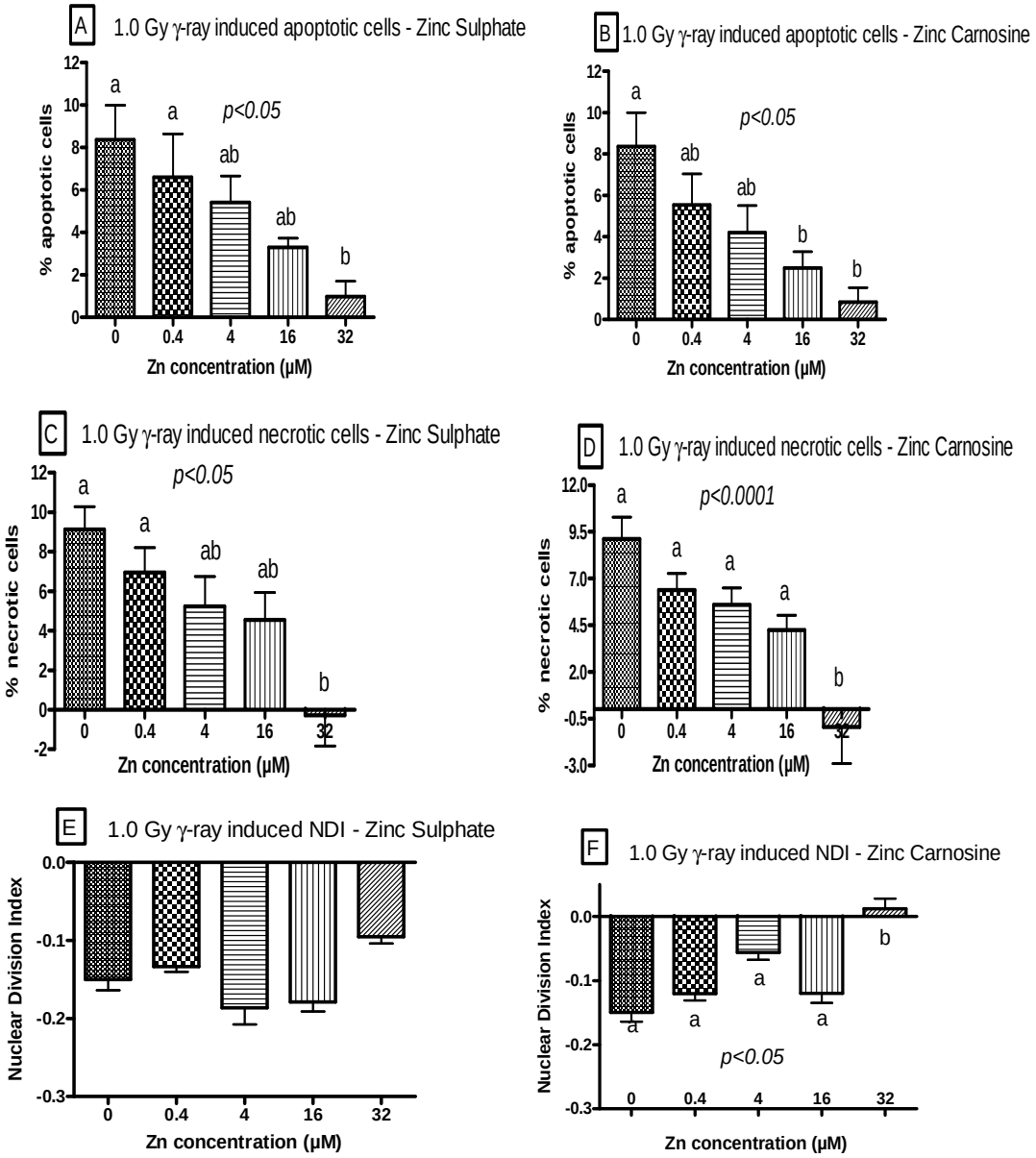

Figure 4.14: γ-ray induced cytotoxicity and cytostatic end points at increasing Zn concentration scored in HOK cells using CBMN-Cyt assay on day 11: (A) percentage of apoptotic cells from cultures treated with $ZnSO_4$, (B) percentage of apoptotic cells from cultures treated with ZnC, (C) percentage of necrotic cells from cultures treated with $ZnSO_4$, (D) percentage of necrotic cells from cultures treated with ZnC, (E) NDI of cultures treated with $ZnSO_4$, and (F) NDI of cultures treated with ZnC. Groups not sharing the same letter are significantly different to each other (p<0.05). Results are shown as mean ± standard error (n=6). NDI – Nuclear Division Index.

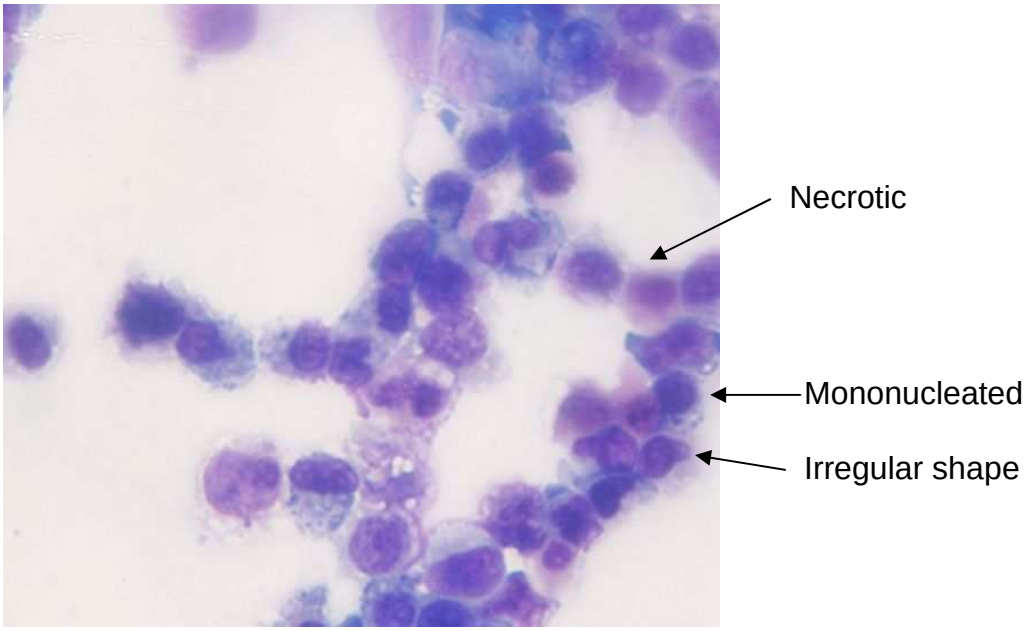

Figure 4.15: Photomicrograph of cells challenged with radiation (40X). Higher frequency of necrotic, mononucleated and irregular size and shapes of cells were observed.

4.4.6 Effect of Zinc concentration on H_2O_2 induced cytotoxicity and chromosome damage as measured by the CBMN-Cyt assay

Figure 4.16A-F showed the cytotoxic and cytostasis effect of H_2O_2 treatment against cells cultured in Zn treatment at various concentrations. Higher percentages of necrotic cells especially in Zn depleted culture (24.23 ± 2.07%) was observed following H_2O_2 treatment as compared to the other treatment groups (*p<0.0001*). Zn at 32 µM showed the lowest percentages of necrotic cells for both Zn type with 0.171 ± 2.375 for $ZnSO_4$ and 0.2726 ± 1.33 for ZnC, respectively. There was no effect on type of Zn on % of necrotic cells (Effect of type of Zn compound: 0.54%, *p*=0.2525, Concentration: 66.52%, *p*<0.0001). Zn depleted cells also showed highest percentages of apoptotic cells with 2.48 ± 1.33%. Zn concentration at 32 µM appeared to be the most optimal concentration for both Zn type to reduce apoptosis with only 0.842 ± 0.700% for $ZnSO_4$ treated culture and 0.599 ± 0.644% for ZnC. In this experiment, concentration of each treatment appeared to explain the most variation observed in this experiment and there was no significant difference observed with type of Zn (Effect of type of Zn compound: 0.00%, *p*=0.9645, Concentration: 38.49%, *p*<0.0001). There were no significant changes for H_2O_2 induced effects on NDI for both Zn treatments.

Frequency of micronucleated cell, nucleoplasmic bridges and nuclear buds were unmeasurable due to higher number of mononucleated cells, necrotic cells and irregular shape of the cells (Figure 4.17).

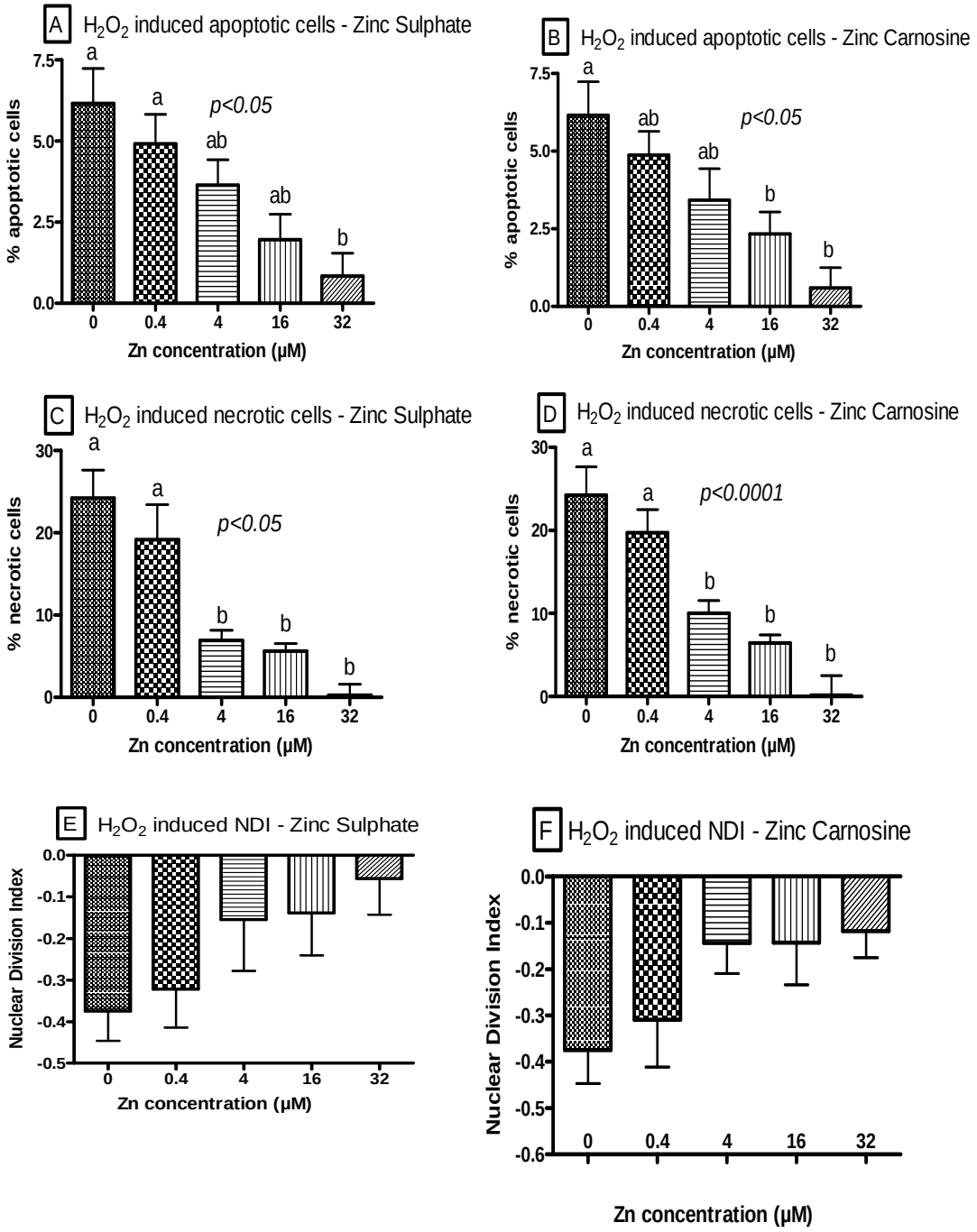

Figure 4.16: H_2O_2 induced cytotoxicity and cytostatic end points at increasing Zn concentration scored in HOK cells using CBMN-Cyt assay on day 11: (A) percentage of apoptotic cells from cultures treated with $ZnSO_4$, (B) percentage of apoptotic cells from cultures treated with ZnC, (C) percentage of necrotic cells from cultures treated with $ZnSO_4$, (D) percentage of necrotic cells from cultures treated with ZnC, (E) NDI of cultures treated with $ZnSO_4$, and (F) NDI of cultures treated with ZnC. H_2O_2 induced values measured by subtracting values for non-treated cultures from those of treated cultures. Groups not sharing the same letter are significantly different to each other (p<0.05). Results are shown as mean ± standard error (n=3). NDI – Nuclear Division Index.

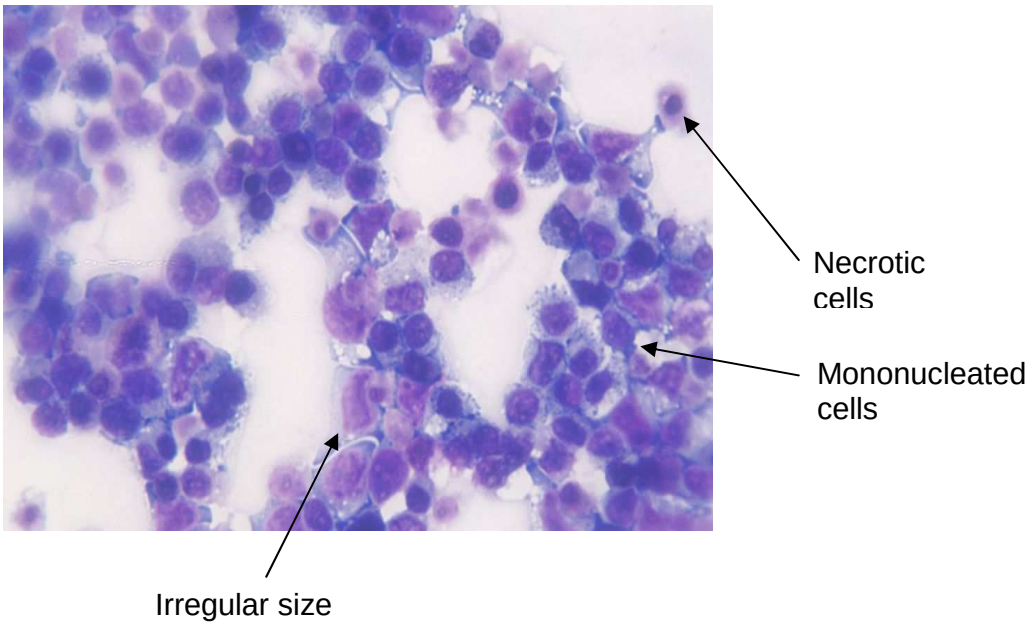

Figure 4.17: Photomicrograph of cells challenged with H_2O_2 treatment (40X). Higher frequency of necrotic, mononucleated and irregular size and shapes of cells were observed.

4.4.7 Western blot analysis

Western blot was used to measure expression of key proteins involved in the molecular mechanisms by which cells respond to Zn status or genotoxic and cytotoxic events induced by Zn depletion or excess. Higher levels of PARP, OGG1 and p53 were observed in Zn depleted cells (*p=0.065, <0.0001,<0.05, respectively*) (Figure 4.18A-C), however, Zn supplemented cells did not show any significantly different levels of these proteins at Zn concentrations ranging from 0.4 to 32 µM. Increased levels of γ-H2AX were observed in Zn depleted cells suggesting increased DNA breaks and γ-H2AX expression was minimised at 4 µM Zn in $ZnSO_4$ cultures (*p<0.05*) (Figure 4.18D). Zn depleted cells also showed higher expression of Caspase 3 as compared to the other groups (*p<0.05*) (Figure 4.18E) indicative of apoptosis activity induced via Caspase 3. Levels of metallothionein (MT) increased in a dose-dependent manner and were significantly higher in cells grown at 16 µM and 32 µM compared with all other groups confirming the relevance of this biomarker as an indicator of Zn status (Figure 4.18F). There was no difference in any of the protein expression biomarkers between $ZnSO_4$ and ZnC at any of the concentrations tested (PARP: Effect of type of Zn compound: 1.56%, *p=0.1794*, Effect of concentration: 49.12%, *p<0.0001*; OGG1: Effect of type of Zn compound: 1.92%, *p=0.0291*, Effect of concentration: 70.55%, *p<0.0001*; p53: Effect of type of Zn compound: 0.55%, *p=0.0004*, Effect of concentration: 95.67%, *p<0.0001*; γ-H2AX – Effect of type of Zn compound: 0.15%, *p=0.6699*, Effect of concentration: 59.43%, *p<0.0001*; Caspase 3: Effect of type of Zn compound: 0.10%, *p=0.5738*, Effect of concentration: 81.59%, *p<0.0001*; MT - Effect of type of Zn compound: 0.21%, *p=0.2059*, Effect of concentration: 91.79%, *p<0.0001*) .

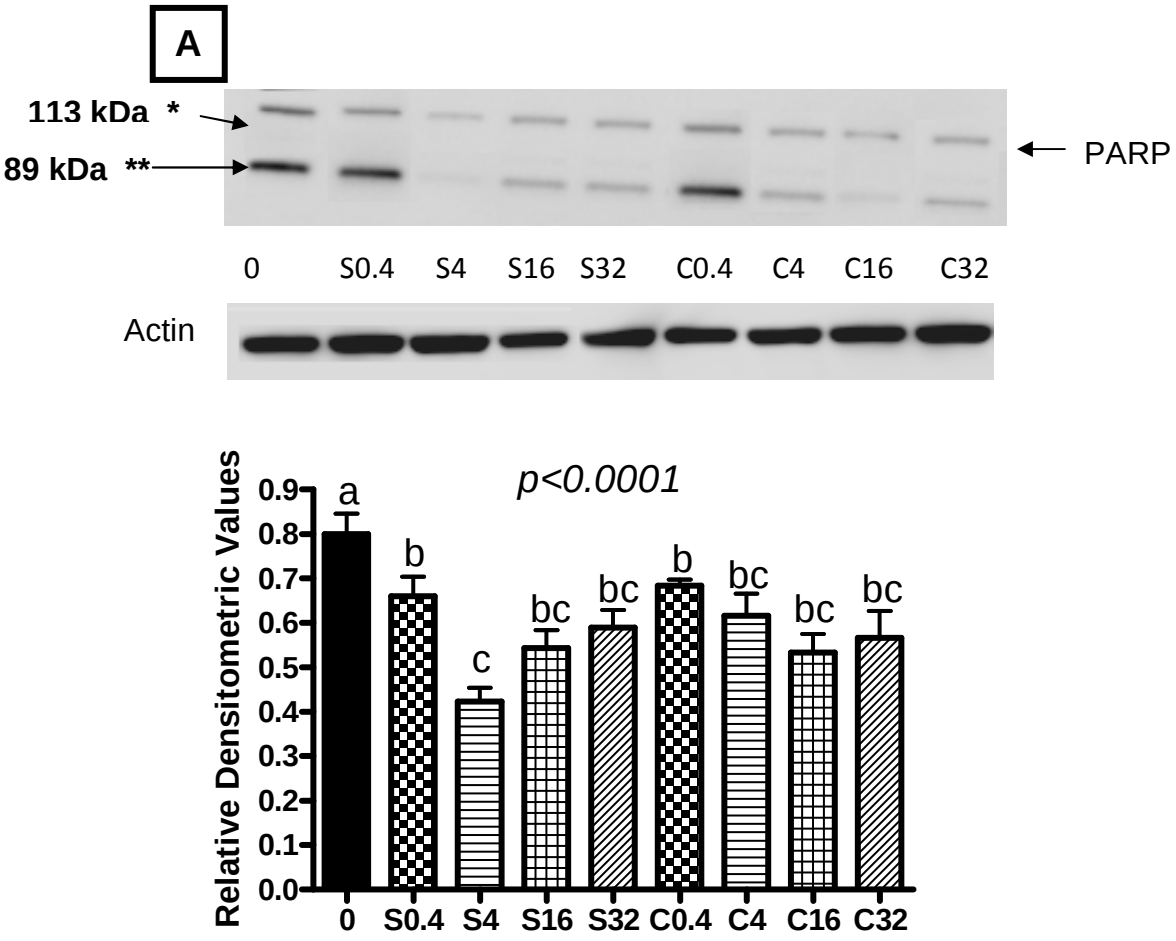
A
113 kDa *
89 kDa **
PARP
0 S0.4 S4 S16 S32 C0.4 C4 C16 C32
Actin
p<0.0001
Relative Densitometric Values
0.9
0.8
0.7
0.6
0.5
0.4
0.3
0.2
0.1
0.0
a b c bc bc b bc bc bc
0 S0.4 S4 S16 S32 C0.4 C4 C16 C32
B
OGG1
0 S0.4 S4 S16 S32 C0.4 C4 C16 C32
Actin
Relative Densitometric Values
0.35
0.30
0.25
0.20
0.15
0.10
0.05
0.00
a b b b b b b b b
p<0.0001
0 S0.4 S4 S16 S32 C0.4 C4 C16 C32

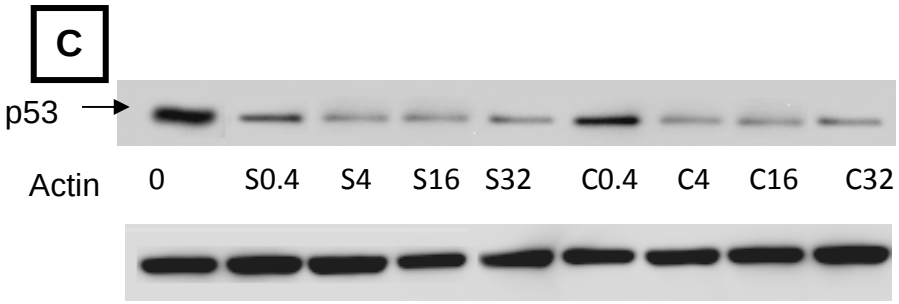
C
p53
Actin
0
S0.4
S4
S16
S32
C0.4
C4
C16
C32

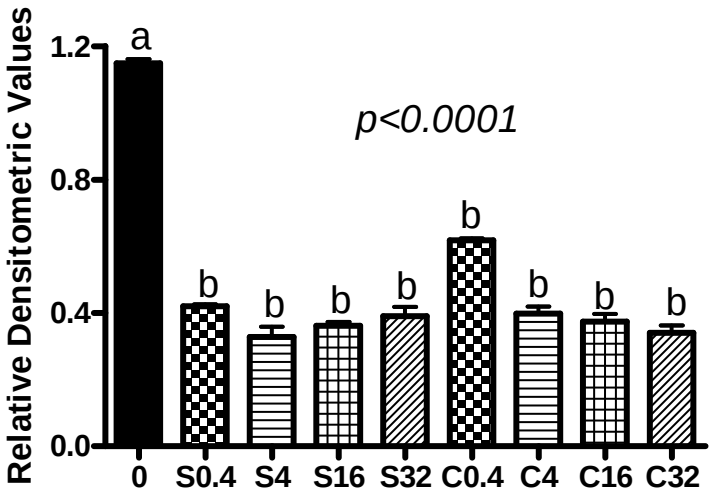
Relative Densitometric Values
1.2
0.8
0.4
0.0
a
b
p<0.0001
0
S0.4
S4
S16
S32
C0.4
C4
C16
C32

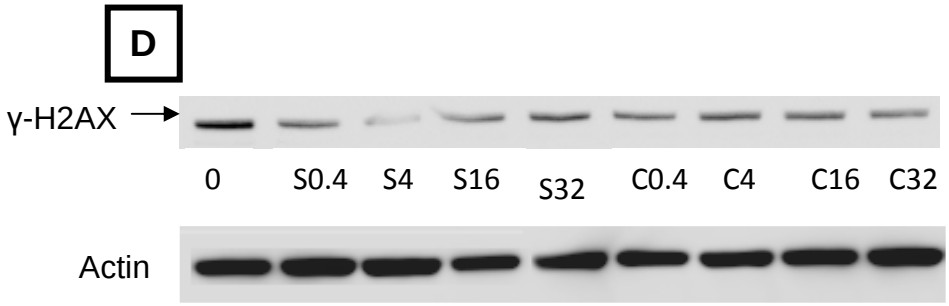
D
γ-H2AX
0
S0.4
S4
S16
S32
C0.4
C4
C16
C32
Actin

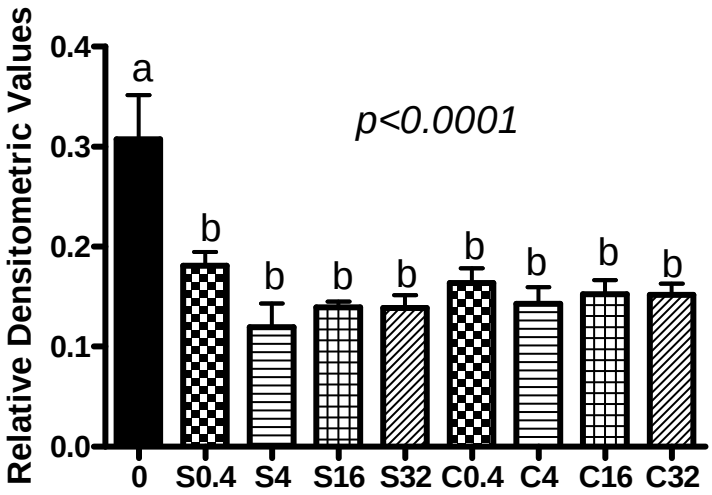
Relative Densitometric Values
0.4
0.3
0.2
0.1
0.0
a
b
p<0.0001
0
S0.4
S4
S16
S32
C0.4
C4
C16
C32

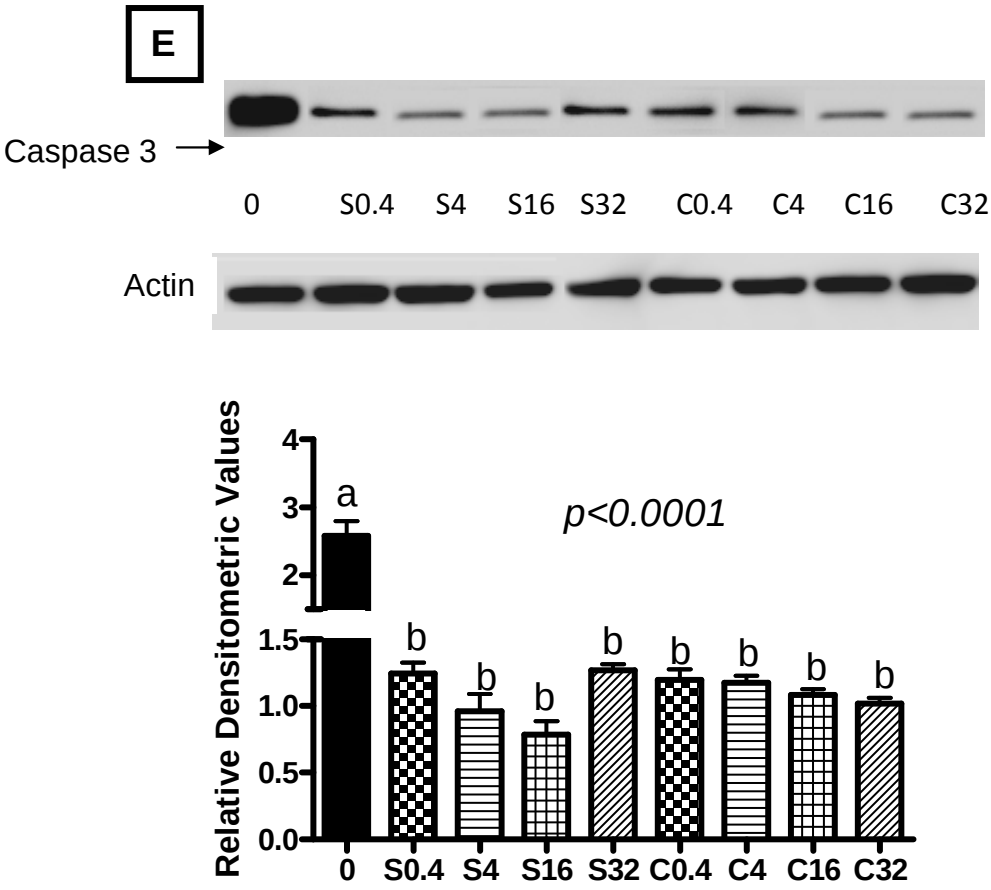
E
Caspase 3
0
S0.4
S4
S16
S32
C0.4
C4
C16
C32
Actin
Relative Densitometric Values
4
3
2
1.5
1.0
0.5
0.0
a
b
b
b
b
b
b
b
b
p<0.0001
0
S0.4
S4
S16
S32
C0.4
C4
C16
C32

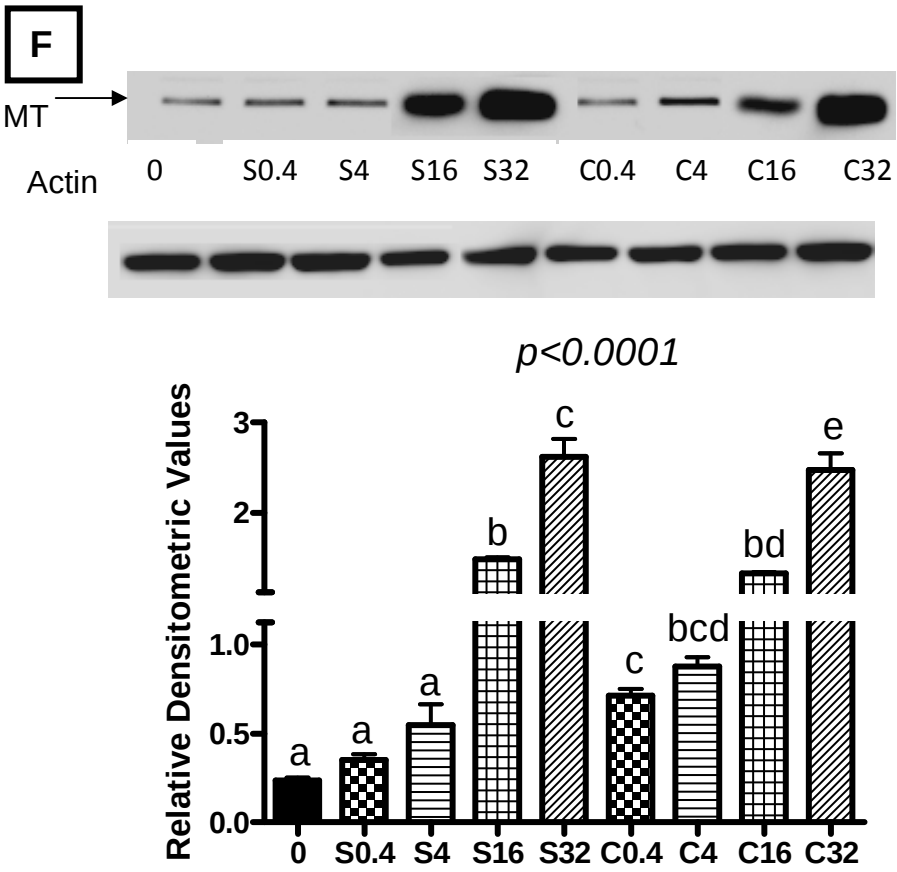

Figure 4.18: The effects of Zn concentration in HOK cells on levels of (A) Poly (ADP-ribose) polymerase (PARP); (B) 8-oxoguanine glycosylase (OGG1); (C) p53; (D) γ-H2AX; (E) Caspase 3; (F) Metallothionein (MT) expressed in HOK cells following 9 days of culture, as determined by western blot analysis. Abbr: S – Zinc Sulphate; C-Zinc Carnosine; 0: Zn depleted cells, 0.4: 0.4 µM ZnS and C, 4: 4 µM ZnS and C, 16: 16 µM ZnS and C, 32: 32 µM ZnS and C, * - intact PARP segments, ** - cleaved PARP segments. Representative western blot are shown in the inserts. Relative densitometric values are values for each sample divided by β-actin. Groups not sharing the same letter are significantly different to each other. (*p* values refer to One way ANOVA analysis: *p<0.05*).

4.4.8 Cytotoxicity and genotoxicity effect of HOK cells in optimal medium

Data on HOK cells grown in optimal medium [Oral Keratinocyte Medium (OKM) which is a complete medium for optimal growth of normal human oral keratinocytes *in vitro*] were presented in Table 4.7. OKM consists of 500 ml of basal medium, 5 ml of oral keratinocyte growth supplement (OKGS, Cat. No. 2652 ScienCell Research Laboratories, Ca, USA) and 5 ml of penicillin/streptomycin solution (P/S, Cat. No.

0503, ScienCell Research Laboratories, Ca, USA). The optimal culture medium used which consists of basal medium with additional oral keratinocyte growth supplement and penicillin/streptomycin solution contains 4 µM of Zn. Cells grown in optimal medium did not show any cytotoxicity and genotoxicity effects as compared to Zn depleted cells. The relationship between DNA damage and cells grown in optimal medium was very similar to cells grown in additional 4 µM of Zn.

Table 4.7: Levels of Zn, cytoxicity and genome stability measurements for HOK cells cultured in standard normal medium.

Levels of Zn(µg/million cells)	Absorbance (570 nm)	Tail moment (arbitrary unit)	Tail intensity (% DNA in tail)	Apoptotic cells (% apoptotic cells)	Necrotic cells (% necrotic cells)	NDI (NDI Indices)	Micronuclei (MNi/1000 BN)	Nucleoplasmic Bridges (NPB/1000 BN)	Nuclear Buds (NBuds/1000 BN)
0.066 ± 0.004	0.585 ± 0.021	0.629 ± 0.043	8.809 ± 0.407	2.735 ± 0.447	4.780 ± 1.011	1.417 ± 0.029	1.275 ± 0.655	2.920 ± 1.340	1.650 ± 0.793

4.5 Discussion

The results of this study show that both Zn deficiency and excess increase cytotoxicity and DNA damage events in HOK cells, and that Zn deficiency induces expression of DNA damage response and/or repair proteins. This study highlights the critical role of Zn in genome maintenance and identifies the optimal concentration of Zn required for maintaining genomic stability in human oral keratinocytes.

Bioavailability of Zn is controlled by Zn homeostatic mechanisms that involve Zn uptake, efflux and Zn distribution in cells [198]. When comparing dose-response effects of Zn concentrations in medium and intracellular Zn (Fig 4.8) and metallothionein expression (Fig 4.18), it is evident that intracellular Zn measurements are a more reliable and specific biomarker of Zn status. In this present study, cellular Zn in cells treated with $ZnSO_4$ was slightly higher compared with cells treated with ZnC. This may be due to the chelating property of carnosine in ZnC that may result in reduced bioavailability compared to $ZnSO_4$ [81]. Carnosine from ZnC may have contributed to the protective effects of this compound and could explain why ZnC was as efficacious in preventing DNA damage and cytotoxicity as $ZnSO_4$ despite a lower intracellular Zn concentration. Carnosine is an antioxidant, derived from the amino acids β-histidine and L-alanine, and has been shown to protect against X-ray irradiation and promote wound healing [174-178]. Several potential antioxidant mechanisms which maybe involved include: a) its chelating action against metal ions; b) superoxide-dismutase (SOD)-like activity, and; c) ROS and free radical scavenging [179-181]. Similarly, it is possible that some observed effects of $ZnSO_4$ may have been influenced not only by Zn but also by the SO_4^{2-} ion. However, evidence for this possibility is lacking in the literature. The observation that metallothionein expression was not different between ZnC and $ZnSO_4$ suggest that differences in Zn status are unlikely to explain any differences in genotoxicity and cytoxicity that may be observed with these two Zn compounds. High Zn concentrations may also compete for uptake of other divalent cationic metals causing toxic effects not directly dependent on Zn. However, no significant

difference was found in the levels of copper and iron in the different Zn concentrations.

Supplementation with Zn at 4 µM and 16 µM proved to be most beneficial in reducing genomic instability *in vitro*. Similar findings were found in a previous study conducted using the WIL2-NS lymphoblastoid cell line using the same protocol and approach [81]. Both deficient (Zn depleted medium, 0 µM) and the higher concentrations of Zn (32 and 100µM) were found, in both this study on HOK cells and in the one on WIL2-NS cells, to induce elevated levels of cell death and DNA strand breaks suggesting a U-shaped dose response in epithelial and lymphoblastoid cells. The physiological range for Zn is reported to be between 2-15 µM [31]. Our data showed that physiological concentrations of Zn had beneficial effects on the genomic stability of HOK cells, whereas, at lower concentrations of Zn and at a maximal pharmacologic concentration of 100 µM, Zn appeared to cause severe cellular toxicity. However, this finding is in contrast to that reported by Sliwinski *et al* (2009) [100] who showed that $ZnSO_4$ at 100 µM did not affect the viability of primary human lymphocytes suggesting that sensitivity to Zn toxicity may be dependent on cell type or cell culture conditions. The mechanism of how Zn excess can cause toxicity is still unknown and is likely to be different to that caused by Zn deficiency.

Reduced cell viability was shown in Zn depleted cells as measured via the MTT assay and this is supported by an increase in both apoptotic and necrotic cells, observed via the CBMN-Cyt assay. Low cellular Zn concentration was found to induce programmed cell death in various cell types including fibroblasts, hepatocytes, T-cell precursors, glioma and testicular cells [35, 36, 80, 150, 151]. In addition, Zn depletion has also been associated with caspase activation and increases in apoptosis in airway epithelial cells, lung and hepatocytes [23, 152]. Under low Zn conditions, Caspase 3 was reported to be involved in apoptosis induction via the intrinsic cell death pathway [27]. Our data confirmed that Zn depleted cells caused an increase in activation of Caspase 3, in parallel with a higher percentage of apoptotic cells as measured via the CBMN-Cyt assay. Previous literature has shown that ZnC has a strong cytoprotective effect that might be due to the synergistic effect of Zn and L-

carnosine [199, 200]. However, there was no difference for effect of the 2 different Zn forms when 2-way ANOVA analysis was performed.

In this study, both the comet assay and CBMN-Cyt assay were used to obtain more comprehensive data on how Zn affects genome stability. The alkaline comet assay provides a measure of single and double strand breaks in DNA and alkaline-labile abasic sites that are induced but remain unrepaired. In contrast, micronuclei and nucleoplasmic bridges may occur due to mis-repair of DNA strand breaks which leads to formation of acentric chromosome fragments and dicentric chromosomes [84]. An increase in DNA strand breaks was found in Zn depleted cells, which is consistent with previous studies [35, 36, 43, 80, 81, 94, 154]. Higher concentrations of Zn further reduced DNA strand breaks (4 and 16 µM) but at the highest concentration tested (32 µM), an increase in DNA strand breaks was observed suggesting a potential genotoxic effect for both Zn compounds when present in excess, however, this increase may have also been affected by a contribution of damaged DNA in necrotic cells which tended to increase at 32 µM Zn. However, the mechanism by which Zn excess can cause toxicity remains unclear. Zn depleted cells also showed higher expression of γ-H2AX which is a sensitive molecular marker for DNA strand breaks [201]. These results further confirmed the hypothesis that low Zn can cause genome instability via an increase in DNA strand breaks.

In the CBMN-Cyt assay, Zn depleted cells expressed a higher frequency of MNi, NPBs and NBuds while Zn supplemented cells showed significant reductions in DNA damage events ($p<0.05$). To date, this is the first cytogenetic study to investigate the effects of various concentrations of Zn on MNi, NPBs and NBud expression simultaneously in HOK cells. The first study using the micronucleus assay, reported in 2001, showed that Zn dimethyl and Zn diisonyldithiocarbamate at 1.53, 15.3 and 153.3 µM did not induce any MNi in human peripheral blood lymphocyte culture [90]. In contrast, Santra *et al* (2002) showed that induction of MNi in Zn chloride treated human lymphocytes at 0.15 mM and 0.3 mM is significant compared to negative controls, but this did not occur in a dose-dependent manner [91]. In our recent study, it was found that concentrations of Zn at 4 µM and 16 µM

reduce DNA damage events in the WIL2-NS lymphoblastoid cell line relative to lower or higher concentrations [81]. This suggests that a narrow physiological range of Zn between 4 μM and 16 μM is required for optimising chromosomal stability. Another previous investigation conducted *in vivo* found excess Zn acetate can induce significant increases of both MNi and sister chromatid exchange in bone marrow cells in an Algerian mouse model [101].

Several mechanisms that could lead to MN formation include simultaneous excision repair of damaged (eg. 8-oxo-deoxyguanosine) or inappropriate bases (eg. uracil) incorporated into DNA that are in close proximity and on opposite complementary DNA strands [202]. Such simultaneous repair events will lead to DNA double strand breaks and MN formation [108, 142]. In addition, hypomethylation of cytosine in centrometric and pericentrometric repeat sequences can also lead to MN formation [202]. There are very few studies that have investigated the relationship between Zn and hypomethylation. However, in one of the previous studies, Zn deficiency was found to reduce the utilization of methyl groups from SAM in rat liver, resulting in genomic DNA hypomethylation and histone hypomethylation [203, 204]. This could lead to an increase in MN formation in Zn depleted cells, as observed in the present study due to whole chromosome loss and malsegregation caused by altered structure of DNA and failure of kinetechore assembly at pericentromeric centromeres [85].

In the current study, it was also found that Zn depletion caused an increase in NPBs which may be due to DNA break mis-repair or telomere end fusion, possibly caused by accelerated telomere shortening or deletion and/or base damage in the telomere sequence [205]. Telomere stability has been extensively correlated with the risk of cancer [106, 156-160] and few studies have investigated the relationship of Zn with telomere stability [99, 109, 161]. Accumulation of cells with short telomeres, which may lead to telomere end fusions, was found to be associated with reduced Zn status in hypertensive patients [110]. Human Tankyrase 1 (TANK1) which plays a key role in maintaining telomere integrity has a Zn binding domain in its catalytic site and is therefore dependent on Zn for its function [111]. TANK1 is a

member of the growing family of (poly ADP-ribose) polymerases (PARPs) that interacts with ADP-ribosylases the telomere-binding protein TRF1 [112]. The role of TANK1 involves displacing TRF1 from telomeric DNA and suggests that TANK1 may be a positive regulator of telomere length in telomerase-expressing cells [113, 114]. It is plausible that optimal Zn concentrations may reduce genomic instability events and the risk of cancer possibly by enhancing telomere stability and limiting the incidence of telomere end fusions [106, 108]. This may lead to reduced formation of dicentric chromosomes which are expressed as NPBs [162].

An increase in DNA damage events in Zn depleted cells may be due to compromised DNA repair functions. In this study, it was found that p53 expression is increased under low Zn conditions, which is consistent with other previous studies [35, 36, 43, 80]. p53 is a Zn finger transcription factor that regulates both G1 and G2 checkpoints and plays a crucial role in regulating DNA repair [206, 207]. It is plausible that low Zn may up-regulate p53 levels via oxidative DNA damage and the induction of ATM kinase, which can be activated by cellular stress that can phosphorylate and stabilize p53 protein [208]. Thus, Zn status can indirectly affect p53 protein levels, yet Zn is also an integral component of p53 at its Zn finger domain. However, although p53 is activated, other previous studies have found that DNA binding activity of p53 is impaired by Zn deficiency [36, 43, 80]. Therefore, p53 which plays the role as a transcription factor may also be dysfunctional when Zn is deficient and may cause activation for gene transcription of some DNA damage response genes to be compromised. Besides p53, two other DNA damage response and repair proteins, PARP and OGG1 were also assessed.

Zn is an essential component for PARP-1, which binds via its Zn domain to DNA strand breaks thereby assisting in the recruitment of DNA repair complexes [153]. PARP was found to be increased in Zn depleted cells and this is consistent with another *in vivo* study that investigated the effect of Zn deficiency in rats [43]. The induction of PARP under Zn depletion conditions as observed in our study suggests the accumulation of DNA damage at the molecular level [43] which coincided with a higher frequency of MNi, NPB and NBuds and higher DNA strand breaks. A positive

correlation between cellular poly(ADP-ribosyl)ation and Zn status in human peripheral blood mononuclear cells [39] was reported, further indicating that Zn is required for PARP activity.

Zn is also part of OGG1, another Zn finger protein which is a DNA repair enzyme that is crucial to base excision repair by removing 8-hydroxy-2'-deoxyguanosine, one of the more prevalent oxidative DNA damage events [41]. This current study showed that OGG1 expression is significantly increased in Zn depleted cells suggesting that oxidative stress is one of the mechanisms by which Zn deficiency may cause DNA damage. Song *et al* (2009) hypothesized that there may be a potential hierarchy of induction of Zn deficiency response proteins when Zn concentration is sub-optimal [43] and our previous finding using WIL2-NS cells is consistent with this hypothesis because OGG1 was highly expressed in low Zn but the expression of PARP was only slightly affected in the same conditions [81]. However, in this study, the increment in OGG1 and PARP expression in HOK cells in Zn deficient medium relative to 4 µM Zn was not markedly different.

Besides the involvement of Zn in certain DNA damage responses and DNA repair protein function, an increase in oxidative stress may also contribute to DNA damage events. In this study, the levels of metallothionein (MT) expression were measured to test whether this is one of the possible induced mechanisms that may exert a genome-protective effect [14]. Zn can modulate the expression of metallothionein which is involved in cellular defence against free radicals and oxidative stress [13]. Our results showed that Zn depleted cells have a lower MT expression indicating that MT is not involved in protecting against Zn deficiency-induced oxidative stress. Cells with low levels of MT are more susceptible to DNA damage and apoptotic death following exposure to stress stimuli, including oxidative stress, whereas prior induction of MT appears to offer cellular protection against oxidants [30, 53, 171, 172]. These results suggest that DNA damaging effects of Zn deficiency may be exacerbated by lower MT concentration.

Similar to our previous study in WIL2-NS cells, there was no significant difference observed in the response to DNA damage between $ZnSO_4$ and ZnC despite

lower intracellular Zn in cells grown in ZnC medium relative to $ZnSO_4$ [81]. Carnosine, which is derived from the amino acids β-histidine and L-alanine, has been shown to protect against radiation and promote wound healing [174-178]. Several mechanisms are suggested in relation to the antioxidant properties of carnosine ie. a) its chelating action against metal ions; b) superoxide-dismutase (SOD)-like activity, and; c) ROS and free radical scavenging [179-181]. Therefore, there is some possibility that the genome protective effects of ZnC observed in our experiments may have been due to carnosine rather than Zn and future studies will require the inclusion of carnosine as a control to test this possibility.

In this study, we did not measure the genome protective effect of this cell against γ-radiation and H_2O_2 treatment due to the irregular shape of the cells and higher number of mononucleated cells as well as necrotic cells. This suggests that this cell type is not suitable for investigation on any induced challenge genome protective effect of any compound which could be due to the characteristics of the cells. Another thing that we observed is that these cells tend to grow slowly after 4-5 passages suggesting that this primary cell line is only suitable for one-off treatment.

In conclusion, both $ZnSO_4$ and ZnC were shown to provide optimal cell viability and minimal DNA damage at 4 μM and 16 μM Zn concentration. Higher concentrations of Zn (32 and 100 μM) or Zn deficiency (≤ 0.4 μM) may cause adverse cellular cytotoxic and genotoxic effects respectively. Although mechanisms of how Zn deficiency can affect genome integrity is becoming clearer with the involvement of Zn in p53, PARP and OGG1, the mechanism by which Zn excess can cause toxicity is still unknown. It is evident that more attention should be given to Zn levels in culture medium, which should be carefully maintained at an optimal concentration to maintain genome stability.

Chapter 5

Zinc Deficiency Increases Telomere Length and is Associated with Increased Telomere Base Damage, DNA Strand Breaks and Chromosomal Instability

---

Chapter 5

Zinc Deficiency Increases Telomere Length and is Associated with Increased Telomere Base Damage, DNA Strand Breaks and Chromosomal Instability

---

5.1 Abstract

This study aimed to investigate the impact of Zinc (Zn) on telomere length and telomere base damage in two different human cell types namely the WIL2-NS lymphoblastoid cell line and the Human Oral Keratinocyte cell line (HOK). Zn deficient medium (0 µM) was produced following Chelex treatment, and two Zn compounds, Zinc Sulphate ($ZnSO_4$) and Zinc Carnosine (ZnC) were tested within the normal physiological range at concentrations of 0.0, 0.4, 4.0, 16.0 and 32.0 µM. Telomere length and telomere base damage (both measured by qPCR) increased in Zn-deficient WIL2-NS and HOK cells ($p<0.05$). The relationship of telomere length and telomere base damage together with DNA damage biomarkers as measured by the comet and the cytokinesis block micronucleus cytome assay, were determined using correlation analysis. For WIL2-NS cells, telomere length was significantly positively correlated ($p<0.05$) with telomere base damage ($r= 0.474$), micronuclei ($r= 0.380$), nucleoplasmic bridges ($r= 0.444$) and nuclear buds ($r= 0.332$). Telomere base damage was significantly positively correlated with micronuclei (r=0.409), nucleoplasmic bridges (r=0.692) and nuclear buds (r=0.351). For the HOK cells, the only significant correlation ($p<0.05$) observed involved a positive association between telomere length and tail moment ($r= 0.607$), tail intensity ($r= 0.425$), micronuclei ($r= 0.420$) and nucleoplasmic bridges ($r= 0.301$). These results suggest that Zn may play an important role in telomere length maintenance. Furthermore, these data indicate that longer telomeres induced by Zn deficiency are not indicative

of improved chromosomal stability and that other parameters, such as telomere base damage, maybe required to obtain a more reliable assessment of telomere integrity and functionality.

5.2 Introduction

The relationship between Zinc (Zn) status and telomere structure and function is currently undefined. Telomeres are repeats of a hexamer sequence $(TTAGGG)_n$, and tend to shorten by 50-150 bp with each cell division due to the inability of DNA polymerase to replicate the 3' DNA strand end [209, 210]. Various studies showed that telomere shortening or telomere dysfunction can lead to chromosomal instability (CIN) and cancer [211-215]. Although the impact of dietary factors on chromosome stability has been well documented [81, 82, 88, 108, 130, 216-219], the knowledge about their effect on telomere integrity is still at a very early stage of investigation. To date, there are only two studies that have investigated the impact of Zn on TL (i) an *in vitro* study suggesting that supra physiological concentration of Zn (80µM) causes telomere shortening [109] and (ii) an *in vivo* study indicating that leukocytes with critically short telomeres are associated with impaired zinc homoestasis [110].

Accumulation of oxidative DNA damage resulting from ROS and various oxidative modifications in purines and pyrimidines may also be important in the maintenance of genome stability [220, 221], as alterations in the telomere sequence can cause defective binding of TRF1 and TRF2 proteins which are essential components of the telosome protein complex that regulate telomere integrity and function [108, 222]. The consequence of DNA lesions in the telomeric sequence on both structure and function and whether or not Zn can protect telomeres from oxidative damage has not been adequately explored. Oxidized bases may lead to altered gene transcription, block DNA replication, or alter the affinity of DNA binding proteins, which will in turn affect cell viability and/or promote tumorigenesis [45, 223]. 8-oxo-2′-deoxyguanosine (8oxodG) is a commonly used reliable measure of cellular oxidative stress [224]. The telomere hexamer repeat TTAGGG is rich in guanine and

may be susceptible to the accumulation of 8oxodG resulting in impaired telomere function. Unrepaired 8-oxo-guanine (8-oxoG) can be mutagenic due to pairing with adenine leading to a GC to TA transversion after two rounds of replication [225, 226].

The aim of this study was to investigate the effect of Zn status on telomere length and telomere base damage in two different human cell types. This study used both the WIL2-NS lymphoblastoid cell line and a Human Oral Keratinocyte (HOK) cell line to identify any differences in the effect between haematopoietic and epithelial cells. The effects of using two different Zn compounds, ie Zn Sulphate ($ZnSO_4$) and Zn Carnosine (ZnC) were investigated. $ZnSO_4$ is one of the common forms of Zn salts used in research whereas ZnC is a novel form of Zn used as a dietary supplement with a high antioxidant capacity. Furthermore, correlations between DNA damage biomarkers measured using the Comet and the Cytokinesis Block Micronucleus Cytome (CBMN Cyt) assay, determined in previously reported studies with the same cultures [81, 82], and their relationship with telomere length and telomere base damage were investigated.

5.3 Materials and methods

5.3.1 WIL2-NS lymphoblastoid cell culture

WIL2-NS cells are a human B lymphoblastoid cell line derived from the spleen of a Caucasian male with hereditary spherocyte anaemia and were obtained from the American Type Culture Collection (ATCC No. CRL-8155, Manassas, VA, USA). Cells were cultured for 9 days and the medium was replaced every 3 days as described previously in Chapter 3 (Section 3.3.1, page 42) [81]. For all experiments, cells were either cultured in Zn-depleted medium (0 µM) or Zn depleted medium to which $ZnSO_4$ (Sigma Aldrich St. Louis, MO, USA) or ZnC (Hamari Chemicals Osaka, Japan) was added to obtain Zn concentrations of 0.4, 4.0, 16.0 and 32.0µM. Zn depleted medium was prepared using RPMI 1640 medium (which lacks Zn) (Sigma Aldrich St.

Louis, MO, USA) and Foetal Bovine Serum (FBS) (Thermo Trace, Australia) that was depleted of Zn as follows : FBS was mixed with 10% Chelex-100 (Sigma, St. Louis, MO, USA) for two hours and the cycle of depletion was repeated again for a further 4 hours.

5.3.2 HOK cell culture

Human oral keratinocytes (HOK) isolated from human oral mucosa, were obtained from the ScienCell Research Laboratories (Cat No 2610; ScienCell, Ca, USA). Cells were cultured in Oral Keratinocyte Medium (OKM) which is a complete medium for optimal growth of normal human oral keratinocytes *in vitro*. OKM consists of 500 ml of basal medium, 5 ml of oral keratinocyte growth supplement (OKGS, Cat. No. 2652, ScienCell, Ca, USA) and 5 ml of penicillin/streptomycin solution (P/S, Cat. No. 0503, ScienCell, Ca, USA). The medium is serum-free, HEPES and bicarbonate buffered and has a pH of 7.4. Cells were cultured for 9 days and the medium was replaced every 3 days as described previously in Chapter 4 (Section 4.3.1, page 92) [82]. For all experiments, cells were cultured in Zn-depleted medium (0 µM) or Zn-depleted medium to which $ZnSO_4$ (Sigma Aldrich St. Louis, MO, USA) or ZnC (Hamari Chemicals Osaka, Japan) was added to obtain Zn concentrations of 0.4, 4.0, 16.0, and 32.0 µM. Zn depleted medium was prepared using HOK medium that was depleted of Zn as follows : HOK medium was mixed with 10% Chelex-100 (Sigma, St. Louis, MO, USA) for two hours and the cycle of depletion was repeated again for a further 4 hours.

5.3.3 Isolation of genomic DNA

Genomic DNA was isolated using the silica-gel-membrane-based DNeasy Blood and Tissue Kit 250 (Qiagen, Melbourne, Australia) and the standard protocol was followed, with minor modifications. These additional steps (described below) were included as it has been shown that under conditions of commonly used DNA isolation protocols, oxidative adducts can spontaneously form thereby affecting the integrity of the acquired DNA [227, 228]. It has been shown as well that telomeres shortened under conditions of oxidative stress [229]. Therefore, prior to isolation all

buffers were purged for 5 minutes in nitrogen and supplemented with 50 µM phenyl-*tert*-butyl nitrone (Sigma B7263) which acts as a free radical trap and scavenger. The use of phenol and high temperatures (>56 °C) were avoided.

The vial content was pipetted into a spin column with a 2 ml Qiagen collection tube. The spin column was then centrifuged at 8000 rpm for one minute. The flow through was discarded and 500 µl of AW1 buffer (wash buffer 1) was added to the column. The spin column was again centrifuged at 8000 rpm for one minute, the flow through was discarded and 500 µl AW2 (wash buffer 2) added to the column. The spin column was centrifuged at 13 000 rpm for three minutes and the column placed in a new collection tube. 100 µl of AE buffer (elution buffer) was added directly onto the column and centrifuged at 8000 rpm for one minute. This step was repeated, giving a final volume of approximately 200 µl of DNA concentrate. The isolated DNA was refrigerated overnight at 4°C to allow it to become homogenous throughout the solution. The concentration of DNA for each sample was determined in duplicate by Nanodrop spectrometric analysis (Biolab, ND 1000).

5.3.4 Telomere length assay

In this study, a quantitative real-time polymerase chain reaction (qPCR) based method was used to measure absolute telomere length (aTL). This method is based on the Cawthon method for relative measurement of telomere length (TL) but modified by introducing an oligomer standard to measure aTL. [230-232].

5.3.4.1 qPCR of DNA for telomere length assay

Absolute telomere length was measured by determining the number of TTAGGG hexamer repeats using a quantitative real-time polymerase chain reaction (qPCR) as described by O'Callaghan *et al* [231]. Assays on serial dilutions were performed to determine a standard curve for measuring kilobases of telomeric sequence. All

samples were run on an ABI 7300 Sequence Detection System with SDS v. 1.9 software (Applied Biosystems, Foster City, CA). Each 20µl reaction was performed as follows: 20 ng of DNA, 1X SYBR Green master mix, 100 nM telomere forward primer (CGGTTTGTTTGGGTTTGGGTTTGGGTTTGGGTTTGGGTT), 100 nM telomere reverse primer (GGCTTGCCTTACCCTTACCCTTACCCTTACCCTTACCCT) as described by O'Callaghan *et al* [231]. Cycling conditions were: 10 min at 95°C, followed by 40 cycles of 95°C for 15 sec, 60°C for 1 min. DNA from the 1301 lymphoblastoid cell line was used as an internal control for each plate run. The number of diploid genomes was calculated using the *36B4* (a single-copy gene) amplicon using the following primers: *36B4* forward primer (CAGCAAGTGGGAAGGTGTAATCC) and *36B4* reverse primer (CCCATTCTATCATCAACGGGTACAA) and the same amplification and cycling conditions as for the telomere amplicon. Similar to the oligomer used for standardization of absolute telomere length, an oligomer was synthesized containing the *36B4* amplicon (CAGCAAGTGGGAAGGTGTAATCCGTCTCCACAGACAAGGCCAGGACTCGTTTGTACCCGTT GATGATAGAATGGG) and used to generate a standard curve for diploid genome quantification.

5.3.5 Telomere base damage assay

In this study, a qPCR based method [233] was used to measure the amount of oxidised residues as well as other base lesions within telomeric DNA that are recognised and excised by the bacterial enzyme, formamidopyrimidine DNA-glycosylase (FPG). FPG is specific for oxidized purines, including 8oxodG, 2,6-diamino-4-hydroxy-5-formamidopyrimidine (FaPyGua) and 4,6-diamino-5-formamidopyrimidine (FaPyAde) and other open-ringed purines [234, 235]. This method is based on differences in PCR kinetics between the DNA template exhaustively digested by FPG and undigested DNA i.e. ΔC_T ($C_T$treated- C_T untreated)

5.3.5.1 Excision of 8oxodG and incision of oligomers at 8oxodG sites using FPG

To excise 8oxodG and generate a strand break at the resulting abasic site DNA was digested with FPG used formamidopyrimidine-DNA glycosylase (FPG). FPG protein has both N-glycosylase and AP-lyase activities and generates a strand break after excision of formamidopyrimidine lesions and 8oxodG residues within the DNA [236]. The single Zn finger motif in the FPG enzyme is utilised by an FPG protein to bind oxidatively damaged DNA [237]. DNA digestion was undertaken using 400 ng of genomic DNA and incubated with 8 units of FPG (formamidopyrimidine-DNA glycosylase) (New England Biolabs[NEB], Australia) in 1x NEB Buffer (10mM Bis-Tris-Propane-HCl, 10mM MgCl2, 1mM Dithiothreitol, pH 7.0). A control incubated with 1 X NEB Buffer, but without FPG (replaced with H_2O) was also prepared. A duplicate digestion was also set up for each of the corresponding samples in mock buffer (enzyme solution was excluded and substituted with H_2O). All samples were set up on ice and incubated at 37°C overnight to allow complete digestion.

5.3.5.2 qPCR of synthetic oligomers and genomic DNA

The quantitative Real-Time amplification of the oligomers was performed as described by O'Callaghan *et al* (2011) [231]. Each 20µL qPCR reaction was composed as follows: 40pg of digested or undigested oligomer DNA or 40ng of digested or undigested genomic DNA, 1xSYBR Green master mix, 100nM telo1 forward (CGGTTTGTTTGGGTTTGGGTTTGGGTTTGGGTTTGGGTT), 100nM telo2 reverse primers (GGCTTGCCTTACCCTTACCCTTACCCTTACCCTTACCCT) [231]. All samples were run on an ABI 7300 Sequence Detection System with the SDS Ver. 1.9 software (Applied Biosystems [AB] Foster City, CA, USA). Each sample was analysed in triplicate. Cycling conditions were: 10 minutes at 95°C, followed by 40 cycles of 95°C for 15 seconds and 60°C for one minute. The amount of base damage in telomeric DNA was calculated by subtracting the C_T of the undigested DNA from the C_T of FPG digested DNA. Based on the standard curve (Figure 5.1), the data is presented as the amount

of FPG damage bases/kb telomere. The intra- and inter-assay CV for the telomere base damage assay were 5.7% and 37.4% respectively.

Equations are as follows:

Amount of FPG damage bases/kb telomere = (Change in C_T value -0.3828)/0.0858

(Values derived from standard curve as reported in [233])

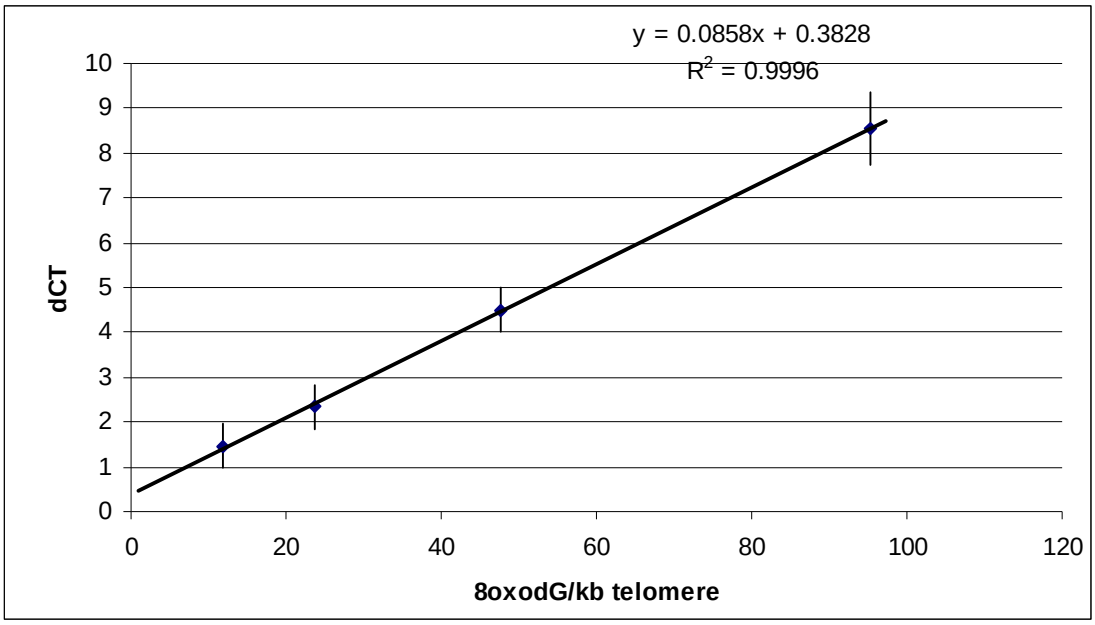

Figure 5.1: An 8oxodG standard Curve. Double-stranded 8oxodG oligomers (1-, 2- or 4-8oxodG bases) were treated with FPG. Following treatment qPCR was performed; resultant amplification profiles (treated and untreated) were then compared. A ΔC_T ($C_T$treated- C_T untreated) was then calculated. The number of 8oxodG in each oligomer was then translated into the number of 8oxodG bases per kb telomeric DNA. Amount of oxidised base pairs per kb of telomere can then be calculated using the equation of the line [dCT=0.0858(oxidised bases/kb telomere) + 0.38] (adapted from [233])

5.3.6 Zinc content of cells, comet assay and CBMN-Cyt assay

The detailed method, and results for the Zn content of cells, comet assay and CBMN-Cyt assay have been reported previously [81, 82]. [Refer to: WIL2-NS – Chapter 3, Section 3.3.5 (page 45), Section 3.3.7 (page 46), Section 3.3.8 (page 47), Section 3.4.1

(page 57), Section 3.4.3 (page 62), Section 3.4.4 (page 63); HOK cells – Chapter 4, Section 4.3.5 (page 96), Section 4.3.7 (page 97), Section 4.3.8 (page 98), Section 4.4.1 (page 111), Section 4.4.3 (page 116), Section 4.4.4 (page 118)].

5.3.7 Experimental design and statistical analysis

All end points measured were tested for Gaussian distribution using the Kolmogorov–Smirnov test. One-way analysis of variance (ANOVA) followed by Tukey's *post hoc* tests for data with Gaussian distribution was performed to compare the effects of different Zn concentrations. The non-parametric Friedman test followed by Dunn's multiple comparison test was used for data that did not exhibit Gaussian distribution. Two-way ANOVA was used to measure the difference in effects between $ZnSO_4$ and ZnC and the % variance for biomarker results that could be explained by Zn concentration or Zn compound used. The partial correlation coefficient was used to study the associations between changes in telomere length and telomere base damage with other DNA damage biomarkers (micronuclei, nucleoplasmic bridges, nuclear buds, comet tail moment and comet tail intensity). The level of statistical significance was set at $p< 0.05$. Data are represented as mean ± standard error of the mean (SEM). Statistical analyses were performed using Prism 4.0 and SPSS for Windows 18 (SPSS, Chicago, IL).

5.4 Results

5.4.1 Cellular Zinc content

Zn depleted cultures in both cell lines as measured using ICPOES showed a significant reduction in cellular Zn levels ($p<0.0001$) and there was no effect on other divalent metals (Copper and Iron) (refer to Chapter 3 and 4). Cells supplemented with either $ZnSO_4$ or ZnC showed a significant dose related increase in cellular Zn ($p<0.0001$) with increasing media Zn concentration. These results are described in previous publications using the same cultures from which DNA was isolated for this study [81, 82] (as shown in Chapter 3 and 4).

5.4.2 Impact of Zinc on telomere length (TL) in WIL2-NS and HOK cells

WIL2-NS cells grown in Zn depleted medium exhibited the highest TL relative to cells that were maintained in Zn supplemented medium (*p<0.05*). For both Zn compounds, the lowest TL was observed in 32 µM treated cells. Cells treated with $ZnSO_4$ showed a significant reduction in TL in a dose dependent manner. Analysis by two-way ANOVA showed statistically significant effects for Zn concentration (*p<0.001*) but not for type of Zn compound (*p=0.9322*) with 68.80% variance attributable to Zn concentration (Figure 5.2A and 5.2B).

TL in HOK cells was at least ten fold greater than in WIL2-NS cells. Despite the large disparity in TL, a similar trend was observed with Zn depleted HOK cells showing highest TL compared to cells in other Zn concentrations (*p<0.001*). A reduction in TL was observed with increasing concentration of Zn for both types of compounds. There were no significant differences in values for TL for cells treated with $ZnSO_4$ or ZnC (Effect of type of Zn compound: 1.08%, *p=0.1025*, Effect of Zn concentration: 76.59%, *p<0.0001*) (Figure 5.2C and 5.2D).

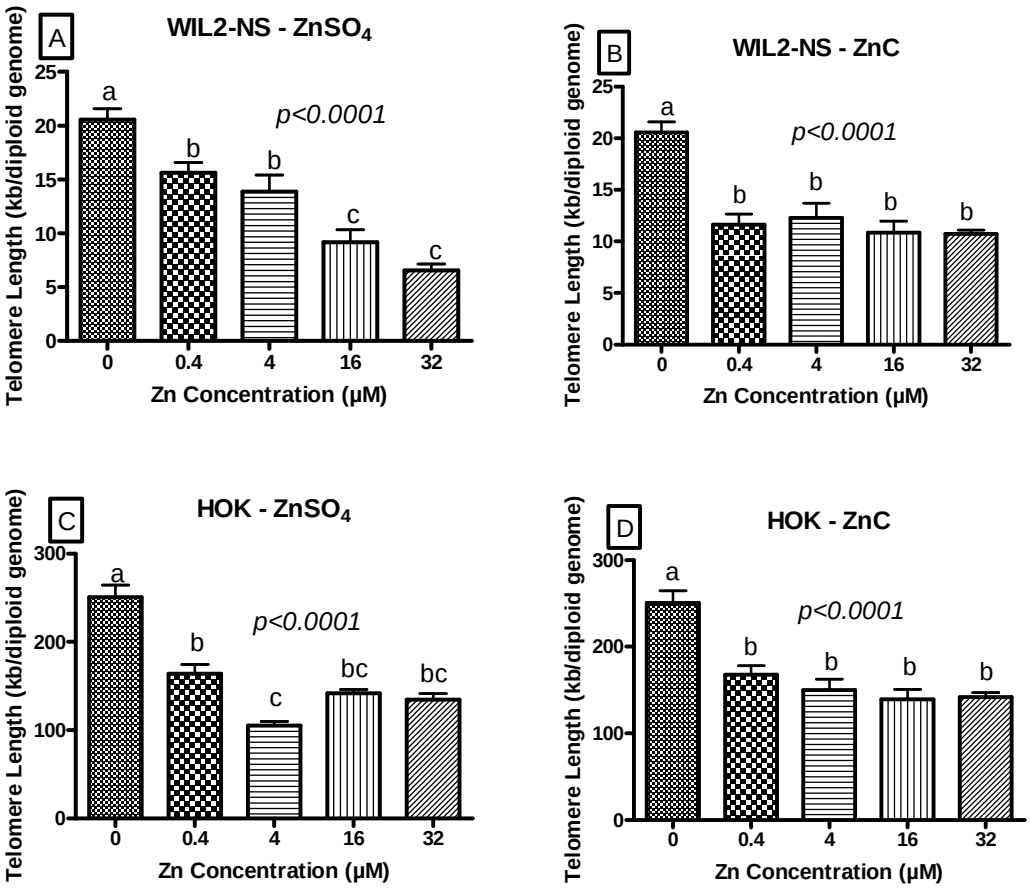

Figure 5.2: Telomere length values for WIL2-NS cells treated with **(A)** $ZnSO_4$ and **(B)** ZnC; Telomere length values for HOK cells treated with **(C)** $ZnSO_4$ and **(D)** ZnC at different concentrations of Zn. Groups not sharing the same letter are significantly different to each other ($p<0.05$). Results are shown as mean ± standard error (n=6). P values in figures refer to One-way ANOVA analysis results.

5.4.3 Impact of Zinc on telomere base damage in WIL2-NS and HOK cells

Both WIL2-NS and HOK cells grown in Zn depleted medium showed the highest amount of telomere base damage relative to cells cultured in medium supplemented with Zn (*p<0.05*). In WIL2-NS cells, both Zn compounds ($ZnSO_4$ and ZnC) at 4 µM showed the lowest amount of base damage (Figure 5.3A and 5.3B). Two way ANOVA analysis did not show any significant difference between cells treated with ZnC or $ZnSO_4$ (Effect of concentration: 35.60%, *p<0.0001*; Effect of type of Zn compound: 0.98%, *p=0.3832*). In HOK cells, $ZnSO_4$ treated cells at 4 µM exhibited the lowest amount of telomere base damage, followed by cells treated at 16 and 32 µM (not significant) (Figure 5.3C). Meanwhile, for ZnC, cells cultured with 16 µM Zn medium showed the lowest amount of telomere base damage indicating a narrow range of Zn concentration for telomere base damage prevention (Figure 5.3D). Despite these apparent consistent trends for HOK cells , two way ANOVA analysis did not show any statistical difference between Zn compound treatments or the effects of Zn concentration (Effect of Zn concentration: *0.00%*, *p=0.9728*, Effect of type of Zn compound: *13.79%*, *p=0.1008*).

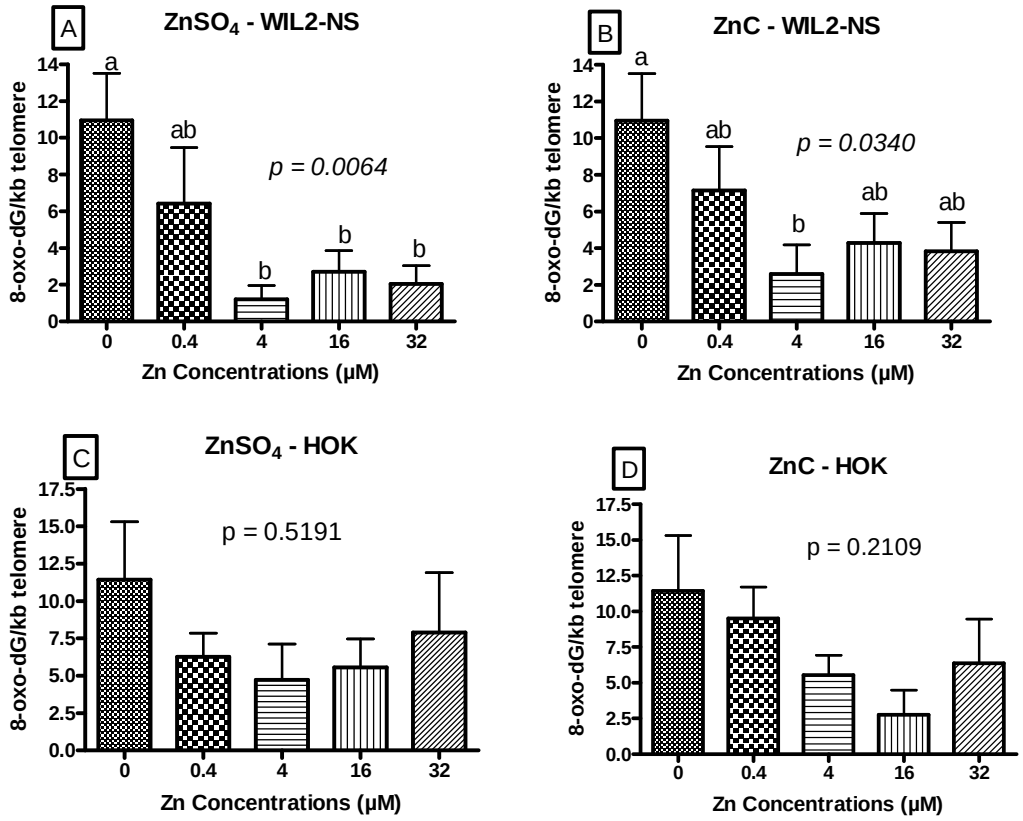

Figure 5.3: Telomere base damage values for WIL2-NS cells treated with **(A)** $ZnSO_4$ and **(B)** ZnC; Telomere base damage values for HOK cells treated with **(C)** $ZnSO_4$ and **(D)** ZnC at different concentrations of Zn. Groups not sharing the same letter are significantly different to each other (*p<0.05*). Results are shown as mean ± standard error (n=6). P values in figures refer to One-way ANOVA analysis results.

5.4.4 Correlation between telomere length and telomere base damage with DNA damage biomarkers (tail moment, tail intensity, micronuclei, nucleoplasmic bridges and nuclear buds)

Chapter 3 and 4 of this thesis outline studies that the Comet and CBMN-Cyt assay DNA damage biomarkers are significantly increased in Zn deficient cells and minimised at a Zn concentration between 4-16µM Zn [81, 82]. Correlations between these DNA damage biomarkers (tail moment, tail intensity, micronuclei, nucleoplasmic bridges and nuclear buds) and telomere length and base damage for each cell line are shown in Table 5.1 and 5.2. For WIL2-NS cells, there were positive correlations between telomere length and telomere base damage (*r= 0.474*),

micronuclei (r=0.380), nucleoplasmic bridges (*r=0.444*) and nuclear buds (*r=0.332*). Meanwhile, telomere base damage was positively correlated with micronuclei (*r=0.409*), nucleoplasmic bridges (*r=0.692*) and nuclear buds (*r= 0.351*) (Table 5.1).

For HOK cells, telomere length was positively correlated with tail moment (*r=0.607*), tail intensity (*r=0.425*), micronuclei (*r=0.420*) and nucleoplasmic bridges (*r=0.301*). There was no significant association observed between telomere base damage and other DNA damage biomarkers in HOK cells (Table 5.2).

Table 5.1: Correlation factors for relationships between genome integrity biomarkers in WIL2-NS cells analysed using partial correlation after adjusting for Zn concentration and type of Zn

r value	Telomere length	Telomere base damage	Tail moment	Tail intensity	Micronuclei	Nucleoplasmic bridges	Nuclear buds
Telomere length	-	**0.474****	0.202	0.010	**0.380****	**0.444****	**0.332***
Telomere base damage		-	-0.04	0.04	**0.409****	**0.692****	**0.351****
Tail moment			-	**0.530****	0.018	**0.343***	0.185
Tail intensity				-	0.167	**0.329***	0.157
Micronuclei					-	**0.535****	**0.399****
Nucleoplasmic bridges						-	**0.413****
Nuclear buds							-

**p<0.05*
***p<0.001*

Table 5.2: Correlation factors for relationships between genome integrity biomarkers in HOK cells analysed using partial correlation after adjusting for Zn concentration and type of Zn

r value	Telomere length	Telomere base damage	Tail moment	Tail intensity	Micronuclei	Nucleoplasmic bridges	Nuclear buds
Telomere length	-	0.134	**0.607****	**0.425****	**0.420****	**0.301***	0.179
Telomere base damage		-	0.161	0.232	0.246	-0.080	0.205
Tail moment			-	**0.705****	0.260	0.260	0.221
Tail intensity				-	0.150	0.237	0.245
Micronuclei					-	0.158	-0.007
Nucleoplasmic bridges						-	0.138
Nuclear buds							-

**p<0.05; **p<0.001*

5.5 Discussion

The results from this study suggest that Zn concentration has an impact on telomere length and telomere base damage. It was shown that Zn deficiency causes increases in both telomere length and telomere base damage particularly in WIL2-NS cells. Although this seems counter-intuitive it suggests that longer telomeres induced by Zn deficiency may be indicative of a homeostatic response to DNA damage in the telomere sequence which is also associated with chromosomal instability possibly due to formation of longer but dysfunctional telomeres. This implies that longer telomeres induced in response to micronutrient deficiency may not be indicative of improved genomic stability which is important for improved health outcomes or reduced biological ageing [238-242]. Some human prospective *in vivo* studies suggest that an increased telomere length in white blood cells may not be associated with increased risk for cancer. An increase in telomere length in peripheral blood leukocytes was associated with an increased risk of non-Hodgkins lymphoma, breast cancer, lung cancer and melanoma [243-246] as well as a negative prognosis in breast cancer patients [238]. Furthermore, several studies have suggested that offspring born to older parents have a longer telomere length [239-242] and increased paternal age at birth may increase the risk of having breast and prostate cancer in the progeny [247, 248].

The impact of Zn deficiency on telomere length is still unclear. Previous studies have showed that a supra physiological concentration of Zn (80μM) causes telomere shortening in hepatoma cells SMMC-7721 measured using flow cytometry and fluorescence in situ hybridization [109]. This is in agreement with our study where we observed that Zn at higher concentrations caused telomere shortening using a qPCR method which has been shown to be a reliable and robust assay for measuring telomere length [230, 249-251]. Another *in vivo* study showed that leukocytes with critically short telomeres are associated with impaired zinc homeostasis in old hypertensive patients using a high throughput Q-FISH assay [110]. In this study, cells with critically short telomeres (<6 kb) were correlated with labile zinc in very old hypertensive individuals with cardiovascular disease.

In addition, evidence is emerging that telomere base damage leading to altered binding affinity of telomere binding proteins (eg TRF1 and TRF2) may be an important determinant of telomere dysfunction and impaired telomere maintenance [252, 253]. These studies shown that oxidative DNA damage may have an impact on telomeres by disrupting both TRF1 and TRF2 [252]. The insertion of a single 8-oxoG instead of G in the telomere sequence reduced at least 50% of bound TRF1 and TRF2 proteins [252]. Our observation that both base damage in the telomere sequence and telomere length increased in Zn deficient conditions supports the hypothesis that oxidation of telomere bases may lead to abnormal telomere length kinetics and maintenance. Furthermore, in both cultures, expression of OGG1 glycosylase that was 8-oxoG was highly expressed in Zn-depleted cultures relative to replete cultures [81, 82], suggesting that Zn deficiency may lead to guanine oxidation explaining the higher telomere base damage frequency observed in Zn depleted cultures. To date, this is the first study that investigates the impact of Zn deficiency on telomere base damage using a qPCR assay. This shows that the qPCR method for measuring telomere base damage is sensitive enough to be used in nutritional studies investigating oxidative stress and its prevention [233].

The fact that Zn is part of the Zn finger protein Human Tankyrase 1 (TANK1) which plays a key role in maintaining telomere integrity [111] may be one of the plausible explanations as to how Zn can influence telomere length. TANK1 is a member of the poly (ADP-ribose) polymerases (PARPs) that interact with the telomere-binding protein TRF1 causing it to be poly(ADP-ribosyl)ated [112]. TANK1 activity involves displacing TRF1 from telomeric DNA, and as a result is a positive regulator of telomere length in telomerase-expressing cells by making the telomere template accessible to TERT [113, 114]. Reduced TANK1 activity may not explain the observed increase in TL with Zn deficiency but in combination with a reduced binding capacity of TRF proteins caused by an increase in telomere base damage may provide a reasonable basis for a hypothetical mechanism. Furthermore, a recent study [254] indicated that TANK1 defective in poly(ADP-ribosyl)ation of TRF1 resulted in telomere elongation suggesting an alternative mechanism by which Zn might affect TL indirectly.

The correlation analysis data showed that TL was positively correlated with telomere base damage and with some of the chromosomal DNA damage biomarkers. This suggests that TL may not reflect telomere integrity at the base sequence or chromosomal instability.

In conclusion, the findings of this study support the hypothesis that inadequate Zn can cause a significant increase in telomere length and telomere base damage and chromosomal instability. Further research is required to unravel the mechanisms that could explain the observed inverse relationship between Zn deficiency induced telomere lengthening and chromosomal instability.

Chapter 6

Genome Health Effect of Zinc Supplement in an Elderly South Australian Population with low Zinc status

---

Chapter 6

Genome Health Effect of Zinc Supplement in an Elderly South Australian Population with low Zinc status

---

6.1 Abstract

An increased intake of Zinc (Zn) may reduce the risk of degenerative diseases but may prove to be toxic if taken in excess. This study aimed to investigate whether taking a daily supplement of 20mg of Zn can improve Zn status, genome stability events and Zn transporter gene expression in an elderly (65-85y) South Australian cohort characterised by having low plasma Zn levels. 208 volunteers were screened for low plasma Zn levels (≤ 0.77 mg/L/11.77 µM) and 90 were selected and randomized into two groups. A 12 week placebo-controlled intervention trial was performed with 84 volunteers completing the study, (Placebo, n=42) and (Zn group, n=42). Fasted blood was collected at baseline and at the end of the 12 week intervention. In the placebo group, plasma Zn showed a significant drop ($p<0.05$) after 12 weeks from 0.907 ± 0.099 mg/L (13.76 ± 1.51 µM) to 0.861 ± 0.080 mg/L (13.15 ± 1.22 µM). Plasma Zn was significantly increased ($p<0.05$) by 5.69% in the Zn supplemented group after 12 weeks raising plasma Zn levels from 0.926 ± 0.096 mg/L (14.16 ± 1.46 µM) to 0.972 ± 0.135 mg/L (14.86 ± 2.06 µM). FRAP and eSOD were increased in the Zn supplemented group but carnosine concentration were unaffected by the improved Zn status. A significant ($p<0.05$) decrease in the micronucleus frequency (-24.18%) was observed for the Zn supplemented cohort relative to baseline compared to the placebo group which recorded a small increase in the micronucleus frequency of 1.77%. There were no significant changes in the frequency of nucleoplasmic bridges and nuclear buds for both groups. Comet assay results showed a significant effect of time and treatment of Zn supplementation for

both tail moment and tail intensity ($p<0.05$). Reductions of -7.09% for tail moment ($p<0.05$) and -8.76% ($p<0.05$) for tail intensity were observed for the Zn group (relative to baseline). Telomere length did not show any significant changes following the 12 weeks Zn intervention. Telomere base damage was found to be significantly decreased in the Zn group ($p<0.05$) (Baseline: 13.82 ± 18.04, 12 weeks: 6.89 ± 15.18 [8 oxodG/kb telomere]), but no significant difference was observed between groups. Both MT1A and ZIP1 expression showed a significant increase in the Zn supplemented group compared to the Placebo group ($p<0.05$). In conclusion, Zn supplementation may prove to have a beneficial effect in an elderly population with low Zn levels by improving Zn status, antioxidant profile and lowering DNA damage events (micronuclei, tail moment and tail intensity). This study also suggests that Zn transporter gene expression may be a useful indicator of Zn status.

6.2 Introduction

Zn can be found ubiquitously in the environment and possesses a number of biological functions that are essential to human health [15]. The function of Zn involves a wide range of biological processes which includes cell proliferation, reproduction, immune function and defence against free radicals [13-18]. In addition, Zn plays an important role in key biological processes such as response to oxidative stress, DNA replication and repair, cell cycle and apoptosis [14]. It is known that more than 100 specific enzymes require Zn for their catalytic functions [18]. Thus, Zn appears to have a critical role in cellular processes and genomic stability.

Previous evidence has shown genomic instability as being one of the main reasons for increased cancer risk [8, 9, 59-62]. The fact that Zn is required as a cofactor in DNA metabolism, is suggestive that deficiency in this micronutrient may induce important chromosomal mutations that increase cancer risk. Several studies show that Zn deficiency causes DNA oxidation, DNA breaks and chromosome damage [13, 14, 219].

Mild Zn deficiency has been reported in various populations such as individuals with gastrointestinal problems, general aging populations, individuals with compromised immunity function and also in vegetarians [255]. Ageing populations are at risk of Zn deficiency because of numerous factors such as those reported by the International Zn Nutrition Consultative Steering Committee (2004) [256], which has shown reductions in total food intake maybe caused by depression, reduced total energy expenditure, maybe reduced mobility and also lower intakes of food with high Zn content (meat or fish) due to dysphagia or dental imperfection. Zn deficiency has been shown to be prevalent in a number of studies investigating Zn status in elderly populations [257-259]. Deficiency of Zn may cause impaired immunity function ([260-262], delayed wound healing [263], depression [264] , impaired cognitive function [265] and increased oxidative stress [266, 267]. As Zn deficiency may have serious implications to the health of ageing individuals, it is important to maintain adequate Zn nutriture among this population.

In 2004, The ZnAge project investigated various health-related impacts of Zn supplementation among the elderly in European countries [122, 123, 129, 264, 266, 268, 269]. Putics and colleagues (2008) reported that Zn supplementation can induce stress responses in the elderly and concluded that proper dietary Zn may have an important role in anti-aging mechanisms involving the immune system [269]. A further report showed that Zn supplementation reduces spontaneous inflammatory cytokine release and restores T cell function [270]. Marcellini and colleagues (2008) showed that Zn supplementation given to the elderly in the ZnAge project affected psychological dimensions dependent on IL-6-174G/C polymorphism [268]. However, the most important finding from this project was presented by Mocchegiani and colleagues (2008) [122] who showed the relevance of the interleukin-6 (IL-6) polymorphism (IL-6-174G/C) for the screening of elderly subjects who effectively need Zn supplementation. IL-6 is identified as a key modulator for intracellular Zn homeostasis, which is influenced by metallothioneins (MT) [271].

Zn supplementation among elderly people (ZnAge project) also reported an increase in the antioxidant enzyme activities such as superoxide dismutase, catalase

and glutathione peroxidise in erythrocytes [128]. Despite all these findings there are still knowledge gaps regarding the affect of Zn supplementation in relation to genomic stability and integrity in an elderly population and was the main focus addressed in this current study.

This study aimed to investigate whether taking a daily supplement of 20mg of Zn can improve Zn status, genome stability events and Zn transporter gene expression in an elderly (65-85y) South Australian cohort characterised by having low plasma Zn levels (<0.77 mg/L/11.7 µM).

6.3 Materials and methods

6.3.1 Screening and recruitment of volunteers

Volunteers were recruited through the CSIRO Clinical Reasearch Unit database and by advertising in local newspapers. The volunteers did not receive any renumeration for their participation. In this study, we excluded 1) individuals supplementing with more than 25% of the recommended dietary intake of Zn, 2) individuals with habitual dietary Zn intake > 20 mg/day, 3) patients undergoing radiotherapy/chemotherapy treatment for cancer and d) individuals with plasma Zn > 0.77 mg/L. A total of 208 volunteers aged 65-85 years old met the selection criteria and were screened for plasma Zn status and those with plasma Zn concentration ≤ 10.0 µM (≤ 0.65 mg/L - cut-off point for Zn deficiency [272]) were given priority for inclusion in the study. As there were too few individuals with plasma Zn ≤ 0.65 mg/L (10.0 µM), we eventually selected all those with plasma Zn status < 0.77 mg/L/11.77 µM (n=90) and the volunteers consented to partipate in the study. The volunteers were randomly divided into two groups (Zn supplement vs placebo). Body mass index (BMI) was also measured during the clinic visits.

6.3.2 Intervention design

The study was designed as a randomised, placebo-controlled intervention in a free-living elderly, healthy population. Volunteers with low plasma Zn (< 0.77 mg/L/11.7 µM) were randomised into two groups; placebo and a Zn supplemented group (Figure 6.1).

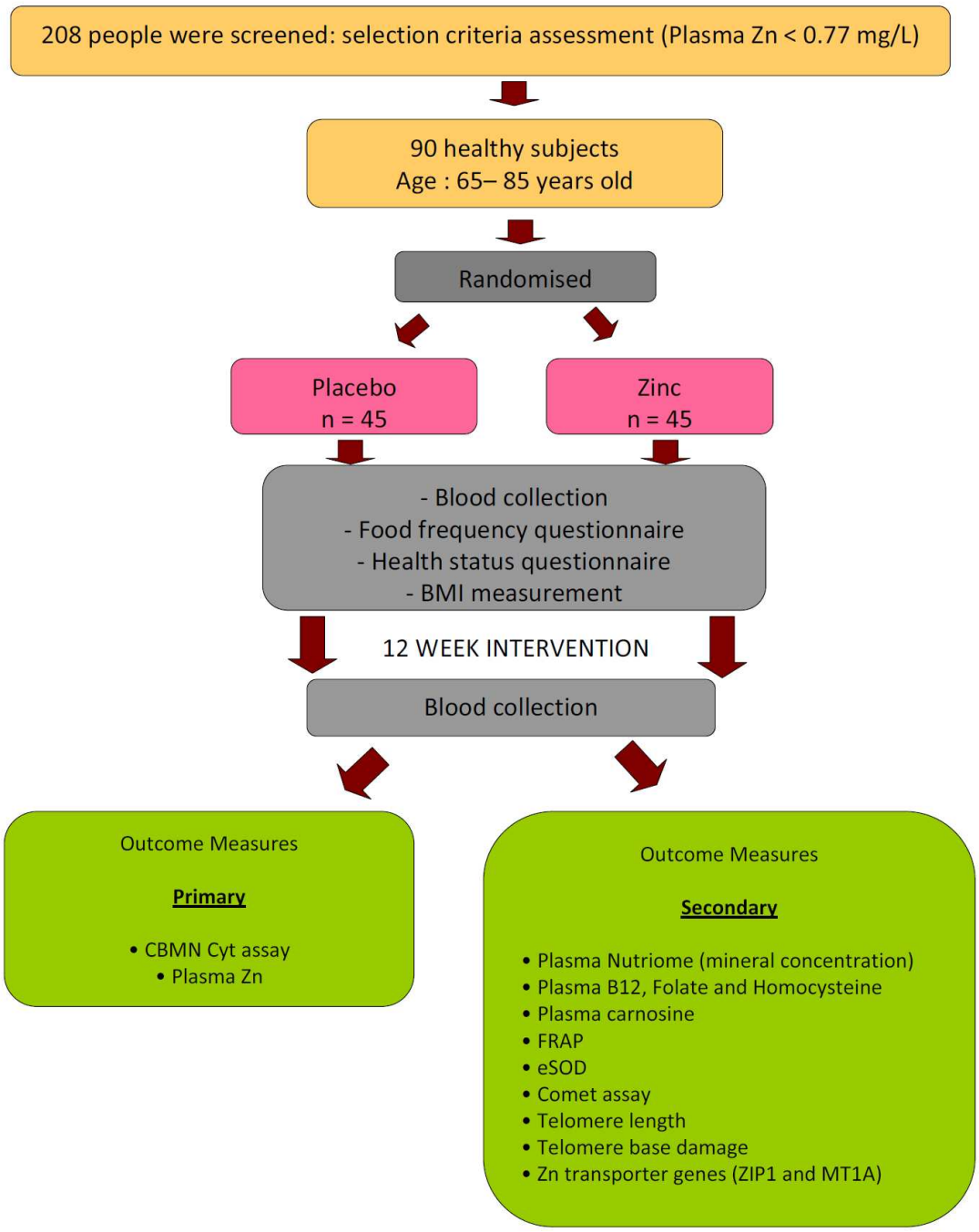

Figure 6.1: Simplified study design. MT1A – MT1A gene; ZIP1 – ZIP1 gene; FRAP – Ferric Reducing Activity in Plasma; eSOD – erthyrocytes Superoxide Dismutase; CBMN Cyt – Cytokinesis Block Micronucleus Cytome assay.

The Zn supplement tablet in this trial is a commercially available Zn carnosine chelate supplement, which was supplied and prepared by Metagenics (Queensland, Australia). Each Zn carnosine supplement tablets contained 86.9 mg of Zn carnosine with maltodextrin as excipient. The Zn dose of each supplement was 20 mg/day which is within the safe physiological range [256, 273-276]. The Zn tolerable upper intake level for individuals aged 65-85 years old is 40 mg/day [277]. Given that dietary Zn intake in this age group is 11.4 mg/day for males and 9.0 mg/day for females [278], it was calculated that it was unlikely that the upper limit would be exceeded. The placebo group received an identical tablet, which only contained the excipient maltodextrin. The volunteers consumed one tablet (Placebo or Zn carnosine) per day.

6.3.3 Nutritional assessment

A nutrition survey was carried out to investigate the estimated dietary intake of Zn in the study cohort. The volunteers who participated in the study were required to complete the validated Anti-Cancer Council of Victoria (ACCV) Food Frequency Questionnaire (FFQ) at the start of the study [279]. The four page format ACCV FFQ includes 74 food items with responses on a 10 point scale (1=never to 10=3 or more times per day) in the frequency section and detailed questions on specific foods over the previous 12 months [280]. A series of photographs is included to enable an estimate of portion size. Also, 10 cross-check questions were used to adjust for overestimation of fruit and vegetable consumption. The completed ACCV FFQs are optically scanned and nutrient intakes are computed from FFQ responses using software developed by the ACCV based on the NUTTAB95 nutrient composition data [280]. Vitamin E and folate intake are computed using the British McCance and Widdowson's database [280].

6.3.4 Blood collection and sample preparation

For screening, one tube of non-fasted blood per volunteer was collected in a lithium-heparin vacutainer (Vacuette, Austria). At baseline and 12 weeks, three tubes of

blood were collected in the morning after an overnight fast by venipuncture into a potassium-EDTA tube for homocysteine (Hcy) measurement, and another two lithium-heparin tubes for further assays. Figure 6.2 shows the fractionation of blood to isolate plasma, erythrocytes and lymphocytes and assays conducted in this study.

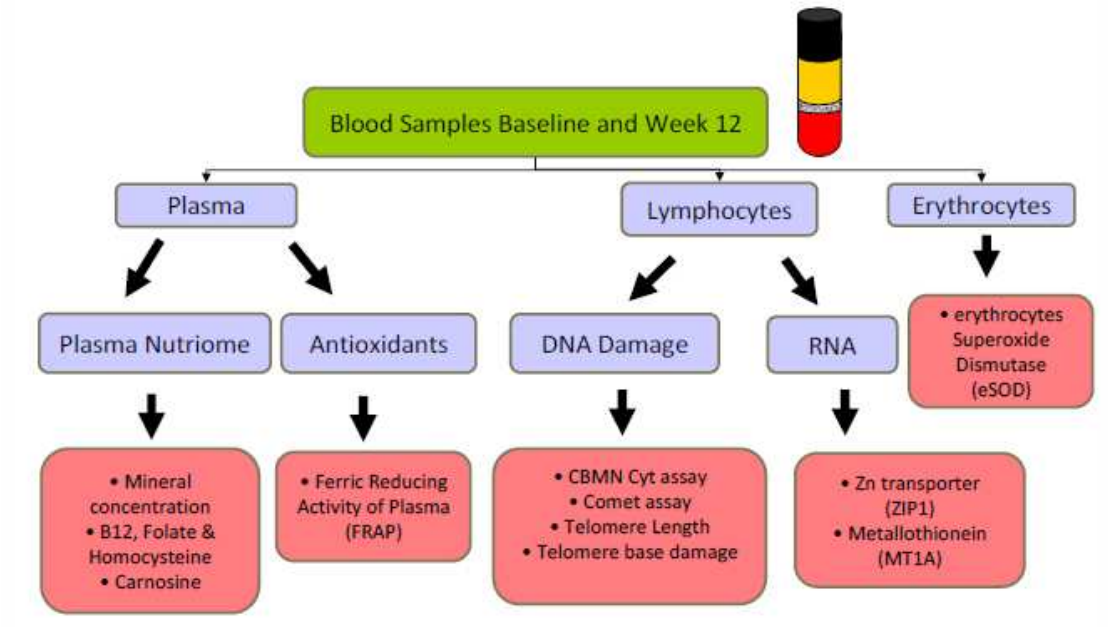

Figure 6.2: Simplified version of assays conducted in this study. MT1A – MT1A gene; ZIP1 – ZIP1 gene; FRAP – Ferric Reducing Activity in Plasma; eSOD – erthyrocytes Superoxide Dismutase; CBMN Cyt – Cytokinesis Block Micronucleus Cytome assay.

a) Plasma Isolation

For plasma isolation, blood was spun at 3000 rpm for 20 minutes at 4°C and plasma was transferred into new tubes according to the assays to be investigated. Spare plasma was labelled and kept at -80°C.

b) Isolation and storage of lymphocytes

The remaining whole blood was then diluted with an equal volume of Hanks balanced salt solution (HBSS, Thermo, US) and mixed. To isolate lymphocytes, 5 ml of Ficoll-Paque™ (Amersham Pharmacia Biotech), a density gradient medium, was

added to a 50 ml falcon tube and 15 ml of diluted blood was gently overlaid. The tubes were centrifuged at 400G for 30 minutes at 22°C. Using a sterile plugged pasteur pipette, the lymphocyte layer was removed into another 50.0 ml Falcon tube and 3X volume (approximately 15.0 ml) of the HBSS was added followed by centrifugation at 180G for 10 minutes. Supernatant was removed and the pellet was resuspended in 2X the original volume of HBSS (1:2 dilutions). The mixture was then spun at 100G for 10 min, supernatant was removed and the pellet was resuspended in 1.0 ml complete medium (RPMI 1640 media (Sigma, St. Louis, MO, USA) supplemented with 10% (v/v) foetal bovine serum (FBS) (Thermo Trace, Australia), 1% (v/v) penicillin [5000 IU/ml]/streptomycin [5 mg/ml] (Sigma, USA), 1 mM L-glutamine (Sigma, USA), 1 mM Sodium Pyruvate (Sigma, St. Louis, MO, USA) warmed to 37°C in the incubator.

For the CBMN Cyt assay, a total cell count was performed and 750 µl cultures were set up at $1x10^6$ /ml, in duplicate labelled clearly with CSIRO ID and date. Cultures were placed in an incubator at 37°C with 5% CO_2 until ready for phytohaemagglutinin (PHA) addition.

For the alkaline comet assay, 500 µl of $1X10^5$ cells/ml suspension was prepared for each volunteer. Spare cells were spun down and resuspended in 500 µl PBS with 10% DMSO (Sigma, Australia), then stored in -80°C prior to DNA/RNA isolation.

The remaining blood was collected and transferred into new tubes and kept at -20 °C prior for erythrocyte superoxide dismutase measurements.

6.3.5 Plasma analysis

6.3.5.1 Plasma mineral, B12, Folate and Homocysteine analysis

For screening, non-fasted blood was spun at 3000 rpm for 20 minutes at 4°C and 2ml of plasma was transferred into new tubes. The plasma samples were stored in -20°C

before being sent to the Waite Analytical Services (WAS, Adelaide University) for plasma Zn analysis.

For both baseline and at the end of 12 weeks intervention period, fasted blood was spun at 3000 rpm for 20 minutes at 4°C and 2 ml of plasma was transferred into new tubes and stored at -80°C before being sent to the Waite Analytical Services (WAS, Adelaide University) for plasma Zn and other mineral analysis. A further 300 µl of plasma was transferred to new tubes and kept at -80°C before being sent to the Institute of Medical and Veterinary Science (IMVS) for B12 and folate analysis. Both of these laboratories are nationally certified and accredited to provide specified analytical measurements for these minerals and vitamins. 3 ml of spare plasma was transferred to a new tube, labelled and stored at -80°C.

The concentration of plasma Zn and other minerals (Iron, Copper, Calcium, Magnesium, Sodium, Potassium, Phosphorus, Sulphur) was determined by Inductively Coupled Plasma Optical Emission Spectrometry (ICPOES, Agilent Technologies 7500c, Japan), following digestion with nitric acid and hydrochloric acid.

The plasma folate, B12 and Hcy analysis were monitored to assess whether there were substantial dietary changes during the trial which may have impacted on the DNA damage biomarkers. For Hcy determination, blood was collected in a special vacutainer containing EDTA and sent to the IMVS within 2 hours of collection for analysis. The concentration of Hcy in samples was expressed as µmol/L. The IMVS reference range for (fasted) plasma samples was 4.0-14.0 µmol/L. Concentration of Hcy was measured using the ARCHITECT® Homocysteine assay (Abbott Laboratories, IL, USA). The ARCHITECT® Homocysteine assay exhibits total imprecision of <10% within the calibration range (0.0-50.0 µmol/L). For folate analysis, the concentration of folate in all samples was expressed as nmol/L. The IMVS reference range for (fasted) plasma samples was 5.0-45.0 nmol/L. Plasma vitamin B12 is expressed as pmol/L. The IMVS reference range for (fasted) plasma samples was 100-700 pmol/L.

6.3.5.2 FRAP analysis

The FRAP assay was used to measure the combined antioxidant effect of the non-enzymatic defences in plasma samples [281]. This method was adapted from one of the standard operating procedures in the lab [281]. At a low pH, antioxidants present in plasma reduce ferric 2,4,6-tripyridyl-s-triazine (Fe^{3+} - TPTZ) to the ferrous form (Fe^{2+} - TPTZ), which has an intense blue colour with absorbance maximum at 593 nm.

$$\mathbf{Fe^{3+}\text{ - TPTZ} \xrightarrow[\text{pH3.6}]{\text{antioxidants}} Fe^{2+}\text{ - TPTZ}}\ \text{(blue colour)}$$

The unit of measurement is the FRAP value (or antioxidant activities-AOA), measured in µmol/L. The FRAP value was calculated by comparing the amount of plasma antioxidants with the amount of ferrous ions (Fe^{2+}) required to give the same absorbance change (ΔA).

The absorbance of the products of the FRAP reaction was measured on an ELISA microplate reader (SpectraMax 250, Molecular Devices, CA, USA) at a wavelength of 593 nm. 96 well plates were used in this assay for multiple readings as only 300 µl solution was used for absorption readings.

Plasma samples that were kept at -80°C were thawed overnight at 4°C in a fridge. The chemicals used in the FRAP assay included the FRAP working reagent and the ferrous sulphate standard solutions. Preparation of the FRAP working reagent is detailed in Table 6.1 and based on one of the laboratory standard operation produres [281].

Table 6.1: Preparation of FRAP working reagent

FRAP working reagent ingredients	Preparation
1. 25 ml 0.3 M Acetate buffer pH 3.6	3.1g of sodium acetate ($C_2H_3O_2Na*3H_2O$) was mixed with 16 ml of glacial acetic acid ($C_2H_4O_2$) and diluted with deionized water (DI) to 1L. The pH was adjusted to 3.6.
2. 25 ml 10 mmol/L TPTZ solution	TPTZ 2,4,6-tripyridyl-s-triazine solution : 0.156g of TPTZ was mixed with 2 ml of HCl (1M) and diluted to 50 ml.
3. 2.5 ml of 20 mmol/L ferric chloride solution	Ferric chloride solution : 0.54g of $FeCl_3*6H_2O$ was dissolved in DI water and diluted to 100 ml.

*the order of mixing the solutions 1, 2 and 3 is important

In this assay, the working standard of 10 mmol/L ferrous ion solution was used to prepare 0, 200, 600, and 1000 µmol/L concentrations of Fe^{2+} standard solutions. This range covered the normal adult FRAP value ranging from 600 – 1600 µmol/l [281].

For this analysis, 30 ml of freshly prepared FRAP reagent was warmed in a 37°C water bath and 300 µl of FRAP reagent transferred to a 96 well plate for reagent blank reading (A_1) at 593nm. Subsequently, 10 µl of the plasma samples were added to the FRAP reagent in the same 96 well plate along with 30 µl of deionized water (DI) and an absorbance reading (A) at 593 nm was recorded after 5 minute reaction time. The change in absorption (ΔA) between the final reading (A) and the reagent blank reading (A_1) was calculated for each sample ($\Delta A = A - A_1$) and related to ΔA of a Fe^{2+} standard solutions tested in parallel.

The calibration curve of the six Fe^{2+} standard solutions was made before each set of sample measurements. An example of a calibration curve used in this study is shown in Figure 6.3.

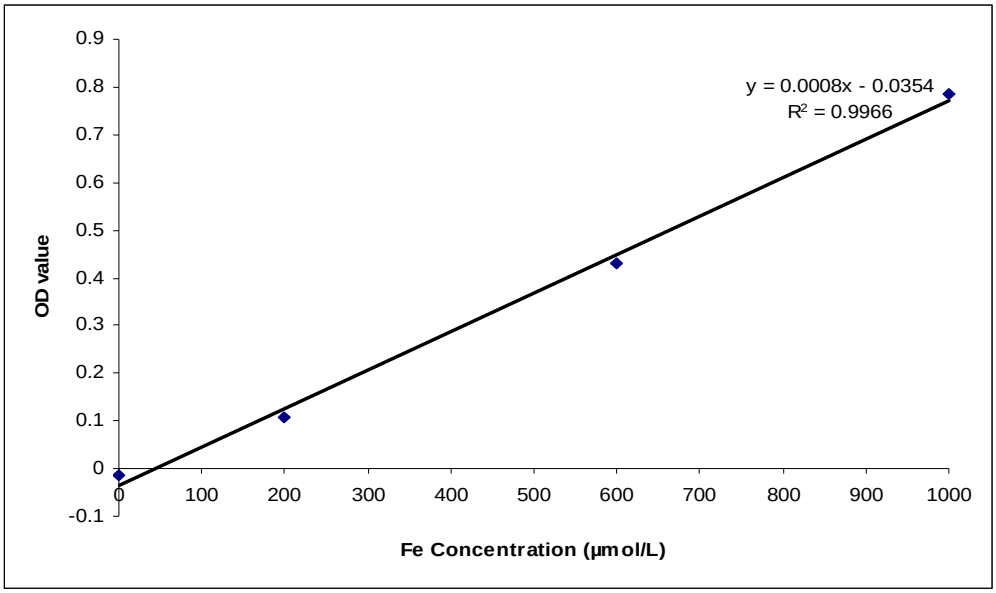

Figure 6.3: Relationship between the concentration of Fe^{2+} standard solutions and the changes in absorption (at 593 nm).

A calibration curve of Fe^{2+} standard solutions was used to demonstrate the linear relationship between the concentration of Fe^{2+} and the change in absorbance ΔA (the formula from the calibration curve was obtained by forcing the linear regression line through zero) and used to calculate the plasma antioxidant activities (AOA).

6.3.5.3 eSOD assay

After lymphocyte isolation, erythrocytes (red blood cells) had cold dH_2O added in order to aid cellular lysis. Lysis occured when the opaque solution changed to a brilliant clear red solution, indicating the release of haemoglobin. Hemoglobin was precipitated by adding 0.25 volumes of ethanol and 0.15 volumes of chloroform. The mixture was shaken for 1 minute and spun at 10 000 rpm for 10 minutes at 4°C. The clear top layer was recovered and dialyzed overnight with 1X PBS. The dialyzed erythrocyte extract was spun the next day to remove any precipitate formed during the dialysis and placed on ice prior to determination of protein. Cell extraction buffer was added to the vial and incubated on ice for 30 minutes with periodic vortexing. The disrupted cell suspension was spun at 10 000 rpm for 10 minutes at 4°C to remove insoluble material. The supernatant was then recovered to a fresh tube

prechilled on ice. Protein concentration of the cleared cell lysate was determined using Protein Quantification Kit-Rapid (Sigma, Australia).

For this analysis, we used the SOD standard curve to verify that the assay is working predictably and that concentration dose-response is linear within the relevant range (Figure 6.4). A serial dilution of the SOD standard was prepared with 1X SOD buffer at the following concentrations: 10 units/25 µl, 5 units/25 µl, 2 units/25 µl, 1 unit/25 µl, 0.5 unit/25µl, 0.2 unit/25 µl, and 0.1 unit/25 µl. 25 µl of 1X SOD buffer was used as activity control in this assay. For protein erythrocytes, a serial dilution between 0.5 µg/25 µl to 50 µg/25 µl protein was prepared and 25 µl of the extract dilutions was added to duplicate wells of the 96 well plate. 150 µl of Master Mix [10X SOD Buffer (Cat# 7501-500-02, Trevigen Inc, USA), 15 µl WST-1 Reagent (Cat# 7501-500-06, Trevigen Inc, USA), 5 µl Xanthine Oxidase (Cat# 7501-500-03, Trevigen Inc, USA), and 5 µl dH2O] was added for each reaction. Xanthine solution was added (Cat# 7501-500-04, Trevigen Inc, USA) to initiate the reactions and the plate was transferred immediately to a plate reader and absorbance readings at 450 nm were taken every minute for 10 minutes at room temperature. SOD activity was determined by the slope and from the curve, the amount of protein that caused 50% inhibition was determined.

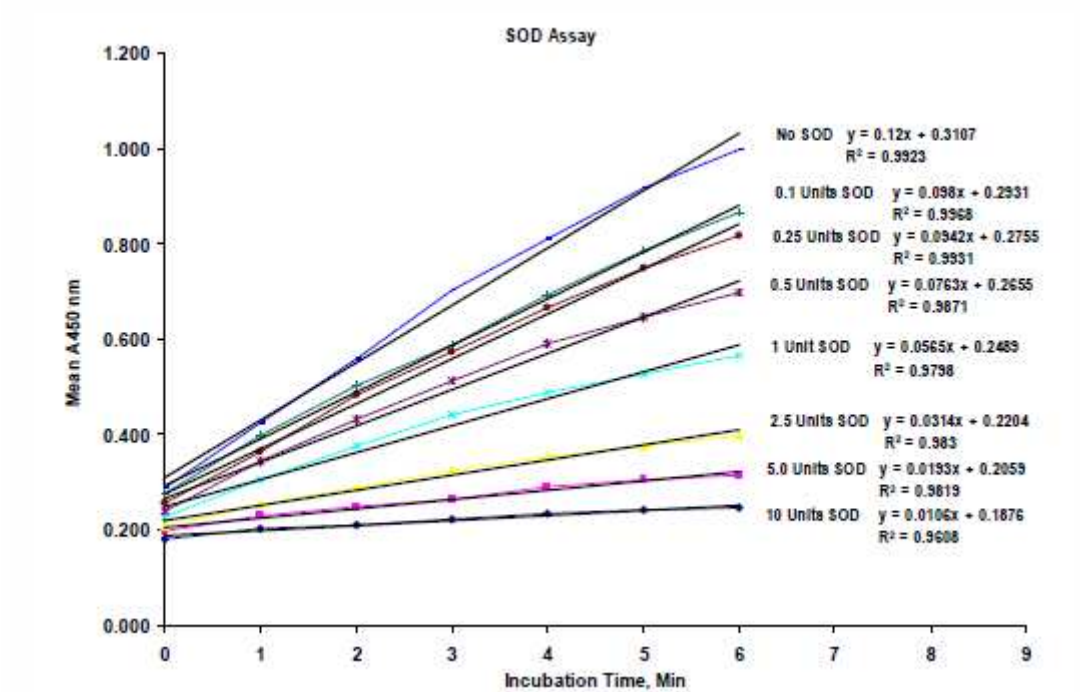

Figure 6.4: Change in absorbance at 450 nm with time for a SOD standard dilution series. A linear regression analysis of the reaction rates during the first 6 minutes of incubation is shown.

6.3.6 DNA Damage assay

6.3.6.1 Cytokinesis Block Micronucleus Cytome assay (CBMN-Cyt)

This assay involves culturing mitogen stimulated primary lymphocytes *in vitro* in the presence of cytochalasin-B (Cyto-B) to block dividing cells at the binucleate stage (BNed cells) to observe any DNA damage, cytotoxic or cytostatic effects. After Cyto-B treatment, cells are harvested onto slides by cytocentrifugation and stained. Chromosomal damage markers are then scored by light microscopy. The standard protocol involves scoring DNA damage biomarkers in 1000 BNed cells per slide, on duplicate slides, from duplicate cultures.

a) Lymphocyte culture and addition of Cytochalasin-B

i- Preparation of phytohaemagglutinin (PHA) stock solution

To prepare the 10X stock solution, 2 ml of sterile isotonic saline was added to a vial containing 5 mg of phytohaemagglutinin (PHA) (Oxoid, Australia), forming a solution of 2.5 mg/ml. 200 µl volumes of the solution were aliquotted into labelled 5 ml polystyrene yellow capped tubes and stored at -20°C for up to 1 month.

ii- Preparation of Cytochalasin-B stock and working solutions

The vial containing 5 mg of Cytochalasin B (Cyto-B) (Sigma, Australia) was removed from storage at -20°C and allowed to equilibrate to RT. The top of the rubber seal was sterilised with 70% ethanol and the seal vented with a 25G needle attached to a 0.2 µm hydrophobic filter to break the vacuum. 8.33 ml of sterile DMSO was transferred to a sterile 50 ml Falcon tube and half of this was then transferred through the seal using a sterile syringe and mixed gently with the Cyto-B. The solution was removed and transferred to a sterile tube to create a final volume of 8.33 ml of 600 µg/ml stock solution. 100 µl volumes of the latter were then aliquotted into a sterile labelled 5 ml polystyrene tubes and stored at -20°C for up to 12 months. Prior to addition into cultured working solution (60 µg/ml) was prepared using culture medium as a diluent.

iii- Establishment of fresh lymphocyte cultures for CBMN-Cyt assay

For CBMN Cyt assay, a total cell count was performed and 750 µl cultures were set up at $1x10^6$ /ml (in duplicate labelled clearly with CSIRO ID and date) in complete medium. PHA was added to cultures to give a final concentration of 30 µg/ml and placed in an incubator at 37°C with 5% CO_2. Following 44 hours incubation after PHA stimulation, cultures were removed and 37.5 µl of 60 µg/ml Cyto B was added to each culture, achieving a final Cyto B concentration of 4.5 µg/ml. Tubes were shaken

to mix well and then returned to the incubator for a further 24 hours. Cells were then harvested onto slides 72 hours after PHA stimulation (Figure 6.5).

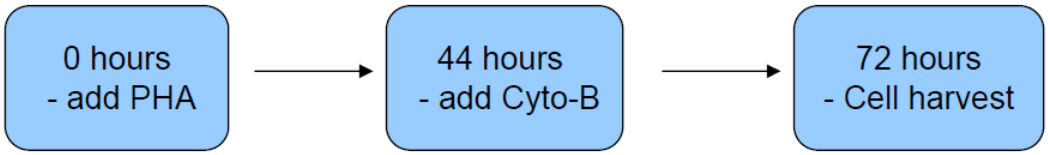

Figure 6.5: Time intervals for CBMN-Cyt assay.

b) Cell harvest and staining

Glass microscope slides (Knittel Gläser, Germany) were washed in absolute ethanol, dried and labelled. They were assembled in a slide holder with a filter card (Thermo Electron, Melbourne, Australia) and cytocentrifuge cup, arranged in the cytocentrifuge (Shandon Scientific Limited, UK) rotor. Cells in each culture tubes were resuspended gently, and a 120 µl sample was transferred into the cytospin cup of the corresponding numbered slide in the rotor. After centrifugation at 600 rpm (5 minutes) at RT, the slides were rotated and the process repeated. Each slide holder was then carefully dismantled and slides were placed in a rack to dry for exactly 10 minutes prior to fixing for 10 minutes in Diff-Quik fixing solution (Diff-Quik Kit, Lab Aids, Australia). The slide rack was then transferred to Diff-Quik solution 1 (orange) (Diff-Quik Kit, Lab Aids, Australia) and stained for 10 dips, and then into Diff-Quik solution 2 (blue) for 6 dips. The slides were then washed gently under running RO water, and allowed to air dry. Each slide was checked by microscopy prior to coverslipping to ensure an even coverage of cells and appropriate staining. When thoroughly dry, slides were coverslipped in a fume hood using DePex (Merck, Germany) and then left overnight in the fumehood to dry, prior to scoring.

c) Slide scoring method

At the end of each week of cultures, two slides from each individual were randomly numbered and coded by an independent operator prior to scoring by the “blinded”

experimenter. Slides were only un-blinded when all slides for the whole intervention had been scored. Slides were scored under 1000X magnification (10X objective, 100X oil immersion lens), using a conventional light microscope (Leica, DMLB). Initially, all cells on the slide were scored for the categories of apoptotic, necrotic, mono-, bi-, and multinucleated, until a total of 500 cells was reached, providing data to calculate the nuclear division index (NDI). Then, only binucleated (BN) cells were scored until a total of 1000 BN was achieved. Chromosomal damage biomarkers (MNi, NBuds and NPBs) were only recorded when they occurred in a BN cell.

d) Calculation of the nuclear division index (NDI)

The NDI provides a measure of the proliferative status of the viable cell fraction [84]. NDI at each time point and for each culture condition was calculated, using the proportions of mono-, bi- and multinucleated cells, to give an estimate of the cell division frequency. NDI is calculated according to a modified form of the equation proposed by Eastmond and Tucker [197].

NDI = {(M1 + (2XM2) + (3XM3))/N}, where M1 and M2 represent the number of cells with one or two nuclei respectively, M3 represents all multinucleated cells (ie. >2 nuclei per cell) and N is the total number of viable cells scored.

e) Cell scoring criteria

Cell types and chromosomal damage markers were scored according to the criteria proposed by Fenech (2007) and detailed below [84].

i- Criteria for scoring viable mono-, bi-, and multinucleated cells

- Mono-, bi- and multinucleated cells are those with an intact cytoplasm and normal nuclear morphology, containing one, two and three or more nuclei, respectively (Figure 6.6).

- These cells may or may not contain MNi, NBuds and in the case of bi- and multinucleated cells (Figure 6.7) [84].

ii- Criteria for scoring BN cells suitable for scoring markers of chromosomal damage

The cytokinesis-blocked BN cells that may be scored for MN, NPB and NBud frequency should have the following characteristics (Figure 6.6B):

- The cells should be binucleate (BN).
- The two nuclei in a BN cell should have intact nuclear membranes and be situated within the same cytoplasmic boundary.
- The two nuclei in a BN cell should be approximately equal in size, staining pattern and staining intensity.
- The two nuclei in a BN cell may be attached by a NPB, which is no wider than $1/4^{th}$ of the nuclear diameter.
- The two main nuclei in a BN cell may touch but ideally should not overlap each other. A cell with two overlapping nuclei can be scored only if the nuclear boundaries of each nucleus are distinguishable.
- The cytoplasmic boundary or membrane of a BN cell should be intact and clearly distinguishable from the cytoplasmic boundary of adjacent cells [84].

iii- Criteria for scoring apoptotic cells

Apoptotic lymphocytes are cells undergoing programmed cell death. They have the following characteristics:

- Early apoptotic cells can be identified by the presence of chromatin condensation within the nucleus and contain intact cytoplasmic and nuclear membranes (Figure 6.6D).

- Late apoptotic cells exhibit nuclear fragmentation into smaller nuclear bodies within an intact cytoplasm/cytoplasmic membrane (Figure 6.6E).
- Staining intensity of the nucleus, nuclear fragments and cytoplasm in both early and late stage apoptotic cells is usually greater than that of viable cells [84].

iv- Criteria for scoring necrotic cells

Necrosis is an alternative form of cell death that is thought to be caused by damage to cellular membranes, organelles and/or critical metabolic pathways required for cell survival such as energy metabolism. Necrotic lymphocytes have the following characteristics (Figure 6.6F):

- Early stage necrotic cells have a pale cytoplasm, the presence of numerous vacuoles (mainly in the cytoplasm and sometimes in the nucleus), damaged cytoplasmic membranes and a fairly intact nucleus.
- Late stage necrotic cells exhibit loss of cytoplasm and damaged/irregular nuclear membrane, with only a partially intact nuclear structure and often with nuclear material leaking from the nuclear boundary.
- Staining intensity of the nucleus and cytoplasm in both types is usually less than that of viable cells [84]

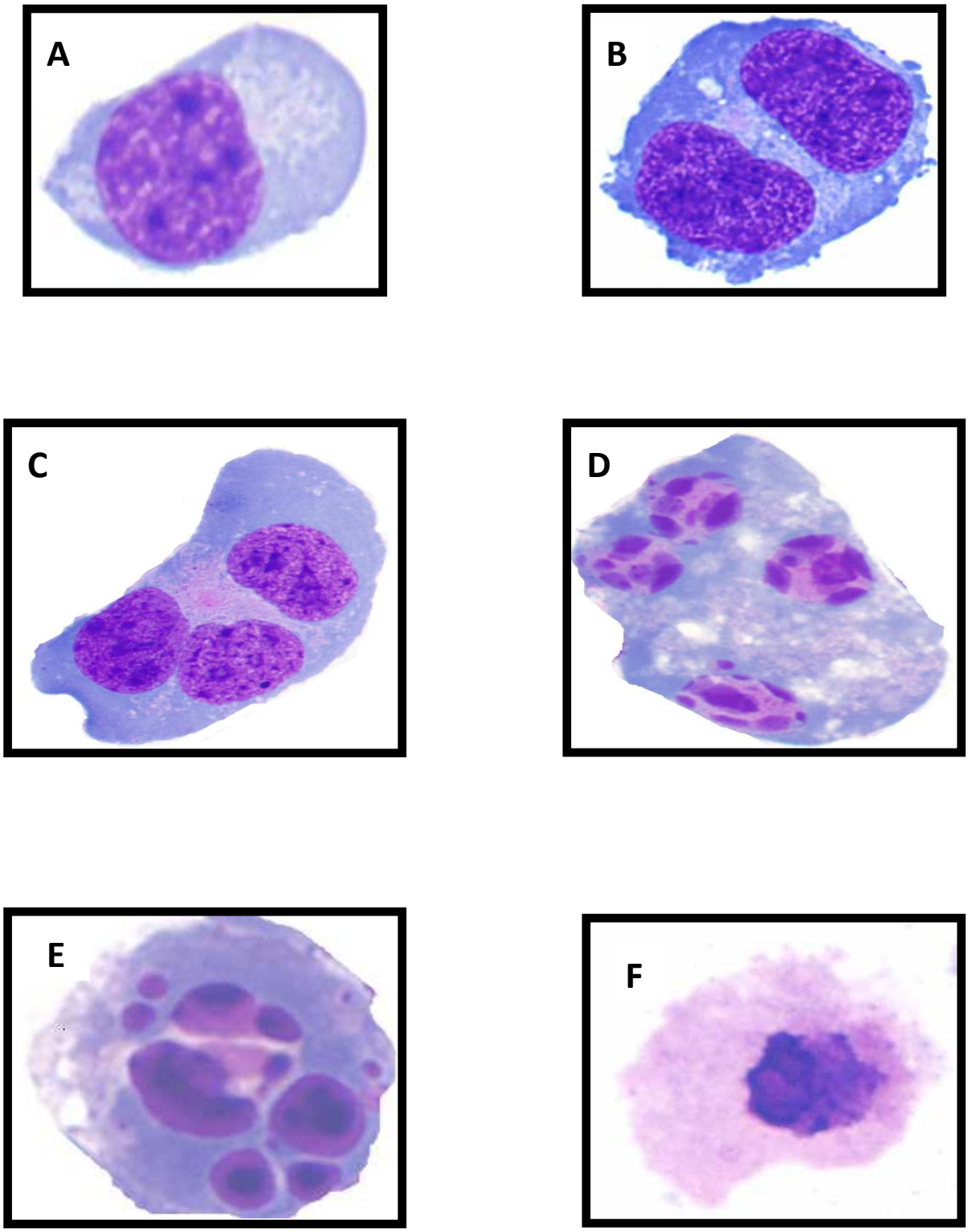

Figure 6.6: Example of morphological characteristics used to score cells in the cytokinesis blocked micronucleus cytome (CBMN-Cyt) assay. (A) mononucleated cell; (B) binucleated cell; (C) multinucleated cell; (D) early multinucleated apoptotic cell; (E) late apoptotic cell; and (F) necrotic cell (1000X magnification)

v- Criteria for scoring micronuclei (MNi)

Micronuclei represent chromosome fragments or whole chromosomes that lag behind at anaphase during nuclear division. They are morphologically identical to, but smaller than, nuclei. The have the following characteristics (Figure 6.7A,B) [84]:

- The diameter of MNi in human lymphocytes usually varies between $1/16^{th}$ and $1/3^{rd}$ of the mean diameter of the main nuclei, which corresponds to $1/256^{th}$ and $1/9^{th}$ of the area of one of the main nuclei in the BN cell, respectively.
- MNi are non-refractile and can therefore be readily distinguished from artefacts such as staining particles.
- MNi are not linked or connected to the main nuclei.
- MNi may touch but do not overlap the main nuclei and the micronuclear boundary should be distinguishable from the nuclear boundary.
- MNi usually have the same staining intensity as the main nucleus but occasionally staining may be more intense.

vi- Criteria for scoring nucleoplasmic bridges (NPBs)

A NPB is a continuous DNA-containing structure linking the nuclei in a BN cell. NPBs originate from dicentric chromosomes (resulting from mis-repaired DNA breaks or telomere end fusions) in which the centromeres are pulled to opposite poles during anaphase. They have the following characteristics (Figure 6.7C) [84]:

- The width of a NPB may vary considerably but usally does not exceed $1/4^{th}$ of the diameter of the nuclei within the cell.
- NPBs should also have the same staining characteristics as the main nuclei.

- ❖ On rare ocassions, more than one NPB may be observed within one BN cell.
- ❖ A BN cell with one or more NPB may also contain one or more MNi (Figure 6.7D).

vii- Criteria for scoring nuclear buds (NBuds)

A NBud represents the mechanism by which a nucleus eliminates amplified DNA and/or DNA repair complexes. They have the following characteristics (Figure 6.7E) [84]:

- ❖ Similar in appearance to MNi with the exception that they are connected with the nucleus via a bridge that can be slightly narrower than the diameter of the bud, or by a much thinner bridge, depending on the stage of the extrusion process.
- ❖ Usually have the same staining intensity as MNi.
- ❖ Occasionally NBuds may appear to be located within a vacuole adjacent to the nucleus.

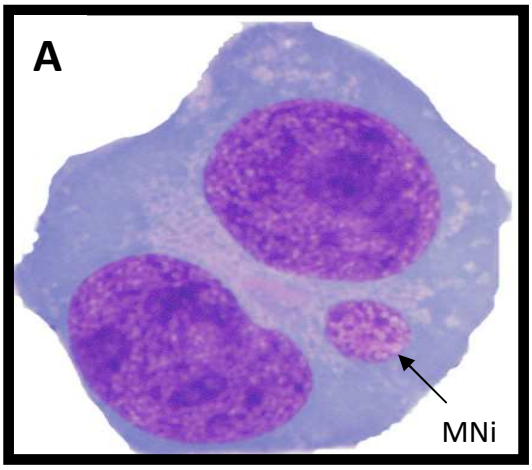

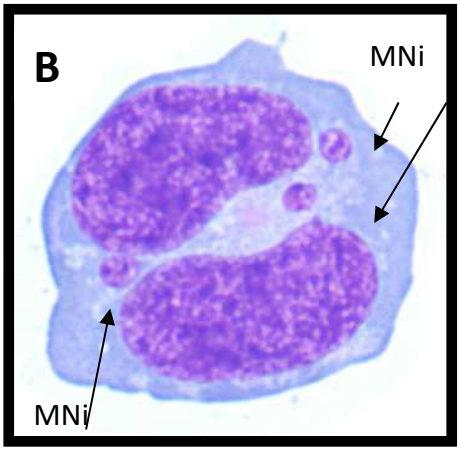

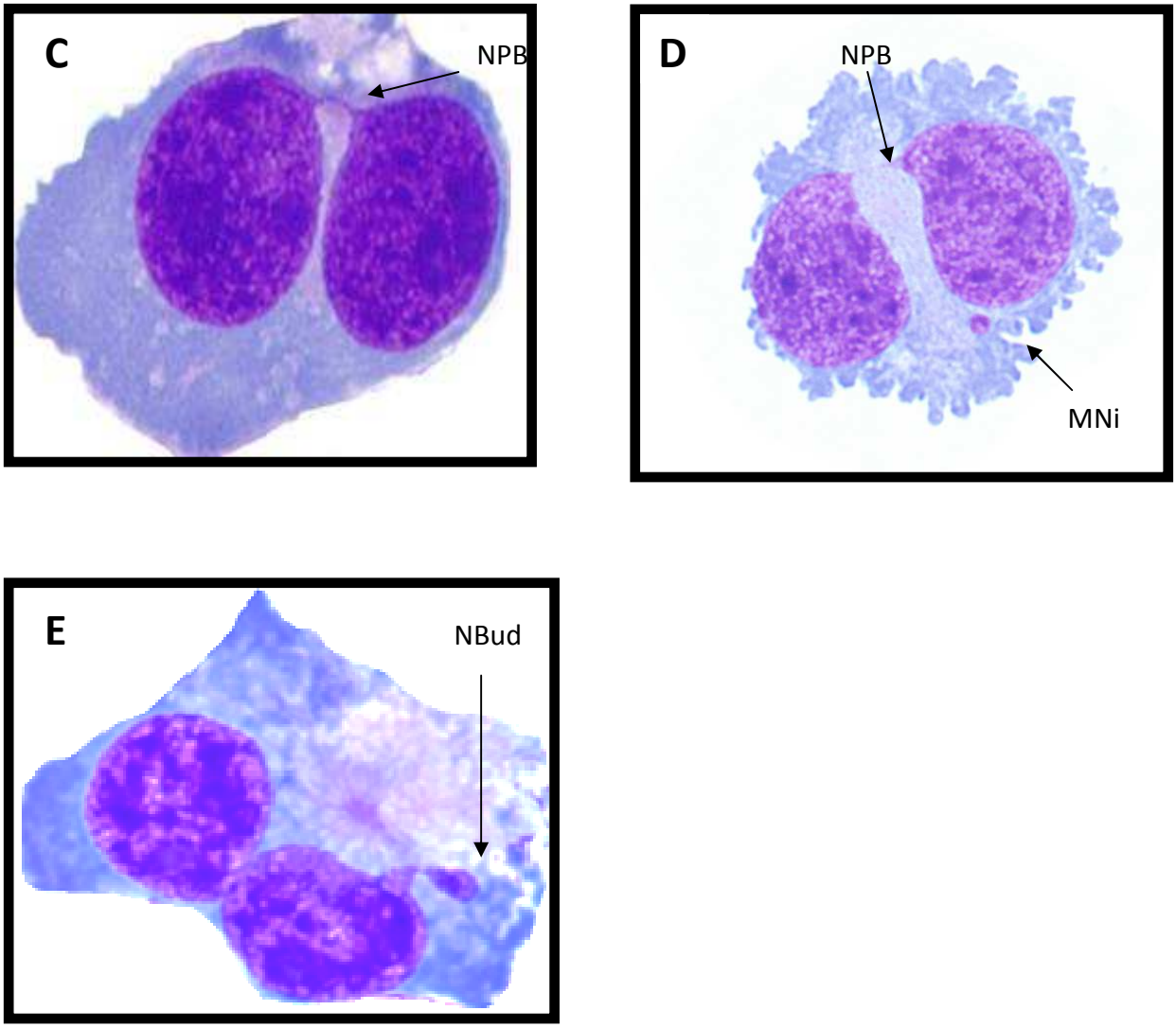

Figure 6.7: Biomarkers of chromosomal damage in lymphocytes scored in Cytokinesis Blocked Micronucleus Cytome assay (CBMN-Cyt) assay. Using these biomarkers, it is possible to measure the frequency of (A,B) chromosome breakage or loss indicated by the presence of one or more micronuclei (MNi); (C) chromosome rearrangement resulting in one or more nucleoplasmic bridges (NPB); (D) chromosome breakage and end fusion, forming a dicentric chromosome (NPB) and one or more acentric fragments (MNi); and (E) gene amplification, indicated by the presence of nuclear bud (NBud) (1000X magnification)

6.3.6.2 Alkaline comet assay

Single cell gel electrophoresis (comet assay) was used to measure DNA strand breaks and alkaline labile sites in the participant lymphocytes. The assay was conducted under alkaline conditions as previously described [147, 148] with slight modification for use with a high throughput CometSlide HT (Trevigen Inc. Cat 4252-02K-01). 100 µl cell suspension in 1% low melting point agarose (Sigma, St. Louis, MO, USA) was spread onto precoated high throughput Comet slides before being immersed in lysis buffer [100 mM EDTA disodium salt dehydrate (Sigma, St. Louis, MO, USA), 2.5 M NaCl (Sigma, St. Louis, MO, USA), 10 mM Trizma base (Sigma, St. Louis, MO, USA), 1% Triton X-100 (Sigma, St. Louis, MO, USA), pH adjusted to 10.0], for 1 hour at 4°C. Slides were incubated in ice-cold alkaline electrophoresis buffer [1 mM EDTA (Sigma, St. Louis, MO, USA), 300 mM NaOH (Sigma, St. Louis, MO, USA), pH adjusted to 13.0] for 20 minutes. Electrophoresis was then conducted at 25V, 350 mA for 20 minutes in the same alkaline buffer in a horizontal Comet assay electrophoresis tank (Thistle Scientific). Slides were washed (3 times with neutralization buffer – 0.4 M Tris-HCl, pH adjusted to 7.5), drained and immersed in 70% ethanol for 5 minutes and air dried at room temperature overnight. Staining was performed using Propidium Iodide solution (Sigma, St. Louis, MO, USA - 50 ug/ml in Phosphate Buffer Saline) for 10 minutes. The above procedures were performed under subdued light conditions using UVA and UVB fliters on fluorescent lamps to avoid light-induced DNA breaks. Nuclei with/without DNA damage were observed at 20X magnification under an Eclipse fluorescence microscope (Nikon, Tokyo, Japan) with a triple band filter (excitation wavelength of 530 nm and emission wavelength of 615 nm) and captured with an attached Spot video camera (Diagnostic Instrument Inc.; Model – 254015, USA). 100 cells were randomly selected from each spot and scored with online software (Tritek - http://autocomet.com/main_home.php) for tail moment and tail intensity. Tail moment (tail length X DNA density) and tail intensity (% DNA in tail) were used as indicators of DNA damage. Figure 6.8 shows an example of damaged and undamaged cells scored in this assay.

A) Undamaged Cells

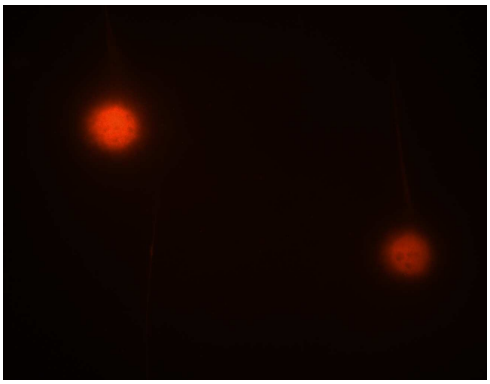

B) Damaged Cells

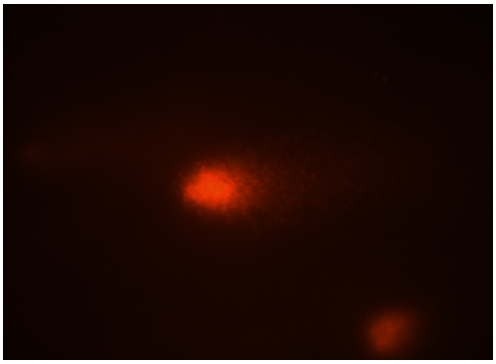

Figure 6.8: Photomicrograph of the cells analysed in the comet assay (400X magnification).

6.3.6.3 Isolation of DNA/RNA

DNA and RNA were isolated from lymphocytes using TRIzol (Ambion), A 0.5 ml volume of trizol was used to homogenise each sample. The only alteration from the manufacturer's directions was the use of 2 µg/ml glycogen (Ambion) and 5 mM sodium acetate to aid RNA precipitation.

To obtain both DNA and RNA from the lymphocytes, we used TRIzol (Invitrogen, Life Technologies) extraction method, as per the manufacturer's directions. Briefly, 0.2 ml of chloroform was added to 1 ml of homogenised lymphocytes in TRIzol reagent. Samples were centrifuged at 12 000 rpm for 15 minutes at 4°C and the

colourless upper aqueous phase containing RNA placed in a new tube. RNA was precipitated by mixing with isopropyl alcohol and washed with 75% ethanol before storage.

0.3 ml of 100% ethanol was added to the organic phase which contained DNA and the genomic DNA was isolated using the silica-gel-membrane-based DNeasy Blood and Tissue Kit 250 (Qiagen, Melbourne, Australia) and the standard protocol followed, with minor modifications. These additional steps were included as it has been shown that under conditions of commonly used DNA isolation protocols, oxidative adducts can spontaneously form affecting the integrity of the acquired DNA [227, 228]. Prior to isolation all buffers were purged for 5 minutes in nitrogen and supplemented with 50 µM phenyl-*tert*-butyl nitrone (Sigma B7263) which acts as a free radical trap and scavenger, the use of phenol and high temperatures (>56 °C) were avoided.

The vial content was pipetted into a spin column with a 2 ml Qiagen collection tube. The spin column was then centrifuged at 8000 rpm for one minute. The flow through was discarded and 500 µl of AW1 buffer (wash buffer 1) added to the column. The spin column was again centrifuged at 8000 rpm for one minute, the flow through was discarded and 500 µl AW2 (wash buffer 2) was added to the column. The spin column was centrifuged at 13 000 rpm for three minutes and the column placed in a new collection tube. 100 µl of AE buffer (elution buffer) was added directly onto the column and centrifuged at 8000 rpm for one minute. This step was repeated, giving a final volume of approximately 200 µl of DNA concentrate. The isolated DNA was refrigerated overnight at 4°C to allow it to become homogenous throughout the solution. The concentration of DNA for each sample was determined in duplicate by Nanodrop spectrometric analysis (Biolab, ND 1000).

6.3.6.4 Telomere length

In this study, a quantitative real-time polymerase chain reaction (qPCR) based method was used to measure absolute telomere length (aTL). This method is based on the Cawthon method for relative measurement of telomere length (TL) but modified by introducing an oligomer standard to measure aTL [230-232].

a) qPCR of DNA for telomere length assay

Absolute telomere length was measured by determining the number of TTAGGG hexamer repeats using a quantitative real-time polymerase chain reaction (qPCR) as described by O'Callaghan *et al* [231]. Assays on serial dilutions were performed to determine a standard curve for measuring kilobases of telomeric sequence. All samples were run on an ABI 7300 Sequence Detection System with SDS v. 1.9 software (Applied Biosystems, Foster City, CA). Each 20µl reaction was performed as follows: 20 ng of DNA, 1X SYBR Green master mix, 100 nM telomere forward primer (CGGTTTGTTTGGGTTTGGGTTTGGGTTTGGGTTTGGGTT), 100 nM telomere reverse primer (GGCTTGCCTTACCCTTACCCTTACCCTTACCCTTACCCT) as described by O'Callaghan *et al* [231]. Cycling conditions were: 10 minutes at 95°C, followed by 40 cycles of 95°C for 15 seconds, 60°C for 1 minute. DNA from the 1301 lymphoblastoid cell line was used as an internal control for each plate run. The number of diploid genomes was calculated using the *36B4* (a single-copy gene) amplicon using the following primers: *36B4* forward primer (CAGCAAGTGGGAAGGTGTAATCC) and *36B4* reverse primer (CCCATTCTATCATCAACGGGTACAA) and the same amplification and cycling conditions as for the telomere amplicon. Similar to the oligomer used for standardization of absolute telomere length, an oligomer was synthesized containing the *36B4* amplicon (CAGCAAGTGGGAAGGTGTAATCCGTCTCCACAGACAAGGCCAGGACTCGTTTGTACCCGTT GATGATAGAATGGG) and used to generate a standard curve for diploid genome quantification.

6.3.6.5 Telomere base damage

In this study, a qPCR based method [233] was used to measure the amount of oxidised residues as well as other base lesions within telomeric DNA that are recognised and excised by the bacterial enzyme, formamidopyrimidine DNA-glycosylase (FPG). FPG is specific for oxidized purines, including 8oxodG, 2,6-diamino-4-hydroxy-5-formamidopyrimidine (FaPyGua) and 4,6-diamino-5-formamidopyrimidine (FaPyAde) and other open-ringed purines [234, 235]. This method is based on differences in PCR kinetics between the DNA template exhaustively digested by FPG and undigested DNA i.e. ΔC_T ($C_T$treated- C_T untreated)

a) Excision of 8oxodG and incision of oligomers at 8oxodG sites using FPG

To excise 8oxodG and generate a strand break at the resulting abasic site DNA was digested with FPG used formamidopyrimidine-DNA glycosylase (FPG). FPG protein has both N-glycosylase and AP-lyase activities and generates a strand break after excision of formamidopyrimidine lesions and 8oxodG residues within the DNA [236]. The single Zn finger motif in the FPG enzyme is utilised by an FPG protein to bind oxidatively damaged DNA [237]. DNA digestion was undertaken using 400 ng of genomic DNA and incubated with 8 units of FPG (formamidopyrimidine-DNA glycosylase) (NewEnglandBiolabs[NEB], Australia) in 1x NEB Buffer (10mM Bis-Tris-Propane-HCl, 10mM MgCl2, 1mM Dithiothreitol, pH 7.0). A control incubated with 1 X NEB Buffer, but without FPG (replaced with H_2O) was also prepared. A duplicate digestion was also set up for each of the corresponding samples in mock buffer (enzyme solution was excluded and substituted with H_2O). All samples were set up on ice and incubated at 37°C overnight to allow complete digestion.

b) qPCR of synthetic oligomers and genomic DNA

The quantitative Real-Time amplification of the oligomers was performed as described by O'Callaghan *et al* (2011) [231]. Each 20µL qPCR reaction was composed as follows: 40pg of digested or undigested oligomer DNA or 40ng of digested or undigested genomic DNA, 1xSYBR Green master mix, 100nM telo1 forward, 100nM telo2 reverse primers [231]. All samples were run on an ABI 7300 Sequence Detection System with the SDS Ver. 1.9 software (Applied Biosystems [AB] Foster City, CA, USA). Each sample was analysed in triplicate. Cycling conditions were: 10 minutes at 95°C, followed by 40 cycles of 95°C for 15 seconds and 60°C for one minute. The amount of base damage in telomeric DNA was calculated by subtracting the C_T of the undigested DNA from the C_T of FPG digested DNA. Based on the standard curve (Figure 6.9), the data is presented as the amount of FPG damage bases/kb telomere.

Equations are as follows:

Amount of FPG damage bases/kb telomere = (Change in C_T value -0.3828)/0.0858

Equations are as follows:

Amount of FPG damage bases/kb telomere = (Change in C_T value -0.3828)/0.0858
(Values derived from standard curve as reported in [233])

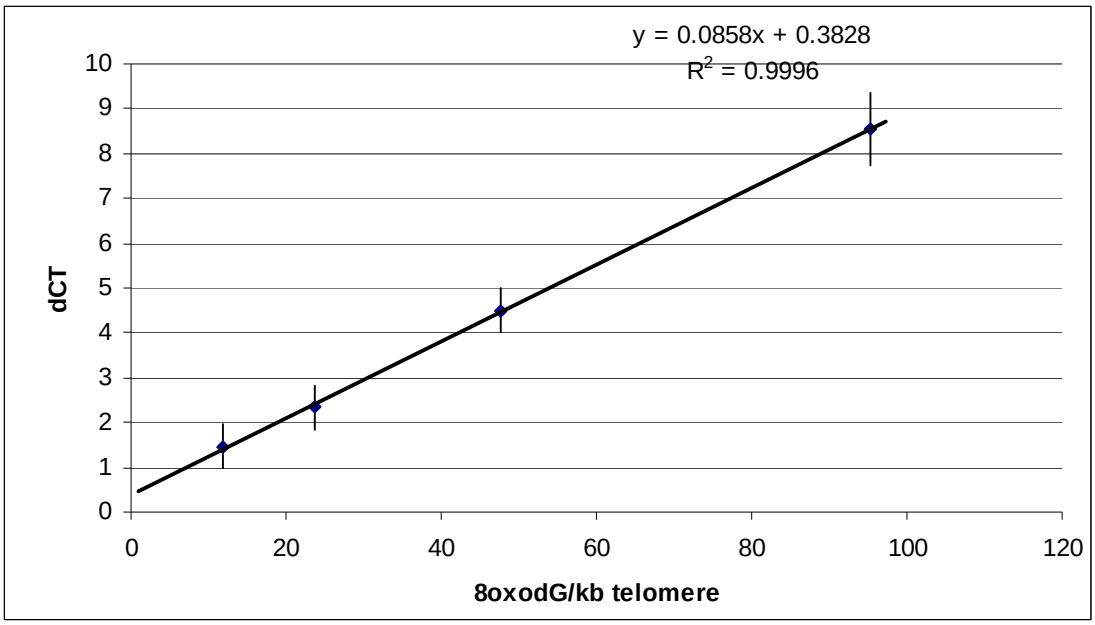

Figure 6.9: An 8oxodG standard Curve. Double-stranded 8oxodG oligomers (1-, 2- or 4-8oxodG bases) were treated with FPG. Following treatment qPCR was performed; resultant amplification profiles (treated and untreated) were then compared. A ΔC_T ($C_T$treated- C_T untreated) was then calculated. The number of 8oxodG in each oligomer was then translated into the number of 8oxodG bases per kb telomeric DNA. Amount of oxidised base pairs per kb of telomere can then be calculated using the equation of the line [dCT=0.0858(oxidised bases/kb telomere) + 0.38] (adapted from [233])

6.3.7 Gene expression

6.3.7.1 MT1A and ZIP expression

a) cDNA synthesis from isolated RNA

RNA samples were thawed on ice prior to measurement of the concentration using a spectrophotometer (Model ND-1000, NanoDrop Technologies, Delaware, USA). Superscript™ III First-Strand Synthesis system for RT-PCR (Invitrogen, Cat No 18080-051) was used to create cDNA from purified RNA, using a modified viral reverse transcriptase enzyme (SuperScript™ III). 5 µg of DNA was then incubated with random hexamer primers, according to the manufacturer's instructions. The mixture was treated at 65°C for 10 minutes (PCR, Corbett Research) to denature any double

strands and to dissociate any bound proteins. Vials were placed immediately on ice for at least 1 minute. 10 µl of synthesis mix was added containing buffer, 25 mM $MgCl_2$, 0.1 M dithiothreitol (DTT), RNAseOUT (RNAse inhibitor) and the polymerase Superscript III RT. Vials were then incubated in the PCR machine for 10 minutes at 25°C during the annealing step. The cDNA synthesis reaction was carried out at 50°C for 50 minutes, followed by a 5 minute heating step at 85°C to inactivate the polymerase and stop the reaction. Samples were then stored at 4°C until required. All steps were performed using surfaces, gloves and equipment that had been cleaned with RNAse Zap. Samples were stored at -20°C until required for RT-PCR.

b) MT1A and ZIP1 expression

In this study, two different types of Zn transporter gene expression were measured using Taqman quantitative Real-Time PCR (ABI 7500 Fast Sequence Detection system, Applied Biosystems). Inventoried Taqman gene expression assays and one custom-designed assay were obtained for *Zip1(Hs00205358_m1) and MT1A (Hs00831826_s1)* mRNA. All samples were quantified in duplicate, using the comparative Ct method for relative quantification of gene expression, normalized to Glyceraldehyde 3-phosphate dehydrogenase (GAPDH). No-template control assays for each mRNA transcript were performed in duplicate on each plate, with diethyl pyrocarbonate-H_2O replacing the cDNA. Minus RT controls were conducted when first extracting RNA to validate that the samples were free from genomic contamination.

All samples were run on an Applied Biosystem 7300 Real Time PCR System and ABI 7300 Sequence Detection System with the SDS Ver 1.9 software (Applied Biosystem, Foster City, CA). Cycling conditions were: 10 minutes at 95°C, followed by 40 cycles of 95°C for 15 seconds, 60°C for 1 minute.

The level of expression of a specific gene in each sample was quantified by measuring the level of fluorescence relative to that of baseline samples.

6.3.8 Statistical analysis

The power calculation was based on the mean and standard deviation of the two main outcome measures: i.e. plasma Zn and micronucleus frequency in lymphocytes. With 40 subjects per group, the study has 80% power to detect an increase in plasma Zn of 0.055 μg/ml and a decrease in micronucleus frequency of 8.30 per 1000 binucleated cells at P=0.05 (one-tailed). These power calculations are based on standard deviation values of 0.095 for plasma Zn and 14.8 for micronucleus frequency in lymphocytes obtained from our own database. The detectable effect size of micronucleus frequency is equivalent to the DNA damage level induced by 0.2 Gy of X-rays which is a carcinogenic dose [282].

Q-Q plots on standard residues of all outcome measures were performed to test the normality of the data sets. Comparisons between groups were performed using general linear models and having treatment and gender as factors. To compare the difference in response between groups at 3 months, the percentage difference relative to baseline values was calculated as recommended by Vickers and Altman (2001) [283]. Correlation analysis between two sets of data was performed using Pearson's test and Partial Correlation Test. A value of $p<0.05$ was considered to be statistically significant. Prism 5.0 (GraphPad Inc, San Diego, CA, USA) and SPSS for Windows (version 17.0, SPSS Inc, Chicago) software were used to obtain these values.

6.4 Results

6.4.1 Screening results

A total of 208 volunteers aged 65-85 years old met the selection criteria and were screened for plasma Zn status and those with plasma Zn concentration ≤ 10.0 μM (≤ 0.65 mg/L - cut-off point for Zn deficiency [272]) were given priority for inclusion in the study. Because there were too few with plasma Zn ≤ 0.65 mg/L (10.0 μM), we increased the cut-off point and eventually selected all those with plasma Zn status <

0.77 mg/L/11.77 µM (n=90) and the volunteers were consented to partipate in the study. The volunteers were then randomly divided into two groups (Zn supplement vs placebo). Figure 6.10 shows the distribution of plasma Zn in screened participants and Figure 6.11 shows prevalence of plasma Zn according to the range based on the iZincG technical document [256]. 45.92% of participants have Zn deficiency while 39.29% have a normal plasma Zn concentration and another 14.80% have a slightly higher plasma Zn concentration.

Figure 6.10: Distribution of plasma Zn from screening (n=208)

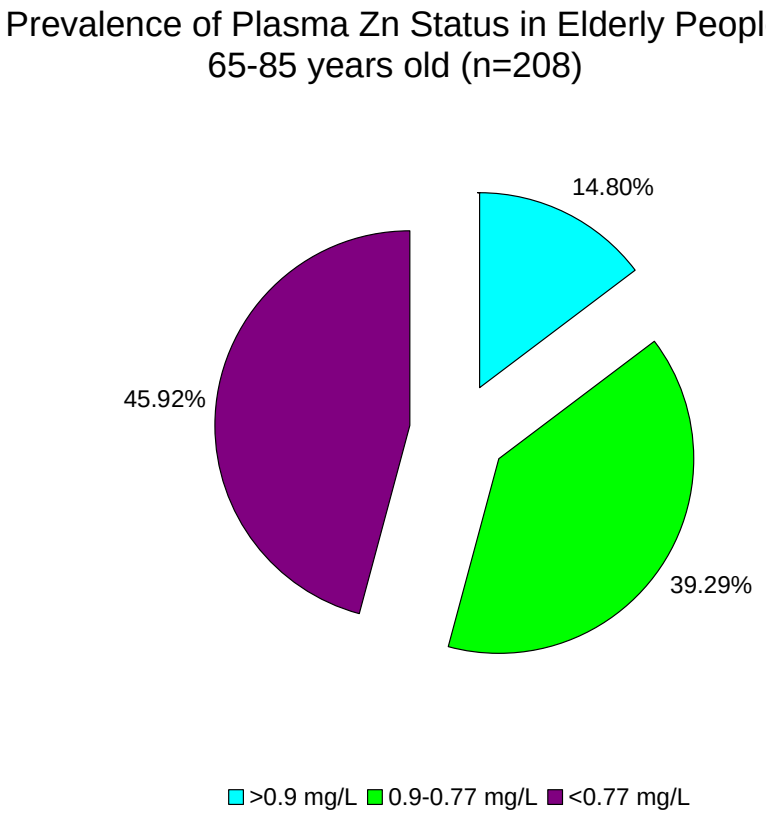

Figure 6.11: Prevalence of plasma Zn according to the range based on the iZincG technical document [256], (n=208)

6.4.2 Characteristics of volunteers

90 participants were randomised into two groups (Placebo and Zn, n=45) and 42 from each group completed the intervention. Reasons for drop-out during the trial included overseas travel (n=2), noncompliance (n=2), adverse events (n=1) and voluntary withdrawal (n=1). Age (Placebo group: 73.12 ± 5.19 years; Zn group: 73.88 ± 4.99 years), BMI (Placebo group: 26.73 ± 4.29 kg/m^2; Zn group: 26.81 ± 4.07 kg/m^2) and the estimated Zn intake (Placebo group: 10.58 ± 3.62; Zn group: 10.97 ± 3.91 mg/day) was not significantly different between Placebo and Zn groups, respectively (Table 6.4). However, plasma Zn values at screening were significantly lower in the Placebo group (0.69 ± 0.06 mg/L) compared to the Zn group (0.71 ± 0.04 mg/L). Compliance rate was high (>98%) with respect to tablet consumption in both groups.

Table 6.4: Characteristics of participants who completed the intervention in each dietary group (n=84).

	Placebo (n=42)	Zn (n=42)	P value
Age (years)	73.12 ± 5.19	73.88 ± 4.99	0.4996 (ns)
BMI (kg/m^2)	26.73 ± 4.29	26.81 ± 4.07	0.9341 (ns)
Gender (%)	Male : 38.1 Female : 61.9	Male : 54.8 Female : 45.2	0.126 (ns)
Plasma Zn (at screening) (mg/L)	0.69 ± 0.06	**0.71 ± 0.04***	**0.0289 (p<0.05)**
Zn intake (mg/day)	10.58 ± 3.62	10.97 ± 3.91	0.6401 (ns)
Compliance rate (%)**	98	99	

*significant compared to placebo, **reported percentage of tablets consumed, ns – not significant

6.4.3 Plasma micronutrients: Zinc, Carnosine, Mineral, B12, Folate and Homocysteine

In this study, plasma Zn levels was one of the main outcome measures. In the placebo group, plasma Zn showed a significant drop of -4.48% after 12 weeks of

intervention from 0.905 ± 0.099 mg/L (13.84 ± 1.51 µM) to 0.863 ± 0.080 mg/L (13.19 ± 1.22 µM) (Figure 6.12). In the Zn group, there was a significant time and dose-related increase in plasma Zn (Table 6.5A). Plasma Zn was significantly increased by 5.69% after 12 weeks of intervention from 0.926 ± 0.096 mg/L (14.16 ± 1.46 µM) to 0.972 ± 0.135 mg/L (14.86 ± 2.06 µM) (Figure 6.13). At baseline, no change between groups was observed, but significant change was found at the end of 12 weeks intervention indicating that plasma Zn responded well to the Zn supplementation. Despite the changes in plasma Zn concentration, there was no significant increase in the carnosine concentration in the group consuming the Zn Carnosine supplement (Table 6.5A).

No significant changes were observed between both groups following intervention for other minerals such as Iron, Copper, Potassium, Magnesium and Phosphorus as well as vitamin B12, Folate and Homocysteine except for Calcium, Sodium and Sulphur levels (Table 6.5A). However, within groups, a significant increase of 92.36 ± 3.77 to 95.56 ± 3.61 mg/L in the Placebo group and 92.86 ± 3.66 to 97.75 ± 3.69 mg/L in the Zn group were observed for calcium levels in plasma ($p<0.05$). For magnesium, an increase from 20.08 ± 1.61 to 20.58 ± 1.49 mg/L was reported in the Placebo group while a significant increase of 5.7% (relative to baseline) was observed in the Zn group (baseline: 19.49 ± 1.76; 12 weeks: 20.61 ± 1.51 mg/L). Plasma folate showed a significant increase in the Zn group from baseline levels at 33.50 ± 7.81 to 35.88 ± 8.81 nmol/L at the end of the 12 week intervention.

6.4.4 Antioxidant activity (FRAP and eSOD)

Antioxidant activity measured via FRAP was significantly increased in Zn group following 12 weeks of supplementation ($p<0.05$) from 1180.62 ± 315.40 to 1447.79 ± 471.58 µmol/L. However, no significant difference between groups was observed following the intervention. eSOD which reflects Cu-Zn SOD activity in erythrocytes was also significantly increased in the Zn group following the 12 week intervention and the changes were significant between groups ($p<0.05$). eSOD showed a 33.07%

increment (relative to baseline), compared to the Placebo group which showed only 2.45% increment (relative to baseline) (Figure 6.14).

Table 6.5A: Comparison of plasma mineral, B12, Folate, Homocysteine, plasma Carnosine, plasma FRAP and eSOD during the stages of the intervention within and between groups. Values are represented as mean ± SD. FRAP – Ferric Reducing Ability of Plasma, eSOD – erythrocyte Superoxide Dismutase. Mean values were significantly different for comparison *P<0.05, **P<0.01.

† p value for comparison between goups for baseline and week 12

‡ p value for comparison between baseline and week 12 within the placebo and Zn group

	Placebo (n=42)		**Zn (n=42)**		**P value †**
	Baseline	12 weeks	Baseline	12 weeks	
Plasma Mineral (mg/L)					
Zinc (Zn)	**0.905 ± 0.099**	**0.863 ± 0.088**	**0.926 ± 0.096**	**0.972 ± 0.135**	Baseline : 0.340 **Week 12 : 0.000****
P value ‡	**0.028***		**0.016***		
Iron (Fe)	1.276 ± 0.977	1.079 ± 0.412	1.231 ± 0.414	1.198 ± 0.487	Baseline : 0.838 Week 12 : 0.106
P value ‡	0.142		0.827		
Copper (Cu)	1.197 ± 0.237	1.195 ± 0.232	1.154 ± 0.191	1.160 ± 0.196	Baseline : 0.138 Week 12 : 0.208
P value ‡	0.842		0.614		
Calcium (Ca)	**92.363 ± 3.772**	**95.557 ± 3.608**	**92.859 ± 3.661**	**97.748 ± 3.690**	Baseline : 0.551 **Week 12 : 0.009****
P value ‡	**0.000****		**0.000****		
Magnesium (Mg)	**20.079 ± 1.611**	**20.575 ± 1.493**	**19.489 ± 1.762**	**20.613 ± 1.514**	Baseline : 0.120 Week 12 : 0.911
P value ‡	**0.005****		**0.000****		
Sodium (Na)	3256.250 ± 121.379	3225.529 ± 77.144	3260.641 ± 85.404	3254.611 ± 79.543	Baseline : 0.756 Week 12 : 0.050
P value ‡	0.097		0.659		
Potassium (K)	150.161 ± 16.860	152.894 ± 15.272	**150.196 ± 11.512**	**156.604 ± 13.614**	Baseline : 0.991 Week 12 : 0.234
P value ‡	0.186		**0.002****		

	Placebo (n=42)		Zn (n=42)		P value ϯ
	Baseline	**12 weeks**	**Baseline**	**12 weeks**	
Phosphorus (P)	128.272 ± 18.892	128.744 ± 17.282	132.349 ± 19.108	133.181 ± 18.708	Baseline : 0.895 Week 12 : 0.765
P value ǂ	0.889		0.645		
Sulphur (S)	**1165.337 ± 66.558**	**1148.990 ± 55.597**	1176.922 ± 61.243	1182.654 ± 58.724	Baseline : 0.369 **Week 12 : 0.004****
P value ǂ	**0.049***		0.543		
Plasma carnosine (µmol/L)	0.664 ± 0.405	0.688 ± 0.382	0.682 ± 0.382	0.739 ± 0.444	Baseline : 0.972 Week 12 : 0.621
P value ǂ	0.969		0.936		
Plasma B12 (nmol/L)	383.065 ± 274.343	392.286 ± 283.529	305.906 ± 105.830	300.835 ± 102.408	Baseline : 0.084 Week 12 : 0.052
P value ǂ	0.441		0.611		
Plasma Folate (nmol/L)	33.639 ± 7.628	33.821 ± 7.691	**33.500 ± 7.812**	**35.882 ± 8.818**	Baseline : 0.741 Week 12 : 0.244
P value ǂ	0.905		**0.024***		
Plasma Homocysteine (µmol/L)	11.389 ± 3.014	11.476 ± 3.049	11.393 ± 2.801	11.623 ± 2.468	Baseline : 0.797 Week 12 : 0.582
P value ǂ	0.851		0.237		
Antioxidants					
FRAP (µmol/L)	1216.589 ± 326.284	1311.345 ± 418.126	**1180.622 ± 315.404**	**1447.799 ± 471.582**	Baseline : 0.610 Week 12 : 0.167
P value ǂ	0.155		**0.000****		
eSOD (U/g Hb)	2920.93 ± 330.2	2980.615 ± 275.645	**2807.957 ± 571.478**	**3190.228 ± 374.159**	Baseline : 0.780 **Week 12 : 0.005****
P value ǂ	0.452		**0.000****		

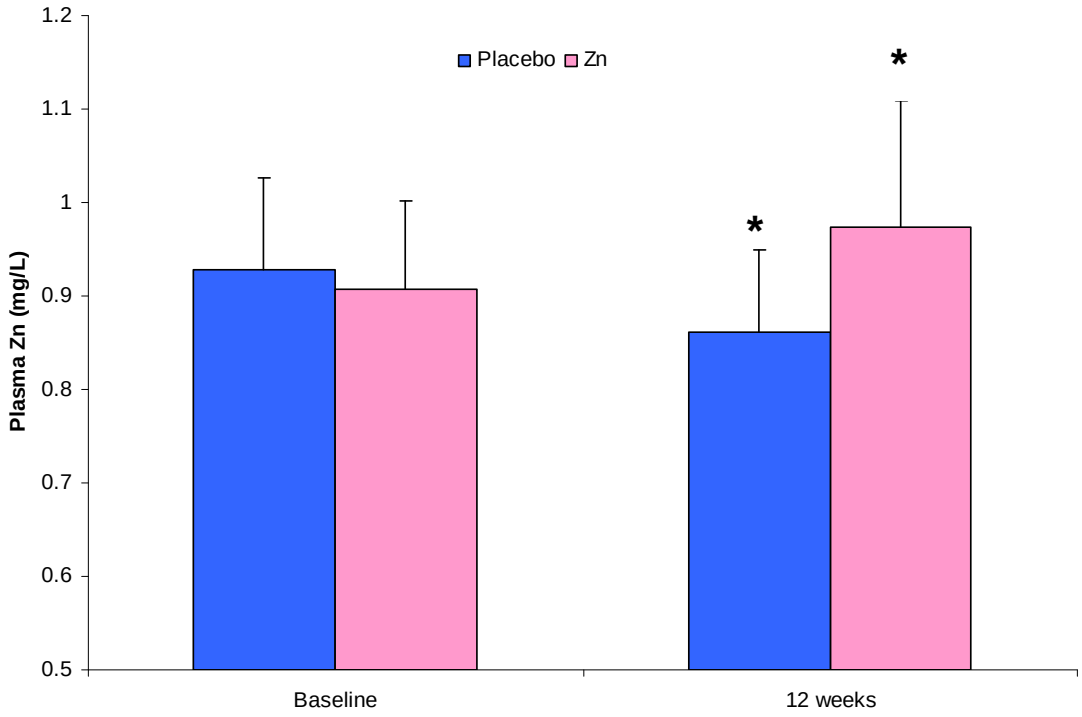

Figure 6.12: **Plasma Zn concentration during the intervention trial**. n=42 for both Zn and Placebo groups, respectively. Results were expressed as mean ± SEM. Mean values with * were significantly different compared to baseline (*p<0.05*).

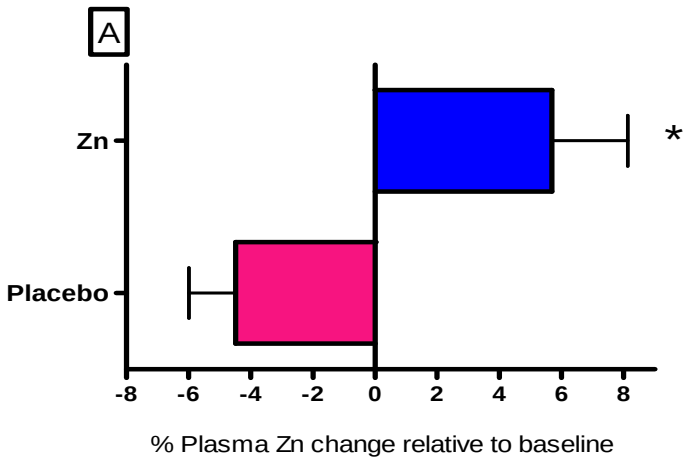

Figure 6.13: Percentage change in Plasma Zn at 12 weeks relative to baseline. Percentage change was adjusted for baseline values. Zn and Placebo refer to the treatment groups; Zn (n = 42) received Zn tablets; Placebo received (n=42) placebo tablet. Values are means with standard errors shown by horizontal bars. Mean values with * were significantly different (*p<0.05*).

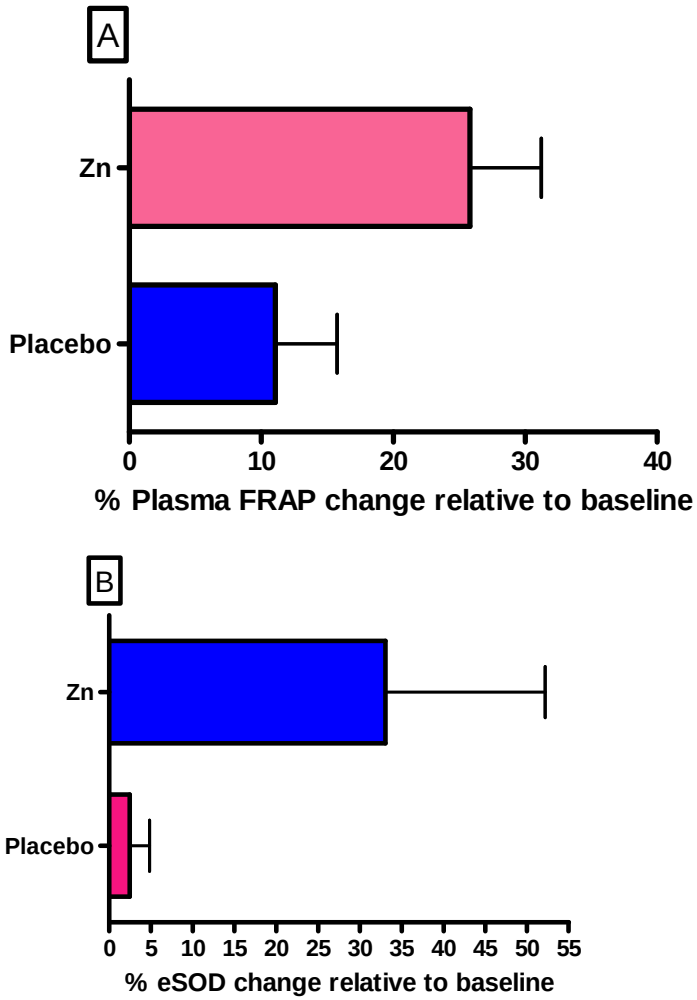

Figure 6.14: Percentage change in A) Plasma FRAP and B) eSOD, at 12 weeks relative to baseline. Percentage change was adjusted for baseline values. Zn and Placebo refer to the treatment groups; Zn (n = 42) received Zn tablets; Placebo received (n=42) placebo tablet. FRAP – Ferric Reducing Activity in Plasma; eSOD – erthyrocytes Superoxide Dismutase. Values are means with standard errors shown by horizontal bars. Mean values with * were significantly different (*p<0.05*).

6.4.5 DNA damage assay: CBMN-Cyt assay and alkaline comet assay

The CBMN-Cyt assay results (Table 6.5B), showed a significant decrease in the frequency of MNi for the Zn group following supplementation (*p<0.05*). The reductions of 24.18% (relative to baseline) were statistically significant compared to the placebo group which showed an increase of 1.77% (Fig 6.15). There were no significant changes in the frequency of NPB and NBuds for both groups. Both tended

to decrease in the Zn supplemented group but the changes were not significant. Necrotic cells were higher in the placebo group following 12 weeks intervention with a significant increase of 44.28% (relative to baseline). However, no change was observed in the percentage of necrotic cells in the Zn supplemented group with only an 18.21% increase relative to baseline. Apoptotic cells were decreased in the Zn group ($p<0.05$) following the duration of intervention with a reduction of -7.53% relative to baseline. NDI was increased in both groups following the 12 weeks of intervention ($p<0.05$) (Table 6.5B) but no significant change between groups was observed.

The comet assay results showed a significant effect of time and treatment of Zn supplementation for both tail moment and tail intensity ($p<0.05$) (Table 6.5B). Tail moment for the placebo group increased from 0.499 ± 0.286 to 0.809 ± 0.354 after 12 weeks of intervention and tail intensity values were also increased from 4.301 ± 1.306 to 5.139 ± 1.953. For the Zn group, both tail moment and tail intensity values were decreased following 12 weeks intervention (Tail moment-baseline: 0.476 ± 0.210; 12 weeks: 0.376 ± 0.229; Tail intensity-baseline: 4.700 ± 1.365; 12 weeks: 2.985 ± 1.587). The reductions of -7.53% for tail moment and -8.76% for tail intensity were observed for the Zn group (relative to baseline) (Fig 6.16). Tail moment and tail intensity in the Placebo group showed a significant 141.6% and 28.95% increase respectively relative to baseline ($p<0.05$).

Table 6.5B: Comparison of DNA damage biomarkers, DNA stability biomarkers and gene expression (MT1A and ZIP1) during the stages of the intervention within and between groups. Values are represented as mean ± SD. BN – binucleates, MNi – Micronuclei, NPB – Nucleoplasmic Bridges, NBuds – Nuclear Buds, kb – kilobase, 8-oxodG - 8-Oxo-2'-deoxyguanosine.
Mean values were significantly different for comparison *P<0.05, **P<0.01
† p value for comparison between goups for baseline and week 12
‡ p value for comparison between baseline and week 12 within the placebo and Zn group

	Placebo		**Zn**		**P value †**
	Baseline	**12 weeks**	**Baseline**	**12 weeks**	
DNA damage					
CBMN-Cyt assay					
Necrosis (%)	8.655 ± 3.302	11.365 ± 4.245	8.755 ± 2.632	9.489 ± 2.835	Baseline : 0.878 Week 12 : 0.018
P value ‡	0.000**		0.275		
Apoptosis (%)	3.283 ± 1.216	3.371 ± 1.723	3.748 ± 1.397	2.951 ± 1.359	Baseline : 0.200 Week 12 : 0.216
P value ‡	0.6785		0.012*		
NDI	1.862 ± 0.165	1.965 ± 0.198	1.877 ± 0.150	1.968 ± 0.222	Baseline : 0.650 Week 12 : 0.949
P value ‡	0.028*		0.030*		
MNi (per 1000 BN)	12.058 ± 5.310	11.125 ± 5.475	11.200 ± 5.034	6.930 ± 3.467	Baseline : 0.456 Week 12 : 0.000**
P value ‡	0.270		0.000**		
NPB (per 1000 BN)	7.469 ± 4.741	7.523 ± 3.886	7.818 ± 3.972	7.486 ± 2.556	Baseline : 0.861 Week 12 : 0.839
P value ‡	0.911		0.555		

	Placebo (n=42)		Zn (n=42)		*P value ϯ*
	Baseline	**12 weeks**	**Baseline**	**12 weeks**	
NBuds (per 1000 BN)	3.244 ± 2.080	3.805 ± 1.968	3.648 ± 2.066	3.405 ± 2.065	Baseline : 0.411 Week 12 : 0.452
P value ǂ	0.294		0.553		
Comet assay					
Tail moment (arbitrary unit)	0.499 ± 0.286	0.809 ± 0.354	0.476 ± 0.210	0.376 ± 0.229	Baseline : 0.686 Week 12 : 0.000**
P value ǂ	0.000**		0.100		
Tail intensity (% DNA in tail)	4.301 ± 1.306	5.139 ± 1.953	4.700 ± 1.365	2.985 ± 1.587	Baseline : 0.178 Week 12 : 0.000**
P value ǂ	0.011*		0.000**		
Telomere Integrity					
Telomere length (kb/diploid genome)	2.878 ± 0.458	3.069 ± 0.463	2.725 ± 0.420	2.929 ± 0.449	Baseline : 0.122 Week 12 : 0.174
P value ǂ	0.054		0.035*		
Telomere base damage (8-oxodG/kb telomere)	14.503 ± 14.870	9.937 ± 10.671	13.879 ± 18.036	6.820 ± 15.181	Baseline : 0.867 Week 12 : 0.291
P value ǂ	0.096		0.009**		
Gene expression					
MT1A (arbitrary units)	4.981 ± 5.371	5.294 ± 5.863	4.287 ± 7.710	8.463 ± 4.697	Baseline : 0.643 Week 12 : 0.009**
P value ǂ	0.658		0.004*		
ZIP1 (arbitrary units)	2.693 ± 0.712	2.760 ± 0.663	2.894 ± 0.705	3.197 ± 0.598	Baseline : 0.294 Week 12 : 0.010*
P value ǂ	0.543		0.045*		

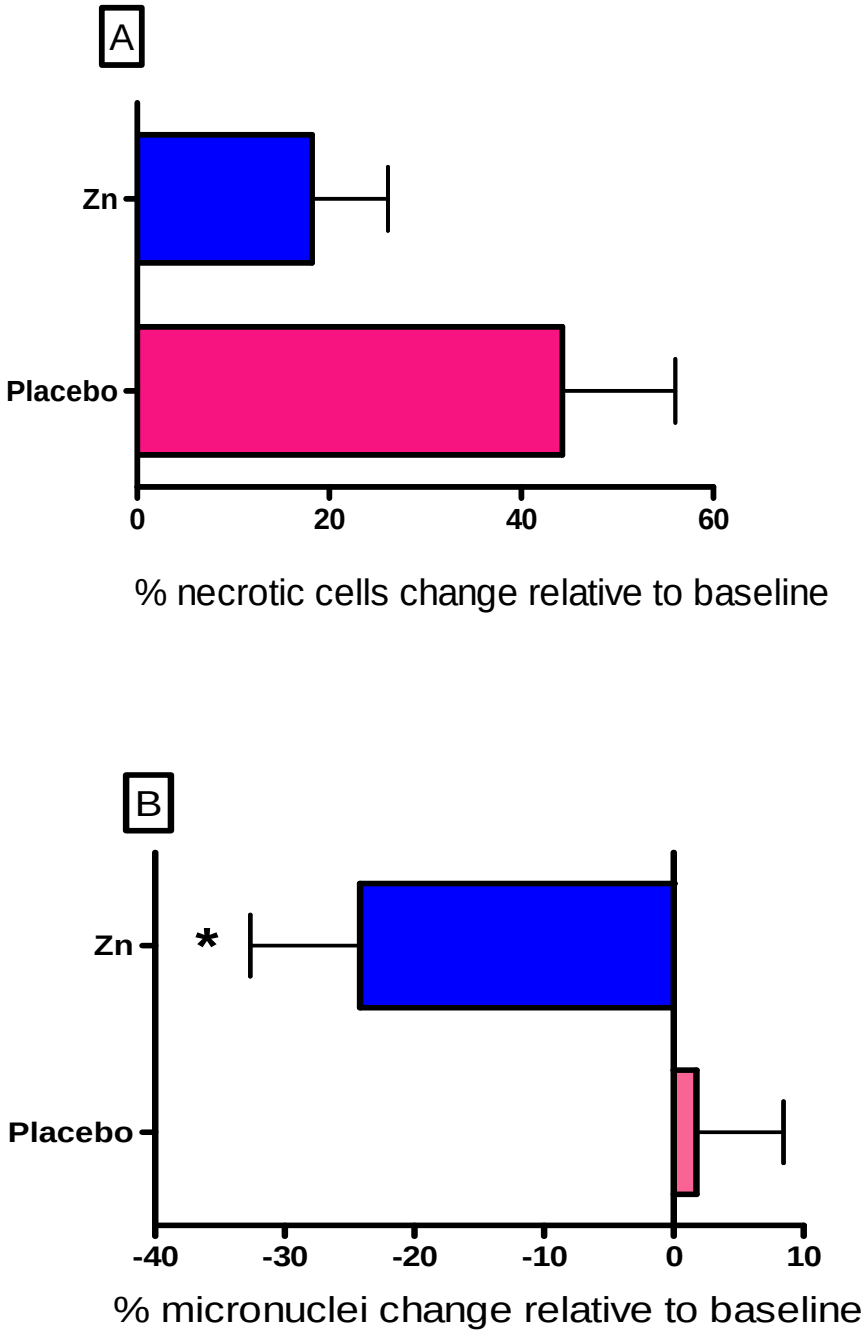

Figure 6.15: Percentage change in A) necrotic cells and B) micronuclei frequency at 12 weeks relative to baseline. Percentage change was adjusted for baseline values. Zn and Placebo refer to the treatment groups; Zn (n = 42) received Zn tablets; Placebo received (n=42) placebo tablet. Values are means with standard errors shown by horizontal bars. Mean values with * were significantly different (*p<0.05*).

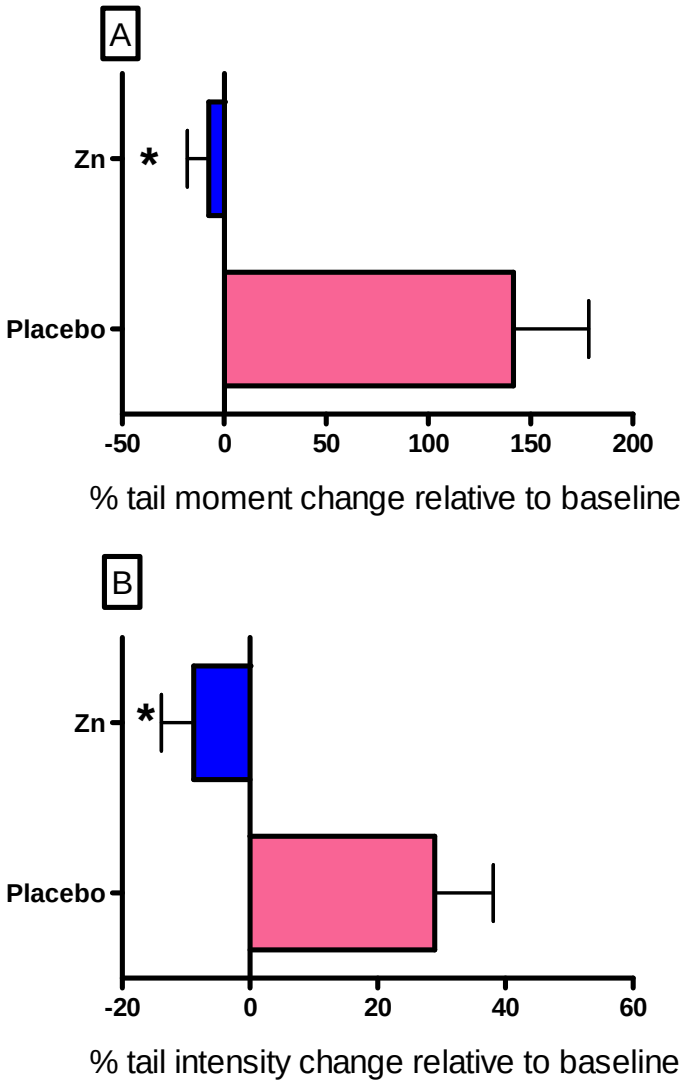

Figure 6.16: Percentage change in A) tail moment and B) tail intensity at 12 weeks relative to baseline. Percentage change was adjusted for baseline values. Zn and Placebo refer to the treatment groups; Zn (n = 42) received Zn tablets; Placebo received (n=42) placebo tablet. Values are means with standard errors shown by horizontal bars. Mean values with * were significantly different (*p<0.05*).

6.4.6 Telomere integrity: Telomere length and telomere base damage

Telomere length was found to be shorter in the Zn supplemented group following the 12 week intervention but the difference was not significantly relative to the placebo group. Both groups showed a significant increase in telomere length within groups following 12 weeks of intervention with an increment of 9.65% for the Zn supplemented group and 10.36% for the Placebo group (relative to baseline) (Fig 6.17). Telomere base damage was found to be significantly decreased in the Zn group ($p<0.05$) (Baseline: 13.88 ± 18.04, 12 weeks: 6.82 ± 15.18 [8 oxodG/kb telomere]), but no difference was observed between groups.

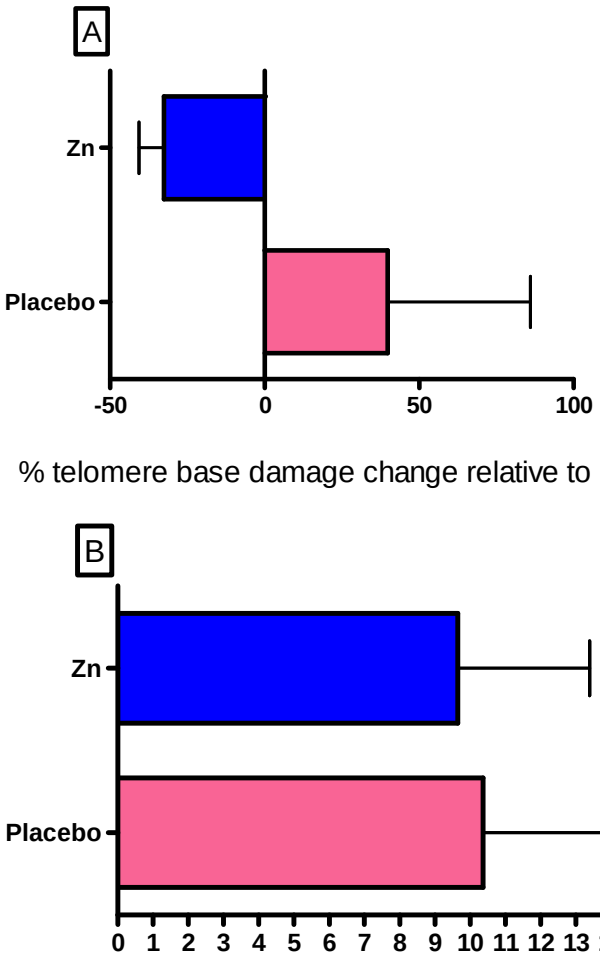

Figure 6.17: Percentage change in A) telomere base damage and B) telomere length at 12 weeks relative to baseline. Percentage change was adjusted for baseline values. Zn and Placebo refer to the treatment groups; Zn (n = 42) received Zn tablets; Placebo received (n=42) placebo tablet. Values are means with standard errors shown by horizontal bars.

6.4.7 Zinc transporter genes: MT1A and ZIP1

In this study, MT1A and ZIP1 were measured as biomarkers for Zn status and Zn transportation measures. Both MT1A and ZIP1 expression showed a significant increase in the Zn supplemented group compared to the Placebo group ($p<0.05$). MT1A expression was significantly higher in the Zn supplemented group ($p<0.05$) following the 12 week intervention compared to the Placebo group (Placebo: 5.29 ± 5.86, Zn: 8.46 ± 4.69 arbitrary unit). ZIP1 expression showed a 19.09% increase relative to the baseline measure, compared to a 9.38% increase in the Placebo group (Fig 6.18).

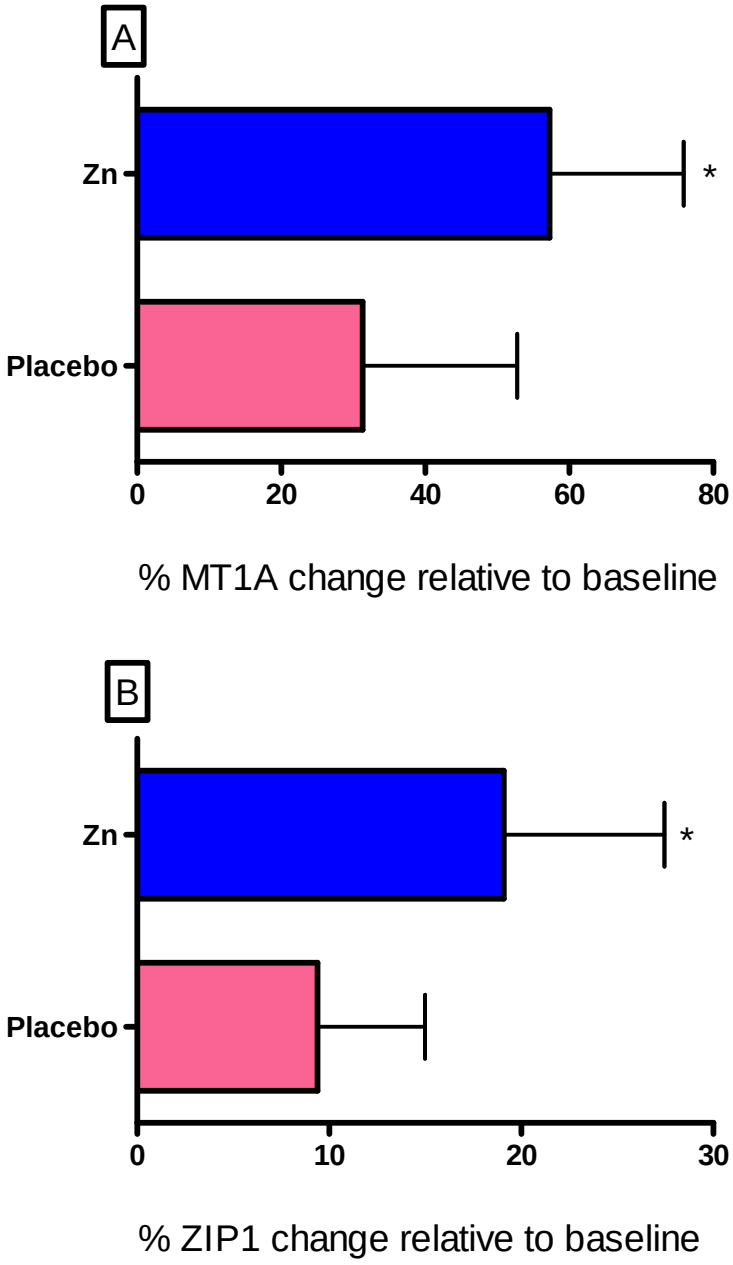

Figure 6.18: Percentage change in A) MT1A and, B) ZIP1 at 12 weeks relative to baseline. Percentage change was adjusted for baseline values. Zn and Placebo refer to the treatment groups; Zn (n = 42) received Zn tablets; Placebo received (n=42) placebo tablet. Values are means with standard errors shown by horizontal bars. Mean values with * were significantly different (*p<0.05*).

6.4.8 Correlation between plasma Zinc and other measured biomarkers

Pearson correlation analysis of the relationship between plasma Zn (at the baseline and at the end of the study) was performed. At baseline, no correlation between plasma Zn and other plasma and DNA damage biomarkers was observed. However, at the end of 12 weeks of supplementation, plasma Zn was significantly correlated with eSOD (r=0.279, p=0.010), tail moment (r=-0.219, p=0.045) and micronuclei (r=-0.235, p=0.032) (Table 6.6).

Partial correlation analysis of the relationships between plasma Zn (at the start and at the end of the trial), after controlling for age and gender, and all biomarkers in this study was also performed. At baseline, no correlation between plasma Zn and other plasma and DNA damage biomarkers was observed (Table 6.7A). At the end of 12 weeks of supplementation, plasma Zn was found to be correlated only with ZIP1 expression (r=0.576, p=0.039) (Table 6.7B).

6.4.9 Correlation between other measured biomarkers

Based on the partial correlation, at baseline, vitamin B12 was correlated with folate (r=0.221, p=0.047) and Hcy was negatively correlated with B12 (r=-0.438, p=0.000) and Folate (r=-0.221, p=0.048). FRAP values were negatively correlated with MT1A gene expression (r=-0.259, p=0.019) and carnosine concentration was negatively correlated with Hcy (r=-0.293, p=0.008). For DNA damage events, tail intensity values was correlated with telomere length (r=0.264, p=0.017) and negatively correlated with carnosine concentration r=-0.236, p=0.034). Necrosis was negatively correlated with folate concentration (r=-0.241, p=0.030) and significantly correlated with ZIP1 expression (r=0.322, p=0.003) and eSOD levels (r=0.222, p=0.046). Apoptosis was also correlated with ZIP1 expression (r=0.265, p=0.017) and necrosis (r=0.541, p=0.000). Nuclear Division Index was significantly correlated only with apoptosis (r=0.232, p=0.037). Nucleoplasmic bridges was significantly correlated with ZIP1 expression (r=0.334, p=0.002), necrosis (r=0.557, p=0.000) and apoptosis (r=0.530, p=0.000). There were more significant correlations observed for nuclear buds.

Nuclear bud frequency was significantly correlated with ZIP1 expression (r=0.274, p=0.013), necrosis (r=0.451, p=0.000), apoptosis (r=0.401, p=0.000), micronuclei frequency (r=0.259, p=0.020) and nucleoplasmic bridges (r=0.615, p=0.000).

Following 12 weeks intervention, Hcy levels was found to be negatively correlated with B12 concentration (r=-0.627, p=0.022). MT1A expression was significantly correlated with folate levels (r=0.660, p=0.014). For antioxidant measures, there was no significant correlation observed for FRAP values with any of the biomarkers measured in the study while eSOD values were found to be negatively correlated with telomere base damage (r=-0.619, p=0.024). With regards to DNA damage events, tail moment was negatively correlated with eSOD values (r=-0.693, p=0.009), while nuclear division index was found to be correlated with tail moment (r=0.623, p=0.023) and negatively correlated with necrosis (r=-0.567, p=0.043). Micronuclei frequency was found to be negatively correlated with telomere length (r=-0.567, p=0.043) and carnosine concentration (r=-0.564, p=0.045) but positively correlated with nuclear division index (r=0.639, p=0.019). Only one positive correlation was found for nucleoplasmic bridges, which was with apoptosis (r=0.572, p=0.041). Nuclear buds were found to be negatively correlated with eSOD values (r=-0.588, p=0.035) but positively correlated with telomere base damage (r=0.564, p=0.045) and strongly correlated with apoptosis (r=0.725, p=0.005).

r value	Plasma Zn	B12	Folate	Hcy	TBD	TL	MT1A	ZIP1	FRAP	eSOD	Carnosine	TM	TI	Necrosis	Apoptosis	NDI	MNi	NPB	NBuds
Plasma Zn	-	**NS**	**NS**	**NS**	**NS**	**NS**	**NS**	**NS**	**NS**	0.279	**NS**	-0.222	**NS**	**NS**	**NS**	**NS**	-0.235	**NS**	**NS**

Table 6.6: Correlation coefficient (r values) between plasma Zn and other biomarkers at week 12 analysed by Pearson's correlation test.

r values 2-tailed (*p<0.05* – significant) ; NS - nonsignificant; B12 – vitamin B12; Folate – Plasma Folate; Hcy – plasma Homocysteine; TBD – Telomere Base Damage, TL – Telomere Length; MT1A – MT1A gene; ZIP1 – ZIP1 gene; FRAP – Ferric Reducing Activity in Plasma; eSOD – erthyrocytes Superoxide Dismutase; Carnosine – Plasma Carnosine; TM – Tail Moment; TI – Tail Intensity; Necrosis – Necrotic cells; Apoptosis – apoptotic cells; NDI – Nuclear Division Index; MNi – Micronuclei; NPB – Nucleoplasmic bridges; NBuds – Nuclear Buds.

Table 6.7A: Cross correlations between biomarkers at baseline analysed using partial correlation after adjusting for age and gender.
r values 2-tailed (*p<0.05* – significant) ; NS - nonsignificant; B12 – vitamin B12; Folate – Plasma Folate; Hcy – plasma Homocysteine; TBD – Telomere Base Damage, TL – Telomere Length; MT1A – MT1A gene; ZIP1 – ZIP1 gene; FRAP – Ferric Reducing Activity in Plasma; eSOD – erthyrocytes Superoxide Dismutase; Carnosine – Plasma Carnosine; TM – Tail Moment; TI – Tail Intensity; Necrosis – Necrotic cells; Apoptosis – apoptotic cells; NDI – Nuclear Division Index; MNi – Micronuclei; NPB – Nucleoplasmic bridges; NBuds – Nuclear Buds.

r value	Plasma Zn	B12	Folate	Hcy	TBD	TL	MT1A	ZIP1	FRAP	eSOD	Carnosine	TM	TI	Necrosis	Apoptosis	NDI	MNi	NPB	NBuds
Plasma Zn	-	**NS**	**NS**	**NS**	**NS**	**NS**	**NS**	**NS**	**NS**	**NS**	**NS**	**NS**	**NS**	**NS**	**NS**	**NS**	**NS**	**NS**	**NS**
B12		-	**0.221**	**-0.438**	**NS**	**NS**	**NS**	**NS**	**0.228**	**NS**	**NS**	**NS**	**NS**	**NS**	**NS**	**NS**	**NS**	**NS**	**NS**
Folate			-	**-0.221**	**NS**	**NS**	**NS**	**NS**	**NS**	**NS**	**NS**	**NS**	**NS**	**-0.241**	**NS**	**NS**	**NS**	**NS**	**NS**
Hcy				-	**NS**	**NS**	**NS**	**NS**	**NS**	**NS**	**-0.293**	**NS**	**NS**	**NS**	**NS**	**NS**	**NS**	**NS**	**NS**
TBD					-	**NS**	**NS**	**NS**	**NS**	**NS**	**NS**	**NS**	**NS**	**NS**	**NS**	**NS**	**NS**	**NS**	**NS**
TL						-	**NS**	**NS**	**NS**	**NS**	**NS**	**NS**	**0.264**	**NS**	**NS**	**NS**	**NS**	**NS**	**NS**
MT1A							-	**NS**	**-0.259**	**NS**	**NS**	**NS**	**NS**	**NS**	**NS**	**NS**	**NS**	**NS**	**NS**
ZIP1								-	**NS**	**NS**	**NS**	**NS**	**NS**	**0.322**	**0.265**	**NS**	**NS**	**0.334**	**0.274**
FRAP									-	**NS**	**NS**	**NS**	**NS**	**NS**	**NS**	**NS**	**NS**	**NS**	**NS**
eSOD										-	**NS**	**NS**	**NS**	**0.222**	**NS**	**NS**	**NS**	**NS**	**NS**
Carnosine											-	**NS**	**-0.236**	**NS**	**NS**	**NS**	**NS**	**NS**	**NS**
TM												-	**NS**	**NS**	**NS**	**NS**	**NS**	**NS**	**NS**
TI													-	**NS**	**NS**	**NS**	**NS**	**NS**	**NS**
Necrosis														-	**0.541**	**NS**	**NS**	**0.557**	**0.451**
Apoptosis															-	**0.232**	**NS**	**0.530**	**0.401**
NDI																-	**NS**	**NS**	**NS**
MNi																	-	**NS**	**0.259**
NPB																		-	**0.615**
NBuds																			-

Table 6.7B: Cross correlations between biomarkers at week 12 analysed using partial correlation after adjusting for age and gender.
r values 2-tailed (*p<0.05* – significant) ; NS - nonsignificant; B12 – vitamin B12; Folate – Plasma Folate; Hcy – plasma Homocysteine; TBD – Telomere Base Damage, TL – Telomere Length; MT1A – MT1A gene; ZIP1 – ZIP1 gene; FRAP – Ferric Reducing Activity in Plasma; eSOD – erthyrocytes Superoxide Dismutase; Carnosine – Plasma Carnosine; TM – Tail Moment; TI – Tail Intensity; Necrosis – Necrotic cells; Apoptosis – apoptotic cells; NDI – Nuclear Division Index; MNi – Micronuclei; NPB – Nucleoplasmic bridges; NBuds – Nuclear Buds.

r value	Plasma Zn	B12	Folate	Hcy	TBD	TL	MT1A	ZIP1	FRAP	eSOD	Carnosine	TM	TI	Necrosis	Apoptosis	NDI	MNi	NPB	NBuds
Plasma Zn	-	**NS**	**NS**	**NS**	**NS**	**NS**	**NS**	**0.576**	**NS**	**NS**	**NS**	**NS**	**NS**	**NS**	**NS**	**NS**	**NS**	**NS**	**NS**
B12		-	**NS**	**-0.627**	**NS**	**NS**	**NS**	**NS**	**NS**	**NS**	**NS**	**NS**	**NS**	**NS**	**NS**	**NS**	**NS**	**NS**	**NS**
Folate			-	**NS**	**NS**	**NS**	**0.660**	**NS**	**NS**	**NS**	**NS**	**NS**	**NS**	**NS**	**NS**	**NS**	**NS**	**NS**	**NS**
Hcy				-	**NS**	**NS**	**NS**	**NS**	**NS**	**NS**	**NS**	**NS**	**NS**	**NS**	**NS**	**NS**	**NS**	**NS**	**NS**
TBD					-	**NS**	**NS**	**NS**	**NS**	**-0.619**	**NS**	**NS**	**NS**	**NS**	**NS**	**NS**	**NS**	**NS**	**0.564**
TL						-	**NS**	**NS**	**NS**	**NS**	**NS**	**NS**	**NS**	**NS**	**NS**	**NS**	**-0.567**	**NS**	**NS**
MT1A							-	**NS**	**NS**	**NS**	**NS**	**NS**	**NS**	**NS**	**NS**	**NS**	**NS**	**NS**	**NS**
ZIP1								-	**NS**	**NS**	**NS**	**NS**	**NS**	**NS**	**NS**	**NS**	**NS**	**NS**	**NS**
FRAP									-	**NS**	**NS**	**NS**	**NS**	**NS**	**NS**	**NS**	**NS**	**NS**	**NS**
eSOD										-	**NS**	**-0.693**	**NS**	**NS**	**NS**	**NS**	**NS**	**NS**	**-0.588**
Carnosine											-	**NS**	**NS**	**NS**	**NS**	**NS**	**-0.564**	**NS**	**NS**
TM												-	**NS**	**NS**	**NS**	**0.623**	**NS**	**NS**	**NS**
TI													-	**NS**	**NS**	**NS**	**NS**	**NS**	**NS**
Necrosis														-	**NS**	**-0.567**	**NS**	**NS**	**NS**
Apoptosis															-	**NS**	**NS**	**0.572**	**0.725**
NDI																-	**0.639**	**NS**	**NS**
MNi																	-	**NS**	**NS**
NPB																		-	**NS**
NBuds																			-

6.5 Discussion

A large body of evidence shows that Zn plays an important role in the cellular response to oxidative stress, in DNA replication and repair of DNA damage, suggesting that it may have a preventative role in the etiology of diseases caused by these pathological events [14, 94, 284, 285]. The aim of the present study was to investigate the impact of Zn supplementation on Zn status, antioxidant profile, DNA damage biomarkers and gene expression in an elderly South Australian cohort. The results of this study show that Zn carnosine supplementation in an elderly population is beneficial in reducing the micronucleus frequency measured by the CBMN Cytome assay and both tail moment and intensity as measured via the comet assay following 12 weeks of intervention. To the author's knowledge, this is the first study conducted to investigate the impact of Zn supplementation on CBMN Cytome biomarkers and telomere integrity in an elderly population.

The result of the present study showed clearly that plasma Zn levels responded well to Zn supplementation and can thus therefore be considered as a reliable and robust Zn status biomarker. However, plasma Zn at baseline (Table 6.5A) was higher than plasma Zn levels at screening (Table 6.4). This may possibly be due to the fasting state and diurnal variation as both can affect plasma Zn concentrations [256]. A previous population study (13 463 subjects) showed that age, sex, time of day that blood was collected [AM, PM or Evening], and fasting status [> 8 hours fasted Vs fasting status unspecified or fasted > 8 hours] were found to have significant effects on plasma Zn concentrations ($p<0.0001$) [256]. Volunteers who were fasting tended to have higher plasma Zn compared to non-fasting volunteers [256]. This explains why in our study, a lower plasma Zn was observed at screening but the value increased at baseline although they were from the same cohort. According to Brown (1998) [286], in a population aged 22-75 years old, the reference value for plasma Zn is 16.6 ± 6.2 µM. The lower limit of fasting plasma Zn levels has been recommended at 10.7 µM [121] and therefore the cut-off level below which a Zn-deficient status is possible [287]. In this study, the cut off point for Zn deficiency was set to 11.6 µM in order to obtain 90 people with the lowest Zn status at screening, which was slightly higher than the 10.7 µM value recommended.

At baseline (4 weeks after screening – washout period), plasma Zn was 13.84 ± 1.51 μM for the Placebo group and 14.16 ± 1.46 μM for the Zn group. After 12 weeks of intervention, plasma Zn concentration in the Zn group showed an increase to 14.86 ± 2.06 μM while plasma Zn in the placebo group dropped to 13.19 ± 1.22 μM. An increase of 5.40% in plasma Zn after 12 weeks of supplementation in the Zn group indicates that daily intake of Zn at 20 mg/day improved Zn status. Savarino *et al* (2001) [288] showed that high plasma Zn in older individuals may contribute to their longevity. The increased plasma Zn levels is in agreement with the beneficial effect of Zn supplementation reported in an older institutionalized population presenting a large prevalence of biological Zn deficiency (< 10.7 μM) [289]. In addition, beneficial effect of a higher Zn status (14.7 vs 12 μM) has been reported in age-related eye disease [290].

This present study also showed that Zn supplementation at 12 weeks with 20 mg/day Zn was effective in improving Zn status and decreasing the percentage of subjects with Zn deficiency. This result is in agreement with another study conducted in a European population, which found similar result after 3 months of Zn supplementation but with 30 mg/day of Zn gluconate [291]. In contrast, Bogden *et al* (1988) found no significant change in plasma Zn values in response to a 15 mg Zn (Zn acetate) supplement taken for 3 months [292]. This discrepancy in results shows that Zn supplementation at 20-30mg/day but not at a lower dose might be beneficial in improving Zn status, particularly in those with lower Zn status.

In this study, levels of plasma B12, folate and Hcy were also measured as these may affect DNA damage and telomere maintenance [108]. It was found that Zn supplementation did not alter levels of B12, folate and Hcy as recorded in Table 6.5A. These results are in agreement with a previous study by Ducros *et al* 2009 [293] that showed after six months of intervention with Zn at 15 mg/day and 30 mg/day, there was no effect on Hcy, B12 and Folate levels. The link between Zn and B12 is unknown. However, marginal or low Zn has been reported to modify vitamin B12 metabolism and decrease absorption of dietary folate due to Zn-dependent intestinal brush-border pteroylglutamate hydrolase, which can cleave dietary folate prior to absorption [294, 295]. It has also been shown that Zn deficiency in

pregnant rats decreases folate bioavailability [296]. Dietary Zn deficiency in rats has been reported to increase hepatic methionine synthase activity and decreased plasma Hcy and folate concentrations without any modification of red blood cell folate [297]. A decreased amount of hepatic 5-methyltetrahydrofolate was observed in Zn-deficient rats compared with pair-fed rats [297, 298]. It is evident that the extent of Zn deficiency in our cohort was not sufficient to substantially alter B12, folate and Hcylevels in plasma.

In this study, the impact of Zn supplementation in relation to the antioxidant profile (FRAP and eSOD) was investigated. It was shown that FRAP and eSOD were increased following Zn supplementation. This result is similar to a previous study that reported Zn supplementation increased the eSOD activity following both 3 and 6 month interventions [299]. However, in the same study, an increase in FRAP was not found. This negative result following Zn supplementation may have been because only 4.8% were middle-aged and 5.6% were older subjects that were below the cutoff level for biological Zn deficiency (10.7 µM) [299]. In another study, Song *et al* [94] found that FRAP activity was unaffected following Zn supplementation while eSOD tended to decrease after marginal Zn depletion and increased after Zn repletion, but the changes were not statistically significant. Results from our current study showed that an increase in antioxidant activity as measured via eSOD activities may have a role in lowering DNA damage following 12 weeks of intervention based on the strong correlation factors with telomere base damage (r=-0.669), tail moment (r=-0.693) and nuclear buds (r=-0.588).

Genomic instability events have been suggested to be one of the main indicators for increased cancer risk [8, 9, 13, 59-62]. There are various methods to measure genome stability but to date, the cytokinesis blocked micronucleus cytome (CBMN-Cyt) assay appears to be the best validated tool for measuring DNA damage as a result of micronutrient deficiency (as reviewed in [83]). This method can provide data on cytostatic and cytotoxic effects as well as chromosomal damage and instability events. In the CBMN-Cyt assay, a cytokinesis blocking agent (cytochalasin B) is used to produce once-divided binucleated cells that can express micronuclei (MNi) which are biomarkers of whole chromosome loss and/or breakage. MNi originate from acentric chromosomal fragments or whole chromosomes that lag behind at anaphase during nuclear division. Other cytome

DNA damage biomarkers include nucleoplasmic bridges (NPBs), which arise from dicentric chromosomes (caused by DNA misrepair or telomere end fusions) and nuclear buds (NBuds), a biomarker of gene amplification, replication stress or unresolved DNA repair-DNA protein complexes [84-86]. The presence of these DNA damage endpoints are a strong indicator of chromosomal damage and instability within a cell [84]. These DNA damage events have been shown to be sensitive to small changes in micronutrient concentration (eg. folic acid, riboflavin, selenomethionine) within the physiological range [87-89]. In a recent review, it was shown that when compared to other DNA damage biomarkers, the micronucleus (MN) index in the CBMN-Cyt assay in human lymphocytes has been substantially validated with respect to its sensitivity to changes in nutritional status with respect to association with health outcomes. This is shown in both cross-sectional and placebo-controlled trials, via cross-sectional and prospective studies, with developmental and degenerative diseases [83]. To complete the measurements of DNA damage events, the comet assay was also used. This assay has become a widely used assay in the toxicology field because it is a quick, sensitive, and relatively inexpensive method for measuring DNA strand breaks as an index of genetic damage after exposure to genotoxic agents although results maybe confounded by cell death or necrosis [148]. The observation that both MNi and tail moment decreases with Zn supplementation strengthens the evidence that improved Zn status is required for optimized genome integrity.

Overwhelming evidence has shown the association of the MN index with nutritional deficiency (as reviewed elsewhere [83, 116]). A recent population study has shown that at least nine micronutrients can affect genome stability in humans *in vivo* [139]. Multivariate analysis of baseline data showed that 1) the highest tertile of intake of vitamin E, retinol, folate, nicotinic acid and calcium is associated with significant reductions in MN frequency and 2) the highest tertile of intake of riboflavin, pantothenic acid or biotin was associated with a significant increase in MN frequency relative to the lowest tertile. This study illustrates how the MN index is sensitive to small variations in micronutrient status within the normal physiological range making it an excellent biomarker for identifying dietary factors that are essential for genome stability by defining their optimal levels. Besides CBMN Cyt assay, DNA damage events were also measured via the alkaline Comet assay which can determine DNA strand breaks [148, 300].

To our knowledge, this is the first study to investigate the effect of Zn supplementation on genome stability in an elderly South Australian population. In this study, a reduction in the micronucleus frequency was observed together with both tail moment and tail intensity as measured via the alkaline comet assay following 12 weeks intervention with Zn at 20 mg/day. A previous study in rats has shown that severe Zn depletion caused an increase in DNA damage in peripheral blood cells compared to Zn replete controls and this was associated with impairment in DNA repair, compromised p53 DNA binding, and upregulation of the base excision repair (BER) proteins, OGG1 and PARP [43]. A further study conducted in rats showed that marginal Zn deficiency (MZnD) caused an increase in oxidative DNA damage in the prostate after chronic exercise. MZnD treated groups also showed increased p53 and PARP expression but no change in plasma 8-OHdG levels compared to Zn Adequate (ZnAD) group. Results utilizing the comet assay showed that the tail moment of peripheral blood cells in MZnD group was 20% higher than in the ZnAD group and prostate 8-OHdG in MZnD group was 32% higher than the ZnAD group. 8-OHdG concentration in the prostate was significantly correlated with the tail moments of peripheral blood cells (*r=0.66, p=0.03*) [42].

Dietary Zn restriction and repletion of Zn to its normal status was found to affect DNA integrity in healthy men aged 19-50 years old [94]. In this study, the number of DNA strand breaks increased significantly during the Zn depletion period (6 weeks). The increase in DNA breaks were shown to be reversible following Zn repletion suggesting that the extent of DNA damage is related to dietary Zn status. Plasma Zn levels measured at the beginning (day 13) and at the end of the Zn depletion period (day 55) did not differ significantly. Mean plasma Zn concentrations were 0.79 ± 0.9 and 0.79 ± 1.0 μg/mL on days 13 and 55, respectively. However, plasma Zn concentrations were found to be 13% higher at the end of the Zn repletion period (0.86 ± 1.0 μg/mL on day 83) than at the end of the Zn depletion period. Plasma Zn concentrations showed a negative correlation with DNA damage measures as measured via the alkaline comet assay (*r=-0.47, p=0.014*) [94].

These studies suggest that Zn deficiency may lead to an increase in DNA damage and in our study it was shown that Zn supplementation may be beneficial in lowering DNA damage especially DNA strand breaks and the frequency of micronuclei. In this study, Zn carnosine

was used and it has been shown that carnosine is well known as a potent antioxidant [135] and may have an impact on DNA damage, the levels of carnosine were very low and did not change significantly in the treatment group versus the placebo (Table 6.5A). However, plasma carnosine was inversely correlated with micronuclei at week 12 (r=-0.564) but not at baseline, and inversely with comet tail intensity at baseline (r=-0.236) but not at week 12. This suggests that significant changes in carnosine concentration in blood may affect genome stability in lymphocytes.

The relationship between Zn status and telomere biology is not clearly defined. Telomeres consist of a conserved hexanucleotide repeat sequence (TTAGGG) that caps the end of chromosomes [210]. They have an important role in protecting the chromosome ends from recombining with each other and prevent chromosomal end-to-end fusions [105]. Accelerated telomere shortening may result in a DNA damage response leading to chromosomal end-to-end fusions, cell arrest and apoptosis [107, 108, 218].

In this study, no difference in telomere length and telomere base damage between the placebo and Zn treatment group was observed. However, telomere length was observed to increase and telomere base damage decreased in the Zn supplemented group when week 12 data was compared to baseline. This suggests that the effects are small or a larger study is required to achieve statistical analysis significant for time and treatment interation by 2-way ANOVA. There are actually very few studies that have investigated the impact of Zn on maintaining telomere integrity. Liu and colleagues (2004) found that Zn sulphate at 80 µM accelerated telomere loss in hepatoma cells (SMMC-7721) after 4 weeks of treatment [109]. Cells with short telomeres are associated with impaired Zn homeostasis in hypertensive patients [110].

Gene expression analysis showed that Zn supplementation over 12 weeks of intervention increased both MT1A and ZIP1 expression significantly. ZIP1 was selected as it is the most abundant Zn transporters in the system [301]. Both genes are expected to be elevated as both are involved in Zn transport and Zn storage [18, 118]. A previous study showed that among all Zn transporter mRNA, ZIP1 is one of the most abundantly expressed [302]. In prostate cancer, a decrease in both cellular Zn and ZIP1 expression was found to be

associated with enhanced tumour growth [73]. Metallothionein (MT) is a small sized protein which serves as a Zn specific chaperone and functions by a similar redox mechanism distributing Zn to enzymes in the metabolic network [55, 56]. MT has been found to affect the release of Zn for the activity of PARP-1, which is involved in base excision DNA-repair [58]. A previous study showed that the abnormal sequester of Zn by MT in ageing is deleterious because it leads to low Zn bioavailability with impairment of PARP-1 and Natural Killer (NK) cell activity [58]. Previous studies have shown that Zn and metallothionein are genome-protective against the insults associated with oxidative stress [30, 53, 54]. In our study, MT expression was increased in the Zn group which may explain the reductions in both tail moment and tail intensity observed in the comet assay and also the frequency of micronuclei.

In particular, polymorphisms of the metallothionein gene MT1A were found to influence the efficacy of Zn supplementation [122, 123]. As MT induction and expression is mediated by IL-6, a multifunctional cytokine which regulates the differentiation and activity of different cell types, stress reactions and inflammatory responses [122-126]. Several studies suggest that the common IL-6-174 G/C and MT1A +647 polymorphisms interactively affect Zn bioavailability and bioefficacy and are likely to be a useful indicator for the selection of elderly people who would benefit from Zn supplementation [122, 123, 126-129]. It would be of interest for future studies to investigate whether polymorphisms in ZnT, ZIP, MT1A and IL6 genes modify the relationship between Zn status and genome stability.

The results from this study show that Zn supplementation in an elderly populations with low Zn status can a) improve Zn status, b) lower DNA damage events, hence improving genome stability, c) increase antioxidant activity which may lower DNA damage risk [14], and d) increase Zn storage and transporter gene expression (MT1A and ZIP1). Given that there is some evidence that the benefits and/or adverse effects of Zn supplementation may depend on genotype variations e.g (MT1A) [122, 266, 268], it will be necessary to find out in future whether there are specific genotypes or polymorphisms in genes in high susceptibility groups, who are more likely to benefit, or be at risk of any toxic effect of Zn supplementation.

Chapter 7

Conclusions, Knowledge Gaps and Future Directions

Chapter 7

Conclusions, Knowledge Gaps and Future Directions

7.1 Introduction

Zn is an essential component for more than 1000 proteins including Copper/Zn super oxide dismutase (SOD) as well as a number of other Zn finger proteins [13, 14]. Various *in vitro* and *in vivo* approaches have also shown that Zn deficiency leads to oxidative stress [19-22, 35, 52]. These findings suggest that Zn depletion may increase DNA damage which leads to genomic instability. However, the optimal concentration of Zn to minimize DNA damage events is still unknown and this hypothesis lead to this research gap being addressed in this thesis. The main aim of this project was to address important knowledge gaps regarding the possible impact of Zn on genomic stability events in both lymphocytes and epithelial cells using both *in vitro* and *in vivo* models. The project also aimed to study the differential impact of Zn Sulphate as the most common form of Zn used within laboratory experiments and Zn carnosine, a newly emerging commercially available supplement known for its antioxidant capacity, on genome stability. Therefore, the experiments and investigations tested the following hypotheses; a) Zn deficiency or excess increase DNA damage in an *in vitro* cell model, b) ZnC will give better genome stability because it is more readily absorbed than $ZnSO_4$ and a stronger antioxidant, c) *In vivo* Zn supplementation improves cellular and plasma Zn status and lowers the rates of DNA damage.

7.2 Zinc and Genomic Stability: *In vitro* (WIL2-NS and HOK cells)

Based on the hypotheses tested (Chapter 2), the first hypothesis in this *in vitro* study is accepted which is Zn deficiency or excess increases DNA damage. The second hypothesis which is ZnC will give better genome stability because it is more readily absorbed than

$ZnSO_4$ and a stronger anti-oxidant is rejected because there were no differences observed in the effect of Zn on genomic stability between these two compounds.

The present *in vitro* study (using both WIL2-NS and HOK cells) showed that a Zn concentration between 4-16 µM is optimal in minimizing DNA damage events and Zn depleted cultures showed an increase in DNA damage events which lead to genomic instability as measured by both the comet and CBMN-Cyt assay. Following gamma-irradiation and hydrogen peroxide challenges (WIL2-NS cells), Zn at 4-32 µM showed a genome-protective effect as determined by the CBMN-Cyt assay. Expression of various proteins were measured in order to further understand the mechanisms underlying the DNA damage events and showed that PARP, OGG1 and p53 protein expression was activated under conditions of Zn deficiency. Metallothionein expression was abundant in Zn supplemented cultures indicating that it may have an impact on low DNA damage events observed in cells supplemented with Zn. Zn depleted cultures also showed longer telomere length, an increase in telomere base damage, and an increase in DNA strand breaks (tail moment and tail intensity) and chromosomal instability (MNi, NPB and NBud). The link between Zn status and telomere biology is still unclear but these current results contribute in filling some of the knowledge gaps on the impact of Zn on telomere stability and provides a pathway for future investigations. Furthermore, they indicate that telomere elongation in response to Zn deficiency is associated with increased DNA damage thus challenging the view that longer telomeres are a good biomarker of genome integrity.

It is evident that more attention should be given to Zn levels in culture medium which should be carefully maintained at an optimal concentration to maintain genome stability. Whether the optimal concentration of Zn should be determined for each specific cell line needs to be tested as it is quite possible that requirements may vary depending on genotype. Optimal Zn concentration to minimize DNA damage *in vitro* is between 4-16 µM while the normal physiological plasma Zn levels in humans are in the range of 12-16 µM [31]. However, optimal levels of plasma Zn to minimize DNA damage is still unknown and this knowledge gap lead to the design of the *in vivo* Zn trial.

The need to conduct further investigations to understand the impact of Zn on telomere stability will be the basis for future research. Using methods such as q-FISH, it may be possible to further analyse telomere functionality also allowing the possibility to detect telomere end fusions. In addition, future investigations including the impact of Zn status on hTERT expression, TRF1 and TRF2 expression as well as telomerase activity would be important in elucidating some of the underlying mechanisms required for telomere maintenance. Besides, the need to further elucidate the mechanisms underlying an increase in DNA damage and Zn excess is still undefined and should be the basis of future investigations. The involvement of free labile Zn transporters may contribute to new knowledge in the investigation of Zn and genomic stability. This will be the focus of future priorities.

7.3 Zinc and Genomic Stability – *In vivo* (Genome Health Effect of Zinc Supplement in an Elderly South Australian Population with low Zinc status)

To test the impact of Zn on genomic stability in an *in vivo* model, a 12 week placebo-controlled human trial was conducted. The study was designed as a randomised, placebo-controlled intervention in a free-living healthy elderly South Australian population. The aim of this study was to determine the effect of Zn status on lymphocyte genomic instability events. The objectives of the study were to investigate the effect of Zn supplementation on DNA strand breaks, telomere length and base damage and chromosomal stability and investigate possible molecular mechanisms underlying such effects.

The results from this study showed that Zn supplementation in an elderly population with lower plasma Zn can a) improve biomarkers of Zn status, b) lower DNA damage, hence improving genome stability, c) increase antioxidant activity which may lower DNA damage risk [14], and d) increase Zn storage and transporter gene expression (MT1A and ZIP1). It is shown that from the *in vitro* study, optimal Zn levels to minimize DNA damage events lies between 4-16 µM while in *in vivo* study conducted, Zn supplemented group manage to reduce DNA damage events. The question that now arises is should Zn concentration or plasma Zn reference values be redefined based on the genome health maintenance as

genome stability maintenance plays an important role in related health outcomes as reviewed in [9, 59, 116].

Recent studies have found that polymorphisms of the metallothionein (MT) gene MT1A influence the efficacy of Zn supplementation [122, 123]. As MT induction and expression is mediated by IL-6, a multifunctional cytokine which regulates the differentiation and activity of different cell types, stress reactions and inflammatory responses [122-126], it has been proposed that the common IL-6-174 G/C and MT1A +647 polymorphism interactively affects zinc bioavailability and bioefficacy and may be a useful indicator for the selection of elderly people who need Zn supplementation [122, 123, 126-129]. Given that there is some evidence that the benefits and/or adverse effects of Zn supplementation may depend on genotype variations (MT1A) [122, 266, 268], it will be necessary to find out in the future whether there are specific genotypes or polymorphisms in genes in higher susceptibility groups, who are more likely to benefit, or be at risk of toxic effects of Zn supplementation.

In addition, it will be interesting to see the impact of Zn supplementation on genome stability in other populations with low Zn status especially infants, prostate cancer patients, populations from third world countries and vegetarians, to determine whether or not Zn supplementation will have the same beneficial effects as those observed in this study. Future directions also include measurements of C-Reactive protein (CRP) as this will determine the infection/inflammation status. An improved method with increased sensitivity for screening people with low plasma Zn is also needed as plasma Zn may not be the best method to identify Zn deficiency. Apart from measuring MT1A and ZIP1 gene expression, other suggestions include measurements of intracellular Zn in monocytes/lymphocytes or measuring labile Zn (free Zn ion) using a Zinquin method [303] that may be beneficial to further characterise people with low Zn status.

References

1. World Health Organizations, W. *Cancer*. 2009 Februray 2009 [cited 2009 February]; WHO - Media Centre - Fact Sheet]. Available from: http://www.who.int/mediacentre/factsheets/fs297/en/index.html.
2. AICR, A.I.C.R., *Food, Nutrition, Physical Activity, and the Prevention of Cancer*. 2007, Washington DC: American Institute for Cancer Research.
3. Milner, J.A., *Molecular targets for bioactive food components.* J Nutr, 2004. **134**(9): p. 2492S-2498S.
4. Finley, J.W., *Proposed criteria for assessing the efficacy of cancer reduction by plant foods enriched in carotenoids, glucosinolates, polyphenols and selenocompounds.* Ann Bot (Lond), 2005. **95**(7): p. 1075-96.
5. Fenech, M. and L.R. Ferguson, *Vitamins/minerals and genomic stability in humans.* Mutat Res, 2001. **475**(1-2): p. 1-6.
6. Ames, B.N., *Micronutrients prevent cancer and delay aging.* Toxicol Lett, 1998. **102-103**: p. 5-18.
7. Ames, B.N., *Micronutrient deficiencies. A major cause of DNA damage.* Ann N Y Acad Sci, 1999. **889**: p. 87-106.
8. Fenech, M., *Chromosomal biomarkers of genomic instability relevant to cancer.* Drug Discov Today, 2002. **7**(22): p. 1128-37.
9. Ames, B.N. and P. Wakimoto, *Are vitamin and mineral deficiencies a major cancer risk?* Nat Rev Cancer, 2002. **2**(9): p. 694-704.
10. Ames, B.N., *DNA damage from micronutrient deficiencies is likely to be a major cause of cancer.* Mutat Res, 2001. **475**(1-2): p. 7-20.
11. Ames, B.N. and L.S. Gold, *Paracelsus to parascience: the environmental cancer distraction.* Mutat Res, 2000. **447**(1): p. 3-13.
12. Blount, B.C., et al., *Folate deficiency causes uracil misincorporation into human DNA and chromosome breakage: implications for cancer and neuronal damage.* Proc Natl Acad Sci U S A, 1997. **94**(7): p. 3290-5.
13. Dreosti, I.E., *Zinc and the gene.* Mutat Res, 2001. **475**(1-2): p. 161-7.
14. Ho, E., *Zinc deficiency, DNA damage and cancer risk.* J Nutr Biochem, 2004. **15**(10): p. 572-8.
15. Falchuk, K.H., *The molecular basis for the role of zinc in developmental biology.* Mol Cell Biochem, 1998. **188**(1-2): p. 41-8.
16. Bray, T.M. and W.J. Bettger, *The physiological role of zinc as an antioxidant.* Free Radic Biol Med, 1990. **8**(3): p. 281-91.
17. Powell, S.R., *The antioxidant properties of zinc.* J Nutr, 2000. **130**(5S Suppl): p. 1447S-54S.
18. Cousins, R.J., et al., *Regulation of zinc metabolism and genomic outcomes.* J Nutr, 2003. **133**(5 Suppl 1): p. 1521S-6S.
19. Oteiza, P.I., V.N. Adonaylo, and C.L. Keen, *Cadmium-induced testes oxidative damage in rats can be influenced by dietary zinc intake.* Toxicology, 1999. **137**(1): p. 13-22.
20. Oteiza, P.I., M.S. Clegg, and C.L. Keen, *Short-term zinc deficiency affects nuclear factor-kappab nuclear binding activity in rat testes.* J Nutr, 2001. **131**(1): p. 21-6.
21. Oteiza, P.I., et al., *Zinc deficiency causes oxidative damage to proteins, lipids and DNA in rat testes.* J Nutr, 1995. **125**(4): p. 823-9.
22. Oteiza, P.L., et al., *Oxidant defense systems in testes from zinc-deficient rats.* Proc Soc Exp Biol Med, 1996. **213**(1): p. 85-91.
23. Hennig, B., et al., *Zinc nutrition and apoptosis of vascular endothelial cells: implications in atherosclerosis.* Nutrition, 1999. **15**(10): p. 744-8.
24. Hennig, B., M. Toborek, and C.J. McClain, *Antiatherogenic properties of zinc: implications in endothelial cell metabolism.* Nutrition, 1996. **12**(10): p. 711-7.
25. Meerarani, P., et al., *Zinc protects against apoptosis of endothelial cells induced by linoleic acid and tumor necrosis factor alpha.* Am J Clin Nutr, 2000. **71**(1): p. 81-7.
26. Paramanantham, R., K.H. Sit, and B.H. Bay, *Adding Zn2+ induces DNA fragmentation and cell condensation in cultured human Chang liver cells.* Biol Trace Elem Res, 1997. **58**(1-2): p. 135-47.
27. Clegg, M.S., et al., *Zinc deficiency-induced cell death.* IUBMB Life, 2005. **57**(10): p. 661-9.

28. Bae, S.N., et al., *Antiproliferative and apoptotic effects of zinc-citrate compound (CIZAR(R)) on human epithelial ovarian cancer cell line, OVCAR-3.* Gynecol Oncol, 2006. **103**(1): p. 127-36.
29. Chung, M.J., et al., *ZINC-mediated gene expression offers protection against H2O2-induced cytotoxicity.* Toxicol Appl Pharmacol, 2005. **205**(3): p. 225-36.
30. Chimienti, F., et al., *Zinc resistance impairs sensitivity to oxidative stress in HeLa cells: protection through metallothioneins expression.* Free Radic Biol Med, 2001. **31**(10): p. 1179-90.
31. Chang, K.L., et al., *Zinc at pharmacologic concentrations affects cytokine expression and induces apoptosis of human peripheral blood mononuclear cells.* Nutrition, 2006. **22**(5): p. 465-74.
32. Hainaut, P. and K. Mann, *Zinc binding and redox control of p53 structure and function.* Antioxid Redox Signal, 2001. **3**(4): p. 611-23.
33. Marchenko, N.D., A. Zaika, and U.M. Moll, *Death signal-induced localization of p53 protein to mitochondria. A potential role in apoptotic signaling.* J Biol Chem, 2000. **275**(21): p. 16202-12.
34. Lane, D.P., *Cancer. p53, guardian of the genome.* Nature, 1992. **358**(6381): p. 15-6.
35. Ho, E., C. Courtemanche, and B.N. Ames, *Zinc deficiency induces oxidative DNA damage and increases p53 expression in human lung fibroblasts.* J Nutr, 2003. **133**(8): p. 2543-8.
36. Ho, E. and B.N. Ames, *Low intracellular zinc induces oxidative DNA damage, disrupts p53, NFkappa B, and AP1 DNA binding, and affects DNA repair in a rat glioma cell line.* Proc Natl Acad Sci U S A, 2002. **99**(26): p. 16770-5.
37. Ra, H., et al., *Essential role of p53 in TPEN-induced neuronal apoptosis.* FEBS Lett, 2009. **583**(9): p. 1516-20.
38. Petrucco, S. and R. Percudani, *Structural recognition of DNA by poly(ADP-ribose)polymerase-like zinc finger families.* Febs J, 2008. **275**(5): p. 883-93.
39. Kunzmann, A., et al., *Effect of zinc on cellular poly(ADP-ribosyl)ation capacity.* Exp Gerontol, 2008. **43**(5): p. 409-14.
40. Oka, S., et al., *Two distinct pathways of cell death triggered by oxidative damage to nuclear and mitochondrial DNAs.* Embo J, 2008. **27**(2): p. 421-32.
41. Boiteux, S. and J.P. Radicella, *The human OGG1 gene: structure, functions, and its implication in the process of carcinogenesis.* Arch Biochem Biophys, 2000. **377**(1): p. 1-8.
42. Song, Y., et al., *Marginal zinc deficiency increases oxidative DNA damage in the prostate after chronic exercise.* Free Radic Biol Med, 2009. **48**(1): p. 82-8.
43. Song, Y., et al., *Zinc deficiency affects DNA damage, oxidative stress, antioxidant defenses, and DNA repair in rats.* J Nutr, 2009. **139**(9): p. 1626-31.
44. Fritz, G., *Human APE/Ref-1 protein.* Int J Biochem Cell Biol, 2000. **32**(9): p. 925-9.
45. Hegde, M.L., T.K. Hazra, and S. Mitra, *Early steps in the DNA base excision/single-strand interruption repair pathway in mammalian cells.* Cell Res, 2008. **18**(1): p. 27-47.
46. Puglisi, F., et al., *Prognostic significance of Ape1/ref-1 subcellular localization in non-small cell lung carcinomas.* Anticancer Res, 2001. **21**(6A): p. 4041-9.
47. Prasad, A.S., *Zinc in human health: effect of zinc on immune cells.* Mol Med, 2008. **14**(5-6): p. 353-7.
48. Chinenov, Y. and T.K. Kerppola, *Close encounters of many kinds: Fos-Jun interactions that mediate transcription regulatory specificity.* Oncogene, 2001. **20**(19): p. 2438-52.
49. Shaulian, E. and M. Karin, *AP-1 in cell proliferation and survival.* Oncogene, 2001. **20**(19): p. 2390-400.
50. Karin, M. and E. Shaulian, *AP-1: linking hydrogen peroxide and oxidative stress to the control of cell proliferation and death.* IUBMB Life, 2001. **52**(1-2): p. 17-24.
51. Mackenzie, G.G., et al., *Low intracellular zinc impairs the translocation of activated NF-kappa B to the nuclei in human neuroblastoma IMR-32 cells.* J Biol Chem, 2002. **277**(37): p. 34610-7.
52. Olin, K.L., et al., *Maternal dietary zinc influences DNA strand break and 8-hydroxy-2'-deoxyguanosine levels in infant rhesus monkey liver.* Proc Soc Exp Biol Med, 1993. **203**(4): p. 461-6.
53. Jourdan, E., et al., *Effects of cadmium and zinc on solar-simulated light-irradiated cells: potential role of zinc-metallothionein in zinc-induced genoprotection.* Arch Biochem Biophys, 2002. **405**(2): p. 170-7.
54. Jourdan, E., et al., *Zinc-metallothionein genoprotective effect is independent of the glutathione depletion in HaCaT keratinocytes after solar light irradiation.* J Cell Biochem, 2004. **92**(3): p. 631-40.

55. Krezel, A., Q. Hao, and W. Maret, *The zinc/thiolate redox biochemistry of metallothionein and the control of zinc ion fluctuations in cell signaling.* Arch Biochem Biophys, 2007. **463**(2): p. 188-200.
56. Bell, S.G. and B.L. Vallee, *The metallothionein/thionein system: an oxidoreductive metabolic zinc link.* Chembiochem, 2009. **10**(1): p. 55-62.
57. Vasak, M., *Advances in metallothionein structure and functions.* J Trace Elem Med Biol, 2005. **19**(1): p. 13-7.
58. Mocchegiani, E., et al., *Metallothioneins/PARP-1/IL-6 interplay on natural killer cell activity in elderly: parallelism with nonagenarians and old infected humans. Effect of zinc supply.* Mech Ageing Dev, 2003. **124**(4): p. 459-68.
59. Fenech, M., *The Genome Health Clinic and Genome Health Nutrigenomics concepts: diagnosis and nutritional treatment of genome and epigenome damage on an individual basis.* Mutagenesis, 2005. **20**(4): p. 255-69.
60. Thompson, L.H. and D. Schild, *Recombinational DNA repair and human disease.* Mutat Res, 2002. **509**(1-2): p. 49-78.
61. Rajagopalan, H. and C. Lengauer, *Aneuploidy and cancer.* Nature, 2004. **432**(7015): p. 338-41.
62. Hambridge, K.M., *Zinc and chromium in human nutrition.* J Hum Nutr, 1978. **32**(2): p. 99-110.
63. Federico, A., et al., *Effects of selenium and zinc supplementation on nutritional status in patients with cancer of digestive tract.* Eur J Clin Nutr, 2001. **55**(4): p. 293-7.
64. Prasad, A.S., *Zinc deficiency in humans: a neglected problem.* J Am Coll Nutr, 1998. **17**(6): p. 542-3.
65. Prasad, A.S., *Zinc and immunity.* Mol Cell Biochem, 1998. **188**(1-2): p. 63-9.
66. Prasad, A.S., et al., *Nutritional and zinc status of head and neck cancer patients: an interpretive review.* J Am Coll Nutr, 1998. **17**(5): p. 409-18.
67. Fong, L.Y., et al., *Induction of esophageal tumors in zinc-deficient rats by single low doses of N-nitrosomethylbenzylamine (NMBA): analysis of cell proliferation, and mutations in H-ras and p53 genes.* Carcinogenesis, 1997. **18**(8): p. 1477-84.
68. Zhang, Z.F., et al., *Adenocarcinomas of the esophagus and gastric cardia: the role of diet.* Nutr Cancer, 1997. **27**(3): p. 298-309.
69. Lipman, T.O., et al., *Esophageal zinc content in human squamous esophageal cancer.* J Am Coll Nutr, 1987. **6**(1): p. 41-6.
70. Newberne, P.M., S. Broitman, and T.F. Schrager, *Esophageal carcinogenesis in the rat: zinc deficiency, DNA methylation and alkyltransferase activity.* Pathobiology, 1997. **65**(5): p. 253-63.
71. Donahue, T. and O.J. Hines, *The ZIP4 pathway in pancreatic cancer.* Cancer Biol Ther, 2010. **9**(3): p. 243-5.
72. Hogstrand, C., et al., *Zinc transporters and cancer: a potential role for ZIP7 as a hub for tyrosine kinase activation.* Trends Mol Med, 2009. **15**(3): p. 101-11.
73. Franklin, R.B., et al., *hZIP1 zinc uptake transporter down regulation and zinc depletion in prostate cancer.* Mol Cancer, 2005. **4**: p. 32.
74. Hansen, C.R., Jr., et al., *Copper and zinc deficiencies in association with depression and neurological findings.* Biol Psychiatry, 1983. **18**(3): p. 395-401.
75. Black, M.M., *Zinc deficiency and child development.* Am J Clin Nutr, 1998. **68**(2 Suppl): p. 464S-469S.
76. Black, R.E., *Therapeutic and preventive effects of zinc on serious childhood infectious diseases in developing countries.* Am J Clin Nutr, 1998. **68**(2 Suppl): p. 476S-479S.
77. Sandstead, H.H., C.J. Frederickson, and J.G. Penland, *History of zinc as related to brain function.* J Nutr, 2000. **130**(2S Suppl): p. 496S-502S.
78. Salgueiro, M.J., et al., *Zinc deficiency and growth: current concepts in relationship to two important points: intellectual and sexual development.* Biol Trace Elem Res, 2004. **99**(1-3): p. 49-69.
79. Salgueiro, M.J., et al., *The role of zinc in the growth and development of children.* Nutrition, 2002. **18**(6): p. 510-9.
80. Yan, M., et al., *Zinc deficiency alters DNA damage response genes in normal human prostate epithelial cells.* J Nutr, 2008. **138**(4): p. 667-73.
81. Sharif, R., et al., *The effect of zinc sulphate and zinc carnosine on genome stability and cytotoxicity in the WIL2-NS human lymphoblastoid cell line.* Mutat Res, 2011. **720**(1-2): p. 22-33.

82. Sharif, R., et al., *Zinc deficiency or excess within the physiological range increases genome instability and cytotoxicity, respectively, in human oral keratinocyte cells.* Genes Nutr, 2011.
83. Fenech, M.F., *Dietary reference values of individual micronutrients and nutriomes for genome damage prevention: current status and a road map to the future.* Am J Clin Nutr, 2010. **91**(5): p. 1438S-1454S.
84. Fenech, M., *Cytokinesis-block micronucleus cytome assay.* Nat Protoc, 2007. **2**(5): p. 1084-104.
85. Fenech, M., et al., *Molecular mechanisms of micronucleus, nucleoplasmic bridge and nuclear bud formation in mammalian and human cells.* Mutagenesis, 2011. **26**(1): p. 125-32.
86. Xu, B., et al., *Replication stress induces micronuclei comprising of aggregated DNA double-strand breaks.* PLoS One, 2011. **6**(4): p. e18618.
87. Kimura, M., et al., *Methylenetetrahydrofolate reductase C677T polymorphism, folic acid and riboflavin are important determinants of genome stability in cultured human lymphocytes.* J Nutr, 2004. **134**(1): p. 48-56.
88. Wu, J., et al., *The effect of selenium, as selenomethionine, on genome stability and cytotoxicity in human lymphocytes measured using the cytokinesis-block micronucleus cytome assay.* Mutagenesis, 2009. **24**(3): p. 225-32.
89. Leopardi, P., et al., *Effects of folic acid deficiency and MTHFR C677T polymorphism on spontaneous and radiation-induced micronuclei in human lymphocytes.* Mutagenesis, 2006. **21**(5): p. 327-33.
90. Zenzen, V., et al., *Mutagenic and cytotoxic effectiveness of zinc dimethyl and zinc diisononyldithiocarbamate in human lymphocyte cultures.* Mutat Res, 2001. **497**(1-2): p. 89-99.
91. Santra, M., et al., *Induction of micronuclei by zinc in human leukocytes: a study using cytokinesis-block micronucleus assay.* Biol Trace Elem Res, 2002. **88**(2): p. 139-44.
92. Bruno, R.S., et al., *Dietary zinc restriction in rats alters antioxidant status and increases plasma F2 isoprostanes.* J Nutr Biochem, 2007. **18**(8): p. 509-18.
93. Shibuya, K., et al., *Protective role of metallothionein in bone marrow injury caused by X-irradiation.* J Toxicol Sci, 2008. **33**(4): p. 479-84.
94. Song, Y., et al., *Dietary zinc restriction and repletion affects DNA integrity in healthy men.* Am J Clin Nutr, 2009. **90**(2): p. 321-8.
95. Xie, H., et al., *Zinc chromate induces chromosome instability and DNA double strand breaks in human lung cells.* Toxicol Appl Pharmacol, 2009. **234**(3): p. 293-9.
96. Zou, L. and S.J. Elledge, *Sensing DNA damage through ATRIP recognition of RPA-ssDNA complexes.* Science, 2003. **300**(5625): p. 1542-8.
97. Falck, J., J. Coates, and S.P. Jackson, *Conserved modes of recruitment of ATM, ATR and DNA-PKcs to sites of DNA damage.* Nature, 2005. **434**(7033): p. 605-11.
98. Wise, S.S., et al., *Comparative genotoxicity and cytotoxicity of four hexavalent chromium compounds in human bronchial cells.* Chem Res Toxicol, 2010. **23**(2): p. 365-72.
99. Bae, S.N., et al., *Cytotoxic effect of zinc-citrate compound on choriocarcinoma cell lines.* Placenta, 2007. **28**(1): p. 22-30.
100. Sliwinski, T., et al., *Zinc salts differentially modulate DNA damage in normal and cancer cells.* Cell Biol Int, 2009. **33**(4): p. 542-7.
101. Tapisso, J.T., et al., *Induction of micronuclei and sister chromatid exchange in bone-marrow cells and abnormalities in sperm of Algerian mice (Mus spretus) exposed to cadmium, lead and zinc.* Mutat Res, 2009. **678**(1): p. 59-64.
102. World Health Organization, W., *Environment Health Criteria 221 : Zinc*. 2001, World Health Organization: Geneva. p. 360.
103. Domingo, J.L., et al., *Acute zinc intoxication: comparison of the antidotal efficacy of several chelating agents.* Vet Hum Toxicol, 1988. **30**(3): p. 224-8.
104. Wang, P., A.B. Guliaev, and B. Hang, *Metal inhibition of human N-methylpurine-DNA glycosylase activity in base excision repair.* Toxicol Lett, 2006. **166**(3): p. 237-47.
105. Blasco, M.A., *Telomeres and human disease: ageing, cancer and beyond.* Nat Rev Genet, 2005. **6**(8): p. 611-22.
106. Callen, E. and J. Surralles, *Telomere dysfunction in genome instability syndromes.* Mutat Res, 2004. **567**(1): p. 85-104.
107. Rodier, F., et al., *Cancer and aging: the importance of telomeres in genome maintenance.* Int J Biochem Cell Biol, 2005. **37**(5): p. 977-90.

108. Bull, C. and M. Fenech, *Genome-health nutrigenomics and nutrigenetics: nutritional requirements or 'nutriomes' for chromosomal stability and telomere maintenance at the individual level.* Proc Nutr Soc, 2008. **67**(2): p. 146-56.
109. Liu, Q., et al., *Effects of trace elements on the telomere lengths of hepatocytes L-02 and hepatoma cells SMMC-7721.* Biol Trace Elem Res, 2004. **100**(3): p. 215-27.
110. Cipriano, C., et al., *Accumulation of cells with short telomeres is associated with impaired zinc homeostasis and inflammation in old hypertensive participants.* J Gerontol A Biol Sci Med Sci, 2009. **64**(7): p. 745-51.
111. Lehtio, L., et al., *Zinc binding catalytic domain of human tankyrase 1.* J Mol Biol, 2008. **379**(1): p. 136-45.
112. Smith, S., et al., *Tankyrase, a poly(ADP-ribose) polymerase at human telomeres.* Science, 1998. **282**(5393): p. 1484-7.
113. Smith, S. and T. de Lange, *Tankyrase promotes telomere elongation in human cells.* Curr Biol, 2000. **10**(20): p. 1299-302.
114. van Steensel, B. and T. de Lange, *Control of telomere length by the human telomeric protein TRF1.* Nature, 1997. **385**(6618): p. 740-3.
115. d'Adda di Fagagna, F., et al., *Functions of poly(ADP-ribose) polymerase in controlling telomere length and chromosomal stability.* Nat Genet, 1999. **23**(1): p. 76-80.
116. Fenech, M., *Micronutrients and genomic stability: a new paradigm for recommended dietary allowances (RDAs).* Food Chem Toxicol, 2002. **40**(8): p. 1113-7.
117. Fenech, M., *Nutrition and genome health.* Forum Nutr, 2007. **60**: p. 49-65.
118. Liuzzi, J.P. and R.J. Cousins, *Mammalian zinc transporters.* Annu Rev Nutr, 2004. **24**: p. 151-72.
119. Sekler, I., et al., *Mechanism and regulation of cellular zinc transport.* Mol Med, 2007. **13**(7-8): p. 337-43.
120. Lichten, L.A. and R.J. Cousins, *Mammalian zinc transporters: nutritional and physiologic regulation.* Annu Rev Nutr, 2009. **29**: p. 153-76.
121. Maret, W. and H.H. Sandstead, *Zinc requirements and the risks and benefits of zinc supplementation.* J Trace Elem Med Biol, 2006. **20**(1): p. 3-18.
122. Mocchegiani, E., et al., *Zinc deficiency and IL-6 -174G/C polymorphism in old people from different European countries: effect of zinc supplementation. ZINCAGE study.* Exp Gerontol, 2008. **43**(5): p. 433-44.
123. Mariani, E., et al., *Effect of zinc supplementation on plasma IL-6 and MCP-1 production and NK cell function in healthy elderly: interactive influence of +647 MT1a and -174 IL-6 polymorphic alleles.* Exp Gerontol, 2008. **43**(5): p. 462-71.
124. Vasto, S., et al., *Zinc and inflammatory/immune response in aging.* Ann N Y Acad Sci, 2007. **1100**: p. 111-22.
125. Giacconi, R., et al., *The -174G/C polymorphism of IL-6 is useful to screen old subjects at risk for atherosclerosis or to reach successful ageing.* Exp Gerontol, 2004. **39**(4): p. 621-8.
126. Cipriano, C., et al., *Polymorphisms in MT1a gene coding region are associated with longevity in Italian Central female population.* Biogerontology, 2006. **7**(5-6): p. 357-65.
127. Mocchegiani, E., et al., *MtmRNA gene expression, via IL-6 and glucocorticoids, as potential genetic marker of immunosenescence: lessons from very old mice and humans.* Exp Gerontol, 2002. **37**(2-3): p. 349-57.
128. Mariani, E., et al., *Effects of zinc supplementation on antioxidant enzyme activities in healthy old subjects.* Exp Gerontol, 2008. **43**(5): p. 445-51.
129. Mocchegiani, E., et al., *Zinc, metallothioneins, and longevity--effect of zinc supplementation: zincage study.* Ann N Y Acad Sci, 2007. **1119**: p. 129-46.
130. Teo, T. and M. Fenech, *The interactive effect of alcohol and folic acid on genome stability in human WIL2-NS cells measured using the cytokinesis-block micronucleus cytome assay.* Mutat Res, 2008.
131. Umegaki, K. and M. Fenech, *Cytokinesis-block micronucleus assay in WIL2-NS cells: a sensitive system to detect chromosomal damage induced by reactive oxygen species and activated human neutrophils.* Mutagenesis, 2000. **15**(3): p. 261-9.
132. Mitchell, C., et al., *Role of oxidative stress and MAPK signaling in reference moist smokeless tobacco-induced HOK-16B cell death.* Toxicol Lett, 2010. **195**(1): p. 23-30.
133. Hiraishi, H., et al., *Polaprezinc protects gastric mucosal cells from noxious agents through antioxidant properties in vitro.* Aliment Pharmacol Ther, 1999. **13**(2): p. 261-9.

134. Arakawa, T., et al., *Effects of zinc L-carnosine on gastric mucosal and cell damage caused by ethanol in rats. Correlation with endogenous prostaglandin E2.* Dig Dis Sci, 1990. **35**(5): p. 559-66.
135. Mahmood, A., et al., *Zinc carnosine, a health food supplement that stabilises small bowel integrity and stimulates gut repair processes.* Gut, 2007. **56**(2): p. 168-75.
136. Ueda, K., et al., *Polaprezinc (Zinc L-carnosine) is a potent inducer of anti-oxidative stress enzyme, heme oxygenase (HO)-1 - a new mechanism of gastric mucosal protection.* J Pharmacol Sci, 2009. **110**(3): p. 285-94.
137. Matsuu-Matsuyama, M., et al., *Protection by polaprezinc against radiation-induced apoptosis in rat jejunal crypt cells.* J Radiat Res (Tokyo), 2008. **49**(4): p. 341-7.
138. Fenech, M., *Micronucleus frequency in human lymphocytes is related to plasma vitamin B12 and homocysteine.* Mutat Res, 1999. **428**(1-2): p. 299-304.
139. Fenech, M., et al., *Low intake of calcium, folate, nicotinic acid, vitamin E, retinol, beta-carotene and high intake of pantothenic acid, biotin and riboflavin are significantly associated with increased genome instability--results from a dietary intake and micronucleus index survey in South Australia.* Carcinogenesis, 2005. **26**(5): p. 991-9.
140. Bonassi, S., et al., *An increased micronucleus frequency in peripheral blood lymphocytes predicts the risk of cancer in humans.* Carcinogenesis, 2007. **28**(3): p. 625-31.
141. El-Zein, R.A., et al., *Cytokinesis-blocked micronucleus assay as a novel biomarker for lung cancer risk.* Cancer Res, 2006. **66**(12): p. 6449-56.
142. Fenech, M. and J.W. Crott, *Micronuclei, nucleoplasmic bridges and nuclear buds induced in folic acid deficient human lymphocytes-evidence for breakage-fusion-bridge cycles in the cytokinesis-block micronucleus assay.* Mutat Res, 2002. **504**(1-2): p. 131-6.
143. Teo, T. and M. Fenech, *The interactive effect of alcohol and folic acid on genome stability in human WIL2-NS cells measured using the cytokinesis-block micronucleus cytome assay.* Mutat Res, 2008. **657**(1): p. 32-8.
144. Zhen, W., et al., *The relative radiosensitivity of TK6 and WI-L2-NS lymphoblastoid cells derived from a common source is primarily determined by their p53 mutational status.* Mutat Res, 1995. **346**(2): p. 85-92.
145. Verbanac, D., et al., *Determination of standard zinc values in the intact tissues of mice by ICP spectrometry.* Biol Trace Elem Res, 1997. **57**(1): p. 91-6.
146. Mosmann, T., *Rapid colorimetric assay for cellular growth and survival: application to proliferation and cytotoxicity assays.* J Immunol Methods, 1983. **65**(1-2): p. 55-63.
147. Singh, N.P., et al., *A simple technique for quantitation of low levels of DNA damage in individual cells.* Exp Cell Res, 1988. **175**(1): p. 184-91.
148. Tice, R.R., et al., *Single cell gel/comet assay: guidelines for in vitro and in vivo genetic toxicology testing.* Environ Mol Mutagen, 2000. **35**(3): p. 206-21.
149. Olive, P.L., J.P. Banath, and R.E. Durand, *Heterogeneity in radiation-induced DNA damage and repair in tumor and normal cells measured using the "comet" assay.* Radiat Res, 1990. **122**(1): p. 86-94.
150. Bao, S. and D.L. Knoell, *Zinc modulates airway epithelium susceptibility to death receptor-mediated apoptosis.* Am J Physiol Lung Cell Mol Physiol, 2006. **290**(3): p. L433-41.
151. Yamaguchi, S., et al., *Zinc is an essential trace element for spermatogenesis.* Proc Natl Acad Sci U S A, 2009. **106**(26): p. 10859-64.
152. Truong-Tran, A.Q., et al., *New insights into the role of zinc in the respiratory epithelium.* Immunol Cell Biol, 2001. **79**(2): p. 170-7.
153. Mazen, A., et al., *Poly(ADP-ribose)polymerase: a novel finger protein.* Nucleic Acids Res, 1989. **17**(12): p. 4689-98.
154. Song, Y., et al., *Marginal zinc deficiency increases oxidative DNA damage in the prostate after chronic exercise.* Free Radic Biol Med, 2009.
155. Mah, L.J., A. El-Osta, and T.C. Karagiannis, *gammaH2AX: a sensitive molecular marker of DNA damage and repair.* Leukemia. **24**(4): p. 679-86.
156. Engelhardt, M., et al., *Telomerase and telomere length in the development and progression of premalignant lesions to colorectal cancer.* Clin Cancer Res, 1997. **3**(11): p. 1931-41.
157. Griffith, J.K., et al., *Reduced telomere DNA content is correlated with genomic instability and metastasis in invasive human breast carcinoma.* Breast Cancer Res Treat, 1999. **54**(1): p. 59-64.
158. Meeker, A.K., *Telomeres and telomerase in prostatic intraepithelial neoplasia and prostate cancer biology.* Urol Oncol, 2006. **24**(2): p. 122-30.

159. Plentz, R.R., et al., *Telomere shortening of epithelial cells characterises the adenoma-carcinoma transition of human colorectal cancer.* Gut, 2003. **52**(9): p. 1304-7.
160. Sieglova, Z., et al., *Dynamics of telomere erosion and its association with genome instability in myelodysplastic syndromes (MDS) and acute myelogenous leukemia arising from MDS: a marker of disease prognosis?* Leuk Res, 2004. **28**(10): p. 1013-21.
161. Nemoto, K., et al., *Modulation of telomerase activity by zinc in human prostatic and renal cancer cells.* Biochem Pharmacol, 2000. **59**(4): p. 401-5.
162. Fenech, M., *Cytokinesis-block micronucleus assay evolves into a "cytome" assay of chromosomal instability, mitotic dysfunction and cell death.* Mutat Res, 2006. **600**(1-2): p. 58-66.
163. Ertekin, M.V., et al., *Zinc sulfate in the prevention of total-body irradiation-induced early hematopoietic toxicity: a controlled study in a rat model.* Biol Trace Elem Res, 2004. **100**(1): p. 63-73.
164. Ertekin, M.V., et al., *Zinc sulfate in the prevention of radiation-induced oropharyngeal mucositis: a prospective, placebo-controlled, randomized study.* Int J Radiat Oncol Biol Phys, 2004. **58**(1): p. 167-74.
165. Ertekin, M.V., et al., *The effects of oral zinc sulphate during radiotherapy on anti-oxidant enzyme activities in patients with head and neck cancer: a prospective, randomised, placebo-controlled study.* Int J Clin Pract, 2004. **58**(7): p. 662-8.
166. Ertekin, M.V., et al., *The effect of zinc sulphate in the prevention of radiation-induced dermatitis.* J Radiat Res (Tokyo), 2004. **45**(4): p. 543-8.
167. Ertekin, M.V., et al., *Effect of oral zinc supplementation on agents of oropharyngeal infection in patients receiving radiotherapy for head and neck cancer.* J Int Med Res, 2003. **31**(4): p. 253-66.
168. Fenech, M., et al., *Necrosis, apoptosis, cytostasis and DNA damage in human lymphocytes measured simultaneously within the cytokinesis-block micronucleus assay: description of the method and results for hydrogen peroxide.* Mutagenesis, 1999. **14**(6): p. 605-12.
169. Suntres, Z.E. and E.M. Lui, *Antioxidant effect of zinc and zinc-metallothionein in the acute cytotoxicity of hydrogen peroxide in Ehrlich ascites tumour cells.* Chem Biol Interact, 2006. **162**(1): p. 11-23.
170. Matsui, H., et al., *Low micromolar zinc exerts cytotoxic action under H2O2-induced oxidative stress: excessive increase in intracellular Zn2+ concentration.* Toxicology, 2010. **276**(1): p. 27-32.
171. Dineley, K.E., T.V. Votyakova, and I.J. Reynolds, *Zinc inhibition of cellular energy production: implications for mitochondria and neurodegeneration.* J Neurochem, 2003. **85**(3): p. 563-70.
172. Maret, W., et al., *The ATP/metallothionein interaction: NMR and STM.* Biochemistry, 2002. **41**(5): p. 1689-94.
173. Dreosti, I.E., *Free radical pathology and the genome*
in *Trace Elements, Micronutrients and Free Radicals*
1991, Humana
Press: New Jersey. p. 149–169.
174. Klebanov, G.I., et al., *Effect of carnosine and its components on free-radical reactions.* Membr Cell Biol, 1998. **12**(1): p. 89-99.
175. Hipkiss, A.R., *Carnosine, a protective, anti-ageing peptide?* Int J Biochem Cell Biol, 1998. **30**(8): p. 863-8.
176. Hipkiss, A.R. and H. Chana, *Carnosine protects proteins against methylglyoxal-mediated modifications.* Biochem Biophys Res Commun, 1998. **248**(1): p. 28-32.
177. Hipkiss, A.R., et al., *Protective effects of carnosine against malondialdehyde-induced toxicity towards cultured rat brain endothelial cells.* Neurosci Lett, 1997. **238**(3): p. 135-8.
178. Hipkiss, A.R., et al., *Protective effects of carnosine against protein modification mediated by malondialdehyde and hypochlorite.* Biochim Biophys Acta, 1998. **1380**(1): p. 46-54.
179. Babizhayev, M.A., et al., *L-carnosine (beta-alanyl-L-histidine) and carcinine (beta-alanylhistamine) act as natural antioxidants with hydroxyl-radical-scavenging and lipid-peroxidase activities.* Biochem J, 1994. **304 (Pt 2)**: p. 509-16.
180. Chan, K.M. and E.A. Decker, *Endogenous skeletal muscle antioxidants.* Crit Rev Food Sci Nutr, 1994. **34**(4): p. 403-26.
181. Chan, W.K., et al., *Effect of dietary carnosine on plasma and tissue antioxidant concentrations and on lipid oxidation in rat skeletal muscle.* Lipids, 1994. **29**(7): p. 461-6.

182. Nersesyan, A. and N. Chobanyan, *Micronuclei and other nuclear anomalies levels in exfoliated buccal cells and DNA damage in leukocytes of patients with polycystic ovary syndrome.* J Buon, 2010. **15**(2): p. 337-9.
183. Nersesyan, A., et al., *Impact of smoking on the frequencies of micronuclei and other nuclear abnormalities in exfoliated oral cells: a comparative study with different cigarette types.* Mutagenesis, 2010.
184. Nersesyan, A.K., *Does cigarette smoking induce micronuclei in buccal cells?* Am J Clin Nutr, 2006. **84**(4): p. 946-7; author reply 947-8.
185. Nersesyan, A.K. and R.T. Adamyan, *Micronuclei level in exfoliated buccal mucosa cells of patients with benign and malignant tumors of female reproductive organs and breast.* Tsitol Genet, 2004. **38**(3): p. 72-5.
186. Li, N., et al., *[Study on the preventive effect of tea on DNA damage of the buccal mucosa cells in oral leukoplakias induce by cigarette smoking].* Wei Sheng Yan Jiu, 1998. **27**(3): p. 173-4.
187. Munoz, N., et al., *Effect of riboflavin, retinol, and zinc on micronuclei of buccal mucosa and of esophagus: a randomized double-blind intervention study in China.* J Natl Cancer Inst, 1987. **79**(4): p. 687-91.
188. Piyathilake, C.J., et al., *Cigarette smoking, intracellular vitamin deficiency, and occurrence of micronuclei in epithelial cells of the buccal mucosa.* Cancer Epidemiol Biomarkers Prev, 1995. **4**(7): p. 751-8.
189. Prasad, M.P., M.A. Mukundan, and K. Krishnaswamy, *Micronuclei and carcinogen DNA adducts as intermediate end points in nutrient intervention trial of precancerous lesions in the oral cavity.* Eur J Cancer B Oral Oncol, 1995. **31B**(3): p. 155-9.
190. Ramirez, A. and P.H. Saldanha, *Micronucleus investigation of alcoholic patients with oral carcinomas.* Genet Mol Res, 2002. **1**(3): p. 246-60.
191. Thomas, P., et al., *Effect of dietary intervention on human micronucleus frequency in lymphocytes and buccal cells.* Mutagenesis, 2010. **26**(1): p. 69-76.
192. Lundqvist, C., et al., *Cytokine profile and ultrastructure of intraepithelial gamma delta T cells in chronically inflamed human gingiva suggest a cytotoxic effector function.* J Immunol, 1994. **153**(5): p. 2302-12.
193. Rouabhia, M., et al., *Interleukin-18 and gamma interferon production by oral epithelial cells in response to exposure to Candida albicans or lipopolysaccharide stimulation.* Infect Immun, 2002. **70**(12): p. 7073-80.
194. Presland, R.B. and B.A. Dale, *Epithelial structural proteins of the skin and oral cavity: function in health and disease.* Crit Rev Oral Biol Med, 2000. **11**(4): p. 383-408.
195. Hambidge, M., *Biomarkers of trace mineral intake and status.* J Nutr, 2003. **133 Suppl 3**: p. 948S-955S.
196. Phillips, H.J., *Dye exclusion test for cell viability*, in *Tissue Culture*, P.F. Kruser, Editor. 1973, Academic Press: New York. p. 407-408.
197. Eastmond, D.A. and J.D. Tucker, *Kinetochore localization in micronucleated cytokinesis-blocked Chinese hamster ovary cells: a new and rapid assay for identifying aneuploidy-inducing agents.* Mutat Res, 1989. **224**(4): p. 517-25.
198. Murgia, C., et al., *Zinc and its specific transporters as potential targets in airway disease.* Curr Drug Targets, 2006. **7**(5): p. 607-627.
199. Nishida, T., et al., *Zinc Supplementation with Polaprezinc Protects Mouse Hepatocytes against Acetaminophen-Induced Toxicity via Induction of Heat Shock Protein 70.* J Clin Biochem Nutr, 2010. **46**(1): p. 43-51.
200. Omatsu, T., et al., *Reactive oxygen species-quenching and anti-apoptotic effect of polaprezinc on indomethacin-induced small intestinal epithelial cell injury.* J Gastroenterol, 2010. **45**(7): p. 692-702.
201. Mah, L.J., A. El-Osta, and T.C. Karagiannis, *gammaH2AX: a sensitive molecular marker of DNA damage and repair.* Leukemia, 2010. **24**(4): p. 679-86.
202. Fenech, M., et al., *Molecular mechanisms of micronucleus, nucleoplasmic bridge and nuclear bud formation in mammalian and human cells.* Mutagenesis, 2010. **26**(1): p. 125-32.
203. Duerre, J.A. and J.C. Wallwork, *Methionine metabolism in isolated perfused livers from rats fed on zinc-deficient and restricted diets.* Br J Nutr, 1986. **56**(2): p. 395-405.
204. Wallwork, J.C. and J.A. Duerre, *Effect of zinc deficiency on methionine metabolism, methylation reactions and protein synthesis in isolated perfused rat liver.* J Nutr, 1985. **115**(2): p. 252-62.

205. Murnane, J.P., *Telomeres and chromosome instability.* DNA Repair (Amst), 2006. **5**(9-10): p. 1082-92.
206. Fanzo, J.C., et al., *p53 protein and p21 mRNA levels and caspase-3 activity are altered by zinc status in aortic endothelial cells.* Am J Physiol Cell Physiol, 2002. **283**(2): p. C631-8.
207. Fanzo, J.C., et al., *Zinc status affects p53, gadd45, and c-fos expression and caspase-3 activity in human bronchial epithelial cells.* Am J Physiol Cell Physiol, 2001. **281**(3): p. C751-7.
208. Siliciano, J.D., et al., *DNA damage induces phosphorylation of the amino terminus of p53.* Genes Dev, 1997. **11**(24): p. 3471-81.
209. Harley, C.B., A.B. Futcher, and C.W. Greider, *Telomeres shorten during ageing of human fibroblasts.* Nature, 1990. **345**(6274): p. 458-60.
210. Blackburn, E.H., *Structure and function of telomeres.* Nature, 1991. **350**(6319): p. 569-73.
211. Shay, J.W. and W.E. Wright, *Role of telomeres and telomerase in cancer.* Semin Cancer Biol, 2012. **21**(6): p. 349-53.
212. Artandi, S.E. and R.A. DePinho, *Telomeres and telomerase in cancer.* Carcinogenesis, 2012. **31**(1): p. 9-18.
213. Jones, C.H., C. Pepper, and D.M. Baird, *Telomere dysfunction and its role in haematological cancer.* Br J Haematol, 2012. **156**(5): p. 573-87.
214. Pino, M.S. and D.C. Chung, *The chromosomal instability pathway in colon cancer.* Gastroenterology, 2012. **138**(6): p. 2059-72.
215. Mirabello, L., et al., *Telomere length and variation in telomere biology genes in individuals with osteosarcoma.* Int J Mol Epidemiol Genet, 2012. **2**(1): p. 19-29.
216. Fenech, M., *The role of folic acid and Vitamin B12 in genomic stability of human cells.* Mutat Res, 2001. **475**(1-2): p. 57-67.
217. Marcon, F., et al., *Diet-related telomere shortening and chromosome stability.* Mutagenesis, 2012. **27**(1): p. 49-57.
218. Moores, C.J., M. Fenech, and N.J. O'Callaghan, *Telomere dynamics: the influence of folate and DNA methylation.* Ann N Y Acad Sci, 2011. **1229**: p. 76-88.
219. Sharif, R., et al., *The role of zinc in genomic stability.* Mutat Res, 2011.
220. Dizdaroglu, M., G. Kirkali, and P. Jaruga, *Formamidopyrimidines in DNA: mechanisms of formation, repair, and biological effects.* Free Radic Biol Med, 2008. **45**(12): p. 1610-21.
221. Memisoglu, A. and L. Samson, *Base excision repair in yeast and mammals.* Mutat Res, 2000. **451**(1-2): p. 39-51.
222. De Boeck, G., et al., *Telomere-associated proteins: cross-talk between telomere maintenance and telomere-lengthening mechanisms.* J Pathol, 2009. **217**(3): p. 327-44.
223. Hu, J., et al., *Repair of formamidopyrimidines in DNA involves different glycosylases: role of the OGG1, NTH1, and NEIL1 enzymes.* J Biol Chem, 2005. **280**(49): p. 40544-51.
224. Shibutani, S., M. Takeshita, and A.P. Grollman, *Insertion of specific bases during DNA synthesis past the oxidation-damaged base 8-oxodG.* Nature, 1991. **349**(6308): p. 431-4.
225. Grollman, A.P. and M. Moriya, *Mutagenesis by 8-oxoguanine: an enemy within.* Trends Genet, 1993. **9**(7): p. 246-9.
226. Boiteux, S. and J.P. Radicella, *Base excision repair of 8-hydroxyguanine protects DNA from endogenous oxidative stress.* Biochimie, 1999. **81**(1-2): p. 59-67.
227. Helbock, H.J., et al., *DNA oxidation matters: the HPLC-electrochemical detection assay of 8-oxo-deoxyguanosine and 8-oxo-guanine.* Proc Natl Acad Sci U S A, 1998. **95**(1): p. 288-93.
228. Collins, A., et al., *Problems in the measurement of 8-oxoguanine in human DNA. Report of a workshop, DNA oxidation, held in Aberdeen, UK, 19-21 January, 1997.* Carcinogenesis, 1997. **18**(9): p. 1833-6.
229. von Zglinicki, T., R. Pilger, and N. Sitte, *Accumulation of single-strand breaks is the major cause of telomere shortening in human fibroblasts.* Free Radic Biol Med, 2000. **28**(1): p. 64-74.
230. O'Callaghan, N., et al., *A quantitative real-time PCR method for absolute telomere length.* Biotechniques, 2008. **44**(6): p. 807-9.
231. O'Callaghan, N.J. and M. Fenech, *A quantitative PCR method for measuring absolute telomere length.* Biol Proced Online, 2011. **13**: p. 3.
232. Cawthon, R.M., *Telomere measurement by quantitative PCR.* Nucleic Acids Res, 2002. **30**(10): p. e47.
233. O'Callaghan, N.J., Baack, N., Sharif, R and Fenech, M, *A PCR based assay to quantifiy oxidised guanine and other FPG-sensitive base lesions within telomeric DNA.* Biotechniques, 2011. **in press**.

234. Smith, C.C., M.R. O'Donovan, and E.A. Martin, *hOGG1 recognizes oxidative damage using the comet assay with greater specificity than FPG or ENDOIII.* Mutagenesis, 2006. **21**(3): p. 185-90.
235. Karakaya, A., et al., *Kinetics of excision of purine lesions from DNA by Escherichia coli Fpg protein.* Nucleic Acids Res, 1997. **25**(3): p. 474-9.
236. Boiteux, S., et al., *Homogeneous Escherichia coli FPG protein. A DNA glycosylase which excises imidazole ring-opened purines and nicks DNA at apurinic/apyrimidinic sites.* J Biol Chem, 1990. **265**(7): p. 3916-22.
237. Tchou, J., et al., *Function of the zinc finger in Escherichia coli Fpg protein.* J Biol Chem, 1993. **268**(35): p. 26738-44.
238. Svenson, U., et al., *Breast cancer survival is associated with telomere length in peripheral blood cells.* Cancer Res, 2008. **68**(10): p. 3618-23.
239. De Meyer, T., et al., *Paternal age at birth is an important determinant of offspring telomere length.* Hum Mol Genet, 2007. **16**(24): p. 3097-102.
240. Kimura, M., et al., *Offspring's leukocyte telomere length, paternal age, and telomere elongation in sperm.* PLoS Genet, 2008. **4**(2): p. e37.
241. Njajou, O.T., et al., *Telomere length is paternally inherited and is associated with parental lifespan.* Proc Natl Acad Sci U S A, 2007. **104**(29): p. 12135-9.
242. Unryn, B.M., L.S. Cook, and K.T. Riabowol, *Paternal age is positively linked to telomere length of children.* Aging Cell, 2005. **4**(2): p. 97-101.
243. Nan, H., et al., *Shorter Telomeres Associate with a Reduced Risk of Melanoma Development.* Cancer Res, 2011. **71**(21): p. 6758-6763.
244. Shen, M., et al., *A prospective study of telomere length measured by monochrome multiplex quantitative PCR and risk of lung cancer.* Lung Cancer, 2011. **73**(2): p. 133-7.
245. Arbeev, K.G., et al., *Leukocyte telomere length, breast cancer risk in the offspring: the relations with father's age at birth.* Mech Ageing Dev, 2011. **132**(4): p. 149-53.
246. Lan, Q., et al., *A prospective study of telomere length measured by monochrome multiplex quantitative PCR and risk of non-Hodgkin lymphoma.* Clin Cancer Res, 2009. **15**(23): p. 7429-33.
247. Xue, F., et al., *Parental age at delivery and incidence of breast cancer: a prospective cohort study.* Breast Cancer Res Treat, 2007. **104**(3): p. 331-40.
248. Zhang, Y., et al., *Parental age at child's birth and son's risk of prostate cancer. The Framingham Study.* Am J Epidemiol, 1999. **150**(11): p. 1208-12.
249. O'Callaghan, N.J., et al., *Weight loss in obese men is associated with increased telomere length and decreased abasic sites in rectal mucosa.* Rejuvenation Res, 2009. **12**(3): p. 169-76.
250. O'Callaghan, N.J., et al., *Colonocyte telomere shortening is greater with dietary red meat than white meat and is attenuated by resistant starch.* Clin Nutr, 2011.
251. Thomas, P., et al., *Grape seed polyphenols and curcumin reduce genomic instability events in a transgenic mouse model for Alzheimer's disease.* Mutat Res, 2009. **661**(1-2): p. 25-34.
252. Opresko, P.L., et al., *Oxidative damage in telomeric DNA disrupts recognition by TRF1 and TRF2.* Nucleic Acids Res, 2005. **33**(4): p. 1230-9.
253. Wang, Z., et al., *Characterization of oxidative guanine damage and repair in mammalian telomeres.* PLoS Genet, 2010. **6**(5): p. e1000951.
254. Muramatsu, Y., et al., *Telomere elongation by a mutant tankyrase 1 without TRF1 poly(ADP-ribosyl)ation.* Exp Cell Res, 2008. **314**(5): p. 1115-24.
255. Hambidge, K.M. and N.F. Krebs, *Zinc deficiency: a special challenge.* J Nutr, 2007. **137**(4): p. 1101-5.
256. Brown, K.H., et al., *International Zinc Nutrition Consultative Group (IZiNCG) technical document #1. Assessment of the risk of zinc deficiency in populations and options for its control.* Food Nutr Bull, 2004. **25**(1 Suppl 2): p. S99-203.
257. Mares-Perlman, J.A., et al., *Zinc intake and sources in the US adult population: 1976-1980.* J Am Coll Nutr, 1995. **14**(4): p. 349-57.
258. Worwag, M., H.G. Classen, and E. Schumacher, *Prevalence of magnesium and zinc deficiencies in nursing home residents in Germany.* Magnes Res, 1999. **12**(3): p. 181-9.
259. Oldewage-Theron, W.H., F.O. Samuel, and C.S. Venter, *Zinc deficiency among the elderly attending a care centre in Sharpeville, South Africa.* J Hum Nutr Diet, 2008. **21**(6): p. 566-74.
260. Chandra, R., *Nutrition and immunity in the elderly: clinical significance.* Nutr Rev, 1995. **53**(4 Pt 2): p. S80-3; discussion S83-5.

261. Bogden, J.D., et al., *Daily micronutrient supplements enhance delayed-hypersensitivity skin test responses in older people.* Am J Clin Nutr, 1994. **60**(3): p. 437-47.
262. Meunier, N., et al., *Importance of zinc in the elderly: the ZENITH study.* Eur J Clin Nutr, 2005. **59 Suppl 2**: p. S1-4.
263. Andrews, M. and C. Gallagher-Allred, *The role of zinc in wound healing.* Adv Wound Care, 1999. **12**(3): p. 137-8.
264. Marcellini, F., et al., *Zinc status, psychological and nutritional assessment in old people recruited in five European countries: Zincage study.* Biogerontology, 2006. **7**(5-6): p. 339-45.
265. Ortega, R.M., et al., *Dietary intake and cognitive function in a group of elderly people.* Am J Clin Nutr, 1997. **66**(4): p. 803-9.
266. Mocchegiani, E., et al., *Zinc, oxidative stress, genetic background and immunosenescence: implications for healthy ageing.* Immun Ageing, 2006. **3**: p. 6.
267. Mocchegiani, E., F. Marcellini, and G. Pawelec, *Nutritional zinc, oxidative stress and immunosenescence: biochemical, genetic, and lifestyle implications for healthy ageing.* Biogerontology, 2004. **5**(4): p. 271-3.
268. Marcellini, F., et al., *Zinc in elderly people: effects of zinc supplementation on psychological dimensions in dependence of IL-6 -174 polymorphism: a Zincage study.* Rejuvenation Res, 2008. **11**(2): p. 479-83.
269. Putics, A., et al., *Zinc supplementation boosts the stress response in the elderly: Hsp70 status is linked to zinc availability in peripheral lymphocytes.* Exp Gerontol, 2008. **43**(5): p. 452-61.
270. Kahmann, L., et al., *Zinc supplementation in the elderly reduces spontaneous inflammatory cytokine release and restores T cell functions.* Rejuvenation Res, 2008. **11**(1): p. 227-37.
271. Maret, W., *Cellular zinc and redox states converge in the metallothionein/thionein pair.* J Nutr, 2003. **133**(5 Suppl 1): p. 1460S-2S.
272. Pepersack, T., et al., *Prevalence of zinc deficiency and its clinical relevance among hospitalised elderly.* Arch Gerontol Geriatr, 2001. **33**(3): p. 243-53.
273. World Health Organization, W., *Trace elements in human nutrition and health*. 1996, Geneva, Switzerland: World Health Organization.
274. World Health Organization, W., *Vitamin and mineral requirements in human nutrition*. 2004, Geneva, Switzerland: World Health Organization.
275. Medicine, I.o., *Dietary reference intakes for vitamin A, vitamin K, arsenic, boron, chromium, copper, iodine, iron, manganese, molybdenum, nickel, silicon, vanadium, and zinc*. 2001, Washington, DC: National Academy Press.
276. Sciences, N.A.o., *Recommended dietary allowances*. 10th Ed ed. 1989, Washington, DC: National Academy Press.
277. Council, N.H.a.M.R., *Nutrient Reference Values for Australia and New Zealand*. 2006: NHMRC Publications.
278. Statistics, A.B.o., *National Nutrition Survey - Nutrient Intakes and Physical Measurements*. 1998, Australian Bureau of Statistics: Australia.
279. Hodge, A., et al., *The Anti Cancer Council of Victoria FFQ: relative validity of nutrient intakes compared with weighed food records in young to middle-aged women in a study of iron supplementation.* Aust N Z J Public Health, 2000. **24**(6): p. 576-83.
280. Ireland, P., Jolley, P., Giles, G., O'Dea, K., Powles, J., Rutishauser, I., Wahlqvist, M., & Williams, J., *Development of the Melbourne FFQ: a food frequency questionnaire for use in an Australian propspective study involving an ethnically diverse cohort.* Asia Pacific Journal of Clinical Nutrition, 1994(3): p. 19-31.
281. Benzie, I.F., W.Y. Chung, and J.J. Strain, *"Antioxidant" (reducing) efficiency of ascorbate in plasma is not affected by concentration.* J Nutr Biochem, 1999. **10**(3): p. 146-50.
282. Fenech, M. and A.A. Morley, *Cytokinesis-block micronucleus method in human lymphocytes: effect of in vivo ageing and low dose X-irradiation.* Mutat Res, 1986. **161**(2): p. 193-8.
283. Vickers, A.J. and D.G. Altman, *Statistics notes: Analysing controlled trials with baseline and follow up measurements.* Bmj, 2001. **323**(7321): p. 1123-4.
284. Hyun, T.H., E. Barrett-Connor, and D.B. Milne, *Zinc intakes and plasma concentrations in men with osteoporosis: the Rancho Bernardo Study.* Am J Clin Nutr, 2004. **80**(3): p. 715-21.
285. Mocchegiani, E., M. Muzzioli, and R. Giacconi, *Zinc, metallothioneins, immune responses, survival and ageing.* Biogerontology, 2000. **1**(2): p. 133-43.
286. Brown, K.H., *Effect of infections on plasma zinc concentration and implications for zinc status assessment in low-income countries.* Am J Clin Nutr, 1998. **68**(2 Suppl): p. 425S-429S.

287. Expert Scientific Working Group, F.o.A.S.f.E.B., *Assessment of the Zinc Nutritional Status of the US populations Based on Data Collected in the Second National Health and Nutrition Examination Survey, 1976-1980*. 1982, federation of American Societies for Experimental Biology: Bethesda, MD.
288. Savarino, L., et al., *Serum concentrations of zinc and selenium in elderly people: results in healthy nonagenarians/centenarians.* Exp Gerontol, 2001. **36**(2): p. 327-39.
289. Girodon, F., et al., *Effect of micronutrient supplementation on infection in institutionalized elderly subjects: a controlled trial.* Ann Nutr Metab, 1997. **41**(2): p. 98-107.
290. Group, A.-R.E.D.R., *The effect of five-year zinc supplementation on serum zinc, serum cholesterol and hematocrit in persons randomly assigned to treatment group in the age-related eye disease study: AREDS Report No. 7.* J Nutr, 2002. **132**(4): p. 697-702.
291. Hininger-Favier, I., et al., *Age- and sex-dependent effects of long-term zinc supplementation on essential trace element status and lipid metabolism in European subjects: the Zenith Study.* Br J Nutr, 2007. **97**(3): p. 569-78.
292. Bogden, J.D., et al., *Zinc and immunocompetence in elderly people: effects of zinc supplementation for 3 months.* Am J Clin Nutr, 1988. **48**(3): p. 655-63.
293. Ducros, V., et al., *Zinc supplementation does not alter plasma homocysteine, vitamin B12 and red blood cell folate concentrations in French elderly subjects.* J Trace Elem Med Biol, 2009. **23**(1): p. 15-20.
294. Milne, D.B., et al., *Effect of oral folic acid supplements on zinc, copper, and iron absorption and excretion.* Am J Clin Nutr, 1984. **39**(4): p. 535-9.
295. Halsted, C.H., *The intestinal absorption of dietary folates in health and disease.* J Am Coll Nutr, 1989. **8**(6): p. 650-8.
296. Favier, M., et al., *Zinc deficiency and dietary folate metabolism in pregnant rats.* J Trace Elem Electrolytes Health Dis, 1993. **7**(1): p. 19-24.
297. Tamura, T., et al., *Increased methionine synthetase activity in zinc-deficient rat liver.* Arch Biochem Biophys, 1987. **256**(1): p. 311-6.
298. Hong, K.H., et al., *Effects of dietary zinc deficiency on homocysteine and folate metabolism in rats.* J Nutr Biochem, 2000. **11**(3): p. 165-9.
299. Andriollo-Sanchez, M., et al., *No antioxidant beneficial effect of zinc supplementation on oxidative stress markers and antioxidant defenses in middle-aged and elderly subjects: the Zenith study.* J Am Coll Nutr, 2008. **27**(4): p. 463-9.
300. Kumaravel, T.S., et al., *Comet Assay measurements: a perspective.* Cell Biol Toxicol, 2007.
301. Gibson, R.S., et al., *Indicators of zinc status at the population level: a review of the evidence.* Br J Nutr, 2008. **99 Suppl 3**: p. S14-23.
302. Foster, M., et al., *Zinc transporter genes are coordinately expressed in men and women independently of dietary or plasma zinc.* J Nutr, 2011. **141**(6): p. 1195-201.
303. Zalewski, P.D., I.J. Forbes, and W.H. Betts, *Correlation of apoptosis with change in intracellular labile Zn(II) using zinquin [(2-methyl-8-p-toluenesulphonamido-6-quinolyloxy)acetic acid], a new specific fluorescent probe for Zn(II).* Biochem J, 1993. **296 (Pt 2)**: p. 403-8.

Appendix and Paper Reprints

Sharif, R., Thomas, P., Zalewski, P. & Fenech, M. (2011) The role of zinc in genomic stability.
Mutation Research/Fundamental and Molecular Mechanisms of Mutagenesis, v. 733(1-2), pp. 111-121

Sharif, R., Thomas, P., Zalewski, P., Graham, R.D. & Fenech, M. (2011) The effect of zinc sulphate and zinc carnosine on genome stability and cytotoxicity in the WIL2-NS human lymphoblastoid cell line.
Mutation Research/Genetic Toxicology and Environmental Mutagenesis, v. 720(1-2), pp. 22-33

Sharif, R., Thomas, P., Zalewski, P. & Fenech, M. (2011) Zinc deficiency or excess within the physiological range increases genome instability and cytotoxicity, respectively, in human oral keratinocyte cells.
Genes and Nutrition, v. 7(2), pp. 139-154

O'Callaghan, N., Baack, N., Sharif, R. & Fenech, M. (2011) A qPCR-based assay to quantify oxidized guanine and other FPG-sensitive base lesions within telomeric DNA.
Biotechniques, v. 51(6), pp. 403-412